Scuola Dottorale di Ateneo
Graduate School

Dottorato di ricerca
in Scienze Chimiche
Cycle XXXIX
Dissertation year 2016

New synthetic routes to bisphosphonates as potential drugs for bone disease treatment

SSD: CHIM/04

Ph.D. Thesis of ANDREA CHIMINAZZO
Student Number 800358

Ph.D. Coordinator	**Tutor**
Prof. Maurizio Selva	**Prof. Alessandro Scarso**
	Co-tutor
	Prof. Giorgio Strukul

Estratto per riassunto della tesi di dottorato

Studente: Andrea Chiminazzo   Matricola: 800358

Dottorato: Scienze Chimiche   Ciclo:XXIX

Titolo della tesi : New synthetic routes to bisphosphonates as potential drugs for bone disease treatment
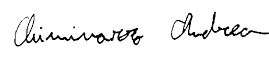
Abstract:

I bisfosfonati (BPs) sono utilizzati come farmaci nel trattamento dell'osteoporosi. BPs contenenti eteroatomi di azoto o lunghe catene alifatiche sono i più potenti inibitori degli osteoclasti, le cellule preposte al riassorbimento osseo. In letteratura un solo BP enantioarricchito è stato testato, osservando una differenza di attività tra i due enantiomeri.

Utilizzando metilenbisfosfonato tetraetil estere (MBP) quale precursore di partenza, è stata sintetizzata un'ampia gamma di precursori BP dotati di doppio legame non sostituito, monosostituito o bi sostituito avente differenti caratteristiche steriche ed elettroniche. L'applicazione su tali precursori di reazioni, anche catalizzate, di addizione di acidi boronici, indoli, tioli o isonitrili, idrogenazione del doppio legame, cicloaddizione o condensazioni aldoliche su derivati isatina-BP hanno permesso la sintesi di nuovi BP, molti dei quali N-BPs o con elevati eccessi enantiomerici. Alcuni dei nuovi BP sono stati sottoposti a deprotezione dei gruppi esterei ottenendo i corrispondenti acidi bisfosfonici che sono stati utilizzati in test su cementi biomedici o materiali a base di ZrO. La *Click Reaction* su un γ-azido BP ha permesso la coniugazione di un nuovo fluoroforo con struttura dichetopirrolopirrolica: la sonda fluorescente ottenuta è attualmente sotto indagine in test di attività e fluorescenza.

Bisphosphonates (BPs) are employed as drugs for the treatment of osteoporosis. N-BP bearing long alkyl chain are the most potent inhibitors of osteoclasts that are the cells deputed to bone resorption. In the literature there is only one example of test on a enantiopure bisphosphonic acid that showed high difference in activity between the two enantiomers. Using methylenebisphosphonate tetraethyl ester (MBP) as building block, a wide range of double bond containing BP precursors with different steric and electronic properties were synthesized. Reactions in many cases mediated by catalysts, like addition of boronic acids, indoles, thiols or isonitriles, double bond hydrogenation, cycloaddition or aldol condensation on isatin-BP derivative allowed to synthesize several new BPs, most of them N-BP or with high enantiomeric excess. Selected BPs were subjected to deprotection of the ester moiety, obtaining the corresponding bisphosphonic acids that were employed in tests on biomedical cement or test ZrO materials. *Click reaction* carried out on γ-azide BP enabled the conjugation of the BP moiety with a new diketopyrrolopyrrole-based fluorophore. Obtained fluorescent BP probe is under investigation for fluorescence and anti-resorption activity tests.

Firma dello studente

_____

To my family

SUMMARY

FOREWORD

This thesis collects the work carried out during the three years of XXIX cycle of PhD course in chemical sciences at the Università Ca' Foscari di Venezia funded by the Italian Ministry of Education on the specific topic concerning "relaunch of pharmaceutical industry through fine chemistry of new active intermediates and natural compounds for new diagnostic applications". No fundings have been provided by private companies.

Some of the results obtained and reported here have been published on international peer reviewed scientific journals, others will be soon submitted for publications. The published results will be highlighted at the beginning of each paragraph.

It is worth to note that the presentation of the results does not follow a strict chronological order. In particular cases appropriately highlighted, the research work permitted the cooperation and synergy with other research groups in Italy and abroad in order to improve the obtained results or test the obtained molecules.

1. <u>INTRODUCTION</u>

1.1 BONE AND MINERAL METABOLISM

1.1.1 *Bone Morphology*

Bone tissue is a complex connective tissue made of associated cells dispersed in an abundant extracellular matrix.[1] It is characterized both by a remarkable hardness and strength and also good flexibility and cover a variety of critical functions on human's physiology, ranging from macroscopic support and movement of the individual, to protection of the internal organs, to molecular properties like mineral deposition and blood pH's control.[2] Bone tissue along with the cartilagenous tissue forms the skeleton of vertebrates (**Figure 1**).
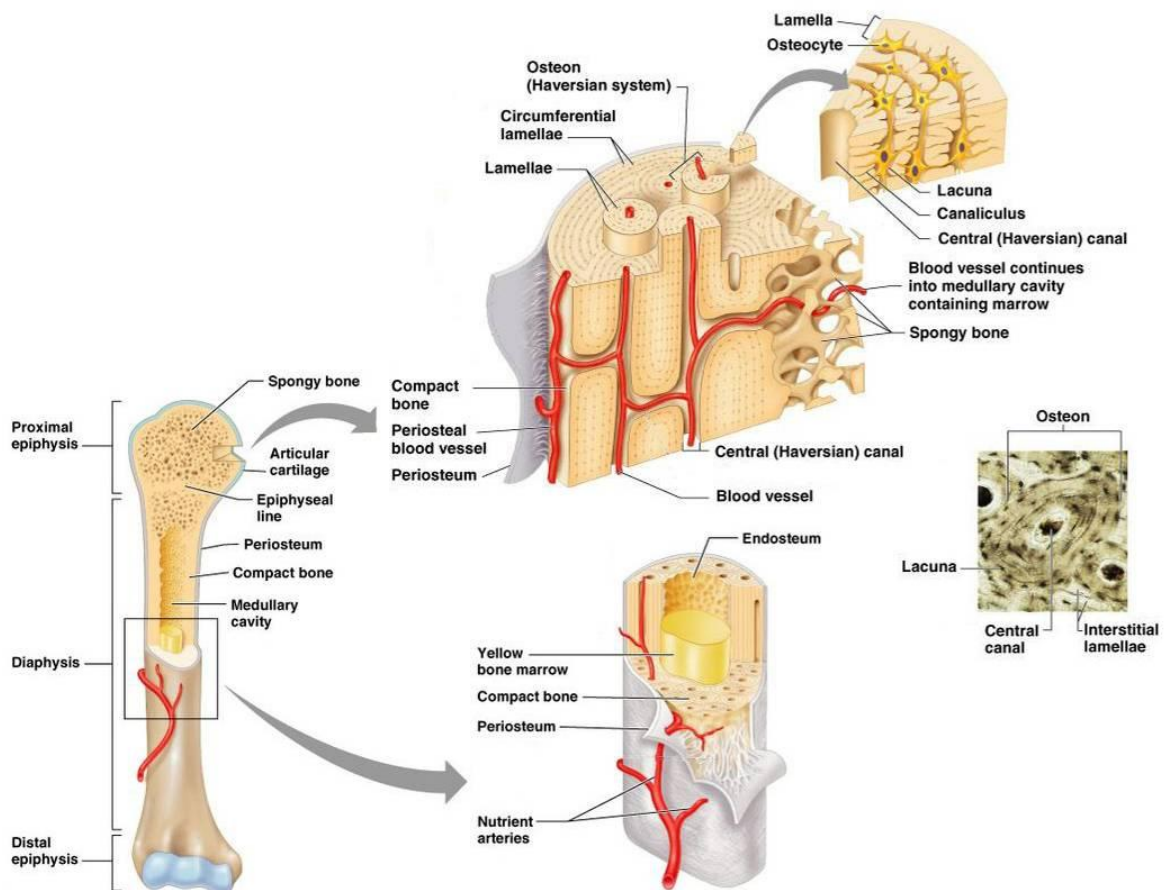
Figure 1: Bone Morphology

Macroscopically, bone can be divided into an inner part named trabecular, cancellous or spongy bone and an outer part called cortical or compact bone, which makes about 80%

of the total weight of the skeleton. Trabecular bone is mainly located on epiphysis of long bones, on the cavities of bone marrow and is the main constituent of short bones (**Figure 1**). While trabecular bone is pore rich and slightly mineralized, the cortical one is dense, mineralized up to 90% and mainly situated on diaphysis of long bones.[3] Microscopically, cortical and spongy bone in the adult skeleton are made of well-ordered parallel collagen fibers, organized in a lamellar pattern made of basic units called bone structural units (BSUs).[4] In cortical bone these are called osteons i.e. cylinders made of concentric lamellae where in the center there is a canal containing the nutrient blood vessels. The trabeculae also consist of structural units, which in this location are called packets. When they are on the surface and not yet terminated, theyare called bone multicellular units (BMUs).

1.1.2 *Bone Composition*

Bone is a composite material consisting of an inorganic and a organic phase on which several cells are dispersed (**Table 1**). By weight, mineral accounts for about 60% of the total dry weight of bone, 8-10% is water and the remainder is organic phase.[5] The inorganic phase is an impure form of hydroxyapatite $Ca_{10}(PO_4)_6(OH)_2$, wich is a naturally occurring calcium phosphate (**Figure 2**). Chemically speaking it is a calcium deficient apatite, containing, however, many other constituents, among others HPO_4^-, carbonate, magnesium, sodium, fluoride and strontium that are incorporated into thecrystal lattice or adsorbed onto the crystal surface reducing the crystallinity of the hydroxyapatite (HAP).[6] Crystals of HAP have the shape of long thin needles that are 2 nm thick and 20-40 nm long and originate from the stacking of the elementar cells present in bone as a flattened hexagonal prism. They are deposited within and between the organic phase of the matrix in a manner which gives the bone tissue its compressive strength and stiffness.
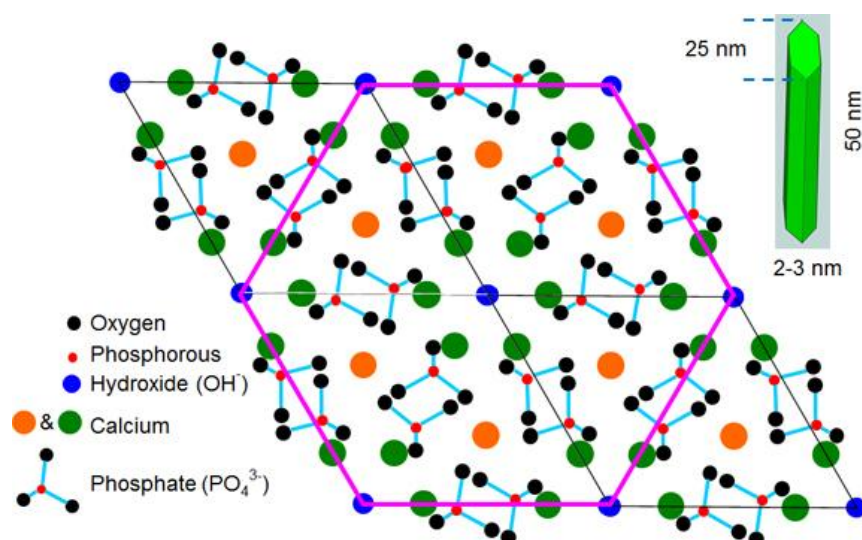
Figure 2: Hydroxyapatite crystal structure

The organic phase is about 30 % of the dry weight of the bone and consists in 90% of type I collagen, which is thus by far the most abundant bone protein characterized by an extremely low solubility. Type I collagen molecule consists of three polypeptide chains of approximately one thousand amino acids each with a complex three-dimensional structure that gives bone tissue a very rigid linear strength. Several non collagenous protein have been identified in the matrix of bone tissue: one of the most abundant is osteocalcin that is closely associated with the mineral phase. Evidences suggest that this non-collagenous protein may play an important role in inhibiting bone formation and maturation.[7]

Other substances, such as polyphosphates and bisphosphonates have a special affinity for calcium phosphate and they can be found on bone tissue. They are deposited preferably on the mineral, specifically on resorption areas. The binding of these substances is usually reversible at sites where the bone surface is accessible to the extracellular fluid. BPs buried inside bone by new bone formation are not available until the bone is destroyed again during modeling or remodeling.[8]

Composition of Bone	
Mineral ~ 60%	Hydroxyapatite
Matrix ~30%	Collagen ~ 90%
	Other proteins
Water	
Cells	Osteoblast
	Osteoclast
	Osteocyes

Table 1: Composition of bones.

1.1.3 *Bone Cells*

Three cell types are typically associated with bone tissue: osteoblasts, osteocytes and osteoclasts. While osteoblasts and osteocytes are derived from mesenchymal cell lineage, osteoclasts are derived from hematopoietic cell lineage (**Figure 3**).

The osteoblasts are the cells that synthesize the protein matrix of bone in an epithelial-like structure at the surface of the bone referred to as osteoid.[9] This organic matrix creates a template for mineralization and production of mature bone that occurs in a second step. As a consequence of the time lag between the formation and calcification, a layer of unmineralized osteoid matrix is present under the osteoblasts. Osteoblast assists, in addition to bone formation, the initiation of bone resorption by secreting factors that

recruit and promote the differentiation of monocytic cells into mature osteoclast. When osteoblast are not forming the bone, they are flat and are called lining cells.

At a certain time some of the osteoblasts stop synthesizing matrix and become embedded within bone. They are then called osteocytes, the other mesenchymal lineage cell type. Osteocytes are the most abundant cellular component of bones making up 95% of all bone cells. With an estimated 25 years lifetime, osteocytes are long living relative to osteoblasts that are estimated to live an average of 3 months.[10] They create an interconnected network in bone allowing for intercellular communications between both neighboring osteocytes and the surface-lining osteoblasts. Gap junctions at the membrane contact sites make a functional syncytium, allowing bone to respond to mechanical and chemical stimuli over large areas.
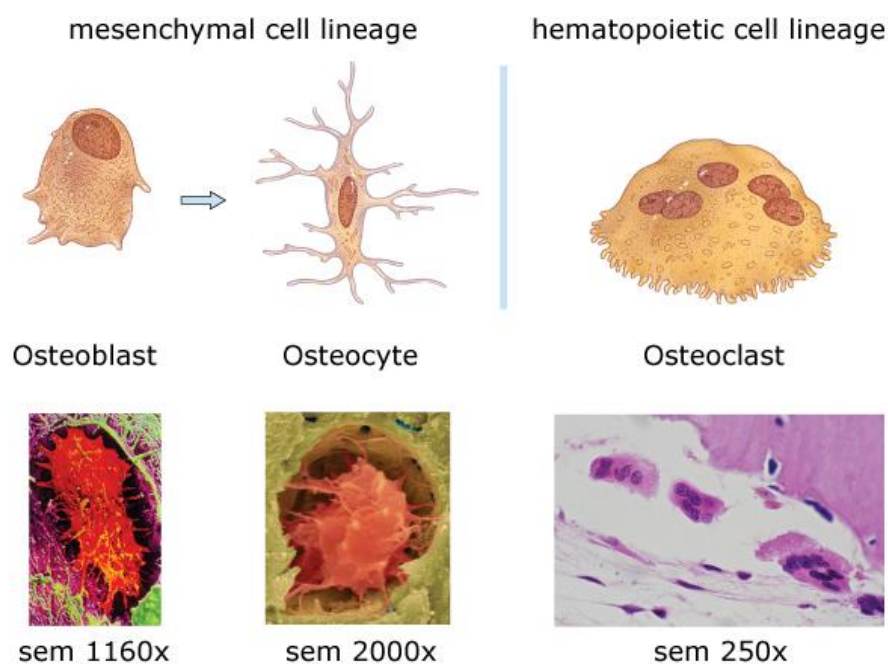
Figure 3: Bone cells types.

The last type of cells in bone are the osteoclasts that are large multinucleated cells derived from hematopoietic mononuclear cells.[11] They are located at the tip of the remodeling units either on the surface of the cortical or trabecular bone, often in depressions called Howship's lacunae, or within the cortical bone. The role of osteoclasts is to resorb bone and this is performed in a closed, sealed-off microenvironment located between the cell and the bone. Cell membrane receptors of osteoclast, called integrins, recognize specific peptide sequences in the matrix covering than the microenvironment with a special part of the cell membrane, called the ruffled border, which secretes two types of products, both leading to bone destruction. The first includes various proteolytic enzymes, such as cathepsin K and collagenases which digest the matrix. The second are H^+ ions, originated from H_2CO_3 as a result of the action of carbonic anhydrase [12] leading eventually to bone dissolution.

Bringing hydroxyapatite into solution at pH 7.4 requires acid secretion on a massive scale [13] as shown in **Equation 1**:

$$14H^+ + Ca_{10}(PO_4)_6(OH)_2 \rightleftharpoons 10Ca^{2+} + 6H_2PO_4^- + 2H_2O \qquad \text{(Eq. 1)}$$

Osteoclasts are able to move along the bone surface or into a cutting cone slowly removing the underlying bone in a defined area without disrupting the surrounding local microenvironment: in one day they approximately degrade their own volume of bone mineral.

Bone resorption can be modulated by altering three basic processes: the activity of mature osteoclasts, the recruitment of new osteoclasts and the life of the latter which is programmed by apoptosis. Recent results indicate that all three processes seem to be under the control of cells of osteoblastic lineage, which synthesize factors influencing directly the osteoclasts and their precursors. The three main hormones modulating bone resorption are parathyroid hormone (PTH), $1,25(OH)_2$ D (calcitriol) and calcitonin: the first two increasing, the latter decreasing resorption. Recently a novel factor inhibiting osteoclast formation and activity, called osteoprotegerin (OPG), has been discovered. Acting as a decoy receptor of an osteoclastic differentiation factor called RANK ligand (RANKL), it inhibits osteoclast recruitment.[13] Furthermore, estrogens in women and testosterone in men inhibit bone resorption. This is why menopause and ovariectomy, as well as orchidectomy, induce an increase in bone resorption.

1.1.4 *Modeling and Remodeling*

Once formed, the shape and structure of the bones is continuously renovated and modified by the two processes of modeling and remodeling. Modeling is the main process by which the skeleton can increase its volume and its mass and it takes place principally during growth. During modeling new bone is formed at a location different from the one destroyed resulting in a change in the shape of the skeleton.

In remodeling, which is the main process in the adult, the two processes are coupled in space and time, so that no change occurs in the shape of the bone resulting in the replacement of old bone by new bone allowing the maintenance of the mechanical integrity of the skeleton.[8] The remodeling rate is between 2 and 10% of the skeletal mass per year. The cancellous bone, which represents about 20% of the skeletal mass, makes up 80% of the turnover, while the cortex, which represents 80% of the bone, makes up only 20% of the turnover. Remodeling in trabecular bone is normally 5–10 times higher than cortical bone remodeling in the adult.[14] Under normal conditions, the remodeling process results in no net change in bone mass and requires up to 5 months to complete a new bone structural unit.

According to the model proposed by Parfitt, [15] the normal remodeling sequence in bone follows a scheme of quiescence, activation, resorption, reversal, formation and return to quiescence. (**Figure 4**)
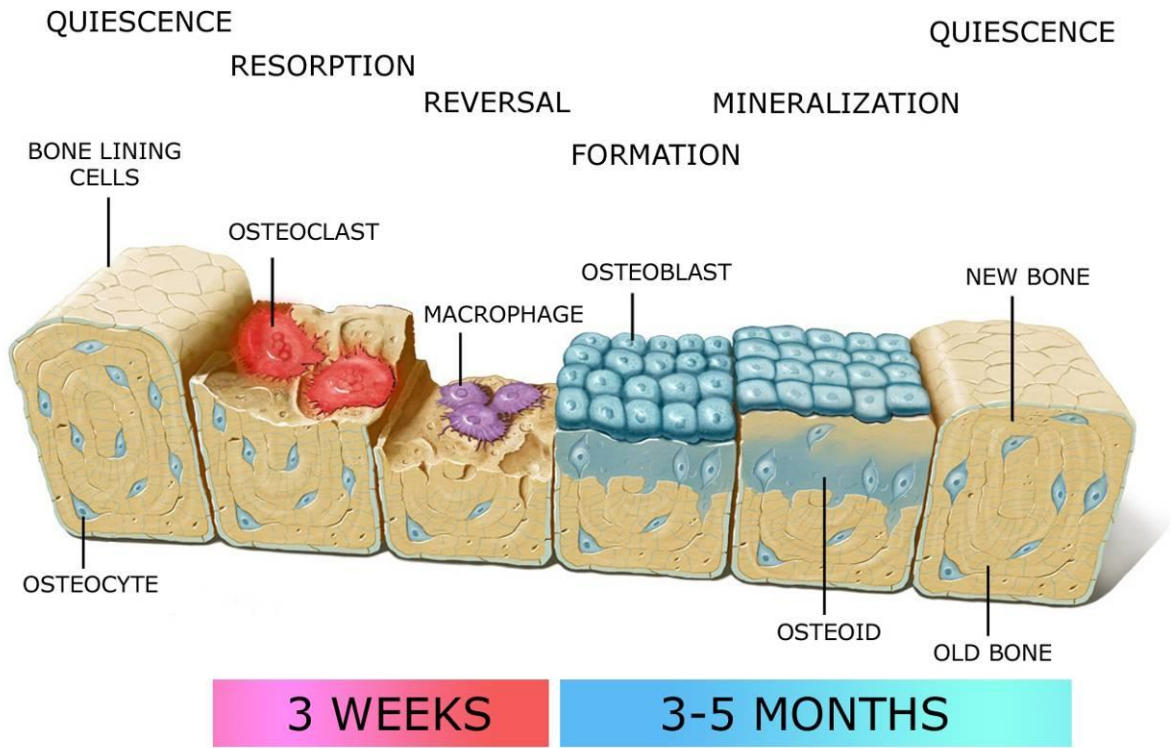
Figure 4: Parfitt's model of the remodeling sequence in bones.

The basic structures of turnover are the packets in cancellous bone and the osteons in cortical bone called in this case bone remodeling unit (BRU). The conversion of a small area of bone surface from quiescence to activity is referred to as activation. Both in the cortex and in the trabeculae, the process of remodeling starts with the recruitment of osteoclasts and proceeds by bone being eroded by osteoclasts. Monolayer of osteoclasts bore holes through the hard bone at a speed of about 20-40 μm per day (in cortical bone), roughly parallel to the long axis of the bone and about 5–10 μm per day perpendicular to the main direction of advance.[16] Recruiting and erosion are increased by thyroxin, parathyroid hormone, $1,25(OH)_2D$ and growth hormone and decreased by calcitonin, estrogen and glucocorticosteroids. They are also stimulated by microfractures and modulated by the mechanical strain environment. The reversal phase is a interval time between the completion of resorption and the initiation of bone formation characterized by the appearance of mesenchymal cells that are progenitors for osteoblasts. The resorption sites are then refilled by the osteoblasts that synthetize the new bone. The formation rate is slower, about 1 μm per day for lamellar, more for woven bone.[16] The terminal transformation of osteoblasts covers the surface of bone by a layer of thin, flattened lining cells that have receptors for a variety of substances, which

are important for initiating bone resorption. Between these lining cells and old bone there is a layer of unmineralized osteoid. By the end of the process (3-5 months) a new mineralized quiescent bone structural unit will have been formed.

1.1.5 *Calcium Homeostasis*

Calcium concentration in plasma is around 100 ppm and approximately only one-half is ionized.[17] The level of ionized plasma calcium is tightly controlled throughout the animal world, leading to ionized calcium being called one of nature's physiological constants. This constancy is explained by the importance of extracellular calcium for many biological processes, like blood coagulation, muscle contraction, ATP and glycogen metabolism.[3, 18] The level of ionized calcium depends on the fluxes between extracellular fluid and blood and the interactions between three target organs: intestine, bone and kidney (**Figure 5**). These three organs are then intimately linked with respect to calcium homeostasis and consequently, a imbalance in one of these affects the others. Because 99% of the body's calcium is located in the skeleton, this organ acts as a mineral storage.
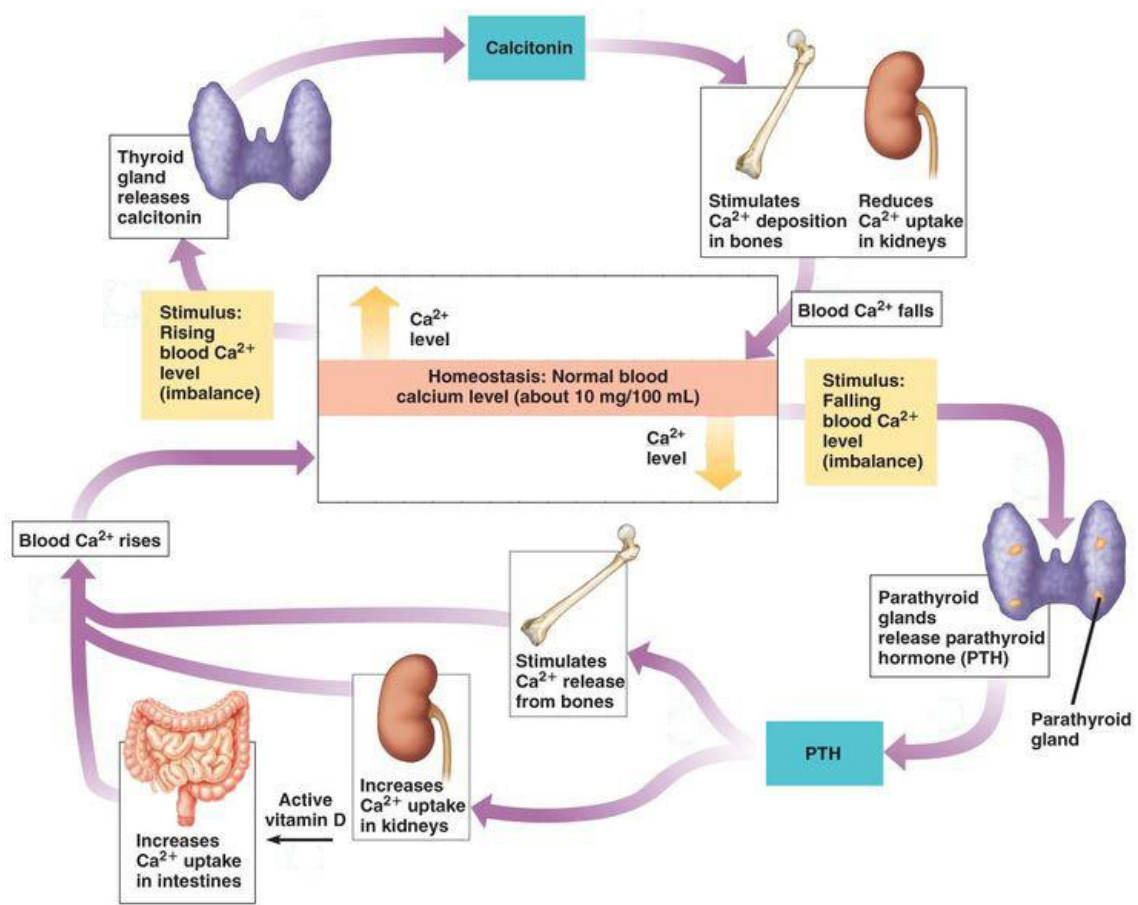
Figure 5: Negative and positive feedback in calcium homeostasis.

Bone homeostasis is maintained by the coordinated actions of osteoblast-mediated formation and osteoclast-mediated bone removal. This coordination is referred to as "coupling." The concept of coupling is based on the idea that osteoblasts influence osteoclast formation and activity likewise osteoclasts influence osteoblast differentiation and activity.[19, 20, 21] The fluxes of calcium are controlled mainly by three hormones, parathyroidhormone (PTH), the vitamin D metabolite $1,25(OH)_2D$ (calcitriol) and calcitonin. All three are directly regulated by plasma calcium levels through a feedback mechanism. Of the three hormones, the most important is parathyroid hormone, which increases plasma calcium by action on all three target organs. The hormone $1,25(OH)_2D$ increases intestinal calcium absorption and bone resorption. Finally, calcitonin inhibits bone absorption and reduce calcium uptake in kidneys. It is not yet clear what is the daily intake of calcium in the humans: it is recommended that at least 1 g is necessary in adult life and 1.5 g in the elderly as well as during pregnancy and lactation.[22] This means that a large part of the population is chronically calcium deficient, since its daily intakeis usually only about 0.5 g.

The coordinated interactions between osteoblasts and osteoclasts regulate not only the balance of ionized calcium but were also adapted to provide means to respond to more global mechanical forces. Bone architecture indeed is under the control of a biomechanical cybernetic system, called mechanostat that controls bone's modification: the induced strains due to the external mechanical forces play an essential role by altering the interconnected osteocyte network that communicate a mechanosensory feedback to the lining osteoblasts [10] altering the remodeling. The mechanical feedback transmission mechanism between cells still remains unclear.[23] A deterioration of the mechanical property of the bone tissue itself, indeed, increases the induced strains, leading to increased bone formation and/or decreased bone resorption. Also the microcracks, which occur constantly during life, stimulate bone remodeling: this allows old bone to be replaced by young bone and permits the skeleton to keep its mechanical strength. When the mechanostat does not sense sufficient input such as in immobilization, rapid and massive bone loss occurs.

1.2   OSTEOPOROSIS

1.2.1 *Nature of Osteoporosis*

The ability of a bone to resist to fracture depends on the bone mass, its spatial shape, its microarchitecture and the intrinsic properties of the materials it is made of. Bone mineral density (BMD) is the amount of bone mineral in bone tissue and it depends by ageing, genetic, physical, hormonal and nutritional factors acting alone or in concert to diminish skeletal integrity. In 1994, Kanis et al. pubblished a definition of osteoporosis based exclusively on bone mass.[24] The authors defined osteoporosis as being present when

the bone mineral density (BMD) at hip level is over 2.5 standard deviations (**Figure 6**) below the young adult reference mean (-2.5 T-scores). If fractures are present, the condition is called severe osteoporosis. In addition they proposed that BMD values of 1–2.5 standard deviations below the young adult mean be designated as "osteopenic".[24] This approach has proven useful for clinical management, but has several limitations like the applicability to young people prior to the completion of peak bone acquisition or the BMD itself measurement.
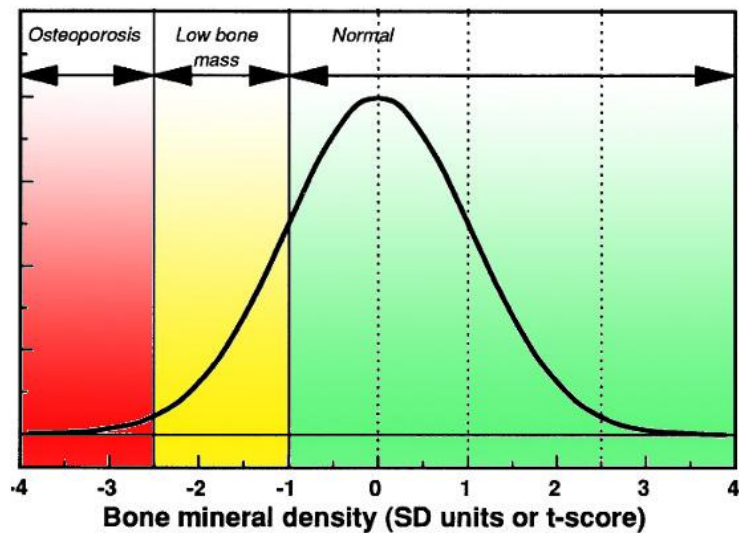
Figure 6: Diagnostic threshold for osteoporosis based on distribution of bone mineral density.

Nowadays osteoporosis has a new definition: from 2001 NIH Consensus Development Conference osteoporosis is "a disease characterized by low bone strength, leading to enhanced bone fragility and a consequent increase in fracture risk".[25] This definition underscores the role of bone strength, attributing to several factors, mainly to low bone mass and microarchitectural deterioration, the enhanced fragility associated with osteoporotic fractures.

Figure 7: Normal bone (A), Osteoporotic bone (B).

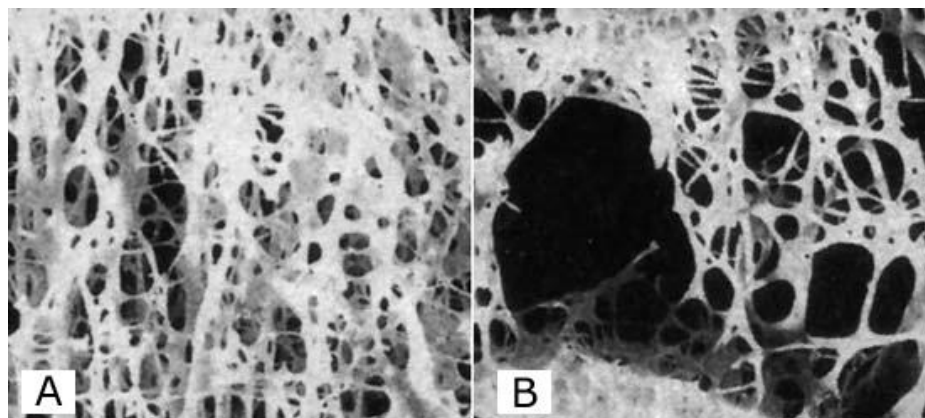An artificial distinction used to be made between primary and secondary osteoporosis: while the former is due to two separate entities, one related to menopausal estrogen loss and the other to aging, [26] the latter is the consequence of other diseases, such as hypogonadism, malignant diseases, liver diseases or immobilization.

The concept of primary osteoporosis was then elaborated by Riggs [27] who used the terms "Type I osteoporosis" to signify a loss of trabecular bone after menopause and "Type II osteoporosis" to represent a loss of cortical and trabecular bone in men and women as the end result of age-related bone loss. Type I disorder directly results from lack of endogenous estrogen and is a rapid bone loss of variable intensity after the menopause that occurs at a rate of a few percent per year. Its duration is variable, 5-8 years and involves mainly cancellous bone. Type II osteoporosis is age-related linear decline in bone mass that involves both cancellous and cortical bone. The age at which this loss starts is generally recognized around age 50, occurring in both women and men with a rate of about 0.5-1% per year. This type of osteoporosis reflects the composite influences of long-term remodeling inefficiency, intestinal mineral absorption, renal mineral handling, adequacy of dietary calcium and vitamin D and parathyroid hormone (PTH) secretion.

At cellular level a discrepancy between bone resorption and formation occurs, with a negative balance in each BMU: less bone is formed than has been destroyed (**Figure 8**). The cause of this imbalance can either be an increase in the amount of bone resorbed or a decrease in the amount formed or both.[28]
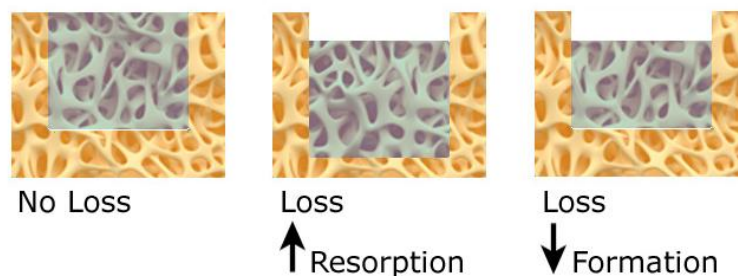
Figure 8: Mechanism of bone loss at the microscopic level of the BMU.

It is important to notice that the overall chemical composition of the bone, and therefore the quality of the bone tissue, is not altered, in contrast to osteomalacia, another bone disease typified by a defect of mineralization. It is known that the properties at cellular, matrix, microarchitectural and macroarchitectural levels may all impact bone mechanical properties.[29] Focusing on trabecular architecture, we can describe it by the shape of the basic structural elements and their orientation. The trabecular structure is generally characterized by the number of trabeculae in a given volume, the average distance between them, their average thickness and the degree to which trabeculae are connected to each other. All of these are the strongest determinants for the biomechanical properties of trabecular bone.[30, 31, 32] So the presence of resorption cavities, in the

absence of bone formation, act as a site of local weakness where cracks may initiate and trabecular bone properties decline.[33, 34]

The clinical manifestations of osteoporosis are fractures, that occur often spontaneously or after minimal trauma or related consequences. The most common osteoporotic fractures are of the wrist, shoulder, spine and hip but their location differs somewhat with age. These fractures may also be asymptomatic. Age-related osteoporotic fractures occur mostly in the vertebrae, leading to a decrease in height and to forward bending of the spine and hip, both in women and in men carrying significant morbidity and mortality. The diagnosis of osteoporosis is made almost exclusively by Dual-energy X-ray Absorptiometry (DXA) which measures only areal bone density (g/cm^2), the output is generally given as BMD. Osteoporosis diagnosis is then calculated using the T-scores method previously reported. Quantitative Computed Tomography (QCT) or ultrasound are also used widely to measure sites such as the finger or heel, fractures detected by X-rays indicate severe osteoporosis.

1.2.2 *Non Skeletal and Lifestyle Factors in Osteoporosis*

There are various nonskeletal and lifestyle risk factors for osteoporosis that impact on both bone mineral density and fracture risk. While nonskeletal factors, like ethnicity, gender, height and weight are unchangeable general physical-genetic characteristics, lifestyle factors like obesity, alcohol consumption or smoking are changeable behaviours.

Bone loss is universal all over the world but there is significant variation in the timing and amount of attainment of peak bone mass as well as variation in the amount and rate of bone loss and its effect on fracture risk due to genetic and environmental factors. There are significant ethnic differences: osteoporosis differs among the ethnic groups as would be expected by the observed differences in the bone mineral density.[35,36] Whites and Asians having the highest incidence of osteoporosis, Africans the lowest, but statistically significant geographic differences in bone markers among U.S. white women [37] emphasizes that ethnic differences should be interpreted with caution.

The incidence of osteoporosis is much higher in women than in men as is the greater risk of fractures. In general, the rate of hip and spine osteoporotic fractures in women is two or three times greater than the risk of these fractures in men.[38] These gender-related differences is only partially explained by the greater bone density and larger bone geometry-size in men than in women.[36,39] Regarding the anthropometric variables, although no ideal weight-to-height ratio has been set for reducing osteoporosis and fracture risk, it is known that a low body weight increases the risk of fracture in older adults up to 2.4-fold [40,41] while women who sustain hip fractures have been reported to be usually taller than those who do not.[42] While all these factors are birth-related, there are other lifestyle elements that could onset to osteoporosis or osteoporotic fractures. There has been a dramatic increase in obesity in recent years resulting from reduced levels of physical activity and an increase in caloric intake [43] and this is

considered as a bad medical condition that has a negative effect on health.[44] This is "not true" regarding osteoporosis because obese people have significantly higher BMD at the spine, hip, and radius than normal weight.[45] This could indicate that obesity helps attenuate bone loss leading to higher peak of BMD. Obviously obesity leads to an increase in various co-morbid conditions, including type 2 diabetes and hypertension.

Smoking is widely considered a risk factor for future fracture and there are numerous relationship between smoking and lower bone mineraldensity. Smoking has been related to lower serum 25(OH)D levels in women [46] and men, [47] finding also adversely affects on other hormones involved in bone regulation, such as parathyroid hormone.[48] It is reported a higher calcium absorption in nonsmokers compared to smokers.[49]

Heavy and chronic alcohol consumption is known to contribute to low bone mass, decrease bone formation and increase the incidence of fractures.[50] Alcohol-induced bone loss appears to relate to a decrease in the rate of bone remodeling, leading to a decrease in active bone formation and active bone resorption.[51, 52, 53] The impact of alcohol on bone formation is reversibile and the osteoblast will quickly recover.[54] While alcohol abuse makes toxic effects, moderate alcohol consumption may actually have a modest favorable effect on bone density, particularly in postmenopausal women, [55, 56] where alcohol may slow down the accelerated bone remodeling rate that is a characteristic of postmenopausal osteoporosis.

1.2.3 *Health Economic of Osteoporosis*

Osteoporosis represents one of the major-non trasmissible disease which will become even more common with the increase in life expectancy. In Europe, India and North America alone there are an estimated 125 million people with osteoporosis.[57] Only in United States, among 43.4 million older adults that have low bone mass there are 10.2 million people with osteoporosis.[58] As previously reported, the incidence is much higher in women than in men and it is estimated that close to one in two women and one in five men over the age of fifty worldwide will sustain an osteoporotic fracture. Hip and spine fractures are the two most serious fracture types, associated with substantial pain and suffering, disability, and even death.[59] It is worth nothing that after a hip fracture, 40% of individuals cannot walk independently and 80% cannot perform basic activities. In the EU27 in 2010 there were 43000 deaths directly attributable to fragility fractures.[60] This disease is therefore, because of its medical and socioeconomic impact on our society, a major public health issue both in women and in men. This will become even more so in the future because of the rapid increase of the elderly population.[61,62]
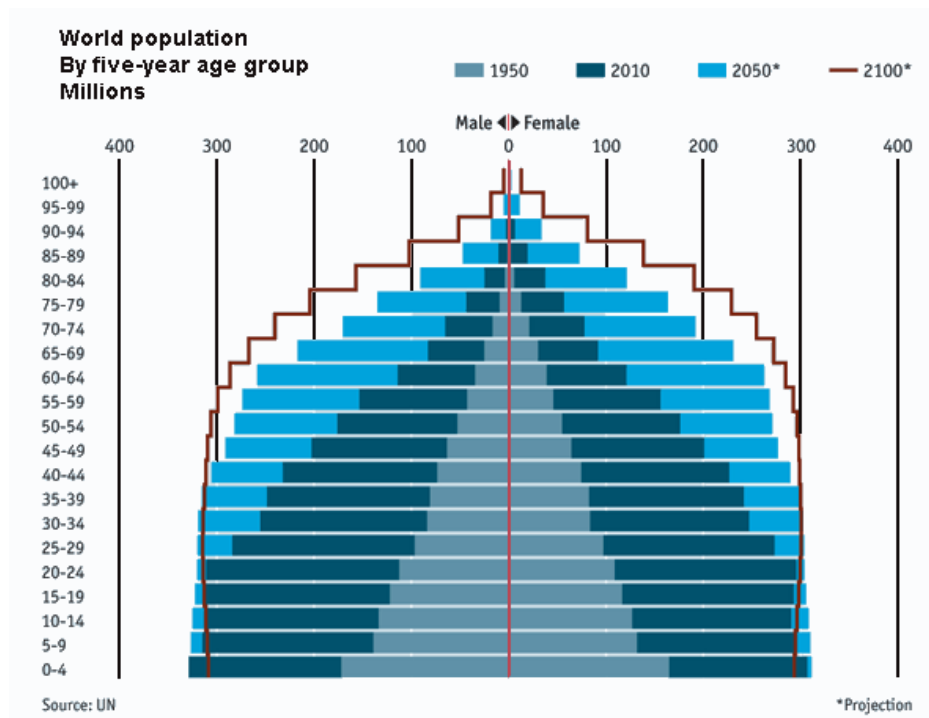
Figure 9:world's population pyramid.
Rapid increase of the elderly population is expected in the next few decades.

Available data on the economic burden of osteoporosis shows that currently, the cost of osteoporosis is 37 billion € per year in the EU27 [59] where 3.5 million new fragility fractures were sustained on the 22 million women and 5.5 million men estimated to have osteoporosis.

The only study that attempted to include pharmacological treatment costs for osteoporosis estimates in 36.2 billion $ the economic burden in USA in 2005.[63] The costs are expected to dramatically rise by 25 % in 2025.

Regarding Italy, in 2003 the Italian Senate included the prevention of the osteoporosis among the primary preventing objectives of the national health system [64] inserting also osteoporosis in the list of chronic and disabling diseases. Despite this, extimated 465000 new fragility fractures occourred in 2010 with an economic impact on national health system of approximately 7 billion €.[59]

1.2.4 *Prevention*

Between birth and maturity, the human skeleton increases substantially in size and strength. Although individual peak bone mass is under genetic control, lifestyle factors such as diet and physical activity also influence bone development in youth and the rate of bone loss later in life. The prevention of osteoporosis begins with optimal bone growth and development in youth: bone mass acquired during youth is an important determinant of the risk of osteoporotic fracture during later life. The higher the peak bone mass, the lower the risk of osteoporosis.[65] Exercise plays an important role in building and

maintaining bone strength and also helps to reduce falls by improving balance and aids rehabilitation from fractures. Therefore, physical activity during childhood and adolescence should be seen as a great opportunity in the prevention of osteoporosis and related fractures. The efficacy is obviously also connected to its continuation throughout life.[66] The direct training effect in old age may be limited, but exercise can be an effective method to prevent falls.

Also nutrition and bone health are closely related. A healthy diet can help prevent and manage osteoporosis and related musculoskeletal disorders by assisting in the production and maintenance of bone.[67] Nutrition affects bone health in two distinct ways. Bone tissue deposition, maintenance, and repair are the result of cellular processes and the cells of bone responsible for these functions are as dependent on nutrition as are the cells of any other tissue. Two of the most important nutrients are calcium and vitamin D. Calcium is the major building-block of bone tissue. In 1979 Matkovic and his colleagues [68] showed that high calcium intake was associated with strikingly reduced hip fracture risk. The calcium that we need to consume changes at different stages in our lives because the body ability to absorb calcium declines, which is one of the reasons why seniors also require higher amounts.[69] Vitamin D is key for its role in assisting calcium absorption from food in the intestine and for ensuring the correct renewal and mineralization of bone tissue. There are a number of nutrients and vitamins, besides calcium and vitamin D that help to prevent osteoporosis and contribute to bone health, including protein, fruits, vegetable and other vitamins and minerals. Fruits and vegetables contain an array of vitamins, minerals and antioxidants some or all of which can have a beneficial effect on bone. Studies have shown higher fruit and vegetable consumption is associated with beneficial effects on bone density in elderly men and women.[70] Adequate dietary protein is essential for optimal bone mass gain during childhood and adolescence as well as for preserving bone mass with ageing. Vitamins B6, B12 and folic acid play a role in changing homocysteine that may be linked to lower bone density into other amino acids for use by the body, so it is possible that they might play a protective role in osteoporosis. Research is ongoing as to whether supplementation with these B vitamins might reduce fracture risk.[71] Magnesium and Zinc play an important role in mineralization of bone as well as vitamin K. Some evidence suggests that low vitamin K levels lead to low bone density and increased risk of fracture in the elderly.[72] Phosphorus also is indirectly involved in the bone health cause, together with calcium, is involved in the balance between absorbed intake and excretory loss of these two minerals.

1.2.5 *Treatment*

A number of effective medications are approved for the treatment of osteoporosis. These medications must be used in conjunction with recommended lifestyle changes and tailored to a person's specific needs.[28] In general, treatments can be divided into two

categories, anti-resorptive and anabolic agents. Some treatments are available that inhibit bone destruction and therefore prevent bone loss.

Today only very few compounds are able to increase bone formation, which include only parathyroid hormone (PTH1-84) and teriparatide (PTH1-34) that need daily subcutaneous injection administration. As they strongly increase BMD in the trabecular compartment [73], the greatest increase in BMD is observed at the spine and hip.

Anti-resorptive agents, which include estrogen, selective estrogen receptor modulators, denosumab and bisphosphonates, reduce bone resorption and preserve bone mineral density (BMD). Estrogen replacement treatment after the menopause is very effective in inhibiting bone loss and even leads to some increase in bone density. The effect on bone stops after discontinuation of the treatment, with resorption increasing again rapidly. Thus, long-term therapy is necessary. Many women, however, refuse this therapy for the fear of a possible increase in the frequency of breast cancer and endometrial carcinoma.[74] A therapeutic area of great promise is selective estrogen receptor modulators (SERMs). They have the ability to bind to estrogen receptors throughout the body and act as estrogen agonists or antagonists depending upon the target organ. Raloxifene and bazedoxifene for example, have been shown to prevent bone loss and reduce the incidence of vertebral and hip fractures.[75, 76]

Also calcium can decrease bone turnover and diminish bone loss: indeed a supplementation of at least 500 mg daily is a standard procedure in the therapy of osteoporosis. Strontium ranelate is another agent that improves bone strength mainly through effects on bone material properties. It slightly inhibits bone resorption but the increasing in BMD is progressively dose-dependent.[77] Denosumab is the most promising compound in the treatment of osteoporosis: it is a fully human monoclonal antibody that binds to RANKL with high affinity and specificity. It blocks the interaction of RANKL with RANK and inhibits bone resorption. Administered subcutaneously it inhibits bone resorption strongly and rapidly.[78]

Bisphosphonates (BP) are the most potent and most used inhibitors of bone resorption that inhibit the activity of osteoclasts. They are available in oral and intravenous formulations, with weekly, monthly and annual dosing schedules, depending on the specific compound.

1.3 BISPHOSPHONATES

1.3.1 *Structure*

Bisphosphonates (BPs) are currently the major class of drugs used for the treatment of osteoporosis and other diseases characterized by increased bone resorption. Bisphosphonates were initially developed as a spinoff from the chemistry of polyphosphates, where their main applications were as antiscaling additives in washing

powders or water and oil brines to prevent deposition of calcium carbonate. It was the scientific observation of Prof. Fleisch and colleagues that led to the knowledge that the first bisphosphonate studied (etidronate) inhibited bone resorption.[79]

Bisphosphonates, formerly called diphosphonates, are biological analogues of naturally occurring pyrophosphates (**Figure 10**). Pyrophosphates (P-O-P) are byproducts of ATP metabolism with no biological activity because of the presence of pyrophosphatases. The substitution of a carbon atom in place of the oxygen atom results in a P-C-P structure called geminal bisphosphonates.[80] The geminal bisphosphonates, as usual in the current literature, are simply called bisphosphonates (BPs). The P-C-P group is resistant to pyrophosphatases as well as to chemical hydrolysis. As a result, BPs are not converted to metabolites in the body and are excreted in the urine unchanged [81] additionally having no effects on the pharmacokinetics of other drugs.
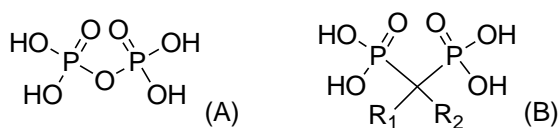
Figure 10: Pyropshosphoric acid (A) and a generic structure of a bisphosphonic acid (B).

These compounds have a strong affinity for metal ions as well as a very high affinity for the bone mineral: bone tissue is nearly the exclusive tissue that takes up bisphosphonates. This selective tissue uptake is due to two major and distinctly different reasons: (i) bisphosphonates bind to the denuded bone resorptive cavity that has exposed hydroxyapatite crystals as a consequence of osteoclastic removal of bone tissue during remodeling and (ii) only phagocytic cells (osteoclasts and macrophages) can take up bisphosphonates.[82, 83]

The P-C-P structure allows a great number of possible variations, either by changing the two lateral chains on the carbon atom or by esterifying the phosphate groups. Nine BPs are commercially available and part of these are sold in their bisphosphonic acid salt form [84]; modifications to one of the phosphonate groups can dramatically reduce the affinity of the BP for bone mineral [85] as well as the biochemical potency.[86]

The R1 and R2 side-chains attached to the carbon atom are responsible for the large range of activity observed among the BPs. R1 substituents such as hydroxyl or amino enhance chemisorption to mineral, [87] while varying the R2 substituents results in differences in antiresorptive potency of several orders of magnitude.[85]

BPs containing nitrogen atoms or nitrogen eterocyclic substituents are very potent, such as ibandronate, risedronate or zoledronate. Ibandronate with its highly substituted nitrogen moiety is more potent than alendronate and pamidronate that have a basic primary nitrogen atom in an alkyl chain. However it is less potent than risedronate and zoledronate that are two of the most potent antiresorptive BPs due to the nitrogen atom within the heterocyclic ring (**Figure 11**). The intensity of the effect is, however, also dependent on the aliphatic side chain and also a three dimensional structural

requirement appears to be involved. The different antiresorptive potency observed with the different R2 groups is linked to the ability to affect biochemical activity and is thought to be linked also to the ability to bind to HAP (**Chapt. 1.3.2**). It is worth to notice that Zhang and collaborators reported that novel lipophilic pyridinium bisphosphonates (**Figure 11**) are approximately 250 times more effective than any other bisphosphonate drugs.[88]
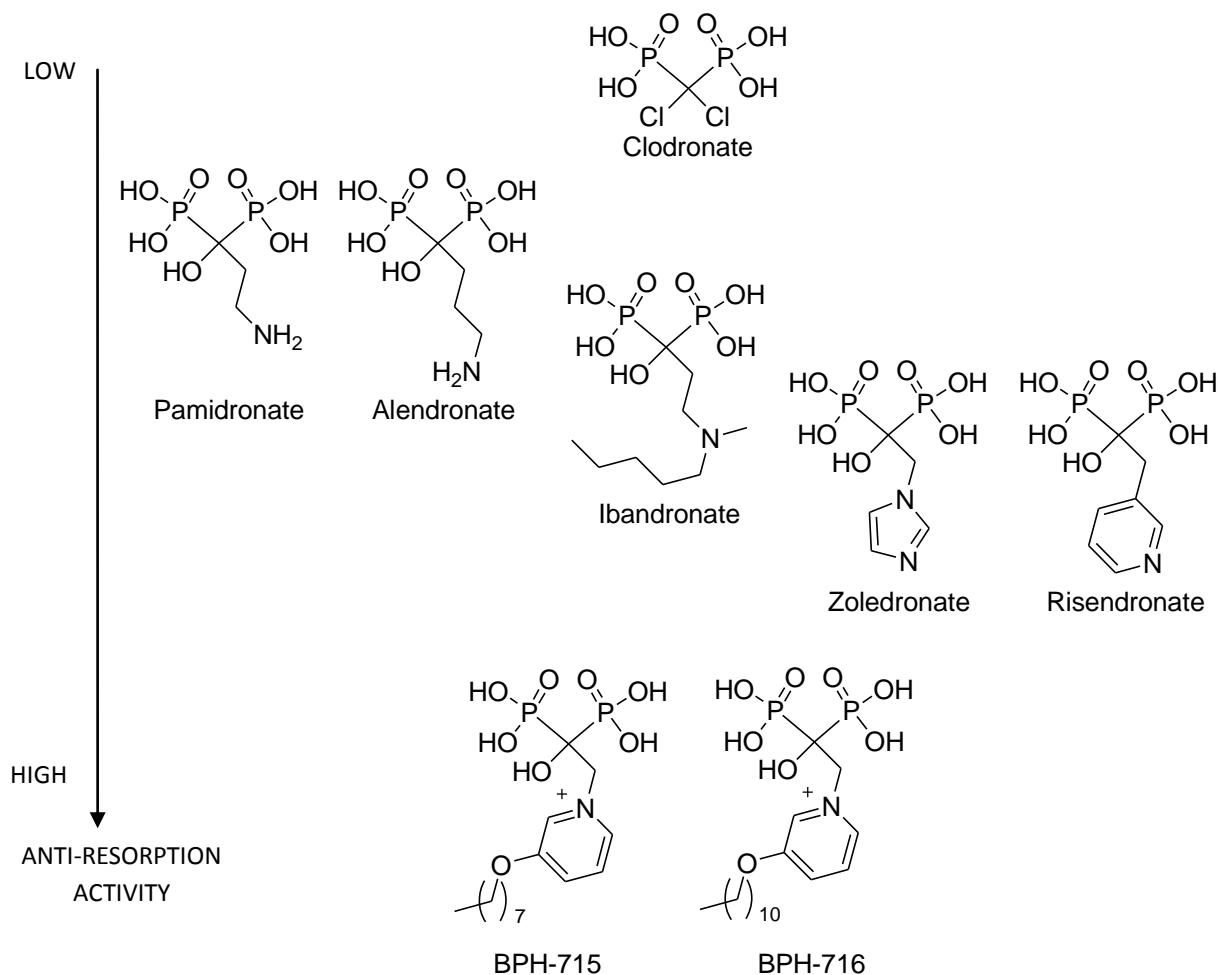

Figure 11: structure/activity relationship of BPs that target FPPS and GGPPS.

Bisphosphonates are poorly absorbed as a class.[89] This poor absorption is related to the heavy negative charge of the bisphosphonate moiety, which makes transport across lipophilic cell membranes difficult: the total dose absorbed lies between less than 1 and 10%. Absorption is proportionally greater when large doses are given but is also dependent on the BP used and differences in retention match the observed order for binding to HAP.[90]

1.3.2 *Mechanism of Action*

Bisphosphonates reduce bone turnover by two major, distinctly different mechanisms of action: a physicochemical effect and a cellular effect.

The physicochemical effects of the bisphosphonates are very similar to those of pyrophosphate. They inhibit the formation, delay the aggregation and also slow down the dissolution of calcium phosphate crystals. There is no doubt, however, that the action *in vivo* is mediated mostly, if not completely, through mechanisms other than the physicochemical inhibition of crystal dissolution.

The preferential uptake of BPs by adsorption to mineral surfaces in bone brings them into close contact with osteoclasts. During bone resorption, the acidic pH in the resorption lacuna should markedly increase the dissociation of a BP from HAP. This is followed by the uptake of the BP into the osteoclasts most likely by fluid-phase endocytosis.[91] With regard to the cellular effect, there are two distinctly different fundamental molecular structures of BPs drugs: the non nitrogen containing bisphosphonates (i.e. etidronate and chlodronate) and the nitrogen containing bisphosphonates (N-BPs, i.e. alendronate, risedronate, ibandronate, pamidronate and zoledronate). Non nitrogen-BPs were found to disrupt the ATP metabolic pathway in osteoclasts. After incorporation into the corresponding non-hydrolyzable analogs of adenosine triphosphate, they induce osteoclast apoptosis by the intracellular accumulation of such metabolites.[92]
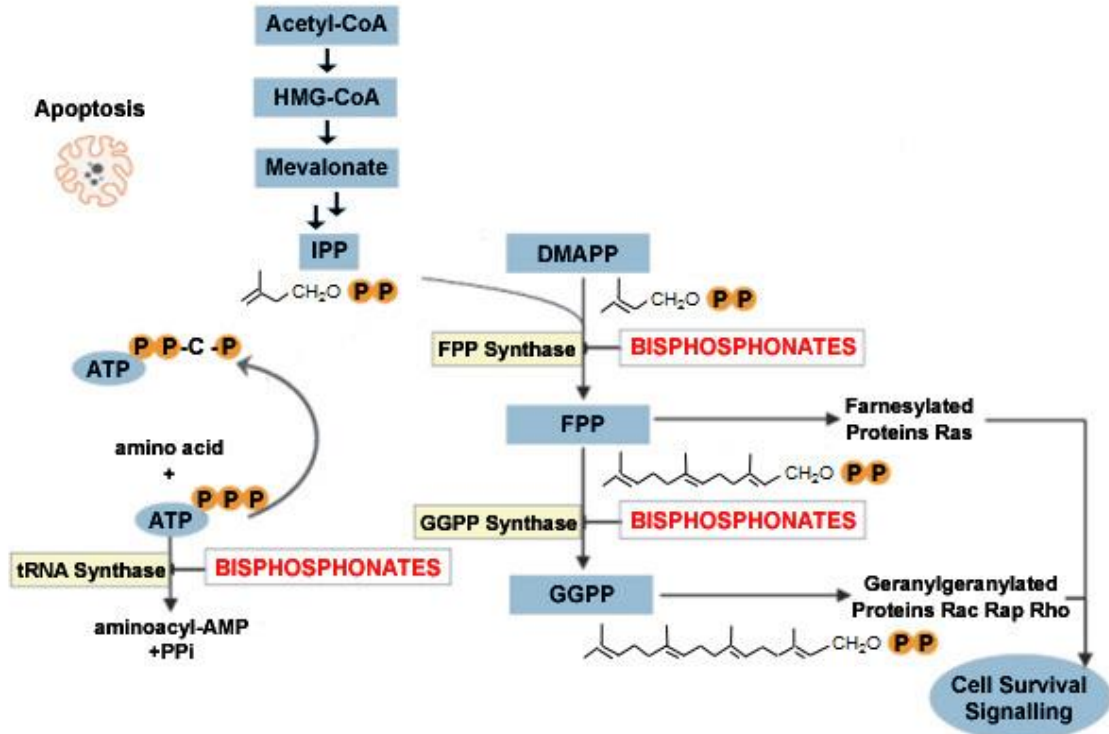
Figure 12: Mechanism of inhibition of FPPS and GGPPS due to Bisphosphonates.

The nitrogen containing bisphosphonates instead, have their biochemical site of action on the mevalonate pathway, known for its role in the cellular biosynthesis of cholesterol and other sterols (**Figure 12**). Several enzymes of this pathway utilize isoprenoid diphosphates as a substrate and the N-BPs could therefore act as substrate analogs of one or more of this isoprenoid. The major target is now known to be Farnesyl Diphosphate Synthase (FPPS), which is inhibited by all of the clinically used N-BPs.[93, 94] This inhibitory effect on FPPS leads to a reduction in the product concentrations of FPP necessary for the production of GeranylGeranyl Diphosphate (GGPP) via cascade pathway. GeranylGeranyl Diphosphate Synthase is also inhibited by N-BPs. Both FPP and GGPP are isoprenoid metabolites required for prenylation of specific intracellular proteins necessary for normal osteoclastic cell function.[95] Nano molar concentrations of N-BPs have shown inhibition only on the FPPS while GGPPS enzyme is inhibited only in the micromolar range. The end result is the impair osteoclast function and the reduction in osteoclast resorption. Eventually, N-BPs may cause apoptosis, but this does not appear to be a mandatory requirement for inhibition by BPs. Even more recent work has identified that N-BPs induces inhibition of another enzyme in the mevalonic acid pathway: adeninenucleotide translocase.[96] Hence, N-BPs may affect up to three intracellular enzymes in the mevalonic acid pathway, leading to disruption of osteoclast cellular function.

The analysis of structure-activity relationships show that, for maximal potency, spatial 3-D requirements are needed: the nitrogen atom in the R2 side chain must be in a critical orientation with respect to the P-C-P group. X-ray crystallography studies of human FPPS, have demonstrated that most BPs bind similarly in an aspartate-rich region of the enzyme. Risedronate and zoledronate appear to display high interactions at these sites, which lead to the greater inhibitory potencies compared with other bisphosphonates such as alendronate, that have more limited interactions at these sites.[97]

The notion of half-life of these drugs can be misleading. The half-life of these drugs are not equivalent to the half-life of their effects. In the body it depends on the rate of bone turnover itself. As the BPs slow down the resorption of the bone their half-life may be longer than the normal half-life of the skeleton, for some bisphosphonates can reach over 10 years. When administered in clinical doses, there seems to be no saturation in BPs total skeletal uptake. In contrast the antiresorbing effect reaches a maximum. Much of the BP is likely to be rapidly "buried" within the mineral phase and therefore become pharmacologically inactive. What is absorbed usually has a powerfull effect on bone turnover, the remainder is excreted in the urine predominantly within the first few hours after administration. It was observed in urinary excretion, the presence of unchanged alendronate also after months from discontinuation of administration. This introduce the concept of the "recycling" of bisphosphonates: it is higly possible that re-released bisphosphonate that re-enters in the systemic circulation during the bone remodeling process could still be metabolically active and reattach to newly formed bone resorptive cavities and maintain clinical activity.[98] Bisphosphonate "recycling" could explain

maintenance of BMD conservation seen in long-term bisphosphonate studies after several years of administration.[99]

1.3.3 *Side Effects*

Bisphosphonates are used orally or intravenously but the skeletal uptake varies with sex and age of the patient and with the dose and nature of the administered compound. The location of the absorption in the gastrointestinal tract can occur in the stomach as well as in the small intestine by passive diffusion. Absorption is diminished when the drug is given with meals, probably because of the conversion of the BP into a non-absorbable form. The rapid uptake by bone means that the soft tissues are exposed to bisphosphonates for only short periods, explaining why in practice only bone is affected *in vivo*. The areas of deposition are generally thought to be mostly those of bone formation.[100] The most common safety issues revolve around the effects of bisphosphonates on the upper gastrointestinal mucosa. There is no doubt that the orally administered bisphosphonates may induce several gastrointestinal side effects including esophageal irritation, dysphagia and heartburn.[101] These problems can occur anytime in the administration of the bisphosphonate and represent a potential barrier to tolerance and adherence to the treatment. The risk of gastrointestinal events can be decreased by ensuring proper drug administration (post-dosing postural positioning and appropriate quantity of water) so patient education is crucial.[102]

Intravenous administration of BPs has been associated with transient moderate inflammatory symptoms, such as fever, myalgia, arthralgias and headache, collectively known as an acute phase response. These symptoms occur in the first 72 hours after the initiation of bisphosphonate therapy in 12-42% of patients only after the first infusion, resolve within two to four days.[103] This is an important consideration for patient adherence because patients who experience this acute phase reaction may be reluctant to continue treatment. Rate of infusion of intravenous BPs is crucial: the formation of aggregates in the blood is thought to occur following rapid intravenous injections of large quantities of BPs. This could explain the rare cases of renal failure that can ensue.[104]

Osteonecrosis of the jaw (ONJ) has emerged as a rare complication of BP use and can be associated with substantial morbidity. Most cases have been reported in patients with cancer who receive high doses of intravenous bisphosphonates for the prevention of skeletal complications of cancer. The risk of ONJ seems to increase when treatment is longer than three years.[105] By inhibiting osteoclastic bone resorption BPs reduce also calcium efflux from bone. This can cause hypocalcemia, a small decrease in serum calcium compared to normal baseline serum calcium. While 85% of patients did not need supplemental calcium, [106] patients with vitamin D deficiency are more likely to experience more severe and prolonged hypocalcemia.

Noteworthy, that the treatment rates are dropped significantly since 2010.[60] There may be several reasons for this, mainly including a fear of these adverse effects.
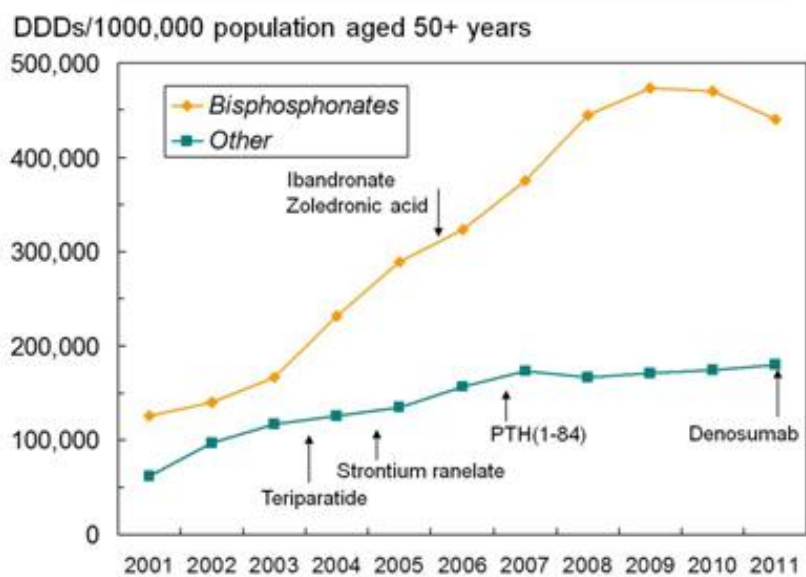
Figure 13: Osteoporosis drugs consumption in the EU. [60]

1.3.4 *Bisphosphonates development*

As BPs are universally recommended as first line therapy for patients with osteoporosis, studies on BP molecules are an area of active research.

In order to improve the bioavailability of BP, a lot of strategis have been attempted such as the use of absorption promoters surfactants, the formulation of polymeric nanoparticles, [107] microemulsions [108] and nano-crystalline TiO_2 particles and colloidal to encapsulate or adsorb the drug.[109] Despite much synthetic research, the molecular structures of commercially available BPs are very simple and in spite of the importance of enantiopure products in pharmacology, only applications of commercial racemic BP are known. Furthermore, these molecules do not possess the complexity and structural diversity necessary to address new fields of application in which BPs promise interesting results such as the development of anti-arthritic drugs, drugs for the diagnosis and treatment of cancer and delivery of proteins.[110] The existing limit in the development of new pharmacologically active molecules, having the properties mentioned above, lies in the lack of suitable chemical methods for the synthesis of a broad spectrum of molecules or molecules able to modulate the three-dimensional atom disposition around the bisphosphonate group so as to increase efficiency and selectivity. Despite the different human body response to molecules with different stereoisomerism is proven, the lack of enantioselective syntheses prevent the development of chiral BPs and only few scientific contributions are known in this field, [111,112,113] none of which shows the biological tests on the corresponding final acid form BP. In the literature only one example (**Figure 14**) of enantio-enriched BP was tested observing a 24 time difference of activity between the enantiomers.[114]
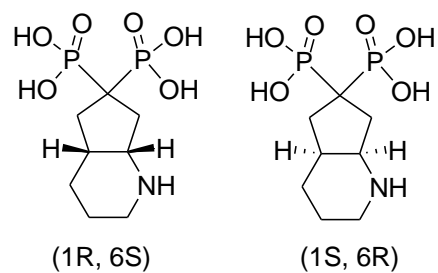
Figure 14: only example of tested enantio-enriched BP. 1R,6S is 24 times more potent than 1S,6R.

An useful synthetic approach that allows the formation of a broad range of BP is based on vinylidenbisphosphonate precursors (VBP). The application of a series of enantioselective catalytic reactions coupled with the use of a wide variety of nucleophilic reagents on these precursors, provides the possibility of obtain a wide range of BP with structural complexity, as well as the opportunity to verify the different behaviors of the synthesized enantiomers.

2. AIM OF THE THESIS

Even though BPs have been known for decades, the molecular structures of commercially available BP are very simple and in spite of the importance of enantiopure products in pharmacology, only commercial applications of achiral BPs are known. Furthermore, these molecules do not possess the complexity and the structural diversity necessary to address new challenges in the treatment of osteoporosis. More suitable chemical methods for the synthesis of a broad spectrum of molecules are therefore an important goal to tackle in this field as well as the syntheses of BP molecules with specific three-dimensional structure in order to increase the drug efficiency and selectivity.

A useful synthetic approach that allows the formation of a broad range of BPs is based on vinylidenbisphosphonate (VBP) precursors. Exploration of new synthetic pathways starting from the synthesis of new substituted prochiral BP precursors was one of the main targets of this work. The application of a series of enantioselective catalytic reactions coupled with the use of a wide variety of reagents on these precursors, could provide the possibility of obtain a wide range of BP with structural complexity, as well as the opportunity to verify the different behaviors of the synthesized enantiomers.

Numerous VBP precursors were synthesized in order to obtain a broad portfolio of molecules characterized by different steric and electronic properties as well as with different steric hindrance in the phosphonate moiety.

Prepared VBP precursors were employed as Michael-acceptor in several addition reactions with nucleophilic reagents like boronic acids, thiols or indoles. Special attention was given to synthetic methods that can provide N-containing BPs, focusing also on the asymmetric version of the reactions, in order to obtain enantiomerically enriched N-containing BPs with potentially high activity in osteoclasts inhibition.

Selected BP molecules were subjected to deprotection of the ester moiety, obtaining the corresponding bisphosphonic acids that were useful in the synthesis and test of biomedical cement or in modified ceramic materials.

Particular interest has been placed on the synthesis of fluorescent BP via Cu(I) catalyzed azido-alkyne cycloaddition with a new diketopyrrolopyrrole-based fluorophore. The derived fluorescent BP probe was found useful in the monitoring of anti-resorption activity tests.

3. RESULTS and DISCUSSION

In this section the results obtained during the thesis work are presented. I will first report the results obtained in the syntheses of the key building blocks followed by the new BP precursors and finally the results obtained in the syntheses of new BP molecules also containing nitrogen atoms. I wish to underline that presentation of the results is not strictly chronological and focusses on the most promising synthetic methodologies.

3.1 BP PRECURSORS

In order to obtain new classes of bisphosphonates the synthesis of methylene bisphosphonate ethyl ester was pivotal. This building-block allows to synthesize a wide range of precursors characterized by the presence of vinyl units namely an unsubstituted double bond (VBP) and a wide range of mono and di-substituted precursors (**Figure 15**). Moreover precursors with reduced steric hindrance were synthesized by changing the protecting ethyl ester groups with methyl ester groups. Some of the synthesized precursors have been used by Prof. Canton's research group at Università Ca'Foscari di Venezia for some affinity test with zirconia-based ceramics.
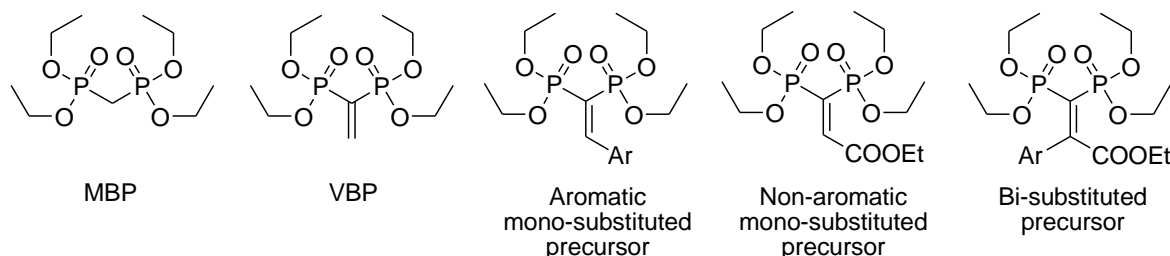
Figure 15: different types of unsaturated BP precursors.

3.1.1 *Methylen Bisphosphonate Tetraethyl Ester (MBP)*

The main BP building block that can produce a wide range of other BP precursors is the methylen bisphosphonate tetraethyl ester (MBP). This molecule is the simplest BP precursor, where R1 and R2 chains are both hydrogen atoms. It looks very similar to pyrophosphoric acid, where oxygen atom is replaced by a carbon atom and the acidic moieties are protected with four identical alkyl groups. In the literature some synthesis of MBP have been reported using carbon disulfide [115] or diazomethane, [116] reagents requiring special precautions and use under severe restrictions: in fact they are toxic, highly flammable and suspected carcinogens.

Another problem limiting the experimentation using tetraalkyl methylenebisphosphonate as starting materials in syntheses is its high commercial price. We used a one pot

procedure described by Hormi and co-workers [117] for the preparation of MBP starting from cheap materials. The synthesis of this precursor takes place with two subsequent nucleophilic attack by deprotonated phosphites on a dichloromethane molecule. The addition order of the reagents is crucial. The deprotonation of the phosphites occurs through the use of a very strong Brønsted base (sodium ethylate) created *in situ* by addition of metallic sodium to ethanol used as the solvent. Then diethyl phosphite is added that is deprotonated and is thus able to nucleophilically attack dichloromethane that is added at the end of the reaction. The reaction is allowed to proceed for two weeks. Recently Mezianeand collaborators reported a faster procedure using microwave technologies to synthesyze the same product.[118] It is noteworthy that the major product is MBP although a large excess of methylene chloride is used. The reason is because the intermediate diethyl chloromethylphosphonate is more reactive than methylene chloride in the subsequent nucleophilic substitution. This methodology described and shown in **Scheme 1** could be performed in 10 g scale and allowed to obtain the product in 54% yield.
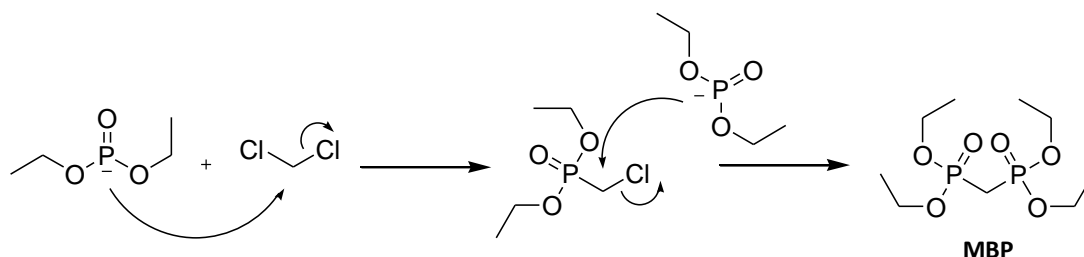
Scheme 1: Synthesis of MBP

3.1.2 *Vinyliden Bisphosphonate Tetraethyl Ester (VBP)*

Tetraethyl vinylidenebisphosphonate (VBP) is a versatile synthetic intermediate that allows access to a variety of highly functionalized compounds bearing the bisphosphonic moiety. As an electron-deficient alkene, this compound is able to undergo conjugate addition with a variety of reagents including strong nucleophiles, such as organometallic reagents and enolates, as well as mild nucleophiles, such as amines, thiols and alcohols. VBP acts as a dipolarophile or dienophile in 1,3-dipolar cycloadditions or Diels–Alder reactions, giving rise to five- or six-membered rings containing the bisphosphonic unit.[119] The synthesis of this precursor occurs by reaction between MBP and formaldehyde [120] in two steps: the first one proceeds at 60°C with depolymerization of paraformaldehyde and deprotonation of the α carbon atom of MBP by diethylamine followed by attack to formaldehyde to give 2-methoxyethan-1,1 bisphosphonate intermediate (**Scheme 2**). The second step carried out at 115°C is characterized by the synthesis of the final VBP product by elimination of a methanol molecule by acid catalysis. The reaction was performed in 2.5 g scale and the product was obtained with a yield higher than 90%.
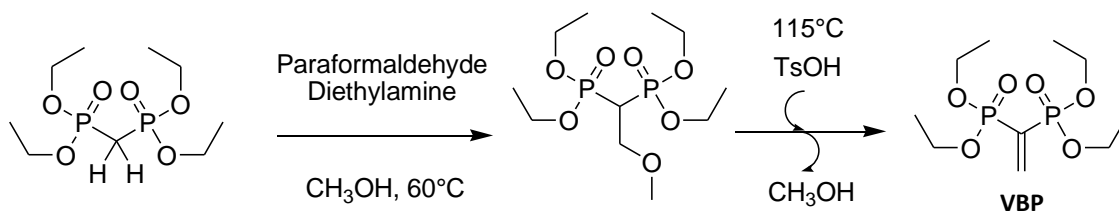
Scheme 2: Synthesis of VBP

The obtained VBP was used, as described below, as a precursor for the synthesis of new BP through Michael addition reactions or 1-3 dipolar cycloadditions.

3.1.3 *Aromatic Mono-Substituted Unsaturated BP Precursors*

The synthesis of mono-substituted prochiral VBPs is known in the literature through two synthetic approaches described in **Scheme 3**. The first (**Scheme 3A**), comprises the reaction between MBP and aldehydes catalyzed by a strong Lewis acid such as $TiCl_4$, [121] which involves some practical issues such as the unavoidable use of inert atmosphere conditions. The second more recent and apparently more accessible method (**Scheme 3B**), comprises the reaction between a phosphonate arylalkyne on which, the addition of a electrophilic phosphate occurs catalyzed by a tertiary alkyl phosphine.[122]
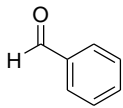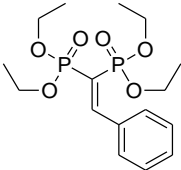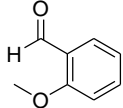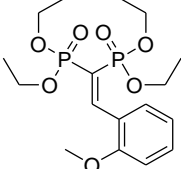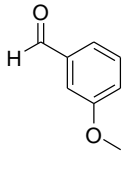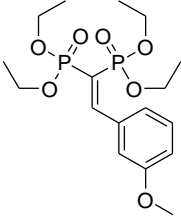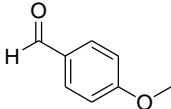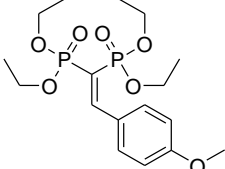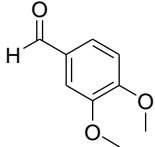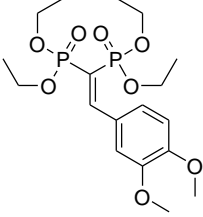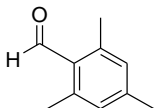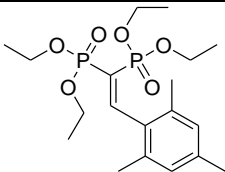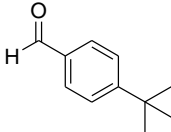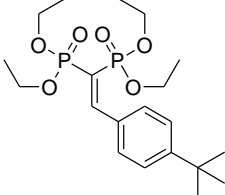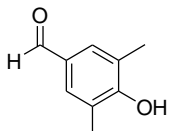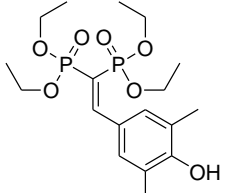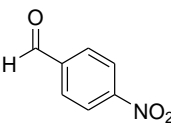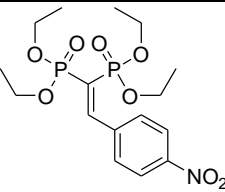
This method has been studied in previous works in our lab. Despite using inexpensive, readily available or easy to synthesize reagents, this methodology showed limitations in terms of yields of the desired products. The formation of phosphine oxide from the alkyl phosphine employed as a catalyst was observed, thus leading to low product yields. Additional failures in purification attempts of the obtained precursors led to abandon this synthetic route, looking for new versatile routes. Attempts to synthesize VBP prochiral precursors by metathesis reactions or Heck reactions (**Scheme 3 C, D**) on VBP were made in our research group [123] leading however to unsatisfying results that pushed to revert to the widely used [124, 125, 126] conventional method involving the condensation of MBP with aldehydes catalyzed by $TiCl_4$.[121]
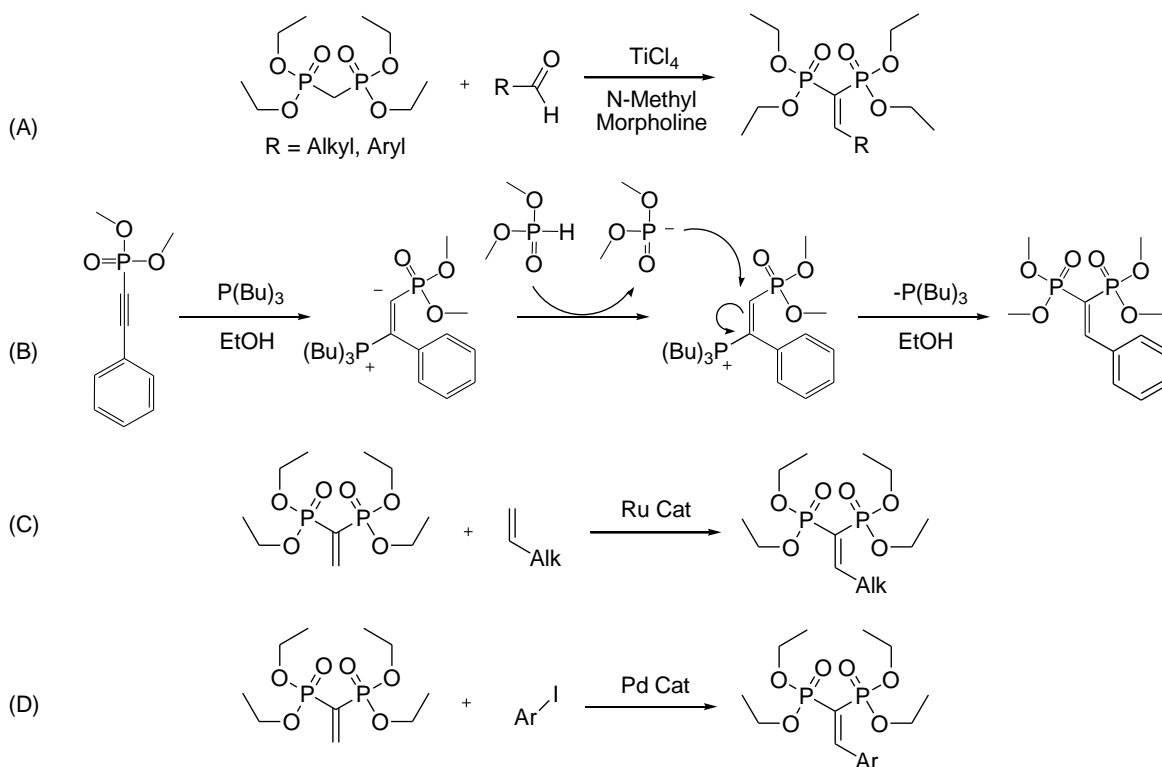
Scheme 3: Literature reported syntheses of BP precursors (A)
and attempted syntheses in the past by this research group (B,C,D).

This reaction is based on a Knoevenagel-type condensation and involves the use of TiCl$_4$ as catalyst which requires special precautions due to its strong Lewis acid character and severe limitations in use. The metal catalyst activates MBP by coordinating the phosphonic groups and increasing the acidity of the α protons of MBP. Deprotonation by N-methyl morpholine base is then easier but an over stoichiometric amount of catalyst of Ti(IV) is anyway necessary. It is quite likely that the Ti(IV) catalyst plays a fundamental role also in the activation of the carbonyl group of the aldehyde. The resulting nucleophilic compound reacts with the activated aldehyde, followed by subsequent dehydration and formation of the double bond. The use of Ti(IV) is crucial because coordination to the phosphonic groups avoids elimination of one phosphonate moiety via a Wittig-type reaction.[121]

Notably with this synthetic route it is possible to form only aromatic monosubstituted VBP. This limits the range of BP intermediates undergoing subsequent reactions, for examples double bond hydrogenation, that could provide enantio enriched BP, can not be performed.

	Aldehyde	BP product		Yield[a] (%)
1			**PPH**	74
2			**POOMe**	63
3			**PMOMe**	67
4			**PPOMe**	63
5			**PVER**	62
6			**PMES**	21
7			**PPtBut**	65
8			**POHMe**	78
9			**PPNO₂**	68
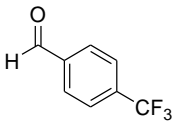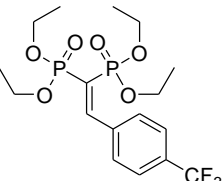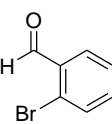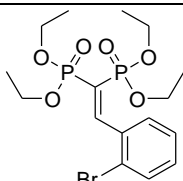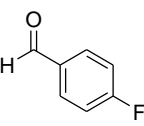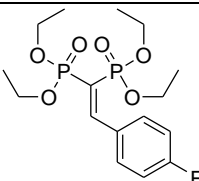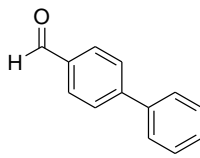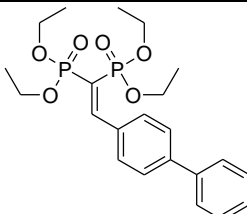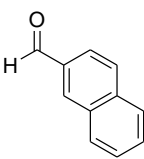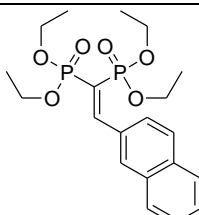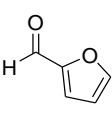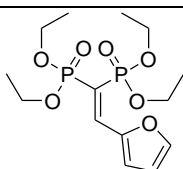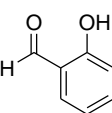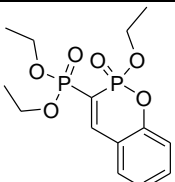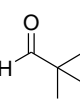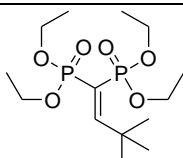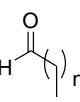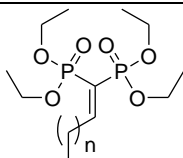
10			**PPCF₃**	75
11			**POBr**	51
12			**PPF**	66
13			**P2Ph**	74
14			**P2NAP**	48
15			**PFUR**	45
16			**PSAL**	51
17			**PtBut**	35
18			**n = 1, 2, 4, 6**	0-5%

Table 2: Ti(IV) catalyzed syntheses of monosubstituted VBP precursors. [a] Isolated yield.

Table 2 shows the results obtained in the Knovenagel-type condensation between MBP and a wide range of aldehydes. Good yields are obtained with the aromatic aldehydes, both bearing electron donating group (**Table 2, entries 1-8**) or electron withdrawing groups (**Table 2, entries 9-12**). A slight decrease in the yields were observed for aldehydes bearing rigid substituent groups in the ortho position of the aromatic ring (**Table 2, entries 6, 11**) including also naphthyl aldehydes (**Table 2, entry 14**). The use of salicyladehyde led to the formation of an intramolecular condensation product between the hydroxyl group of the aldehyde and one ethyl ester protection group (**Table 2, entry 16**). Use of heteroatom containing aldehydes such as furaldehyde allows the formation of the desired precursor but in lower yield. Contrary to what reported in the literature, [127] many aliphatic aldehydes (**Table 2, entry 18**) showed a very low reactivity despite the precautions taken such as washing of the starting material with aqueous solution of $NaHCO_3$ and further distillation to remove traces of acid and impurities. Only with trimethylacetaldehyde moderate yield was observed (**Table 2, entry 17**). It seems likely that Ti(IV) can form enolates due to presence of α hydrogen atoms in the aldehyde. These species can undergo aldol condensation inactivating the reagent for the desired reaction.

As previously explained, with this synthetic route it is possible to form only monosubstituted aromatic VBP, thus limiting the range of BP precursors available for further functionalization. The products were obtained in 0.1 to 1.5 g scale, purified by flash chromatography and characterized by NMR spectroscopy and GC-MS. PPH characterization is reported as an example: ^{1}H-NMR spectra show typical resonances for vinylic proton (doublet of doublets) at high field (**Figure 16**). The HMBC 2D-NMR spectrum show long range ^{13}C-^{1}H resonances, helping to assign ^{13}C signals as reported on **Figure 17**.
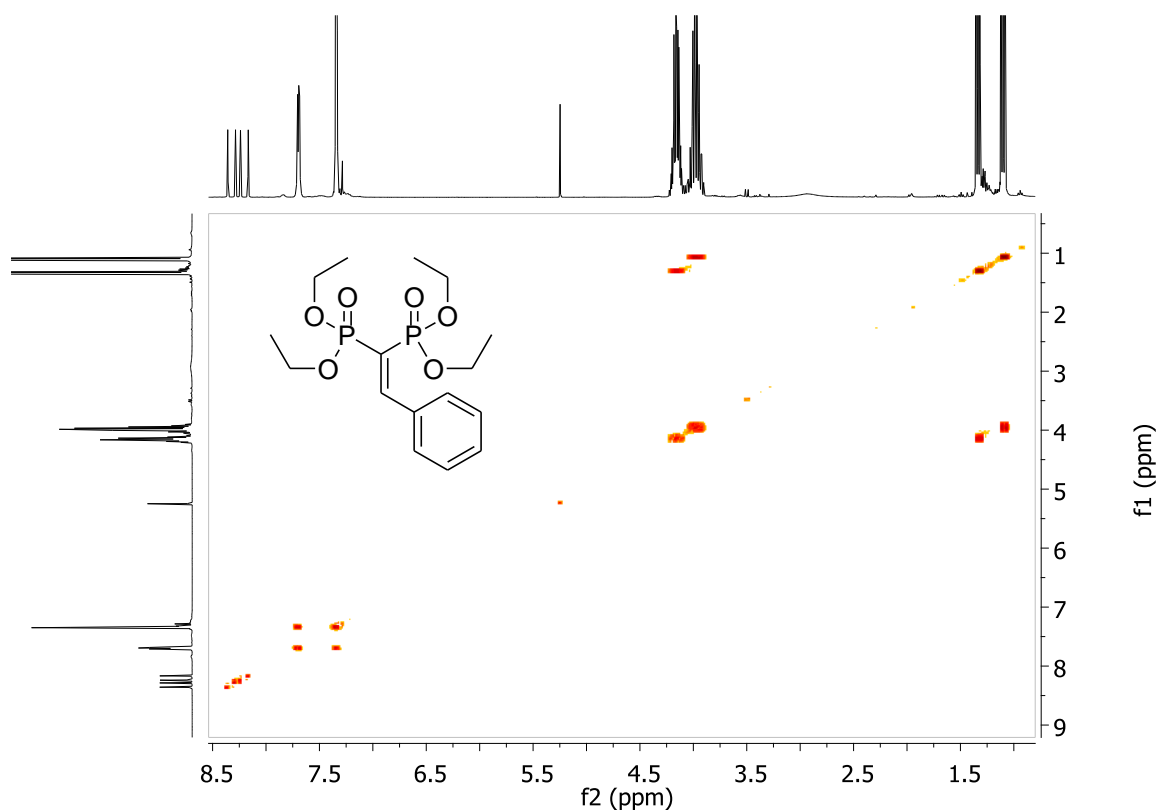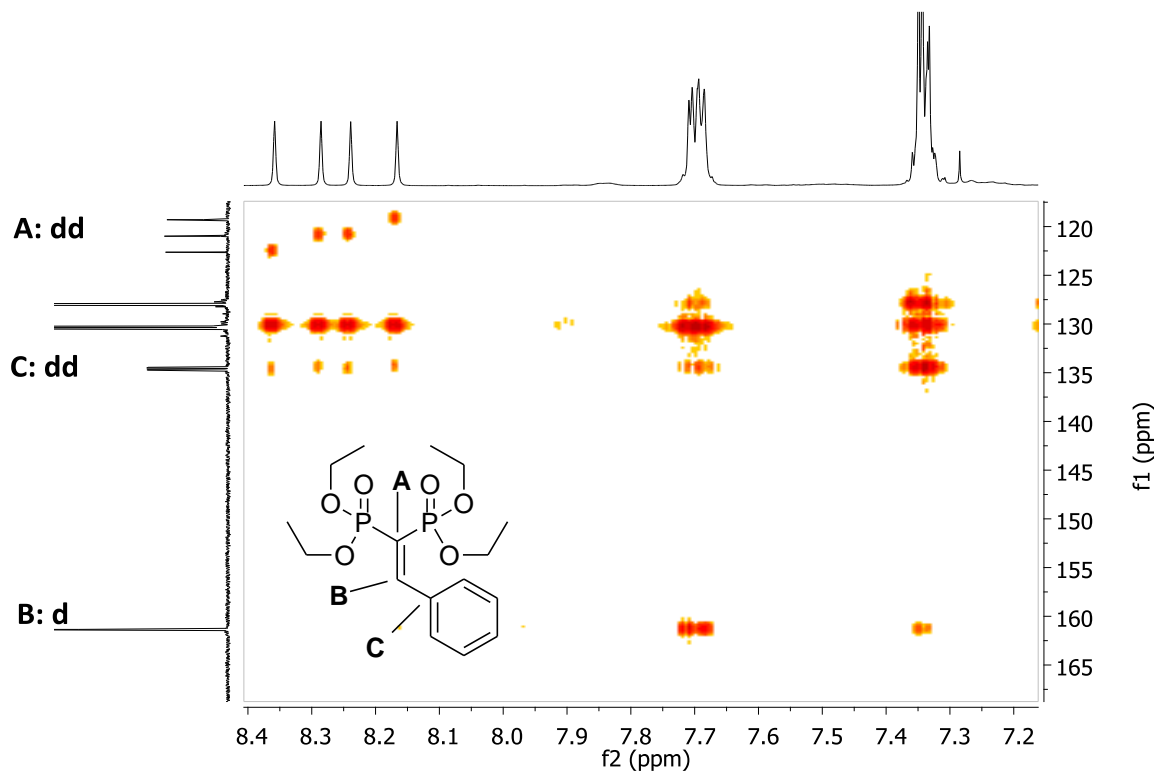
Figure 16: 2D-NMR COSY of PPH.

Figure 17: 2D-NMR HMBC of PPH.

3.1.4 *Bis-Substituted Unsaturated BP Precursors*

Part of the results discussed in this chapter were presented at ChemCYS 2016 in Blankenberge, Belgium, resulting in the third prize of "Organic Chemistry Poster Presentation".

An innovative synthetic strategy for the synthesis of enantioenriched BPs is represented by the preparation of prochiral precursors having two different substituents in the α position on which to perform e.g. simple asymmetric catalytic hydrogenation of carbon-carbon double bond to give enatioenriched chiral products. There are only few examples in the literature of bis-substituted VBP prochiral precursors. The older one shows the synthesis of a phosphonic dithioacetal ketene obtained by condensation of MBP with carbon disulfide under mild basic conditions in high yield, [128] or through the formation of 2,2-dichlorovinylbisphosphonate intermediate.[129] However the substituents to the double bond of the BP precursor are identical. Abdou and co-workers recently reported a one-pot procedure where the reaction between halosubstrates and cyanomethylphosphonate, followed by reaction with dialkyl phosphonates gave a series of branched N-heterocycle-substituted VBP bisphosphonates.[130] Another example was reported using copper-promoted domino condensation/S-arylation/heterocyclization process for the synthesis of series of 2-C-substituted benzothiazoles containing gem-bisphosphonates.[131] In this case both substituents at the vinyl position are constituted by the heterocyclic ring.

Only Abdou and collaborators reported the reactions of MBP with N1- and N3-allyl-2-thiouracils under phase-transfer catalysis conditions, showing the synthesis of two bis-substituted VBP precursors in which the substituent groups of the double bond are two different chains: an alkyl chain and a pyrimidine ring (**Scheme 4**).[132]
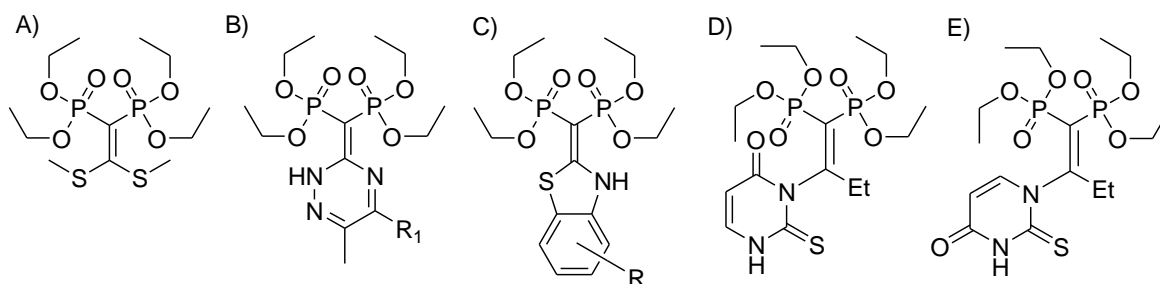
Scheme 4: Bis-substituted VBP structures reported in literature by A) Villemin et al. B) Abdou et al. C) Xiang et al. D-E) Abdou et al.

Previous work in our group [133] demonstrated that the use of an organocopper reagent is a useful way for the introduction of an alkyl chain on a substituted alkynphosphonate, leading to bis-substituted vinyliden monophosphonate intermediate with high regioselectivity. The next step of the reaction showed that the electrophilic addition of a phosphonate group, and more in general of phosphorus containing electrophiles, did not

take place, making this synthetic route useless for the formation of bis-substituted VBP intermediates (**Scheme 5**).
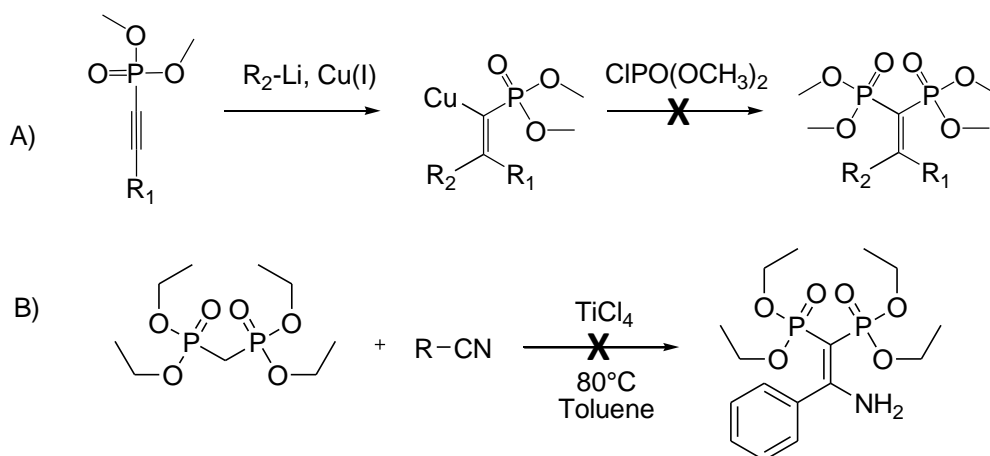
Scheme 5: attempted syntheses of Bi-substituted VBP by Scarso's research group.

A useful synthetic route for the formation of enamino keto esters that use nitriles and ethyl acetoacetate has been reported recently by Pei et al.[134] This synthesis is performed with TiCl$_4$ as catalyst and it is very similar to the previously reported synthesis for the formation of monosubstituted VBP precursors. The extension to MBP, which is structurally very similar to ethyl acetoacetate, can lead to the synthesis of VBP precursors with two different substituent groups, one of which is an amino group. However, the TiCl$_4$ catalyzed reaction between MBP and benzonitrile under the conditions reported in the literature (**Scheme 5**), led only to the decomposition of the reagents without formation of any useful product. Yu and collaborators [135] have similarly reported the synthesis of benzylidene malonate intermediate using α-keto ester reagents. The condensation is effectively catalyzed by TiCl$_4$ on dimethylmalonate, the latter being also a structurally very similar reagent to MBP. Inspired by this work it was decided to investigate the condensation of ethyl phenylglyoxylate with MBP catalyzed by TiCl$_4$ and NEt$_3$ in order to check the possibility of obtaining bis-substituted VBP precursors. Luckily, the application of this procedure to MBP led to the formation of bis-substituted VBP precursor in a higher than 90% yield. The bis-substituted VBP has one aromatic and one ester substituent, the latter useful for further functionalization.
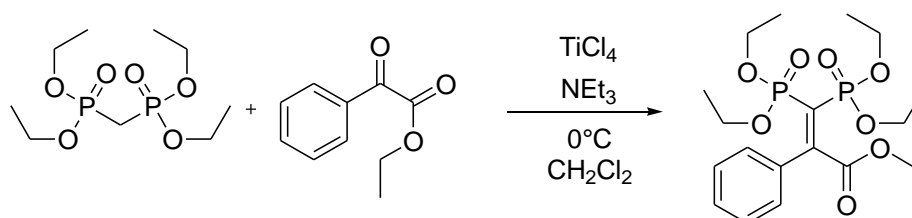
Scheme 6: Condensation reaction of ethyl phenylglyoxylate catalyzed by TiCl$_4$ and NET$_3$ to the MBP.

We thus investigated a wide spectrum of commercially available and synthetic α-keto esters with different steric and electronic properties and the presence of sensitive functional groups in order to test the generality of the synthetic method. The results obtained are reported in **Table 3**:

	α-keto esters	BP product		Yield[a] (%)
1			**BPHEt**	90
2			**BMeEt**	0
3			**BMeMe**	0
4			**BtBut**	0
5			**BOEtEt**	0
6			**PCOOEt**	90
7			**BPHMe**	84
8			**BPOMe**	73
9			**BOOMe**	58

10			**BOPOMe**	63
11			**BOMe**	60
12			**BPNO$_2$**	92
13			**BOCl**	22
14			**BPCF$_3$**	64
15			**B5F**	28
17			**BPYR**	40

Table 3: Synthesized bi-substituted VBP precursors. Reaction conditions: 1 mmol MBP, 1 mmol α-keto esters, 4 mmol NEt$_3$, 1 mmol TiCl$_4$, 25 mL CH$_2$Cl$_2$, 0°C. [a] Isolated yield.

Commercially available molecules structurally similar to ethyl phenylglyoxylate are methyl and ethyl pyruvates (**Table 3, entries 2, 3**) that unfortunately did not react under the conditions of **Table 3**. Use of a non aromatic glyoxylate (**Table 3, entry 4**) did not lead to the formation of the desired product as did diethyl oxalate (**Table 3, entry 5**). Similarly to what reported for Ti(IV) catalyzed synthesis of monosubstituted VBP precursors, it seems likely that this catalyst could easily give an enolate due to presence of α hydrogen atoms in the α-keto esters. This form undergo aldol condensation inactivating the reagent for the desired reaction. The use of a commercial solution of ethyl glyoxylate in toluene

unexpectedly led to the formation of a condensation product with excellent yields identified as the monosubstituted ethyl 3,3-bis(diethoxyphosphoryl)acrylate (PCOOEt, **Table 3, entry 6**) a sterically and electronically different mono substituted VBP precursor compared to those reported so far. Use of numerous glyoxalates synthesized according to the procedures reported in the literature [136, 137] allowed to study the scope of this reaction varying the steric and electronic character. The presence of electron-donating groups on glyoxylates led to slightly lower yields than using glyoxylates having electron-withdrawing groups **(Table 3, entries 1, 6, 8, 12)**. The reaction proved very sensitive to the steric characteristics of the reagent used: the presence of substituents in the ortho position in the phenyl group led to a significant decrease of the reaction yield that was not higher than 60% (**Table 3, entries 9, 10, 11, 14**). The presence of very bulky electroattractive atom such as chlorine in the same position of the phenyl ring (**Table 3, entry 13**) led to a drastic decrease in yield as did the presence of a double substitution in the ortho position (**Table 3, entry 15**). It is interesting to observe that the VBP precursor is obtained even by varying the ester of the glyoxylate (**Table 3, entry 7**), allowing a wider range of products also having an alkyl side chain which, as explained above, is of considerable importance to promote the biological activity of the BP. Nitrogen heteroatoms containing glyoxylates (**Table 3, entry 16**) made possible the synthesis of the corresponding VBP precursors. The new bis-substituted VBP obtained are all stable at room temperature except PCOOEt that undergoes decomposition when stored at room temperature. Storage at low temperature makes the product less susceptible to decomposition and allow a prolonged use over time.

The class of compounds here reported has no precedent in the literature and includes a new prochiral monosubstituted BP building-block with a non-aromatic chain. The products were all obtained in hundreds mg scale, purified by flash chromatography and characterized by NMR spectroscopy and GC-MS. BPPHEt characterization is reported as an example: 2D-NMR ^{1}H-COSY showed typical cross resonances among the ethyl esters protective groups emphasizing the presence of three magnetically different protective groups present (**Figure 18**). HMBC 2D-NMR showed long range ^{13}C-^{1}H resonances, helping to assign ^{13}C signals as reported on **Figure 19**.
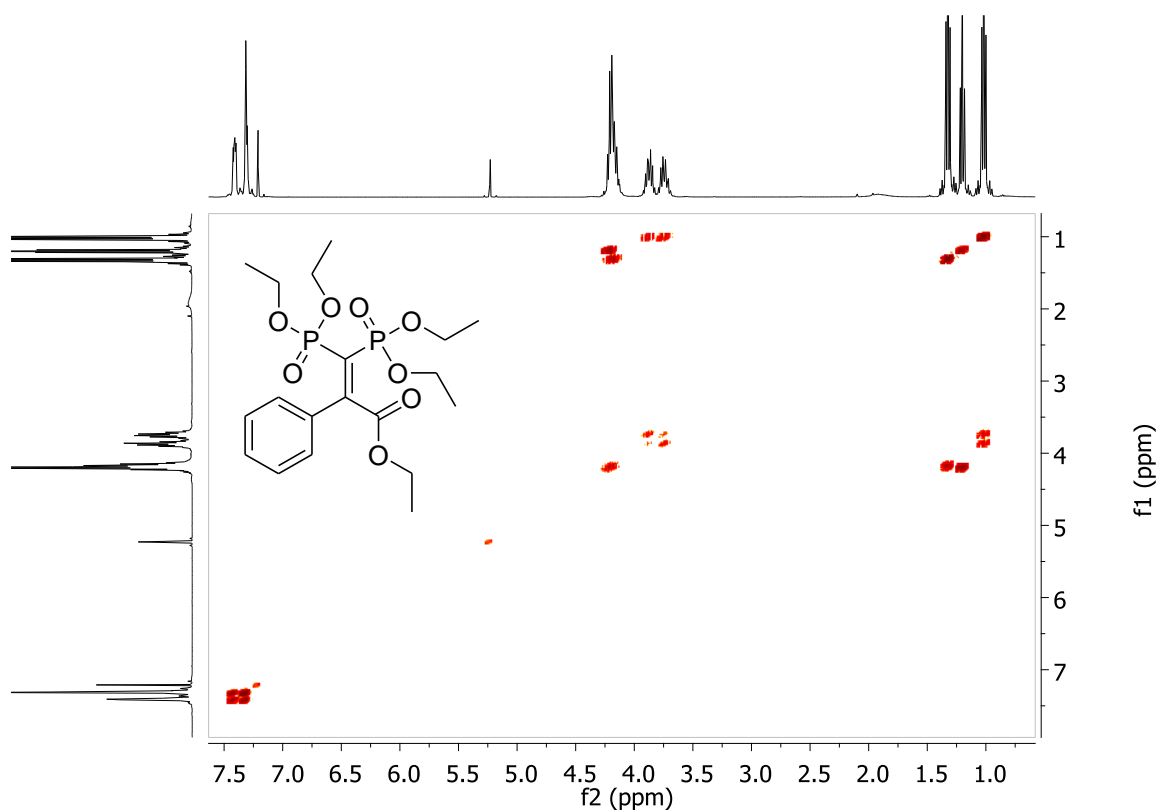
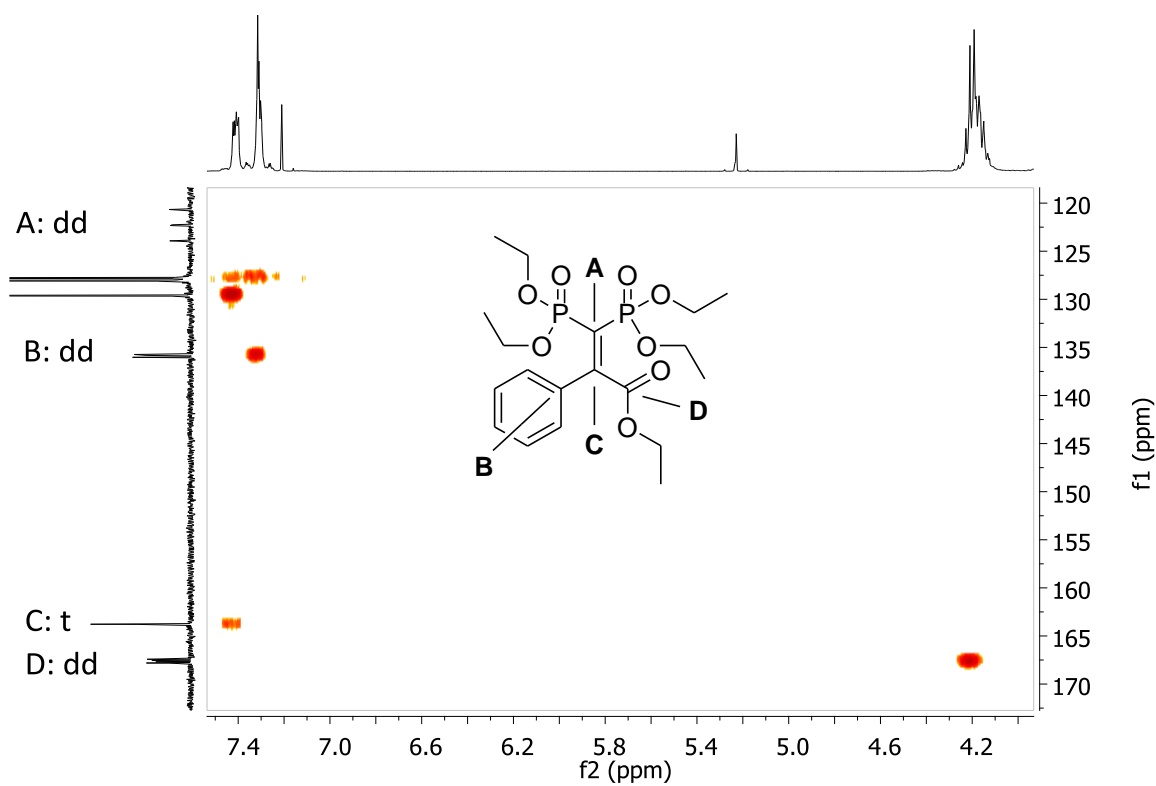Figure 18: 2D-NMR COSY of BPPHEt.

Figure 19: 2D-NMR HMBC of BPPHEt.

3.1.5 *Reduced Steric Hindrance BP Precursors*

As described in the previous sections, MBP tetraethylester represents the starting building block to produce a large variety of BP precursors on which to perform subsequent studies. However, the ethyl ester groups on the phosphonate moieties cause a significant sterical hindrance leading to possible complications in the subsequent reactions. Of crucial importance is therefore the synthesis of protected precursors bearing less bulky groups such as the methyl ester group. In the literature some synthesis of MBP tetramethylesters (MBP-Me) have been reported based on the use of carbon disulfide [115] and diazomethane, [116] all reagents that requires special precautions for use and severe restrictions, in fact they are toxic, highly flammable and suspected carcinogens.

Therefore we thought to modify the method already in use in our group using a different phosphite and a different base for the synthesis of MBP-Me in a single synthetic step. Reaction of metallic sodium with methanol provide sodium methylate that was reacted with dimethylphosphite eventually leading to the double nucleophilic attack to dichloromethane in two stages, following the same mechanism reported for the MBP. Despite the anhydrous atmosphere condition of the reaction, the analysis of the obtained product showed the formation of a completely different molecule i.e. dimethoxy methylphosphonate (**Scheme 7**).
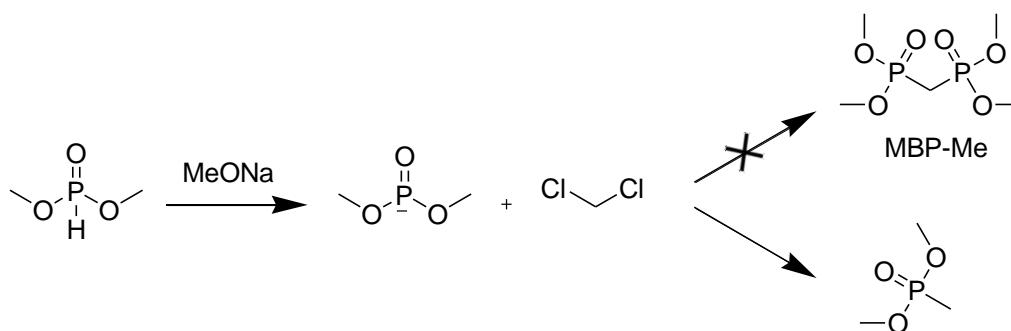
Scheme 7: Direct synthesis of MBP-OMe.

Since it was not possible to prepare MBP-Me in a single step starting from dimethyl phosphite, it was decided to investigate the synthesis of this fundamental building block in three consecutive synthetic steps (**Scheme 8**):

- Traditional synthesis of tetraethyl MBP with the procedure reported by Hormi et al. [117] and described above;
- Deprotection of ethyl ester functions with bromo trimethylsilane (TMSiBr) followed by hydrolysis to give the corresponding bisphosphonic acid;
- Protection of the acid moieties with trimethyl orthoformate.[138]

If treated with bromo trimethylsilane (TMSiBr), the ester groups of MBP, and more generally of the BPs, can be removed by forming a silylester intermediate that can be

subsequently hydrolyzed at room temperature to give the corresponding bisphosphonic acid [139,140] (medronic acid) in quantitative yield. This method is widely used for the synthesis of the acid form of BPs which are the real potential inhibitors of bone resorption. The next synthetic step is the re-protection of the acid groups using trimethyl orthoformate (TOF) that is the simplest molecule in a class of compounds having a carbon atom bound to three alkoxide groups. This reagent causes the esterification on the hydroxyl groups [141] and provides the MBP with new methyl ester substituents characterized by low steric hindrance. Appropriate reaction times allow the re-protection reaction in a quantitative yield without the occurrence of unwanted reactions or partial re-protection even when the reaction scale is fifteen times larger.
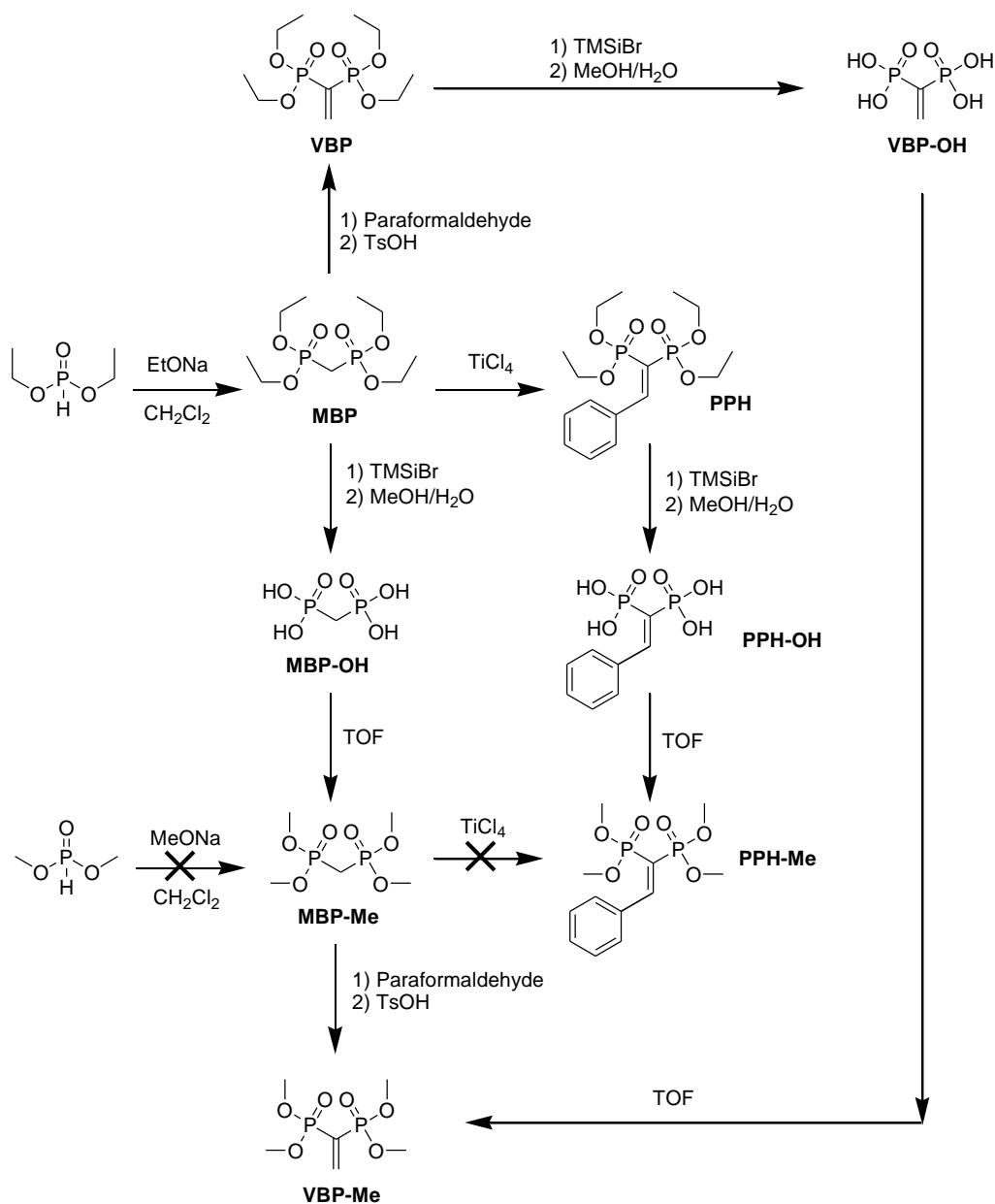
Scheme 8: syntheses of reduced steric hindrance BP precursors.

The same synthetic steps of deprotection by TMSiBr and re-protection using trimethyl orthoformate previously described for MBP-Me were also applied to VBP leading to the synthesis of VBP tetramethylesters (VBP-Me) in 71% yield. The analysis of the crude reaction by GC-MS showed the formation of the VBP-Me together with smaller quantities of two by-products. These are due probably to the reaction with TMSiBr, an extremely aggressive reagent, which tends to react not only with protective groups, but also with the vinyl group of the VBP through a not completely understood mechanism. Given the good results obtained with the MBP-Me synthesis, it was decided to change the procedure described by Degenhardt et al.[120] in order to obtain VBP-Me from the corresponding MBP-Me by reaction with formaldehyde and subsequent removal of methanol in order to reduce the synthetic steps. The changing in the synthesis and the elimination of the deprotection step with TMSiBr led to a significant increase in the reaction yield that increased up to 97% (**Scheme 8**). Despite the excellent yields, isolation and purification of the obtained product were rather complex. The replacement of the ethyl ester function with another one with lower steric hindrance led to a drastic change in the hydrophilicity of VBP-Me, preventing the elimination by simple aqueous extraction of the used acid in the second step of the reaction. Purification attempt was carried out by reduced pressure distillation observing the decomposition of the precursor. Only multiple extractions with ethyl acetate of the aqueous solution made it possible to isolate the desired VBP-Me but at the expence of the isolated yield that decrease to 45%. Similarly, it was decided to change the reported procedure by Lehnert et al. [121] for the synthesis of monosubstituted aromatic VBP. The reaction between MBP-Me and benzaldehyde catalyzed by TiCl$_4$ was explored. Despite the high yields in the condensation reaction using MBP-Et, the similar procedure performed using MBP-Me did not give the desired results. ^{1}H and ^{31}P NMR analysis of the crude reaction mixture demonstrated the total absence of reactivity between the reagents. To PPH bearing ethyl esters protection (**Scheme 8**) the deprotection step with TMSiBr and re-protection with trimethyl orthoformate described above were applied. In **Figure 20** the ^{1}H NMR spectra of the synthetic steps for the synthesis of PPH-Me are shown.
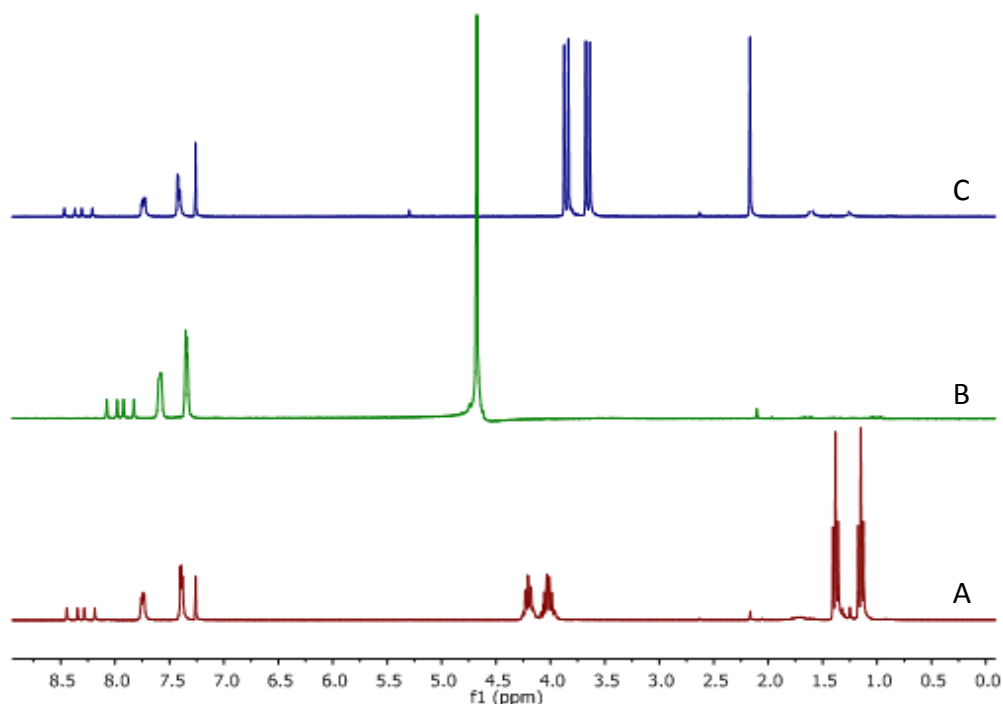
Figure 20: 1H NMR Spectra of PPH (A), PPH-OH (B), PPH-Me (C).

Despite the monosubstituted BP-Et (PPH) precursor presents a similar structure compared to VBP-Et, application of the synthetic steps of deprotection and re-protection seems not to interfere on the double bond of the molecule, allowing the synthesis in excellent yield of the methyl esters protected VBP precursor. The application of this methodology to a few monosubstituted aromatic VBP with different electronic character allowed to obtain the corresponding tetramethyl esters as shown in **table 4**:
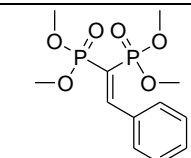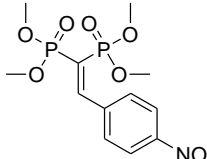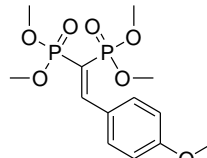
Tetraethyl esters VBP precursor	Tetramethyl esters BP product		Yield [a] (%)
PPH		**PPH-Me**	95
PPNO$_2$		**PPNO$_2$-Me**	95
PPOMe		**PPOMe-Me**	95

Table 4: reduced steric hindrance VBP precursors synthesized. [a] Isolated yield.

Although in all cases the reactions gave excellent yields, it was found that the most critical step was still the TMSiBr deprotection, which is strongly influenced by the reagent concentration. Concentrated reaction environments result in the formation of by-products due to the phosphonate groups decomposition.

3.1.6 *BPs Functionalized Zirconia Mesoporous Nanoparticles*

Recently Prof. Canton and her research group at the Università Ca' Foscari di Venezia published a simple and highly efficient method for the synthesis of spherical mesoporous zirconia nanoparticles (MZNs) with a high surface area through a neutral surfactant-assisted sol–gel method, demonstrating that MZNs were biocompatible, cell permeable and degradable providing a proof of concept for theranostic applications. [142] In order to continue the exploration of this new field, Canton's group tried to functionalize these zirconia materials also with organic phosphates in order to introduce molecules such as amino acids with biological properties. This occurrence stimulated a cooperation in which the BP obtained in the acid form or with different protective ester groups prepared during this thesis, were considered among the tested compounds. PPH-OH, PPH-Me and PPH bisphosphonates were tested to check different binding affinities on the zirconia-based nanoparticles. MZN functionalization with PPH-OH did not lead to any morphological change on the surface of the nanoparticles, as verified by FEG-SEM analysis (**Figure 21 A-B**).
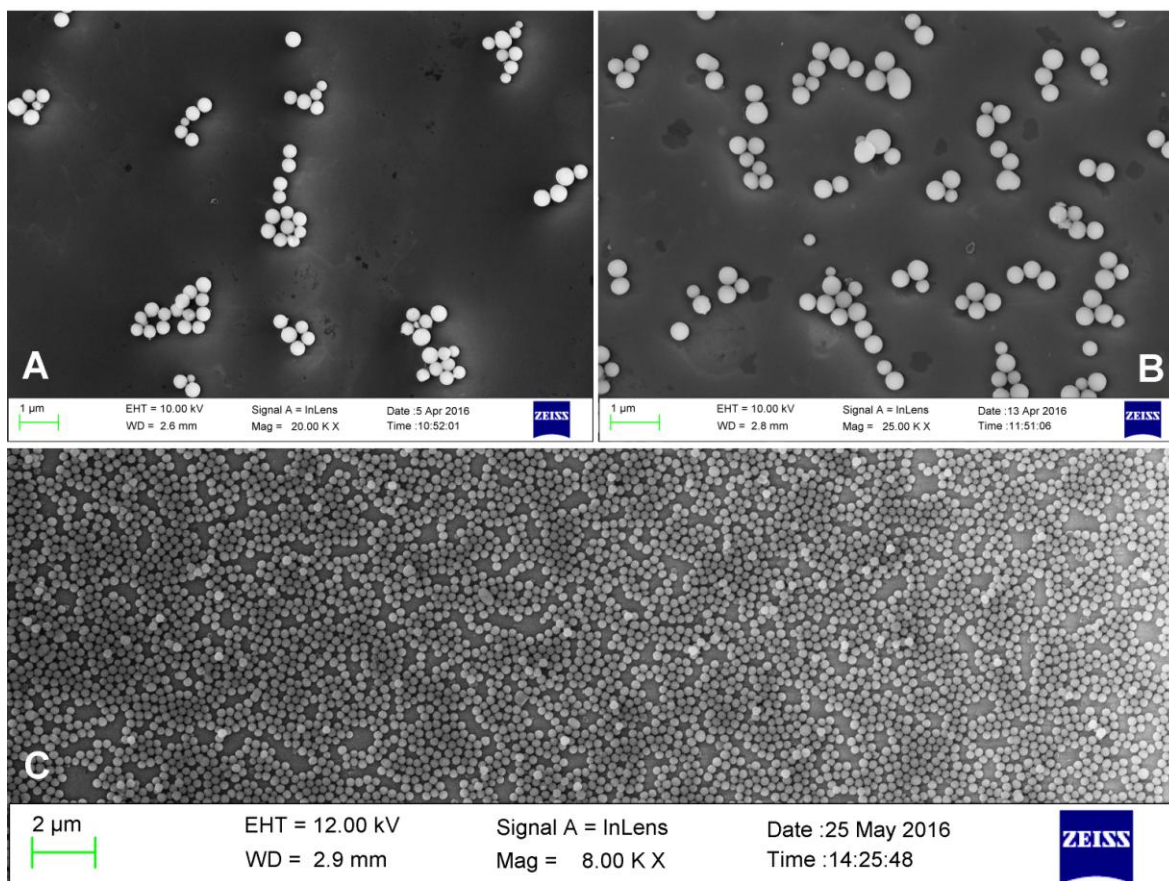
Figure 21: FEG-SEM microscopy of a solution of MZN (A) and MZN/PPH-OH (B). (C) FEG-SEM microscopy of dry monolayer of MZN/PPH-OH on aluminum foil.

Nevertheless, XPS analysis showed that phosphorous was actually present on the surface of the functionalized nanoparticles, providing also a shift of the corresponding peak in comparison with other functionalized MZN by organic phosphates (**Figure 22-A**). Macroscopically, a dramatic change occurred in the behavior of MZN/PPH-OH particles giving rise to a very stable colloidal suspension when redispersed in aqueous solution. Zeta potential analyses confirmed the variation of the electrokinetic properties of MZN/PPH-OH revealing the presence on the surface of these particles of a strong negative charge also at different pH, contrary to what reported for non-functionalized MZN (**Figure 22-B**). PPH and PPH-Me/MZN functionalizations led to formation of colloidal suspensions with stability intermediate between non-functionalized MZN and MZN/PPH-OH but zeta potential values were similar to non-functionalized nanoparticles, indicating a very limited number of functionalization of the nanoparticles. Of particular interest is the property of MZN/PPH-OH to form individual monolayers of particles on solid surfaces even in the dry form (**Figure 21-C**) that could be exploited for biomechanical implants coating.

These preliminary observations seem to have opened a new interesting field of application for BP and the collaboration with Prof. Canton will continue in order to extend the promising obtained results.
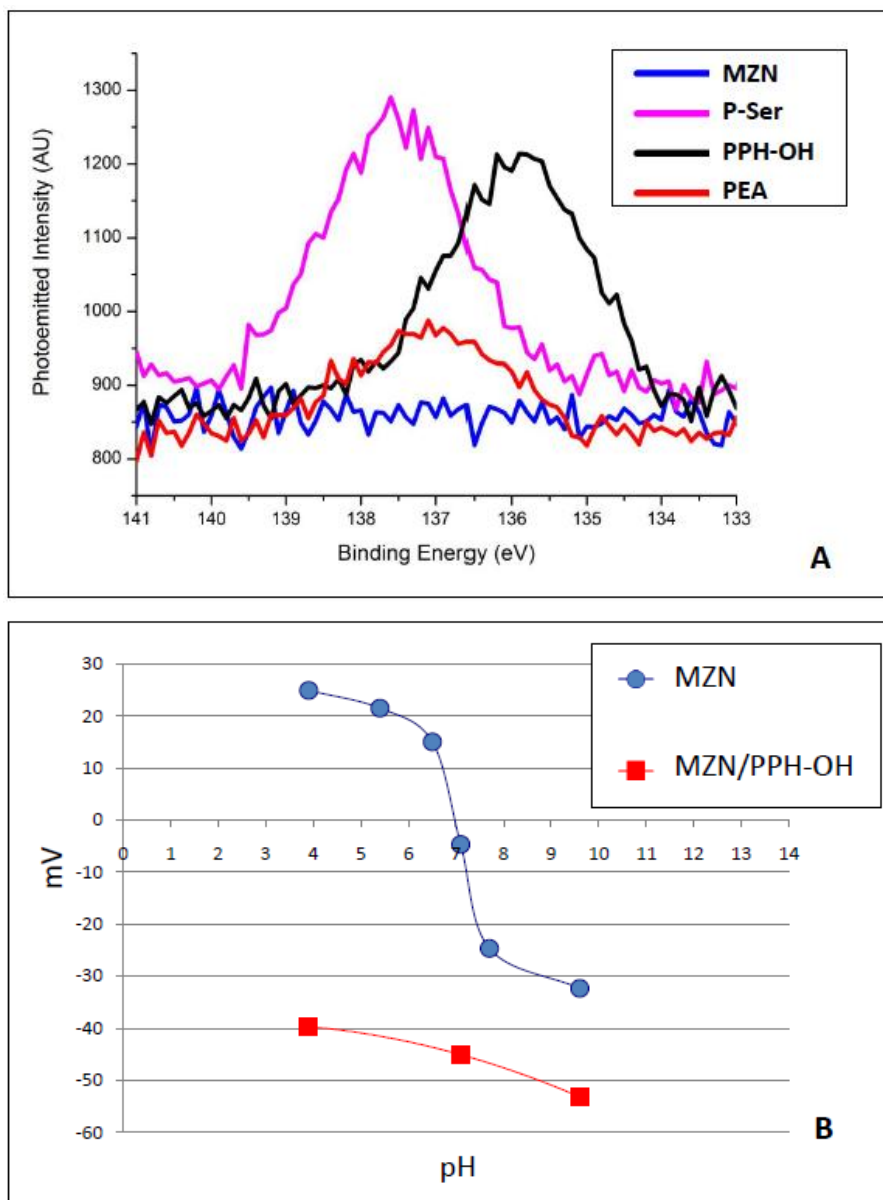
Figure 22:

A) XPS analyses of mesoporous zirconia nanoparticles (MZN), functionalization with phosphoserine (P-Ser), functionalization with bisphosphonate PPH-OH (PPH-OH) and functionalization with phosphoetanolamine (PEA).

B) Zeta potential analyses of mesoporous zirconia nanoparticles (MZN) and with functionalization with bisphosphonate PPH-OH (MZN/PPH-OH)

3.2   NON NITROGEN BISPHOSPHONATES

Non nitrogen BPs such as etidronate, clodronate, and tiludronate are the oldest drugs used to contrast osteoporosis. While the former does not contain heteroatoms, the latter two include respectively chlorine and sulphur in their structure. Non N-BPs were found to disrupt the ATP metabolic pathway in osteoclasts. After incorporation into the corresponding non-hydrolyzable analogs of adenosine triphosphate, they induce osteoclast apoptosis by the intracellular accumulation of such metabolites.[92]
The development of new synthetic routes to a wide range of new BPs with molecular complexity, also in an enantioenriched form, is a primary goal for further studies of new application fields and give the opportunity to verify the different behavior of different enantiomers.

3.3   COPPER-MEDIATED 1,4-CONJUGATE ADDITION of BORONIC ACIDS to VBP PRECURSORS

Part of the results presented in this chapter were published in:

A. Chiminazzo, L. Sperni, M. Damuzzo, G. Strukul, A. Scarso, " *Copper-mediated 1,4-Conjugate Addition of Boronic Acids and Indoles to Vinylidenebisphosphonate leading to gem-Bisphosphonates as Potential Antiresorption Bone Drugs*", *ChemCatChem*, **2014**, 6, 2712 – 2718.

3.3.1 *Cu(II)-Catalyzed Addition of Aryl Boronic Acids to VBP*

The conjugate addition of nucleophiles to VBP is the most common synthetic strategy to synthesize BPs with R_1=H. By using this method, BPs bearing heterocycles, [143] steroid conjugates, [144] or other functional groups in the β position have been prepared. In this chapter I will describe the synthesis of a wide range of β-aryl substituted BP with R_1=H through a highly versatile Cu(II)-catalyzed conjugate addition of aryl boronic acids to VBP. The conjugate addition of boronic acids [145] to electron-poor alkenes can be catalyzed efficiently by Pd(II) [146] and Rh(I) [147] species. The latter metal promotes the synthesis of a wide range of β substituted functional groups such as acrylic acids, [148] enesulfonamides, [149] and others.[150] This class of catalytic reactions well tolerates the presence of water as described in the addition of boronic acids to acrylic acid [148] and substituted acrylic esters, [151] with positive effects on the reactions. In contrast, when this reaction was applied to alkenylphosphonates, [152] the presence of a large amount of water as a cosolvent was detrimental for the scope of the reaction.
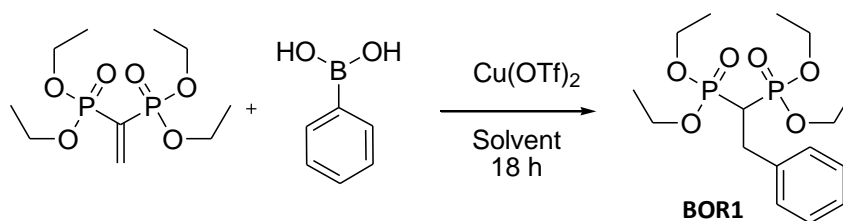
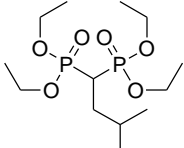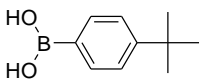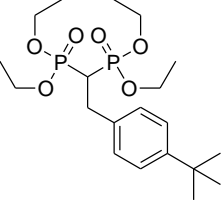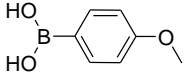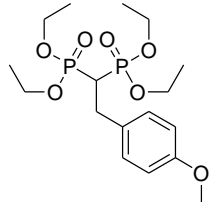Scheme 9: Copper mediated conjugate addition of phenylboronic acid to VBP.
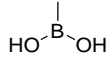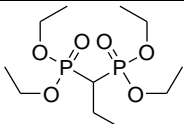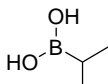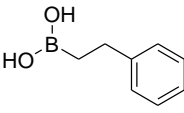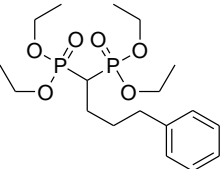
In fact, the reaction between phenylboronic acid and VBP was investigated (**Scheme 9**) with different metal precursors in the presence of 10 mol% catalyst loading and it was found that Pd(II) precursors as well as Zn(OTf)$_2$ (OTf=trifluoromethanesulfonate) and CuI were not effective in the reaction under different experimental conditions (**Table 5, entries 1–5**). In contrast, Cu(OTf)$_2$ demonstrated moderate catalytic activity and provided the corresponding BP product in 40 and 44% yield at 70 and 85°C with 1,2-dichloroethane (DCE) (**Table 5, entries 6 and 9**). A higher yield of the BP product could be obtained by increasing the amount of phenylboronic acid to 5 equiv. (75% yield; **Table 5, entry 7**), whereas by maintaining the same amount of phenylboronic acid and by decreasing the catalyst loading to 2 mol%, the yield decreased to 45% (**Table 5, entry 8**). A rapid solvent screening revealed that the reaction could be performed in a water/1,4-dioxane mixture (9:1) with a small increase in yield (47 %; **Table 5, entry 10**), whereas a good yield of the BP product was obtained with an apolar solvent such as toluene (90% yield; **Table 5, entry 11**). A slight increase in yield was observed (up to 94%) with a higher amount of phenylboronic acid (5 equiv.), which allowed to decrease the Cu(OTf)$_2$ amount to 2% mol (**Table 5, entries 12 and 13**). It is worth of notice that our research group reported the general addition reaction between boronic acids and VBP with 2.4 mol% of dimeric Rh(I) in the water/1,4-dioxane mixture (9:1) at 110°C, [153] which gave BPs in extremely good yields (**Table 5, entries 14**). In comparison to the latter protocol, the new Cu(OTf)$_2$-based system makes use of a comparable amount of a much less expensive and non-hazardous metal catalyst under milder experimental conditions, giving only slightly lower yields with some boronic acids and higher yields with aliphatic boronic acids. The Cu(II) optimized catalytic system was applied also to reduced steric hindrance VBP-Me resulting in an unexpected complete inactivity of the BP (**Table 5, entries 15**). Attempts to use a Rh(I) catalyst [153] with VBP-Me demonstrated that the latter is a less stable reagent, giving half amount of products compared to VBP (**Table 5, entries 14 and 16**) and resulting in a range of decomposition by-products.
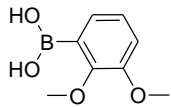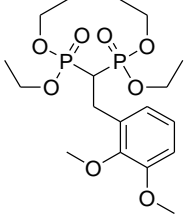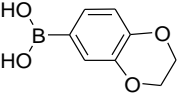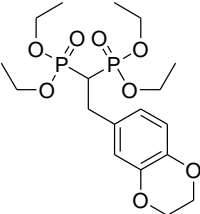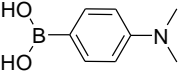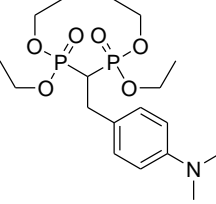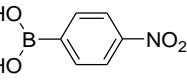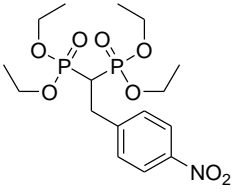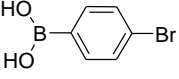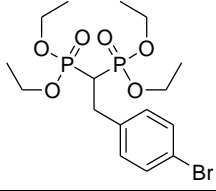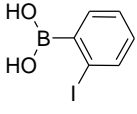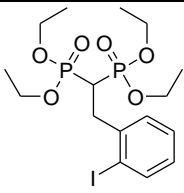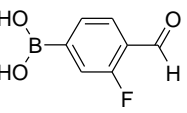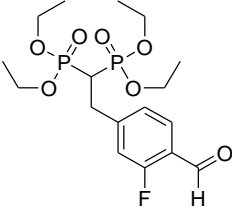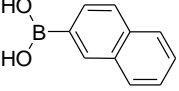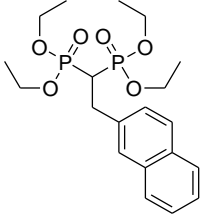
	Catalyst	Catalyst Loading [mol%]	Amount of boronic acid [eq.]	Solvent	T [°C]	Yield [a] (%)
1	CuI	10	1.5	DCE	70	0
2	PdCl$_2$	10	2	DMF	70	0
3	Pd(OAc)$_2$	10	2	DMF	70	0
4	Pd(P(Ph$_3$)$_4$)	10	2	DMF	70	0

5	Zn(OTf)$_2$	10	2	Toluene	110	0
6	Cu(OTf)$_2$	10	1.5	DCE	70	40
7	Cu(OTf)$_2$	10	5	DCE	70	75
8	Cu(OTf)$_2$	2	5	DCE	70	45
9	Cu(OTf)$_2$	10	1.5	DCE	85	44
10	Cu(OTf)$_2$	10	1.5	Water/1,4-dioxane 9:1	70	47
11	Cu(OTf)$_2$	10	1.5	Toluene	70	90
12	Cu(OTf)$_2$	5	5	Toluene	70	94
13	Cu(OTf)$_2$	2	5	Toluene	70	93
14	[Rh(COD)Cl]$_2$	2.4	3	Water/1,4-dioxane 9:1	110	>98[b]
15	Cu(OTf)$_2$	10	5	Toluene	70	0[c]
16	[Rh(COD)Cl]$_2$	2.4	3	Water/1,4-dioxane 9:1	110	52[c]

Table 5: Conjugate addition of phenylboronic acid to VBP under different experimental conditions.
Reaction conditions: 0.33 mmol of VBP, 2 mL of solvent, t=18 h; [a] Isolated yield, [b] Bianchini et al. [153], [c] VBP-Me used.

The optimized catalytic system was used with a wide range of boronic acids with different steric and electronic properties as well as bearing different secondary functional groups (**Table 6**).

	Boronic acid	BP Product		Yield[a] (%)
1			**BOR2**	56
2			**BOR3**	26
3			**BOR4**	46
4			**BOR5**	77
5			**BOR6**	83

#	Boronic acid	Product		Yield
6	(structure)	(structure)	**BOR7**	96
7	(structure)	(structure)	**BOR8**	79
8	(structure)	(structure)	**BOR9**	74
9	(structure)	(structure)	**BOR10**	59
10	(structure)	(structure)	**BOR11**	60
11	(structure)	(structure)	**BOR12**	69
12	(structure)	(structure)	**BOR13**	71
13	(structure)	(structure)	**BOR14**	91

14		**BOR15**	>98
15		**BOR16**	78
16		**BOR17**	66
17		**BOR18**	69
18		**BOR19**	91
19		**BOR20**	83
20		**BOR21**	91
21		**BOR22**	>98
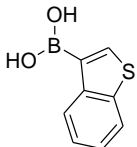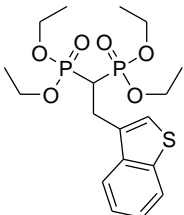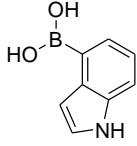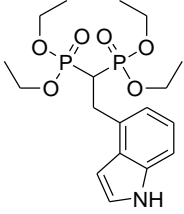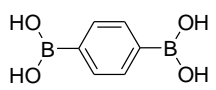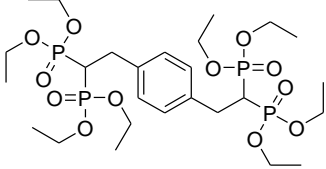
|				
22			**BOR23**	53
23			**BOR24**	95
24			**BOR25**	71[b]

Table 6: Substrate scope of the addition of boronic acid to VBP mediated by Cu(OTf)$_2$.
Reaction conditions: 0.33 mmol of VBP, 0.5 mmol of boronic acid, 10 mol% Cu(OTf)$_2$, 2 mL of toluene, t=18 h, T=70°C; [a] Isolated yield, [b] 3 eq. of VBP with respect to the bis-boronic acid.

Usually poorly reactive alkyl boronic acids provided BP products in modest to moderate yields (**Table 6, entries 1–3**), whereas aromatic boronic acids provided higher yields. The reaction with aryl boronic acids bearing electron-donating groups, such as p-tert-butyl, p-methoxy, bis-alkoxy and dimethylamino, gave BP products in good yields (**Table 6, entries 4–8**). Boronic acids bearing nitro or halogen atoms led to a slight decrease in product formation, even for an ortho-substituted boronic acid (**Table 6, entries 9–11**). The reaction well tolerates the presence of other functional groups on boronic acids such as the aldehyde moiety (**Table 6, entry 12**). Naphthyl boronic acids bearing alkyl, alkoxy, or halogenated substituents provided the corresponding BP products in good to excellent yields, even if the substituents are close to the boronic moiety, which thus generated steric effects (**Table 6, entries 13–19**). Heteroaromatic boronic acids did not perform well in the reaction, such as in the cases of pyridine-, quinoline-, isoquinoline-containing substrates. In contrast, the electron-rich aminopyridine boronic ester (**Table 6, entry 20**) was found to be a suitable substrate. Thiophene- and benzothiophene-containing boronic acids demonstrated optimal to good conversion to the corresponding BPs (**Table 6, entries 21 and 22**), whereas furane-based boronic acids did not work at all. A ditopic substrate such as indole-5-boronic acid preferentially led to the formation of the corresponding 5-substituted indole (**Table 6, entry 23**) but no formation of the 3-substituted indole product, as reported later (**Chapt. 4.9**) for typical indole substrates. The reaction also proceeds smoothly with bis-boronic acids such as in the case of the substrate reported in **Table 6 (entry 24)**, which in the presence of 3 equiv. of VBP provided the doubly substituted BP in 71% yield. The Cu(II)-mediated reaction could be also scaled up: the reaction between (4-

methyl-1-naphthyl)boronic acid and VBP was repeated with 3 mmol of VBP, which gave the corresponding addition product in 90% isolated yield.

3.3.2 *Cu(II)-Catalyzed Addition of Aryl Boronic Acids to Substituted VBP*

Several attempts were made to tackle the asymmetric version of the reaction by investigating the addition of phenylboronic acid to tetraethyl esters protected PPH under Cu(II)-optimized catalytic conditions (**Scheme 10**). The desired product was not obtained even with use of the highly electrophilic substrate PPNO$_2$ when the chiral bis(oxazoline) ligands (+)-2,2'-isopropylidenebis[(4R)-4-benzyl-2-oxazoline] (Box) and 2,6-bis[(4S)-(-)-isopropyl-2-oxazolin-2-yl]pyridine (PyBox) (**Table 7**, **entries 2 and 3**) were employed as suitable ligands, as found in the asymmetric Cu(II) catalyzed 1,4-addition of phenylboronate to electron deficient olefins.[154] In order to reduce the steric hindrance of the tetraethyl esters derivatives, several attempts were made with tetramethyl ester protected PPH-Me that, however, showed a total lack of reactivity using the copper based catalytic system (**Table 7, entry 4**). On the contrary, the Rh(I) catalyzed addition led to some reactivity, but only causing a phosphonate group elimination from the BP reagent, even if EWG or EDG phenylboronic acids were used (**Table 7, entries 5-7**).
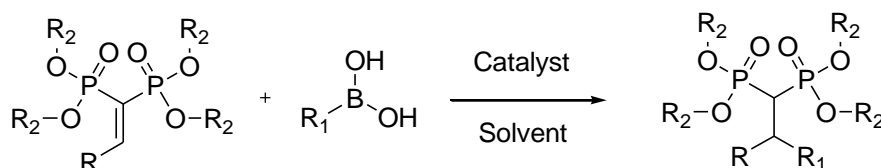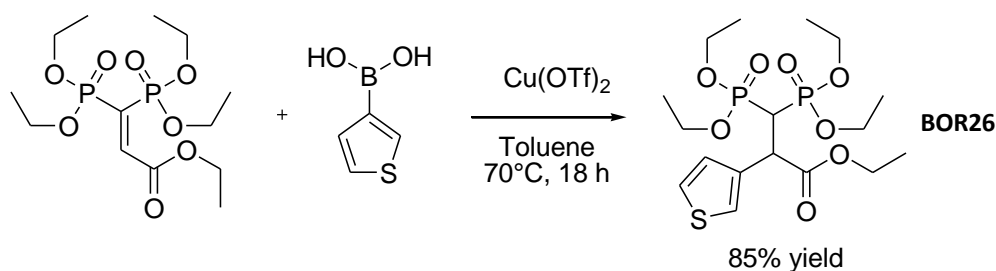

Scheme 10: asymmetric addition of boronic acid to BP precursors

	BP (R)	R$_1$	R$_2$	Catalyst	Solvent	T [°C]	Yield (%)
1	Ph	Ph	Et	Cu(OTf)$_2$	Toluene	70	0
2	p-NO$_2$ Ph	Ph	Et	Cu(OTf)$_2$/Box	Toluene	70	0
3	p-NO$_2$ Ph	Ph	Et	Cu(OTf)$_2$/PyBox	Toluene	70	0
4	Ph	Ph	Me	Cu(OTf)$_2$	Toluene	70	0
5	Ph	Ph	Me	Rh(COD)Cl]$_2$	Water/1,4-dioxane 9:1	110	0
6	Ph	p-NO$_2$ Ph	Me	Rh(COD)Cl]$_2$	Water/1,4-dioxane 9:1	110	0
7	Ph	p-OMe Ph	Me	Rh(COD)Cl]$_2$	Water/1,4-dioxane 9:1	110	0
8	COOEt	Ph	Et	Cu(OTf)$_2$	Toluene	70	0
9	COOEt	3Thienyl	Et	Cu(OTf)$_2$	Toluene	70	85[a]
10	COOEt	Isopropyl	Et	Cu(OTf)$_2$	Toluene	70	0

Table 7: Attempts of asymmetric addition of boronic acid to BP precursors.
Reaction conditions: 0.33 mmol of VBP, 0.5 mmol of boronic acid, 10 mol% Cu(OTf)$_2$, 2 mL of toluene, t=18 h, T=70°C; [a] Isolated yield, [b] 3 eq. of VBP with respect to the bis-boronic acid.

In order to investigate the effect of the steric hindrance at the β-position of the BP, several attempts were made with the non aromatic PCOOEt (**Table 7, entries 8-10**) showing that the reaction is intrisically influenced by the dimension of the boronic reagent. While Cu(II) addition of phenylboronic acid did not lead to the desired product (**Table 7, entries 8**), the use of less bulky reagents like 3-thienyl boronic acid led to an adduct product in excellent yield (**Scheme 11, Table 7, entry 9**). Alkyl boronic acids like isopropyl boronic acid led only to decomposition of the BP precursor by loss of a phosphonate moiety (**Table 7, entry 10**).

Scheme 11: Addition of 3-thienylboronic acid to PCOOEt.

The BOR26 product (**Scheme 11**) was characterized by NMR spectroscopy and GC-MS. The NMR characterization of BOR26 is reported in **Figure 23**: comparison between the ^{1}H (A) and the ^{1}H {^{31}P} (B) NMR spectra shows a simplification of the resonance peaks in the latter spectrum. ^{31}P {^{1}H}-NMR of BOR26 showed formation of two doublets shifted from PCOOEt with a small J coupling constant of 2.4 Hz.
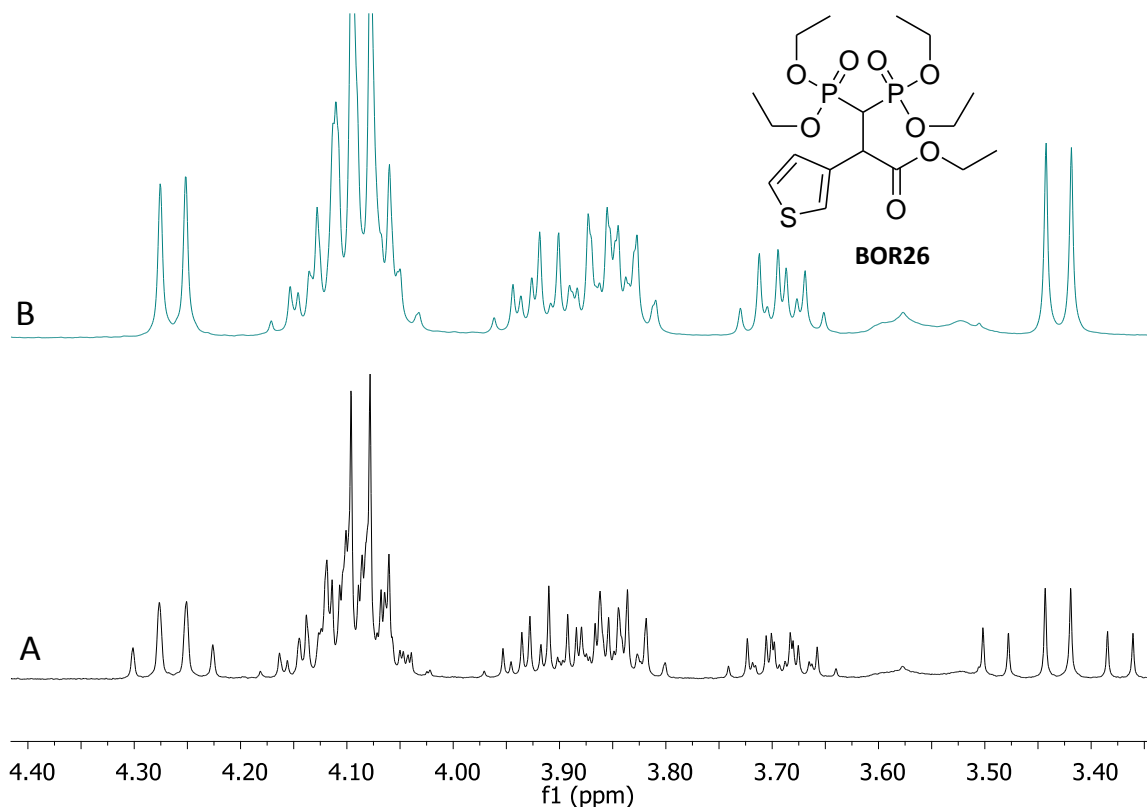
Figure 23: (A) ^{1}H-NMR and (B) ^{1}H {^{31}P}-NMR of BOR26.

3.4   SULFUR CONTAING BPs

There is only one commercially available BP, containing a sulfur atom in the β-position, named tiludronate. Like other non N-containing BPs, tiludronate can be incorporated into molecules of ATP, creating non hydrolysable cytotoxic analogs of ATP molecules. Nevertheless, tiludronate has low cellular potency and low mineral affinity in comparison to the more potent N-containing BPs and its clinical use is limited to the treatment of Paget's disease or in veterinary orthopedics.[155] VBP can undergo facile Michael-type addition reaction with sulphur nucleophiles to give γ-substituted BPs with fewer by-products than those involving amines or phosphites. Thiol BP products could be readily isolated and deprotected removing the phosphonic ester moieties to give the corresponding bisphosphonic acids. [156]

S-containing BPs are an underinvestigated class of BPs. Recent literature showed only a limited number of contributions, in particular a new synthetic procedure reported is based on a rapid and solvent-free microwave-assisted method.[157] Studies on Thienopyrimidine-based bisphosphonates showed that these sulfur-nitrogen containing BPs were identified as a new class of inhibitors of the human farnesyl pyrophosphate synthase (FPPS).[158] Notably, our research group reported, in collaboration with Prof. Granchi's group at the Istituto Ortopedico Rizzoli in Bologna, a comparative study on the toxicity and osteoclast inhibition activity of a known *N*-containing BPs with respect to a new S-containing BP demonstrating good antiosteoclast activity of the latter while maintaining a low toxicity level, which is a really positive aspect for the development of new drugs.[159] Hence, new sulphur-containing BPs were synthesized as reported below.

3.4.1   *Michael-Type Addition of 6-(ferrocenyl)hexanethiol to VBP*

The use of ferrocene in bio-organometallic chemistry has been growing rapidly and several promising applications have been developed since ferrocene is a stable, nontoxic compound bearing good redox properties. The use of ferrocene-based compounds for medicinal applications is an active research area. Many reports have demonstrated that some ferrocenyl derivatives are highly active against several diseases, including cancer, malaria or HIV.[160, 161] It was only in 2015, during the completion of this PhD thesis, that Mukaya et al. [162] synthesized and characterized the first example of macromolecular co-conjugates between a bisphosphonate and ferrocene analogue in order to improve the anticancer activity of the drug and solve the critical question of drug solubility. This approach uses a terminal amino BP.

Based on the ability of mercaptane derivatives to undergo 1,4-conjugate Michael-type addition reactions to VBP, [163] it was decided to synthesize a sulfur containing BP-ferrocene conjugate. The resulting product could present good antiosteoclast activity while maintaining a low toxicity coupled with the anti-cancer properties of ferrocene unit.
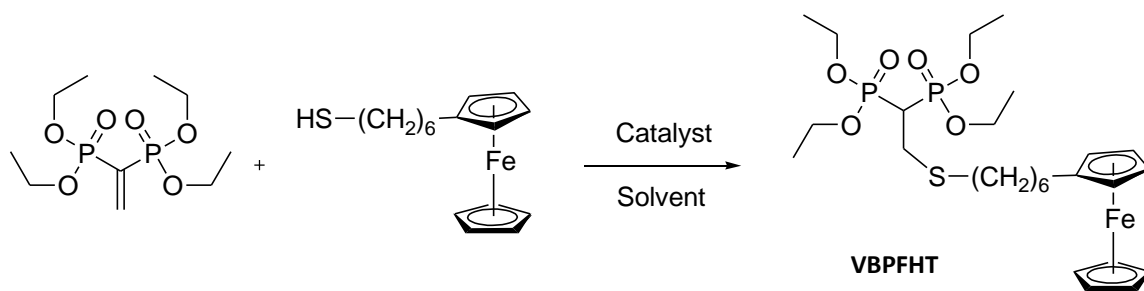
Scheme 12: Michael-type addition between commercial 6-(ferrocenyl)hexanethiol and VBP.

The reaction between commercial 6-(ferrocenyl)hexanethiol (FHT) and VBP was investigated (**Scheme 12**) under different experimental condition and it was found that spontaneous reaction was not effective (**Table 8, entry 2**). Increasing the temperature up to 60°C led to low yield in BP product (**Table 8, entry 3**) showing that triethyl amine did not provide any improvement in the reaction (**Table 8, entry 4**) at variance with what reported in the literature for mercaptanes.[163]

	Reagent	Catalyst	Solvent	T [°C]	Yield [a] (%)
1	FCC	-	CHCl$_3$	rt	0
2	FHT	-	CHCl$_3$	rt	0
3	FHT	-	CHCl$_3$	60	17
4	FHT	NEt$_3$	CHCl$_3$	60	17
5	FHT	PdCl$_2$	DCE	70	19
6	FHT	Cu(OTf)$_2$	DCE	70	48
7	FHT	Zn(OTf)$_2$	DCE	70	93
8	FCC	Cu(OTf)$_2$	DCE	70	0
9	FCC	Zn(OTf)$_2$	DCE	70	0
10	FHT	Zn(OTf)$_2$[b]	DCE	70	56
11	FHT	Zn(OTf)$_2$[c]	DCE	70	85

Table 8: Michael-type addition of 6-(ferrocenyl)hexanethiol to VBP under different experimental conditions. Reaction conditions: 0.067 mmol of VBP, 0.067 mmol of FHT, 2 mL of the solvent, t=18 h, 10 mol% of catalyst; [a] ^{31}P-NMR yield, [b] 5 mol% catalyst, [c] 0.3 mmol of VBP, 0.3 mmol of FHT.

The use of Pd(II) precursors as catalysts (**Table 8, entry 5**) did not provide any improvement in product formation, while 10 mol% Cu(OTf)$_2$ or Zn(OTf)$_2$ demonstrated moderate to excellent catalytic activity providing the corresponding BP product in 48 and 93% yield respectively at 70°C in 1,2-dichloroethane (DCE) (**Table 8, entries 6 and 7**). When decreasing the catalyst loading to 5 mol%, the yield decreased to 56% (**Table 8, entry 10**). As reported in the literature, [156] use of a oxygen nucleophile like ferrocenylcarbinol (FCC) under the same reaction conditions, did not lead to any product formation (**Table 8, entries 1, 8, 9**). The Zn(II) mediated thio-Michael addition could be scaled up to 0.3 mmol of VBP, giving the corresponding addition product in slightly lower yield (**Table 8, entry 11**). The sulfur-containing bisphosphonic acid was successfully prepared via hydrolysis of this tetraethyl intermediate by treatment with TMSiBr in dichloromethane. Further reaction with wet

MeOH for four hours provided the free bisphosphonic acid in quantitative yield (**Scheme 13**).
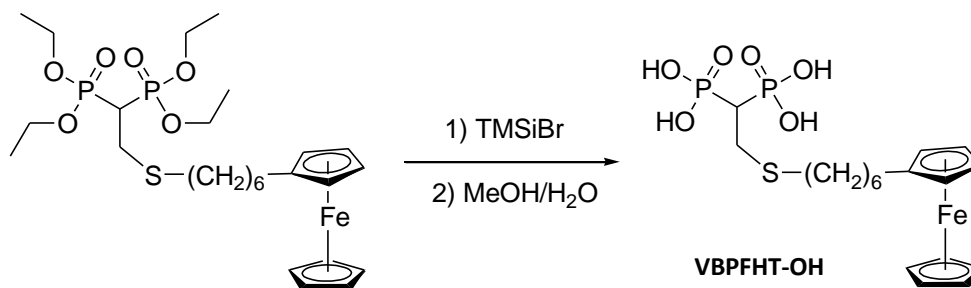

Scheme 13: Deprotection steps of PPFHT.

The intermediate and the product were characterized by ^{1}H and ^{31}P NMR spectroscopy. While sharp resonances were observed in the spectra of VBPFHT in CDCl$_3$, the spectra of VBPFHT-OH in D$_2$O showed the presence of aggregation phenomena providing only a single broad signal. To overcome these problems spectra were run in DMSO-d$_6$, but while the ^{31}P spectrum confirmed the presence of only one product, the ^{1}H spectrum still remained very broad. Electrospray MS analysis of VBPFHT-OH was performed in methanol observing good matching between the [M-H]$^-$ ion and the ESI spectra on negative ion mode, thus confirming the structure of the BP products. VBPFHT-OH will be tested to assess its toxicity and activity inthe inhibition of the osteoclast as well as its anticancer properties.

3.4.2 Synthesis and NMR Quantification of Low Toxicity S-Containing BP

Our previously reported work on a new S-containing BP showing good antiosteoclast activity and low toxicity in a comparative study with some known N-containing BP [159] attracted the curiosity of Prof. Bigi, Università di Bologna, interested in bisphosphonate functionalized hydroxyapatites for biomedical uses.[164,165] It was therefore established to synthesize and test a functionalized hydroxyapatite with 2-(2-hydroxyethylthio) ethane-1,1-diyldiphosphonic acid (VBPTIO-OH) [159] known for its low toxicity properties and interesting for the presence of a free hydroxyl group at the end of the side chain which could favor the interaction with hydroxyapatite. Such materials were prepared reacting a solution of Ca(NO$_3$)$_2$·4 H$_2$O with another of (NH$_4$)$_2$HPO$_4$ at 80°C and pH 10. The obtained precipitate, after filtering and drying, represents a synthetic hydroxyapatite that can be used as a support for bone cells in biochemical tests. The addition of a BP to the phosphate solution leads to the synthesis of functionalized HAP with different antiosteoclastic activities depending on the structure-incorporated drug.[166]
The synthesis of VBPTIO was accomplished by reaction of mercaptoethanol with VBP under triethylamine catalysis, providing almost quantitative yield for the corresponding

BP tetraethyl ester precursor (**Scheme 14**). The latter was treated with trimethylbromo-silane with an improved procedure compared to that reported in the literature.[139]
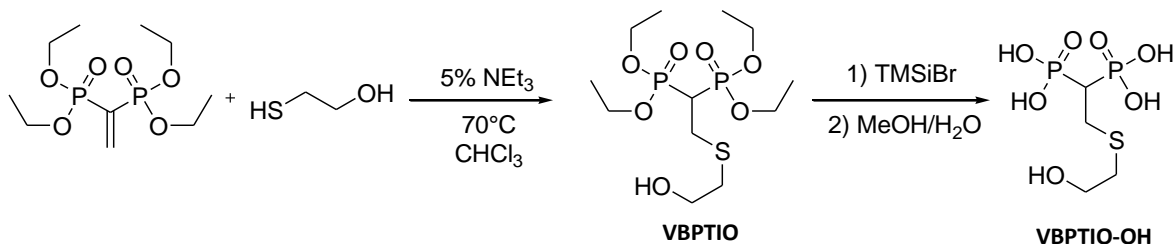
Scheme 14: Synthesis of VBPTIO-OH.

While the room temperature deprotection step with TMSiBr in dichloromethane gave the desired product in 18h, the new deprotection at 70°C in dichloroethane allowed the formation of the silylester intermediate in only 1.5 hours. Further reaction with MeOH/water for 4 h provided the free bisphosphonic acid VBPTIO-OH in quantitative yield. (**Scheme 14**)

The syntheses of functionalized hydroxyapatite at different concentrations of VBPTIO-OH are usually carried out on gram scale, therefore five grams of BP were necessary, an amount 250 times larger than the one normally used in our laboratory. The scaling up process revealed that the deprotection with TMSiBr is the most delicate step, requiring a careful adjustment of appropriate concentrations of reagents. It was possible to proceed with the deprotection step using less than 250 mg (0.66 mmol) of VBPTIO with a solvent volume of 5 mL. Larger solvent volumes led to stirring problems with only partial deprotection; reactions carried out with higher concentrations of VBPTIO gave partial decomposition of the intermediate. Overall, about five grams of the final bisphosphonic VBPTIO-OH were prepared summing up several 250 mg syntheses. The product was characterized by ^{1}H and ^{31}P NMR spectroscopy; a sharp resonance was observed in the ^{31}P spectra in D_2O indicating high water solubility and absence of aggregation phenomena. ^{31}P spectra in D_2O of VBPTIO-OH showed no decomposition even after two hours at 90°C at pH 10. Electrospray MS analysis of VBPTIO-OH was performed in methanol observing the exact mass for the anion [M-H]⁻, thus confirming the structure of the BP product.

VBPTIO-OH was used by the group of Prof. Bigi for the synthesis of functionalized HAP at different concentrations of BP, monitoring the association of the BP on the new material by monitoring the residual BP in solution. The quantitative determination normally used by the group of prof. Bigi for commercial BP such as alendronate and zoledronic acid is based on spectrophotometric analysis of the complex between Fe (III) and BP.[167] The latter analytical method was not effective for the determination of VBPTIO-OH because of the lack of suitable chromophores for the UV analysis. We therefore analyzed the remaining VBPTIO-OH in the aqueous phase using ERETIC2 (TopSpin, Bruker) NMR method.

The ERETIC2 (Electronic REference To access *In vivo* Concentrations) method is a new quantitative NMR experimental technique to measure analytes based on a refence (mainly external) signal generated from the NMR spectrometer.[168] This technique is widely used istance in metabolomics methodology [169] in biomedical research and *in vitro* quantitative analysis of complex matrices.[170,171] ERETIC2 is an internal standard method which correlates the absolute intensities of two different samples, one taken as the reference. This method only needs a 1D spectrum of a sample in known concentration acquired with exactly tuned and matched probe, a calibrated 90° pulse and high signal to noise ratio. An initial calibration of the area of the ERETIC signal for a standard of known concentration is needed, then the method permits the use of this signal to quantify components of unknown concentration avoiding the drawbacks associated with the use of internal chemical references.[172]

Experiments are fast, non-destructive, with easy sample handling and preparation, giving also the possibility of a simultaneous determination of more than one analyte in a mixture. The approach is not restricted to ^{1}H analyses but can be easily extended to the quantification of other NMR active nuclei.

The typical precision of this method is comparable to other internal references methods, resulting in lower than 2% of the mean. The accuracy is slightly better for the ERETIC method than for the internal reference.[173]

	Sample	Found concentration [mM]
1	BL	1.3[a]
2	BLTpH	1.3[a]
3	HAP7	0
4	HAP7BP	<0.05[a]
5	HAP14	0
6	HAP14BP	<0.05[a]
7	HAP28	0
8	HAP28BP	<0.05[a]

Table 9: ERETIC2 quantification of VBPTIO-OH on residual waters of functionalyzed HAP syntheses. [a] the experiment was repeated twice.

As a calibration standard for the ERETIC signal, a 28 mM D_2O/H_2O 50/50 phenylphospinic acid solution was used. The quantification was performed by ^{1}H NMR rather than ^{31}P NMR to increase the sensitivity. The original aqueous samples derived from the hydroxyapatite-BP syntheses were diluted to 50% with D_2O and subjected to NMR analysis using the solvent suppression technique in order to reduce the non deuterated water signal.

The analysis of an aqueous solution of VBPTIO-OH showed that this BP is stable for several months (BL, **Table 9, entry 1**) and no degradation of the molecule was observed after treatment at 80°C at pH 10 (BLTpH, **Table 9, entry 2**). [31]P analysis of BLTpH showed

only the presence of one peak shifted at lower ppm due to the effect of the pH of the solution. Three different concentrations of BP were used in the aqueous syntheses of VBPTIO-OH functionalized HAPs carried out in Bologna, namely 7, 14, 28 mM respectively. The remaining water solutions were analyzed to determine the unreacted BP amount. In parallel non-functionalized HAP syntheses for each sample were carried out, using the remaining waters as control. As expected these samples did not reveal any presence of BP (**Table 9, entries 3, 5, 7**). Conversely the analysis on all the samples coming from the synthesis in the presence of BP showed concentrations of VBPTIO-OH lower than 0.05 mM (**Table 9, entries 4, 6, 8**). This means that less than 1% of the original BP (in all the HAP syntheses) remained in solution, confirming the almost quantitative binding of the BP to the newly synthesized hydroxyapatite. The amount of VBTIO-OH embedded on HAP was double compared to the maximum amount usually loaded on the HAP using commercial BP. This result can be explained considering the presence of a free hydroxyl group at the end of the side chain of VBPTIO-OH that can act as a further point of attack on the crystal structure of the synthesized HAP. The functionalized HAP samples will soon be characterized by the group of Prof. Bigi by thermal gravimetric analysis and X-ray diffraction to confirm the presence and the amount of VBPTIO-OH on the hydroxyapatite structure. The materials will be used as supports for bone cells in bone resorption tests. These data require additional time for acquisition and are not included in this thesis.

3.5   HYDROGENATION of BI-SUBSTITUTED VBPs

The possibility of obtaining new disubstituted prochiral compounds not yet existing in the literature, allowed to explore new synthetic route having as ultimate goal the formation of enantio-enriched molecules. As previously mentioned the lack of enantioselective syntheses hinders the development of chiral BPs [111,112,113]: in the literature only one example of enantio-enriched BP was tested observing a difference of activity between the enantiomers equal to 24 times.[114]

The easiest way to obtain a chiral product starting from prochiral bi-substituted BP is, in fact, a simple hydrogenation of the double bond. Enantioselective hydrogenation of the double bond of disubstituted prochiral BP compounds could give the opportunity to obtain enantio-enriched BP molecules.

3.5.1 *Non Asymmetric Hydrogenation*

In order to optimize a chiral HPLC analytical method for enantiomeric excess determination of the saturated BP products useful for the exploration of possible asymmetric hydrogenation tests, the simple non-stereoselective hydrogenation was carried out on bis-substituted BP precursors.
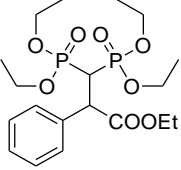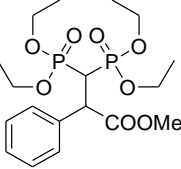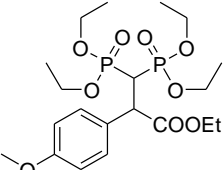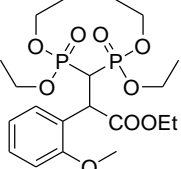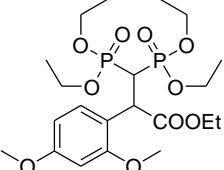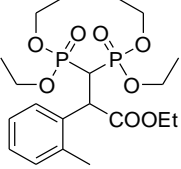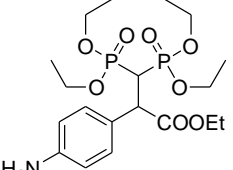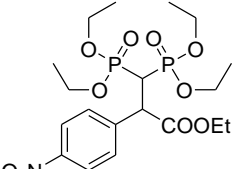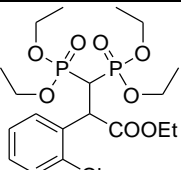
Metal catalyst belonging to the 10th group supported on carbon are the best known and the most widely used for lab scale hydrogenation reactions. In particular, palladium is used in hydrogenation reactions, hydrogenolysis, dehydrogenation, oxidation and formation of new C-C bonds.[174] In the literature several examples of hydrogenation reactions of phosphonate monosubstituted alkenes are reported [175,176] most of which employing Pd supported on carbon as catalyst. There are also examples of hydrogenation of double bonds substituted with one phosphonate groups using sodium borohydride as reducing reagent.[177,178]

Using Pd/C as heterogeneous catalyst in bis-substituted BP precursors hydrogenation, it was possible to obtain the racemic mixtures of hydrogenated products (**Scheme 15**) that were useful for optimization of the chiral HPLC analytical method.
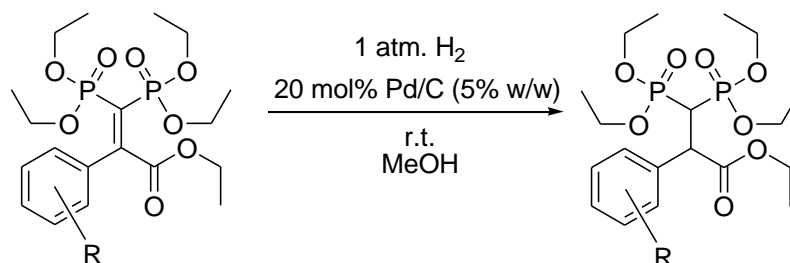
Scheme 15: Pd/C catalyzed hydrogenation of Bi-substituted VBP precursors.

The results obtained from the di-substituted VBPs hydrogenation tests with Pd/C are reported in **Table 10**.

	Di-substituted VBP precursors	BP product		Isolated yield (%)
1	BPHEt		H2BPHEt	>98
2	BPHMe		H2BPHMe	>98
3	BPOMe		H2BPOMe	>98
4	BOOMe		H2BOOMe	>98
5	BOPOMe		H2BOPOMe	>98
6	BOMe		H2BOMe	>98
7	BPNO$_2$		H2BPNH$_2$	82[a]
			H2BPNO$_2$	18[a]
8	BOCl		H2BOCl	0
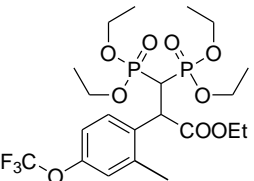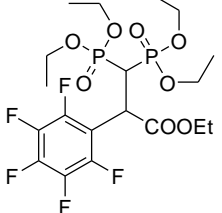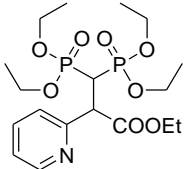
9	BPCF$_3$		H2BPCF$_3$	>98
10	B5F		H2B5F	>98
11	BPYR		H2BPYR	>98

Table 10: Non stereoselective bis-substituted VBP precursors Pd/C catalyzed hydrogenation. Reaction conditions: 1 mmol of BPs, 20 mol% of Pd/C 5%, 1 atm H$_2$, MeOH, r.t., t=1 night. [a] Isolated yield.

The reaction was carried out at room temperature in methanol, showing an excellent reactivity using 20 mol% (relative to VBP precursor) Pd/C 5% w/w (**Table 10, entries 1-11**). The amount of catalyst was relatively high to ensure high conversions. As long as the structure of the substrates is concerned, BPNO$_2$ hydrogenation led predominantly to H2BPNH$_2$ presenting a para-amino phenyl substituent together with H2BPNO$_2$ (**Table 10, entry 7**) as a minor secondary product. The result could be explained by the lack of chemoselectivity of palladium and was confirmed by mass spectrometry analysis. ^{31}P NMR spectra also clearly showed four doublets downfield shifted with respect to the starting prochiral VBP. It is worth to notice that H2BPNH$_2$ allows further functionalization of the amino group but chromatography is needed to isolate the product. In contrast, BOCl hydrogenation under identical experimental conditions not only led to double bond hydrogenation but ended up with the hydrodechlorination of the aromatic unit, leading to quantitative formation of H2BPHEt (**Table 10, entry 8**). The racemic products obtained were used to optimize chiral HPLC analytical methods for the subsequent asymmetric hydrogenation tests. In order to bypass the purification step, the methods were optimized allowing the elution of the separated enantiomers in the presence of the unsaturated reagent, with good separation of all species (see experimental). All obtained products were also characterized by NMR spectroscopy and GC-MS.

In **Figure 24** are reported some typical ^{1}H NMR spectra of a hydrogenated product. In particular, the characterization of H2BOOMe is reported with the comparison between ^{1}H-NMR (A) and ^{1}H {^{31}P}-NMR (B) showing in the latter spectrum the simplification of the resonances of the α and β protons that are characterized only by H-H coupling with a ^{3}J of 9.8 Hz. The ^{31}P {^{1}H}-NMR of H2BOOMe showed the presence of two doublets downfield shifted with respect to BPOOMe with a small coupling constant of 0.8 Hz (**Figure 25**).
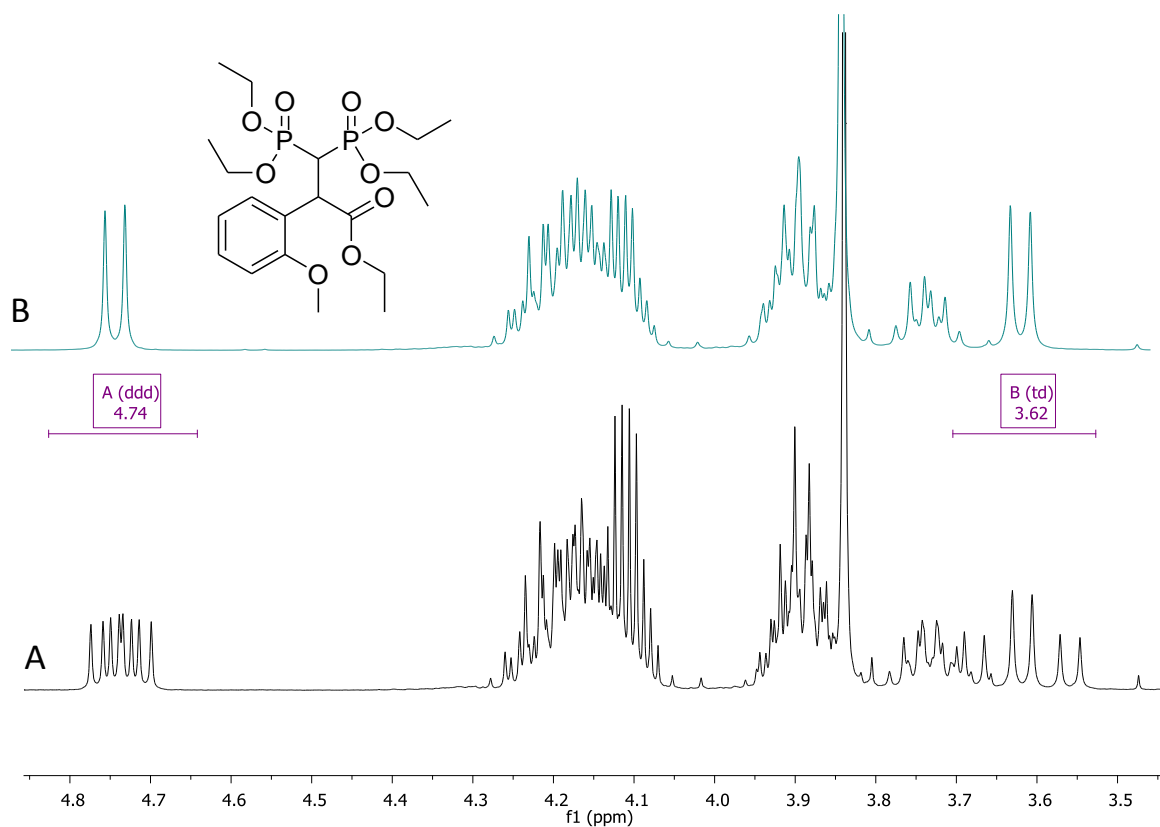
Figure 24: (A) ^{1}H-NMR and (B) ^{1}H {^{31}P}-NMR of H2BOOMe.
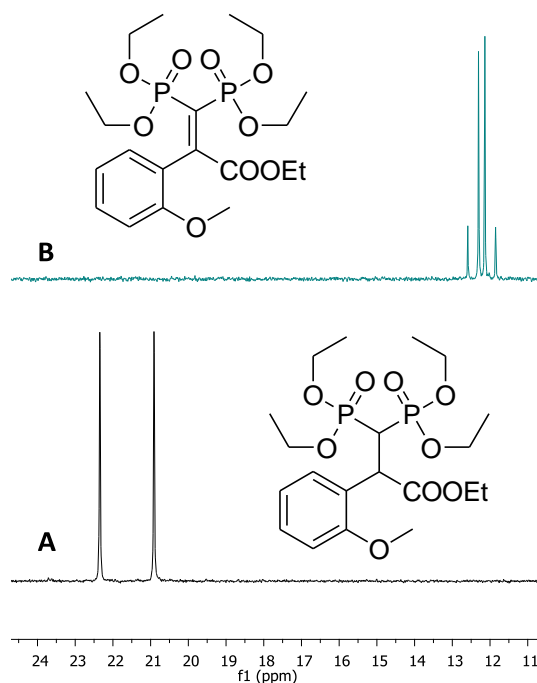
Figure 25: (A) ^{31}P {^{1}H}-NMR of H2BOOMe and (B) ^{31}P {^{1}H}-NMR of BOOMe.

2D-NMR HMBC of H2BOOMe shows long range ^{13}C-^{1}H resonances that turned out to be very useful to assign ^{13}C resonances as reported in **Figure 26 A-B**.
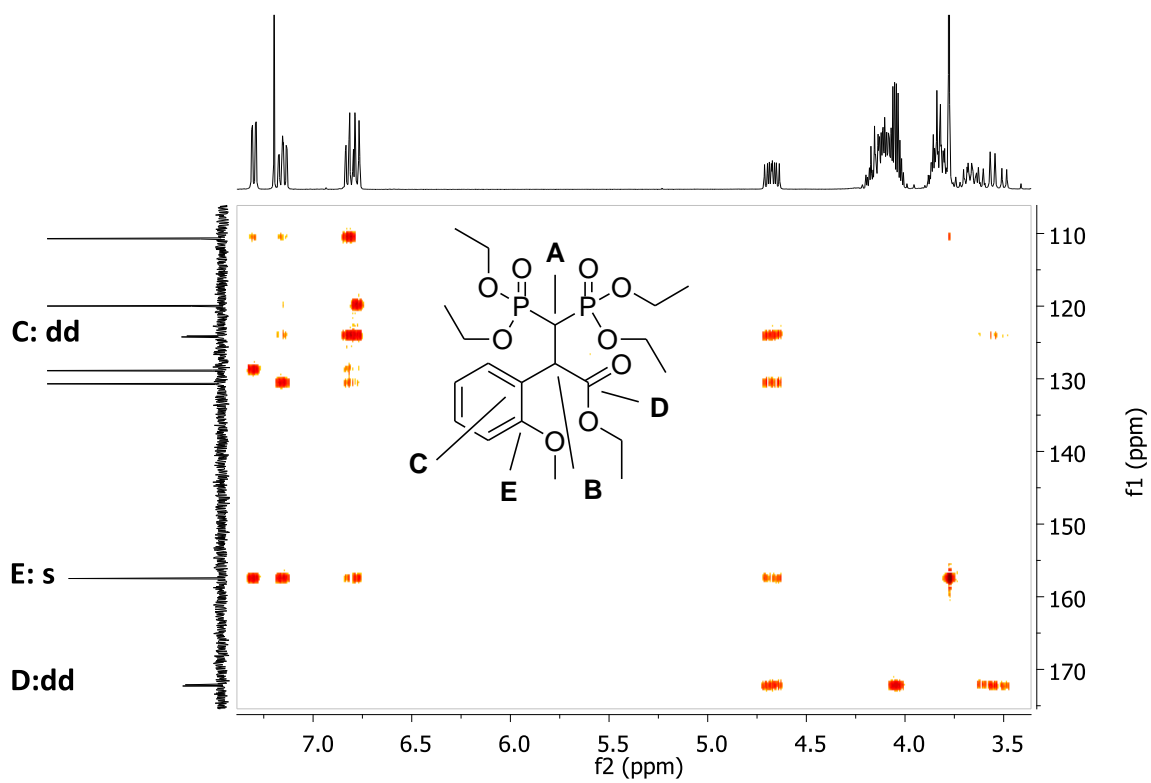
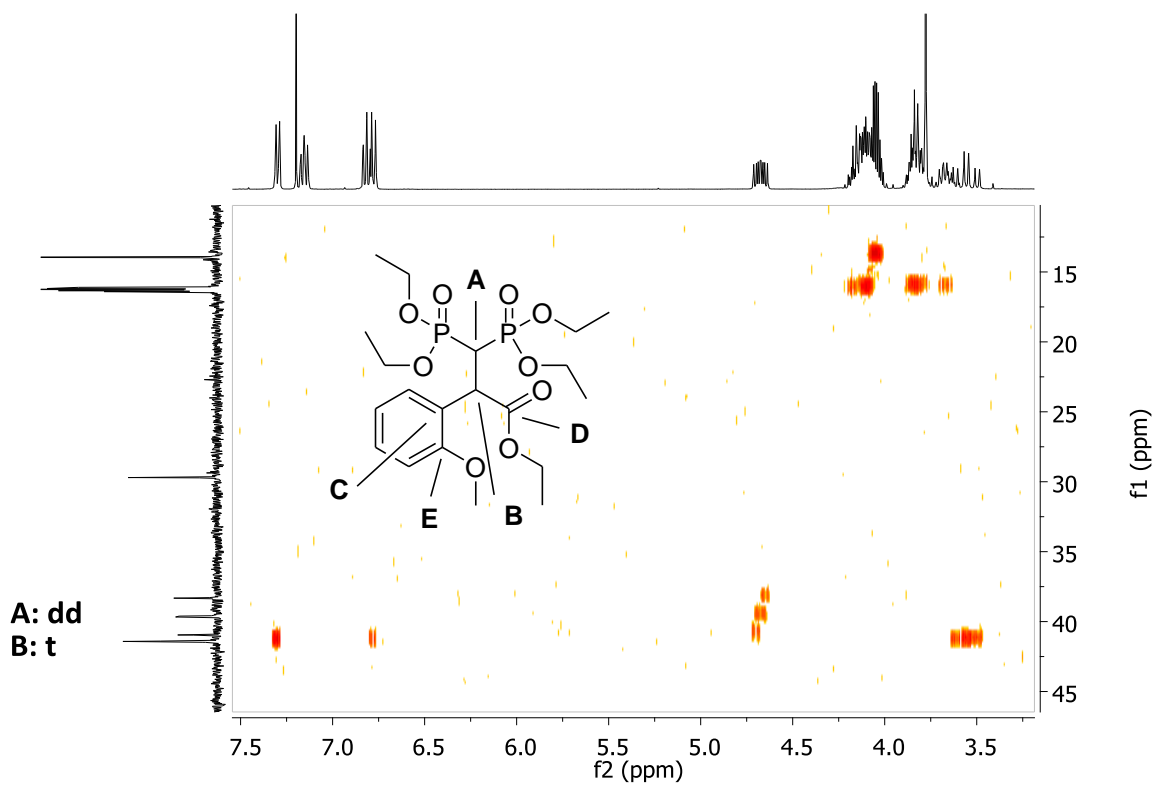Figure 26-A: 2D-NMR HMBC of H2BOOMe

Figure 26-B: 2D-NMR HMBC of H2BOOMe.

3.5.2 *Asymmetric Hydrogenation*

Rhodium, in comparison to other nobel metals like ruthenium and iridium, appears to be the best in asymmetric hydrogenations of olefin or α, β-unsaturated compounds as demostrated by a vast literature.[179] As long as the stereoselective hydrogenation of alkenes bearing the phosphonate moiety is concerned, previous studies demonstrated that best ligands were chiral phosphines. [180] BPPH was used as substrate for the stereoselective Rh(I) catalyzed hydrogenation reaction with the aim of screening some chiral enantiopure phosphinic ligands.

The use of 0,5% mol with respect of BP of (acetylacetonato)dicarbonylrhodium(I) coupled with (S)-BINAP or (*R*)-1-[(*S*)-2-(Diphenylphosphino)ferrocenyl]ethyldicyclohexylphosphine (JOSIPHOS) did not lead to any formation of the desired hydrogenation product at room temperature and 10 bar pressure of H_2. Use of the same catalytic systems under forced reaction conditions (higher pressure and temperature, 50 bar and 50°C) led to the same results. These drastic reaction conditions were used also with the metal precursor chloro(1,5-cyclooctadiene)rhodium(I) dimer without any ligands showing that Rh(I) is not able to catalyze the hydrogenation of the double bond of the di-substituted BP precursor. These results show that the formation *in situ* of the catalytically active species is an inefficient process in this specific case and suggest future reinvestigations of this enantioselective reaction using preformed Rh(I) chiral metal complexes as well as alternative metal centers like Ir(I) or Ru(II).

Metal catalysis was therefore abandoned and other reducing agents were considered. $NaBH_4$ is a reducing agent used in organic chemistry for more than a century, selective for the carbonyl groups of aldehydes, ketones, acyl chlorides and imines.[181] Use of enantiopure organocatalysts coupled with this reducing agent might lead to the desired stereo selective hydrogenation (**Scheme 16**). In this case the amount of organocatalyst is rather high as usually observed in most organocatalytic systems compared to metal catalyzed reactions.
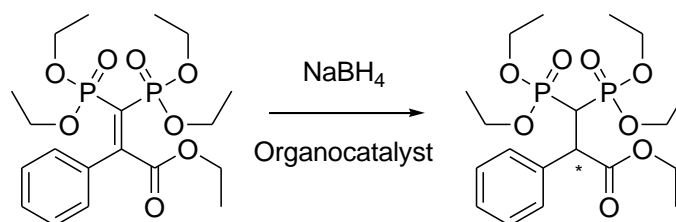
Scheme 16: PPH BP precursor organocatalyst-NABH$_4$ mediated hydrogenation.

	BP precursor	Organocatalyst	Yield [a] (%)	e.e. (%)
1	PPH	-	>99	-
2	PCOOEt	-	>99	-
3	PPH	TioQN	>99	0
4	PCOOEt	TioQN	>99	0
5	PPH	TioQD	>99	0
6	PCOOEt	TioQD	>99	0

Table 11: Asymmetric organocatalyzed NABH$_4$ hydrogenation of PPH.
Reaction conditions: 0.1 mmol of BP precursor, 20 mol% of organocatalyst, 3 eq. NaBH$_4$, 1 mL cyclohexane, T = 2 h. [a] Isolated yield.

Substitution with phosphonate residues results in an electron-poor double bond that should favor the nucleophilic attack of a hydride ion on the α carbon to the carbonyl group. In the absence of catalyst, NABH$_4$ hydrogenation of PPH and PCOOEt resulted in the quantitative formation of saturated products (**Table 11, entries 1 and 2**). The asymmetric reactions were performed with quinine-thiourea and quinidine-thiourea as organocatalyst (**Figure 27**) in order to verify if they were able to develop an asymmetric environment for the hydride addition in a enantioselesctive fashion. These organocatalysts are pseudo enantiomers derived from natural products, already used with phosphonate compounds [182] also in our group for some BP epoxidation reactions.[133]
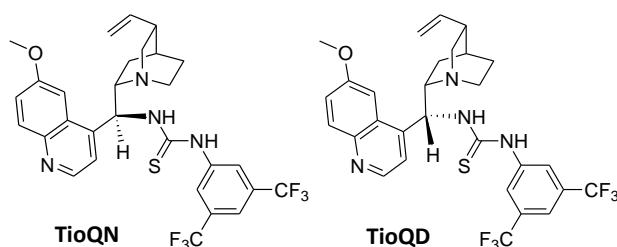
Figure 27: Thiourea quinine (TioQN) and thiourea quinidine (TioQD) organocatalysts.

The organocatalyzed hydrogenation led to quantitative yields of hydrogenated products with PPH (**Table 11, entries 3 and 5**) as well as PCOOEt (**Table 11, entries 4 and 6**). Chiral HPLC analyses showed howewer no asymmetric induction indicating that NaBH$_4$ is a too strong hydrogenation reagent to allow any (chiral) catalyst to display its action.

Other reducing agents extensively used in asymmetric organocatalytic protocols are 1,4-dihydropyridines. In particular, readily available Hantzsch ester (**Figure 28**) is used as a hydrogen equivalent giving often unsurpassed degrees of stereocontrol in the reduction of α,β-unsaturated carbonyl compounds, cyclic/acyclic imines and activated olefins.[183]
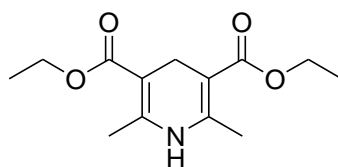
Figure 28: Diethyl 1,4-dihydro-2,6-dimethyl-3,5-pyridinedicarboxylate known as "Hantzsch ester".

For all these reactions, there is general consensus that hydrogen transfer takes place via a hydride. Experimental tests of asymmetric hydrogenation of PPH using the Hantzsch ester mediated by L-proline in apolar solvent at room temperature as well as at 60 °C resulted in no formation of the expected hydrogenated product.

Despite in literature are known enantioenriched compound with similar structure [184, 185] and albeit several metal-ligand combinations and organocatalysts have been investigated for the stereoselective hydrogenation, it seems that no promising method has yet been found. So future studies are called in order to obtain a new class of enantio-enriched BPs as new potential anti-resorptive drugs.

3.6   NITROGEN BISPHOSPHONATES

BPs containing nitrogen atoms or nitrogen eterocyclic substituents are very potent drugs to contrast osteoporosis, such as alendronate, ibandronate or risedronate. Imidazolyl substituted BP like zoledronate is up to date the most potent BP used in osteoporosis treatment. This active pharmaceutical ingredient (API) has its biochemical site of action on the mevalonate pathway with inactivation of osteoclasts already at nano molar concentrations. Development of new synthetic routes that allow to obtain nitrogen containing BPs is therefore a primary goal in the study of potential highly activity and highly effective osteoporosis drugs, focusing the attention on new derivatives with hopefully lower side effects.

3.7   β-NITRILE BISPHOSPHONATES

The exploration of new strategies to prepare a wide range of highly efficient N-BPs is a big challenge for the scientific community and several synthetic approaches have been proposed in the past. These procedures often use the VBP intermediate that undergoes nucleophilic attack leading to BPs bearing heterocycles like imidazole, pyrazole, purine [186] and other functional groups in the β position.[119]
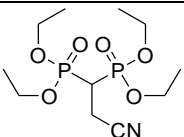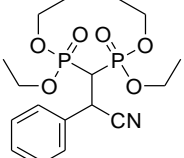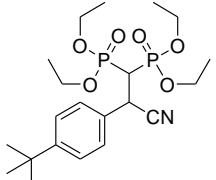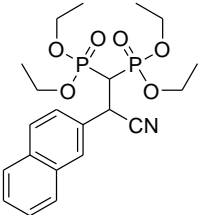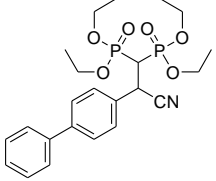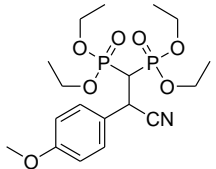
Compared to the extensively investigated catalytic cyanation of carbonyl moieties [187] catalytic cyanation of the alkene double bond is far less explored. Examples of catalytic hydrocyanation of activated electronpoor olefines are reported using Cu(I) or rare earth catalysts [188, 189] showing that also ionic liquid can be used. [190] Wang et al. used a titanium based catalyst in asymmetric catalytic cyanation of diethyl alkylidenemalonate with ethyl cyanoformate (NC-COOEt) as organic cyanide source.[191] Only one example of cyano-BP has been reported in the literature, using KCN solution in water/ethanol mixture as cyanide source.[192]

In the present section we describe an facile synthesis of a new series of β-nitrile substituted BPs without the gem hydroxyl function via a highly versatile catalytic addition of trimethylsilyl cyanide (TMSiCN) to VBP and other mono-substituted unsaturated BP precursors. The subsequent reduction and functionalization of β-nitrile BPs could form a new class of γ-amino BPs.

R: H, Ph
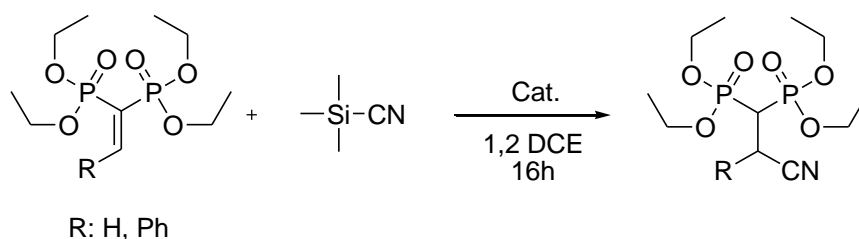
Scheme 17: addition of TMSiCN to VBP and mono-substituted BP precursors.

The reaction was initially investigated with VBP and PPH precursor (**Scheme 17**): while with VBP the reaction proceeded at 70°C in good yield without requiring a catalyst (**Table 12, entry 1**), the reaction on aryl substituted prochiral BPs must be catalyzed (**Table 12, entry 2-6**). The addition reaction between TMSiCN and PPH was investigated with different metal precursors (10 mol% catalyst loading) observing that Pd(II) and Cu(II) were less effective than Zn(II) (**Table 12, entries 3-5**). Zn(OTf)$_2$ showed the best catalytic activity providing the corresponding BP product in >98% yield at 70°C in 1,2-dichloroethane (DCE) even decreasing the catalyst loading to 5 mol% (**Table 12, entry 6**).

	Reagent	Product		Catalyst	Cat. [mol%]	Yield [a] (%)
1	**VBP**		**CNVBP**	-	- -	0[b] > 98
2	**PPH**		**CNPPH**	-	- -	0[b] 28
3	**PPH**	**CNPPH**		Cu(OTf)$_2$	10	79
4	**PPH**	**CNPPH**		Pd(OAc)$_2$	10	87
5	**PPH**	**CNPPH**		Zn(OTf)$_2$	10	> 98
6	**PPH**	**CNPPH**		Zn(OTf)$_2$	5	> 98
7	**PtBut**		**CNPtBut**	Zn(OTf)$_2$	5	85
8	**P2NAP**		**CNP2NAP**	Zn(OTf)$_2$	5	> 98
9	**P2PH**		**CNP2PH**	Zn(OTf)$_2$	5	> 98
10	**PPOMe**		**CNPPOMe**	Zn(OTf)$_2$	5	> 98
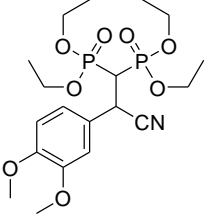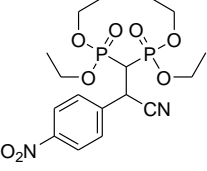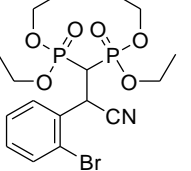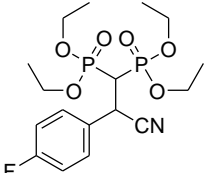
11	**PVER**		**CNPVER**	Zn(OTf)$_2$	5	> 98
12	**PPNO$_2$**		**CNPPNO$_2$**	Zn(OTf)$_2$	5	90
13	**POBr**		**CNPOBr**	Zn(OTf)$_2$	5	86
14	**PPF**		**CNPPF**	Zn(OTf)$_2$	5	90

Table 12:Catalyzed addition of TMSiCN to mono-substituted BP precursors.

Reaction conditions: VBP and BP precursors (20 mg), TMSiCN (5 eq.), DCE (1 mL), T= 70°C, 16 hours.

[a] Isolated yield, [b] T= r.t.

The optimized catalytic system was applied to a wide range of mono-substituted BPs caracterized by different properties: the steric and electronic character of the precursors did not influence much the outcome of the reaction (**Table 12, entries 7-14**). All used precursors showed excellent yields, apart for substrates bearing EWG (**Table 12, entries 12-14**). It is worth to notice that asymmetric conjugate cyanation of alkylidenemalonates is reported in literature, [193] obtaining cyano malonate derivatives with high enatioselectivity (up to 95%). So several attempts were made in order to investigate the asymmetric version of the reaction. These were carried out in the presence of N-polydentate chiral ligands such (+)-2,2'-Isopropylidenebis[(4R)-4-phenyl-2-oxazoline] (Box) or 2,6-Bis[(4S)-(−)-isopropyl-2-oxazolin-2-yl]pyridine (Pybox). Even though a sufficient activity was maintained, no asymmetric induction was observed (**Table 13, entries 1-6**). In order to understand these results, ^{1}H NMR analysis of the two ligands were initially registered. To these, Zn(OTf)$_2$ was added observing a shift of the signals most likely due to coordination to the metal. After addition of VBP the resonances of the ligands returned to be those typical of the free species in solution. This experiment likely indicates that the BP, acting as a bidentate ligand towards the metal, displaces the chiral ligand Box or PyBox that, being now free in solution, is no longer able to induce asymmetry to the reaction. Chiral complexes of metals such as Pt(II) and Pd(II) with (S,S)-Chiraphos or (s)-BINAP did not lead to any product formation (**Table 13, entries 7-9**). Chiral HPLC analysis confirmed that even the use of enantiopure organocatalysts such as quinine (QN), quinidine (QD) and their thioderivatives [194] (**Table 13, entries 10-13**) led to

comparable yields with respect to the use of the Zn(II) catalyst, but only as racemic product.
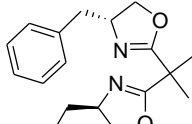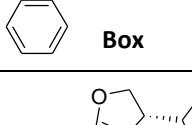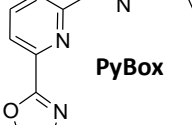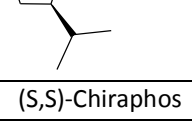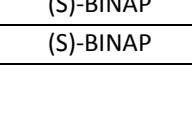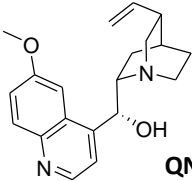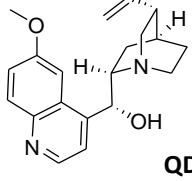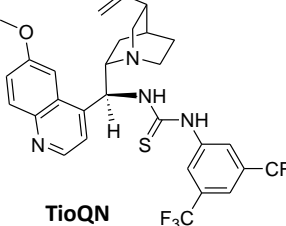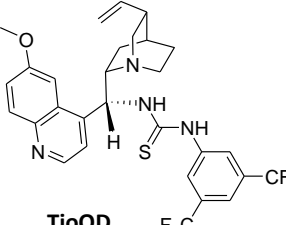
	Reagent	Product	Catalyst	Ligand	Lig. [mol%]	Yield[a] (%)	e.e. (%)
1	**PPH**	**CNPPH**	Zn(OTf)$_2$	**Box**	1	70	0
2	**P2NAP**	**CNP2NAP**	Zn(OTf)$_2$		1	66	0
3	**PPF**	**CNPPF**	Zn(OTf)$_2$		1	45	0
					3	65	0
4	**PPH**	**CNPPH**	Zn(OTf)$_2$	**PyBox**	1	68	0
5	**P2NAP**	**CNP2NAP**	Zn(OTf)$_2$		1	66	0
6	**PPF**	**CNPPF**	Zn(OTf)$_2$		1	25	0
					3	27	0
7	**PtBut**	**CNPtBut**	PdCl$_2$	(S,S)-Chiraphos	10	0 [b]	-
8	**PtBut**	**CNPtBut**	Pt(OTf)$_2$	(S)-BINAP	10	0 [b]	-
9	**PtBut**	**CNPtBut**	Pd μOH(BF$_4$)$_2$	(S)-BINAP	10	0 [b]	-
10	**PPF**	**CNPPF**	**QN**	-	-	82 [bc]	0
11	**PPF**	**CNPPF**	**QD**	-	-	73 [bc]	0
12	**PPF**	**CNPPF**	**TioQN**	-	-	>98 [bc]	0
13	**PPF**	**CNPPF**	**TioQD**	-	-	>98 [bc]	0

Table 13: Asymmetric addition of TMSiCN to mono-substituted BP precursors.

Reaction conditions: BP precursors (20 mg), TMSiCN (10 eq.), Cat. 5 mol%, DCE (1 mL), T= 70°C, 16 hours.

[a] Isolated yield, [b] Cat. 10 mol%, [c] n-hexane (1 mL), T= 50°C.

The new β-nitrile BP derivatives were subjected to deprotection of the phosphonate ester moiety by treatment with bromotrimethylsilane followed by hydrolysis with methanol.[139] The corresponding bisphosphonic acids were isolated in good yields and all substrates led to the corresponding bisphosphonic acid maintaining the newly introduced unit. The products were characterized by ^{1}H and ^{31}P NMR spectroscopy; in **Figure 29** the ^{1}H-NMR spectrum of CNPPH is reported showing the typical ^{1}H signals of the molecule.
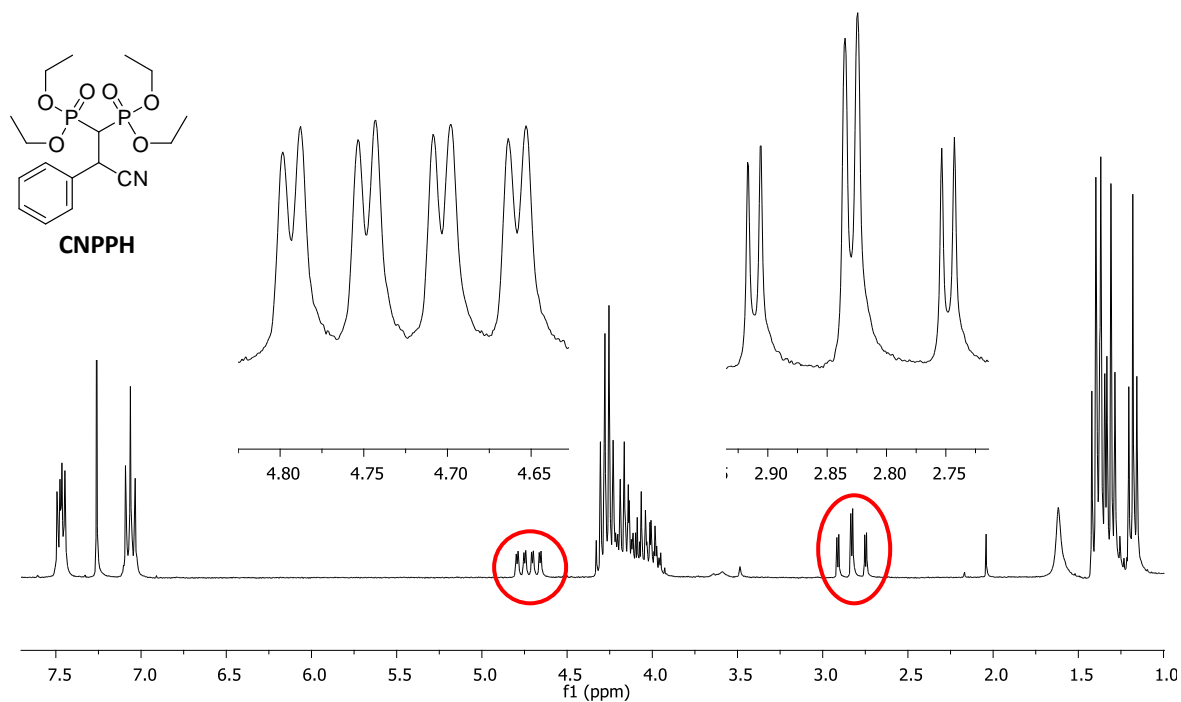
Figure 29: ^{1}H NMR (300 MHz, CDCl$_3$) of CNPPH.

While sharp resonances were observed in the ^{31}P spectrum of the protected compounds, NMR spectroscopy in D$_2$O of the deprotected bisphosphonic acids was characterized by very broad resonances indicating extensive aggregation phenomena. Electrospray MS analyses of the products were performed in methanol observing good matching between the [M-H]$^-$ ion and the ESI spectra on negative ion mode, thus confirming the structure of the BP products. In **Figure 30** the ESI-MS spectrum on negative mode of CNPPH is reported showing [M-H]$^-$ ion and other fragmentations.
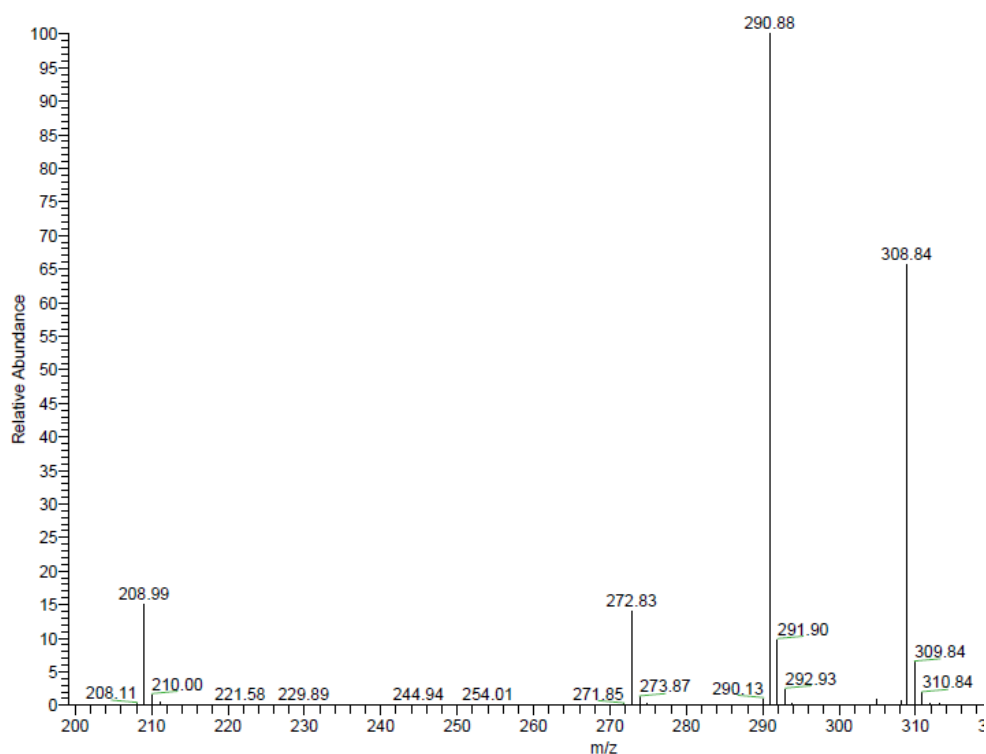
Figure 30: ESI-MS spectrum on negative mode of CNPPH.

The importance of the nitrile group in the side chain of the BP opens the way to the possibility reduction of this moiety to the corresponding amino group, that could further react to give substituted N-BPs. Several examples of cyano group reduction are reported in the literature using different reducing agents such as as hydrogen [195], sodium borohydride [196], lithium aluminum hydride [197] or other. [198, 199]

Reduction attempts and functionalization of nitrile group will be the subject of future studies in order to obtain a new class of γ-amino BPs as potential new N-BPs.

3.8 β-AZIDO BISPHOSPHONATES

It is known that a wide range of compounds containing the 1,2,3-triazole structural moiety exhibits diverse biological properties, [200] such as anti-HIV [201] or antimicrobial activities.[202] Concerning the introduction of 1,2,3-triazole groups into organic molecules, one of the most popular reactions is the Cu(I)-catalyzed azide-alkyne cycloaddition, known for the click chemistry developed by the groups of Sharpless [203] and Meldal.[204] This useful approach leads to 1,4-di-substituted 1,2,3-triazoles with high regioselectivity. As a consequence of the versatility of the click reactions and despite the azido-phobia related to the difficult handling of this class of compounds in medium amounts, there is a considerable interest in synthetic methodologies for the preparation of organic azides. In addition, several metodologies for azide reduction leading to the corresponding amines have been reported [205, 206] giving the opportunity to obtain terminal amino compound useful for further reactions.

While in the literature there are only a few examples of synthesis of α-azido [207] or γ-azido BPs, [208] syntheses and reactions with β-azido BP compounds is a highly debated topic. In particular, Chen et al. [209] published in 2013 the synthesis of tetraethyl 2-azidoethane-1,1-diyldiphosphonate (β-N$_3$BP) starting from VBP: the free azide product was obtained after only 15 minutes reacting sodium azide in water and acetic acid (1/1, v/v) at room temperature without observing the formation of by-products. On the contrary, in the same year Rodriguez and collaborators [210] showed that treating an excess of VBP with sodium azide in water at room temperature, did not lead to the direct formation of β-N$_3$BP (**Scheme 18**) but rather to the formation of double BP compoud (2BP) supposedly because of the 1,3-dipolar cycloaddition leading to the triazole-BP intermediate. Once produced, it reacted immediately with another molecule of VBP to undergo a Michael-type reaction yielding 2BP. NMR spectroscopic data supported this structure.
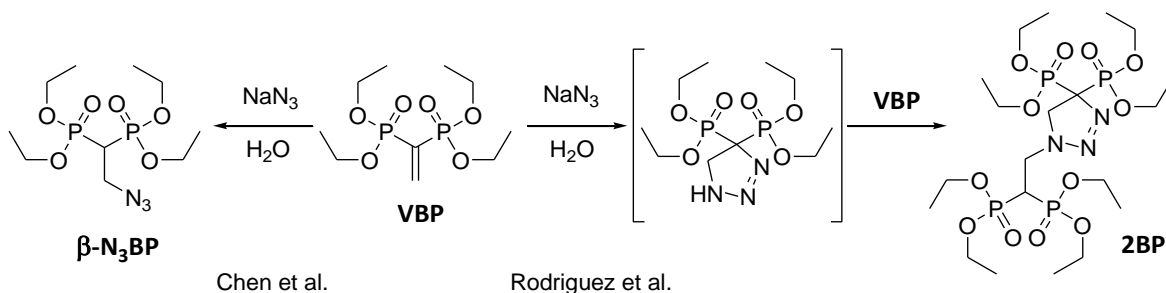
Scheme 18: Reported contrasting syntheses of β-azido bisphosphonate.

In this thesis a synthetic route is proposed, alternative to the use of NaN$_3$, enabling to work in organic medium to facilitate both the reactivity of hydrophobic substituted BP precursors and the isolation of the azido-products. Similarly to the previously reported metal catalyzed addition of cyanide to BP precursors, it was decided to investigate the

azide addition reaction using trimethylsilyl azide (TMSiN$_3$) as organic reagent to obtain β-azido BPs (**Scheme 19**). The resulting azido BP products could be useful for further Cu(I) mediated click cycloadditions or could be reduced to provide β-amino BPs.
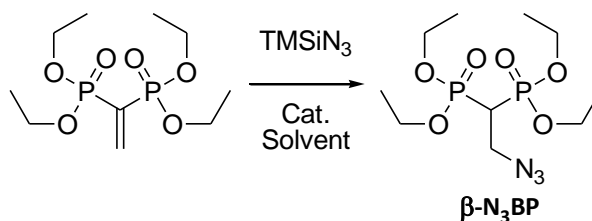
Scheme 19: Addition of trimethylsilyl azide to VBP under different experimental conditions.

The reaction between trimethylsilyl azide and VBP was initially investigated under different experimental conditions as reported in **Table 14**.

	BP Precursor	Catalyst	Solvent	Temperature (°C)	Yield[a] of Azido BP (%)	Yield[a] Of Amino BP (%)
1	**VBP**	Cu(OTf)$_2$	DCM	r.t.	0	0
2	**VBP**	Cu(OTf)$_2$	Toluene	110	0	0
3	**VBP**	Zn(OTf)$_2$	DCM	r.t.	0	0
4	**VBP**	Zn(OTf)$_2$	Toluene	110	0	20
5	**VBP**	PdCl$_2$	DCM	r.t	>98 26[b]	0 0[b]
6	**VBP**	Pd(OAc)$_2$	DCM	r.t	>98 >98[c]	0 0[c]
7	**VBP**	Pd(OAc)$_2$	Toluene	110	0	90
8	**VBP**	Pd(OAc)$_2$	Toluene	90	0	90
9	**VBP**	Pd(OAc)$_2$	Toluene	60	15	75
10	**VBP-Me**	Pd(OAc)$_2$	DCM	r.t	>98	0
11	**VBP-Me**	Pd(OAc)$_2$	Toluene	110	0	90

Table 14: Addition of TMSiN$_3$ to VBP under different experimental conditions.
Reaction conditions: 0.07 mmol of VBP, TMSiN$_3$ 5 eq., 5 mol% Cat., 2 mL of the solvent, t=18 h; [a] Isolated yield, [b] 2 mol% Cat, [c] 0.8 mmol of VBP.

The reaction was initially investigated with different metal precursors in 5 mol% catalyst loading, observing that Cu(II) as well as Zn(II) did not lead to the formation of the desired product at room temperature (**Table 14, entries 1 and 3**). While Cu(II) catalyst was inactive also under high temperature conditions (**Table 14, entry 2**), Zn(II) showed formation in moderate yield of the unexpected product tetraethyl 2-aminoethene-1,1-diyldiphosphonate (VBPNH$_2$) (**Table 14, entry 4**). Pd(II) metal catalyst (5 mol%) showed outstanding activity, giving the desired tetraethyl 2-azidoethane-1,1-diyldiphosphonate (β-N$_3$BP) in excellent yields at room temperature, while decreasing the metal loading to 2 mol% resulted in only partial conversion (**Table 14, entries 5 and 6**). Pd(II) catalyzed addition

of trimethylsilyl azide to VBP under high temperature (**Table 14, entry 7**) did not lead to formation of β-N$_3$BP but provided the unexpected VBPNH$_2$ in good yields (**Scheme 20**).
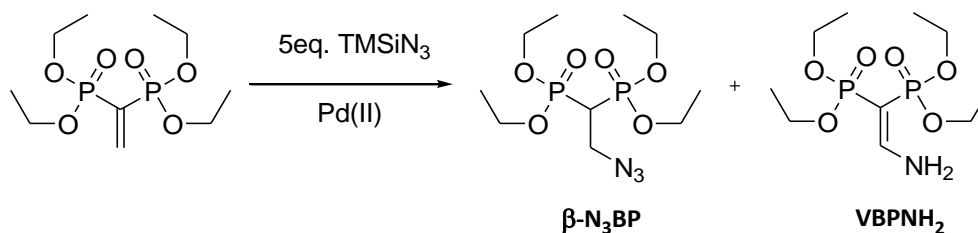
Scheme 20: Addition of TMSiN$_3$ to VBP provides different nitrogen BP products depending on the reaction temperature.

Decreasing the reaction temperature to 60°C led to the formation of both products (**Table 14, entry 9**). The formation of VBPNH$_2$ could probably be due to a thermal elimination of an N$_2$ molecule as described in **Scheme 21**.
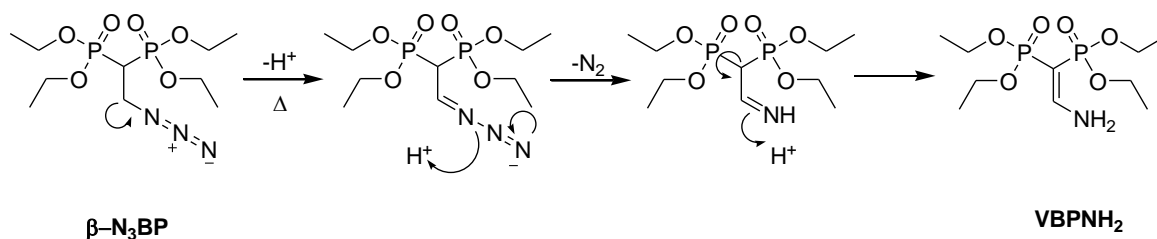
Scheme 21: proposed N$_2$ thermal elimination mechanism.

Tetramethyl 2-azidoethane-1,1-diyldiphosphonate (β-N$_3$BP-Me) was obtained under Pd(II) catalyzed addition of TMSiN$_3$ to VBP-Me (**Table 14, entry 10**) as well as tetramethyl 2-aminoethene-1,1-diyldiphosphonate (VBPNH$_2$-Me) when temperature was raised up to 110°C (**Table 14, entry 11**). The resulting azido-BP was found stable for several days if stored at -20°C, while decomposition and 2BP partial formation was observed if kept at room temperature. This phenomena could be explained assuming a retro-Michael reaction giving back VBP; 1,3 cycloaddition with the remaining β-N$_3$BP leads to the formation of 2BP as by-product. The reaction was repeated in 0.8 mmol VBP scale (**Table 14, entry 6**), showing that it can be easily scaled-up without relevant loss in product yield and allowing to use β-N$_3$BP for further Click Chemistry or reduction reactions. New azido and amino BP products were isolated and characterized by ^{1}H and ^{31}P NMR spectroscopy. In **Figure 31** it is reported a comparison of the ^{1}H-NMR (A) and ^{31}P {^{1}H}-NMR (B) spectra between VBP, β-N$_3$BP and VBPNH$_2$ showing presence of typical ^{1}H and ^{31}P signals of the molecules.
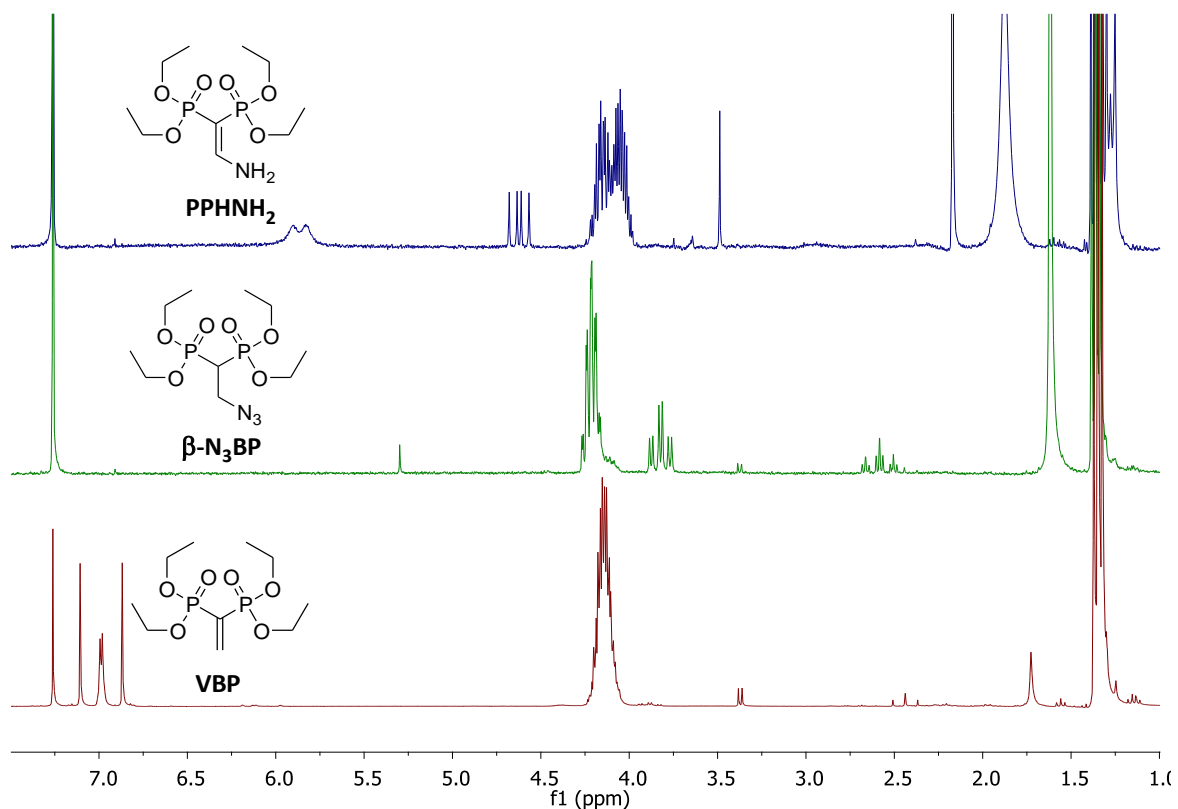
Figure 31: (A) ^{1}H-NMR comparison between VBP, β-N$_3$BP and VBPNH$_2$.
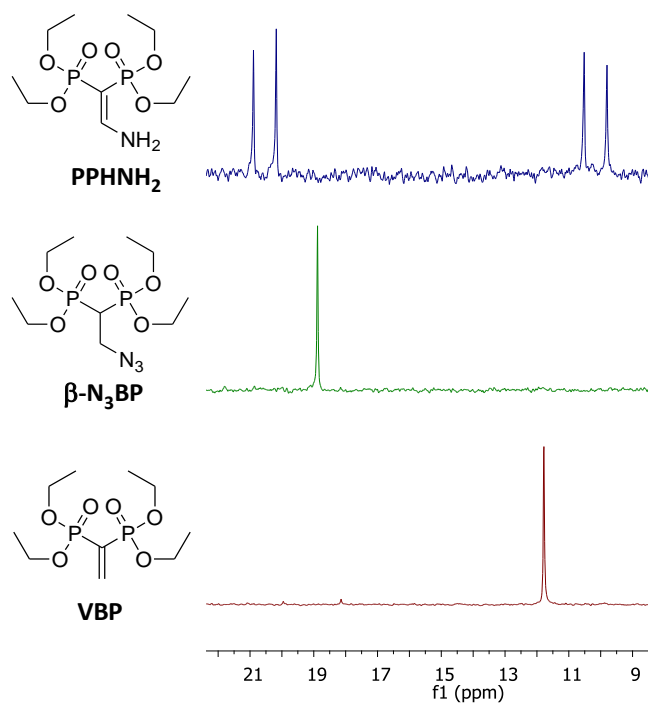
Figure 31: (B) ^{31}P {^{1}H}-NMR comparison between VBP, β-N$_3$BP and VBPNH$_2$.

In order to investigate the addition of TMSiN$_3$ to substituted VBP precursors, optimized catalytic conditions were tested also with PPH (**Scheme 22**).
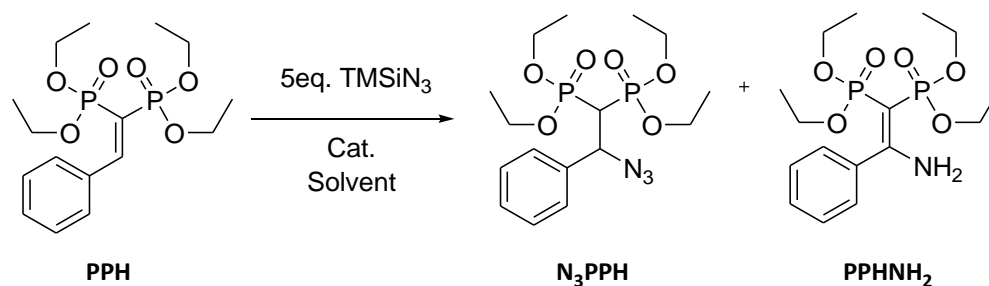
Scheme 22: Addition of TMSiN$_3$ to PPH forming different nitrogen BP products depending on the reaction temperature.

While Pd(II) was an excellent metal catalyst in TMSiN$_3$ addition to VBP, it was found less reactive with respect to monosubstituted VBP precursors like PPH (**Table 15, entries 1-4**). Increasing catalyst amount up to 10 mol% did not show a substantial increase in reaction yields (**Table 15, entries 2 and 3**), even using drastic temperature conditions (**Table 15, entries 4 and 5**). The use of Zn(OTf)$_2$ that showed modest reactivity with VBP (**Table 14, entry 4**), led to the formation of the desired tetraethyl 2-azido-2-phenylethane-1,1-diyldiphosphonate (N$_3$PPH) in moderate yield (**Table 15, entry 6**). Increasing the temperature, moderately increased the reaction yield (**Table 15, entry 7**) but at the same time led to predominant formation of tetraethyl 2-amino-2-phenylethene-1,1-diyldiphosphonate (PPHNH$_2$). Further increase in the reaction temperature led only to the formation of PPHNH$_2$ (**Table 15, entry 8**).

	Catalyst	Cat. Loading [mol%]	Solvent	Temperature (°C)	Yield [a] of Azido BP (%)	Yield [a] of Amino BP (%)
1	PdCl$_2$	5	DCM	r.t.	5	0
2	Pd(OAc)$_2$	5	DCM	r.t.	5	0
3	Pd(OAc)$_2$	10	DCM	r.t.	7	0
4	Pd(OAc)$_2$	10	Toluene	90	7	0
5	Pd(OAc)$_2$	10	Toluene	110	10	0
6	Zn(OTf)$_2$	10	Toluene	r.t	30	0
7	Zn(OTf)$_2$	10	Toluene	60	20	60
8	Zn(OTf)$_2$	10	Toluene	90	0	90

Table 15: Addition of TMSiN$_3$ to PPH under different experimental conditions.
Reaction conditions: 0.07 mmol of PPH, TMSiN$_3$ 5 eq., 2 mL of solvent, t=18 h; [a] ^{31}P-NMR yield.

Despite numerous purification attempts, it was not possible to isolate N$_3$PPH as pure product. Reduction of the azido moiety as well as functionalization of other substituted VBP precursors will be the subject of future studies in order to obtain a new class of β-amino BPs or β-azido BPs as potential new N-BPs.

3.9 COPPER-MEDIATED ADDITION of INDOLES to VBP PRECURSORS

Part of the results presented in this chapter were published in:

A. Chiminazzo, L. Sperni, M. Damuzzo, G. Strukul, A. Scarso, " *Copper-mediated 1,4-Conjugate Addition of Boronic Acids and Indoles to Vinylidenebisphosphonate leading to gem-Bisphosphonates as Potential Antiresorption Bone Drugs", ChemCatChem*, **2014**, 6, 2712 – 2718.

3.9.1 *Friedel–Crafts Reaction between Indoles and VBP*

3-Substituted indoles are important structures that are widely present in many common natural products [211] as well as in pharmacophores characterized by several biological activities.[212] Cu(II)-based catalysts bearing chiral ligands can efficiently promote the Friedel-Crafts reaction of indoles with alkylidene malonates or nitroalkenes in the enantioselective way.[213, 214, 215, 216] Although the reaction between indoles and VBP has been investigated under Brønsted basic and acidic conditions with emphasis on the regioselectivity of the reaction, [217] no examples of the reaction involving metal catalysis can be found in the literature.
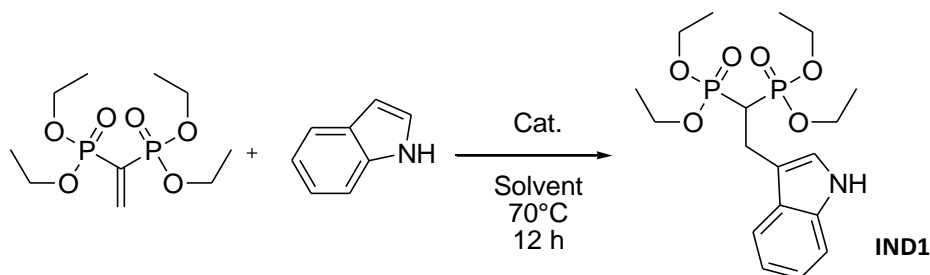
Scheme 23:General conjugate addition of indole to VBP.

Copper precursors were therefore tested in the Friedel–Crafts reaction between indole and VBP (**Scheme 23**), and it was found that Cu(OTf)$_2$ in 1,2 Dichloroethane (DCE) led to the expected reaction, forming the desired 3-substituted indole derivative in increasing amounts (up to 97% yield) as a function of the catalyst loading (**Table 16, entries 3–5**). In contrast, other copper catalysts with different anions and oxidation states, such as CuI, or other metal complexes such as PdCl$_2$ were found to be ineffective in promoting the reaction (**Table 16, entries 1 and 2**). The reaction did not give good yields in toluene (**Table 16, entry 6**) but in water with sodium dodecyl sulfate (SDS) used as a surfactant to improve substrate solubilization, the desired product was obtained in 94% yield, which was comparable to what observed in DCE (**Table 16, entries 5 and 7**). The use of water as a reaction medium has also been confirmed for other Friedel–Crafts-type conjugate additions of indoles by using a Lewis acid–surfactant combined catalyst in water;[218] however, this is the first example, to our knowledge, in which this approach has been
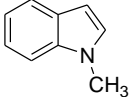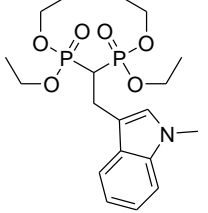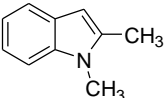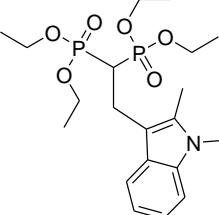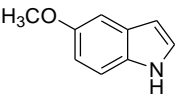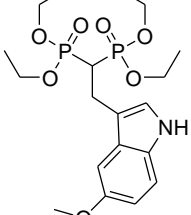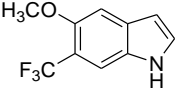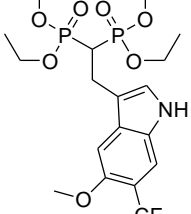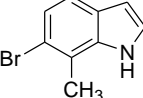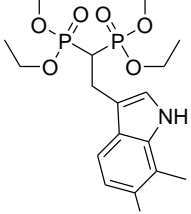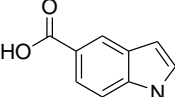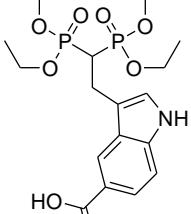
applied to the synthesis of BPs. The possibility to use either an organic solvent or a micellar medium in this reaction was further investigated.

	Catalyst	Cat. Loading [mol%]	Solvent	Yield [a] (%)
1	CuI	10	DCE	0
2	PdCl$_2$	10	DCE	0
3	Cu(OTf)$_2$	2	DCE	39
4	Cu(OTf)$_2$	5	DCE	47
5	Cu(OTf)$_2$	10	DCE	97
6	Cu(OTf)$_2$	10	Toluene	56
7	Cu(OTf)$_2$	10	Water/SDS	94

Table 16: Conjugate addition of indole to VBP mediated by different metal precursors.
Experimental conditions: VBP (0.3 mmol), indole (0.5 mmol), 2 mL solvent, T= 70°C, t= 12 hours.
[a] Isolated yield, [b] [SDS]=100 mM.

For the reaction in DCE, the optimized catalytic system was used with a wide range of indoles characterized by different electronic and steric properties (**Table 17**). The reaction is intrinsically sensitive to the electronic properties of the indole used.[219] Thus, indoles bearing electron-donating substituents such as 1-methylindole and 1,2-dimethylindole provided the corresponding Friedel-Crafts products in high yield (**Table 17, entries 1 and 2**). The electron-rich substrate 5-methoxyindole provided the corresponding BP addition product in 98% yield, whereas the presence of an extra trifluoromethyl moiety in position 6 of the same structure drastically reduced the yield to 44% and a similar effect was observed with 6-bromo-7-methyl-indole (**Table 17, entries 3-5**). Notably, electron-poor substrates such as the ester 5-(carboxymethyl) indole and the corresponding free acid 5-carboxyindole led to the formation of BP products in moderate yields (**Table 17, entries 6 and 7**) whereas 5-carboxamide indole was found to be completely inactive. With the above-mentioned indole substrates, the reaction in water/SDS led in most cases to comparable and in few cases even better yields related to the ability of the micellar medium to dissolve the reagents and place them close to the metal catalyst. Indoles with substituents in position 2 showed moderate to good activity: the reaction with 2-phenylindole, which is an extremely important structure in medicinal chemistry, led to the formation of the corresponding BP derivative in 77% yield in DCE and 53% yield in water/SDS (**Table 17, entry 8**). A similar reagent bearing a *p*-Cl residue led to the formation of the product in moderate yield, whereas a substrate like 2-(hydroxymethyl)indole, even if more electron rich than indole, did not lead to product formation. The use of water/SDS as a reaction medium was beneficial for the 2-*p*-Cl-phenyl-substituted indole, which led to the formation of the corresponding BP product in 88% yield (**Table 17, entry 9**). A ditopic substrate such as indole-5-boronic acid led only to the formation of the corresponding 5-substituted indole (**Table 17, entry 10**) but no formation of the 3-substituted indole product confirmed what reported for typical boronic substrates (**Chapt. 3.3**). The reaction could easily be scaled up using 3 mmol of VBP with 1.5 eq. of 1,2-dimethylindole in the

presence of 10 mol% Cu(OTf)$_2$ in DCE, which led to the formation of the corresponding isolated product in 94% yield.

	Indole	Product		Yield [a] (%)
1			IND2	67 78[b]
2			IND3	>98 96[b]
3			IND4	98 85[b]
4			IND5	44 82[b]
5			IND6	84 49[b]
6			IND7	50 51[b]
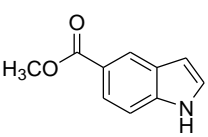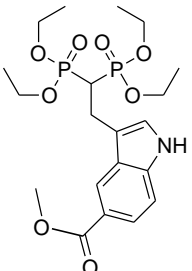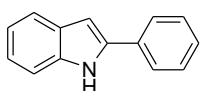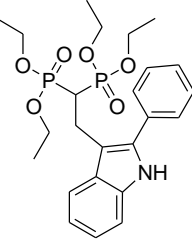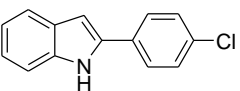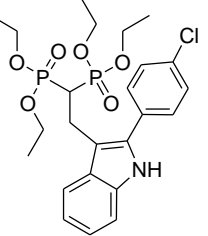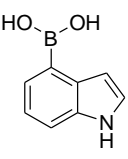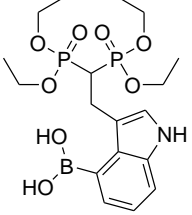
7	H₃CO—indole structure	IND8 structure	**IND8**	48 41 [b]
8	2-phenylindole structure	IND9 structure	**IND9**	77 53 [b]
9	2-(4-chlorophenyl)indole structure	IND10 structure	**IND10**	38 88 [b]
10	boronic acid indole structure	IND11 structure	**IND11**	0

Table 17: Friedel-Crafts reaction of indoles to VBP mediated by $Cu(OTf)_2$ under optimized experimental conditions.
Experimental conditions: VBP (0.3 mmol), indole (0.5 mmol), 10 mol% of Cu(OTf)2, 2 mL DCE, T= 70°C, t= 18 hours. [a] Isolated yield, [b] [SDS]=100 mM.

In some cases the yields in aqueous micellar environment were modest compared to the organic solvent (**Table 17, entries 1, 3, 5, 8**) probably because of the poor solubility of the corresponding indoles in water despite the presence of SDS. Where the reactions in an aqueous environment led to an increase in yield, or to a result comparable to the organic medium (**Table 17, entries 2, 4, 6, 7, 9**), it is reasonable to assume that the micellar system dissolves the reactants inside the micelles, leading to a more intimate proximity with beneficial effects on the reaction. The increase of reactivity moving from an organic solvent to a micellar environment could also be explained considering the positioning of the Cu(II) cation: in water it can act as countercation of sodium dodecyl sulfate in place of sodium. This favors an even better proximity between reagents present inside the micelles and the catalyst likely placed close to the hydrophilic head of the surfactant (Stern layer).

Selected new indolyl BP products were subjected to subsequent deprotection of the phosphonate ester moiety by treatment with trimethylbromosilane[139] followed by

hydrolysis with the water/methanol solution (9:1). The corresponding bisphosphonic acids were isolated in good yields and were characterized by ^{1}H and ^{31}P-NMR spectroscopy in D_2O. Not all indole BP esters led to the formation of the corresponding bisphosphonic acids owing to side reactions observing in some cases the release in solution of the original indole due to retro-Michael side reactions.
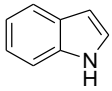
3.9.2 *Friedel–Crafts Reaction between Indoles and Substituted VBP Precursors*
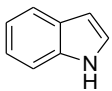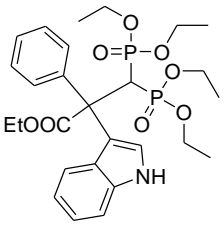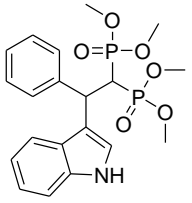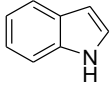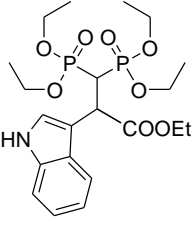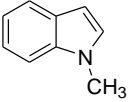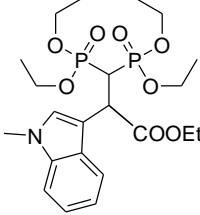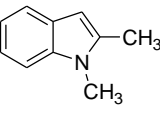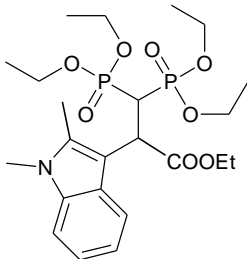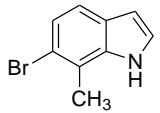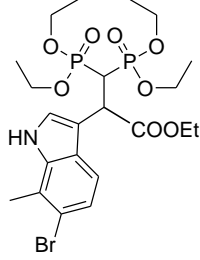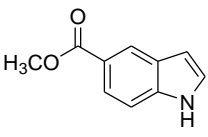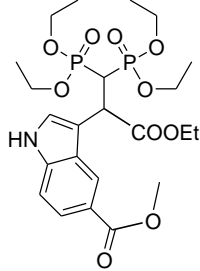
Several attempts were made to investigate the asymmetric version of the indole Friedel-Crafts reaction using substituted bisphosphonate precursors (**Scheme 24**) with different electronic properties under the above optimized catalytic conditions.
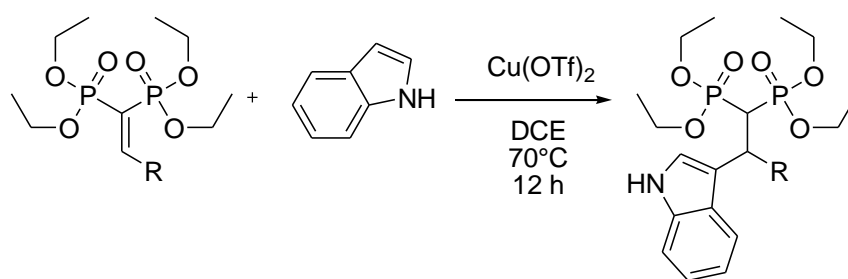
Scheme 24: General Friedel-Crafts reaction of indole to substituted VBP precursors.

Tests on PPH and PPNO$_2$ precursors were performed with free Cu(OTf)$_2$ as well as in the presence of chiral ligands like (+)-2,2'-Isopropylidenebis[(4R)-4-benzyl-2-oxazoline] (Box) or 2,6-bis[(4S)-(−)-isopropyl-2-oxazolin-2-yl]pyridine (PyBox) but unfortunately, no evidence of product formation was obtained (**Table 18, entries 1 and 2**) recovering in both cases, only the unconverted prochiral bisphosphonate reagent.

	VBP reagent	Indole	Product	Yield [a] (%)
1	**PPH**		IND1PPH	0 0[b] 0[c]
2	**PPNO$_2$**		IND1PPNO$_2$	0 0[b] 0[c]

3	**BPHEt**			**IND1BPHEt**	0
4	**PPH-Me**			**IND1PPH-Me**	0
5	**PCOOEt**			**IND1Et**	49 43[d]
6	**PCOOEt**			**IND2Et**	37
7	**PCOOEt**			**IND3Et**	64
8	**PCOOEt**			**IND6Et**	28
9	**PCOOEt**			**IND8Et**	18
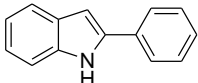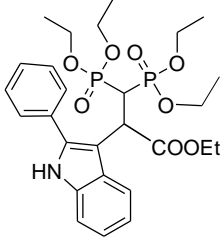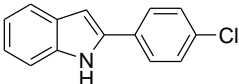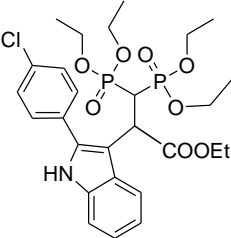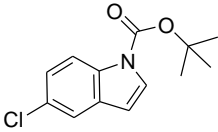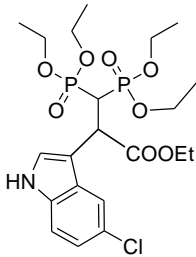
10	**PCOOEt**			**IND9Et**	26
11	**PCOOEt**			**IND10Et**	13
12	**PCOOEt**			**IND11Et**	22

Table 18: Addition of indoles to substituted VBP precursors mediated by Cu(OTf)$_2$.
Reaction conditions: 1 mmol monosubstituted VBP, 1.5 mmol indole, 10 mol% Cu(OTf)$_2$ in DCE, T=70°C, t=12h. [a] Isolated yield, [b] 2 mol% of Box, [c] 2 mol% PyBox, [d] [SDS]=100 mM.

Even the use of a di-substituted BP precursor did not lead to the formation of the desired product (**Table 18, entry 3**) as well as monosubstituted reduced steric hindrance precursors like PPH-Me (**Table 18, entry 4**); so the lack of reactivity is probably due to intrinsic steric hindrance present in the β position of the aromatic substituted BP precursors.

The addition of indole on PHCOOEt (**Table 18, entry 5**), a non aromatic monosubstituted precursor, confirmed the formulated hypothesis, showing a successful addition reaction. As previously observed, indole reacted on carbon 3 of the five membered ring, which is the most electron-rich position. The reaction took place also in aqueous micellar media (**Table 18, entry 5**) as previously reported for the addition of indoles to VBP, obtaining yields similar to those obtained in an organic solvent. PCOOEt was then used with a wide range of indoles with different electronic and steric properties applying the optimized catalytic system (**Table 18, entries 6-12**). In general the presence of electron-donating groups as substituents in the nitrogen five membered ring of substituted indoles led to higher reaction yields (**Table 18, entries 6 and 7**) compared to the presence of electron withdrawing groups (**Table 18, entries 8 and 9**). Moreover, with sterically hindered indoles containing phenyl substituents, a lowering of the reaction yields was observed (**Table 18, entries 10 and 11**). With 1-(tert-butoxycarbonyl)-5-chloroindole (**Table 18, entry 12**) partial loss of the tert-butoxycarbonil group occurred during the reaction, leading to the completely deprotected product after chromatographic purification, presumably because of the acid character of silica. The results were confirmed by GC-MS analysis and ^{1}H NMR that

showed the presence of signals typical of the indolyl nitrogen proton. Comparing the results for the addition of indoles to PCOOEt with those previously observed for the reaction on VBP, generally lower yields were observed most likely due to steric effects at the β position.

All products obtained were characterized by ^{1}H, ^{31}P, ^{13}C NMR spectroscopy and GC-MS. In **Figure 32** the ^{31}P {^{1}H}-NMR of IND1Et is reported showing two doublets with a really small coupling constant (J = 2.4 Hz) down-field shifted compared to BPPHEt.
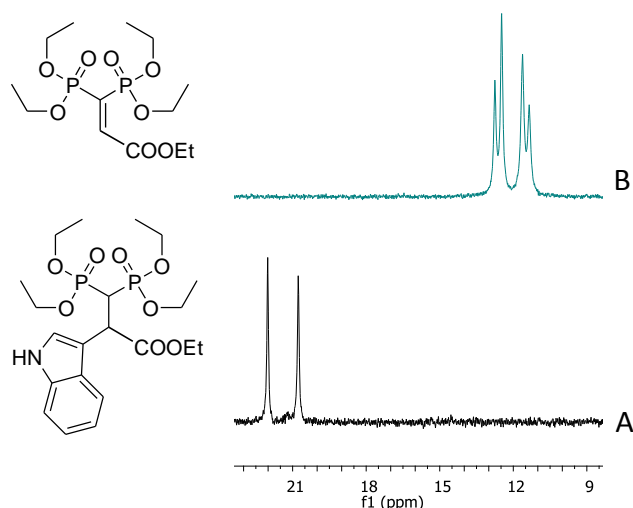
Figure 32: (A) ^{31}P {^{1}H}-NMR of IND1Et and (B) ^{31}P {^{1}H}-NMR of BPPHEt.

2D-NMR COSY (**Figure 33**) showed unusual cross-peak between ethyl ester protections protons highlighting [1]H-^{1}H resonances between α and β protons. 2D-NMR HSQC (**Figure 34**) helped to confirm the synthesis of desired indolyl-BP product, giving the possibility to verify ^{13}C assignements.
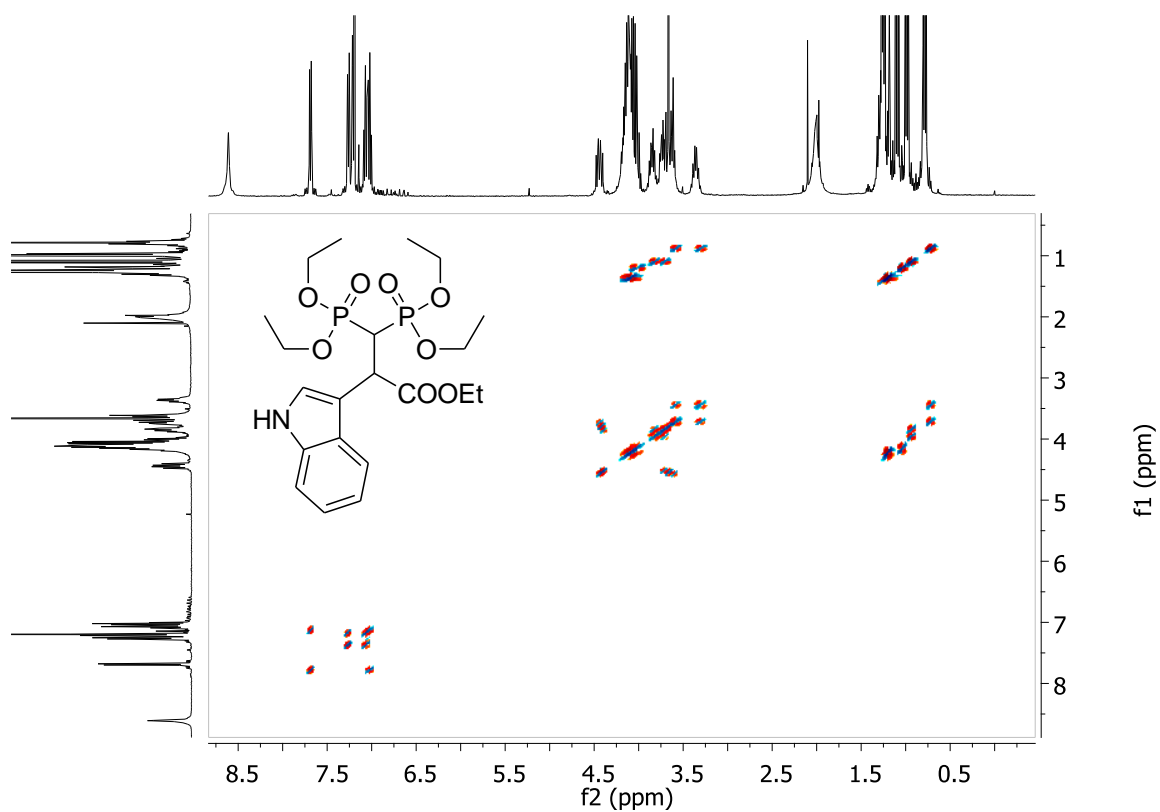
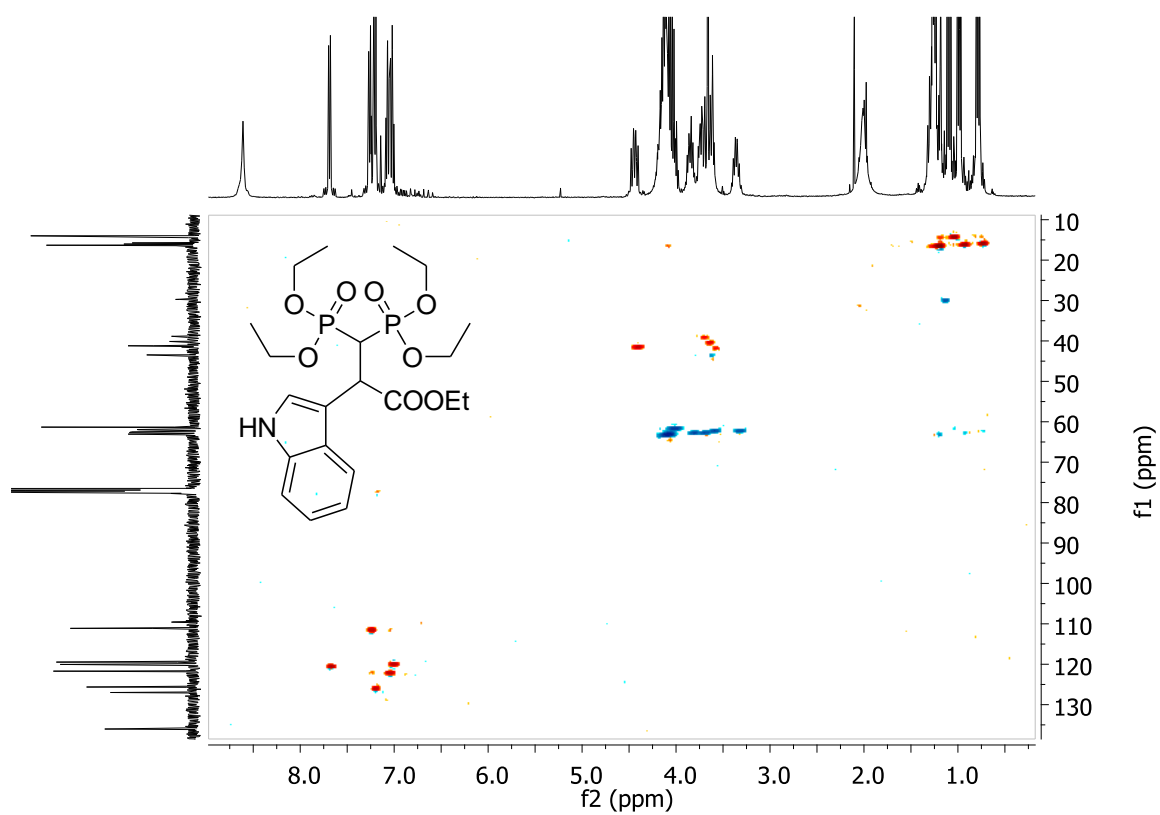Figure 33: 2D-NMR COSY of IND1Et.

Figure 34: 2D-NMR HSQC of IND1Et.

The new indolyl BP products IND1Et was deprotected with trimethylsylil bromide following an improved procedure compared to those reported in the literature [139] (**Chapt. 3.4.2**). The corresponding bisphosphonic acid IND1Et-OH was isolated in good yields and characterized by ^{1}H and ^{31}P-NMR spectroscopy in D_2O.

Very recently Weng and co-workers [220] reported about the highly enantioselective Friedel–Crafts reactions of indoles with α,β-unsaturated esters and nitroalkenes using chiral bis-oxazoline-Cu(II) as catalysts, affording chiral indole derivatives in good to excellent yields (up to 99%) and enantioselectivities (up to 96% ee). Despite the above reported observation that BPs can act as ligands towards certain metals (**Chapt. 3.7**),the Friedel-Crafts addition of indoles to PCOOEt in the presence of asymmetric oxazoline ligands will be tested in future studies to achieve a new class of enantio-enriched indolyl BPs as potential anti-resorptive drugs with better permeability properties as reported by other authors.[221]
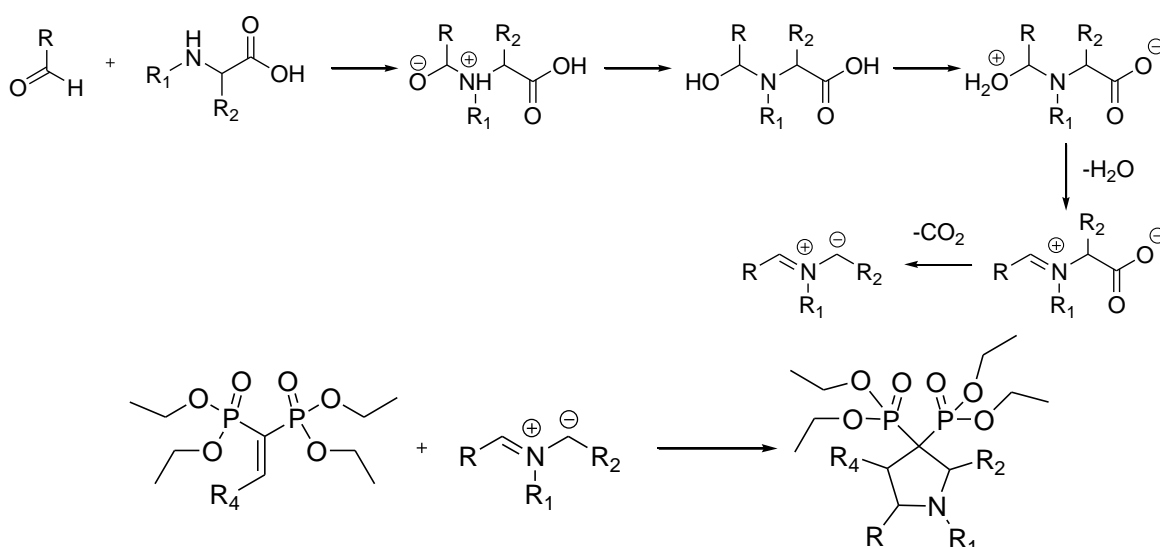
3.10 PYRROLIDINE BISPHOSPHONATES

One of the main methods to obtain nitrogen containing heterocycles compounds is represented by cycloaddition reactions. The 1,3-dipolar cycloaddition, also known as the Huisgen cycloaddition, [222] are concerted pericyclic reactions that are exploited for the synthesis of molecules of fundamental importance for both academic research and industrial applications. These reactions take place between a 1,3-dipole and a dipolarophile, generally an unsaturated bond, to form a five-membered ring as shown in **Scheme 25**.
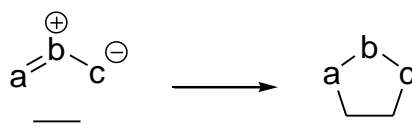
Scheme 25: General scheme of the 1,3 dipole and dipolarophile cycloaddition.

It was after the discovery of the Diels-Alder reactions in 1928 [223] that the synthetic value of the cycloaddition reactions became evident and constant evolution occurred over the years discovering new classes of 1,3-dipoles, such as nitrile compounds, azomethine ylides or diazoalkanes [224] that find common application in syntheses.

VBP efficiently acts as a dienophile [210] in Diels-Alder cycloadditions reacting with dienes [225] providing cyclic carbon BPs as well as in 1,3-dipolar cycloaddition reacting with nitrones [139] giving isoxazolidine N-BPs. Taking inspiration from the numerous examples of 1,3-dipolar cycloadditions of azomethine ylides to electron poor alkenes known in the literature, also in the enantioselective version, [226] in the present section it is described the synthesis of a large series of substituted BPs containing pyrrolidines via 1,3-dipolar cycloaddition of azomethine ylides [227] to VBP and other substituted BP precursors as dipolarophiles (**Scheme 26**).


Scheme 26: Formation of the intermediate azomethine ylide species by reaction of aminoacids and aldehydes followed by 1,3 cycloaddition with BP precursors.

The obtained products are therefore pyrrolidine derivatives with the bisphosphonate unit on carbon atom in position 3. BP with similar structures have been reported in the literature only marginally. Examples are the Grigg azometin ylide 1,3-dipolar cascade cycloaddition [228] reaction of VBP with an aldehyde and diethyl aminomalonate [210] (**Scheme 27**) and the reaction between proline with aromatic aldehydes and VBP catalyzed by cerium(IV) oxide (**Scheme 28**) forming (3-substituted-hexahydro-1H-pyrrolizine-1,1-diyl)bis(phosphonate) products in the protected tetraethyl ester form.[229]
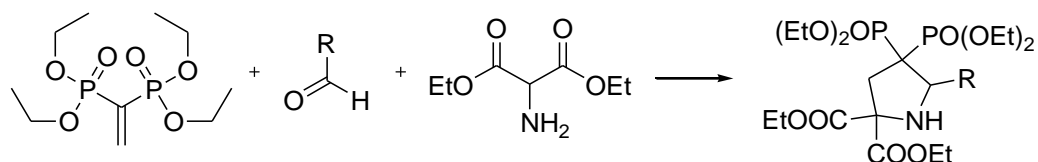

Scheme 27: 1,3-dipolar cycloaddition reaction between VBP with diethyl aminomalonate and aldehydes.
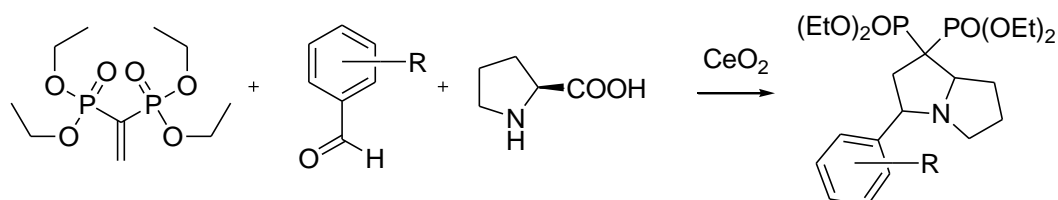
Scheme 28: Ce(IV) catalyzed 1,3-dipolar cycloaddition reaction between VBP, L-proline and aldehydes.

It was decided to deeply investigate the reaction between the VBP and similarly monosubstituted prochiral dipolarophiles in the 1,3-dipolar cyclization reaction with azometin ylides. The latter *in situ* formed intermediate reagents were obtained by combination of several amino acids and derivatives coupled with different aldehydes. Different combinations of reagents and experimental conditions were investigated to produce an as wide as possible range of multisubtituted pyrrolidine BP derivatives. Firstly the role of the amino acid in the reaction between VBP and paraformaldehyde was considered in order to investigate the steric and electronic effects of the side chain on the reaction (**Scheme 29**). Depending on the amino acid employed, differently C-2 substituted pyrrolidines rings were obtained.
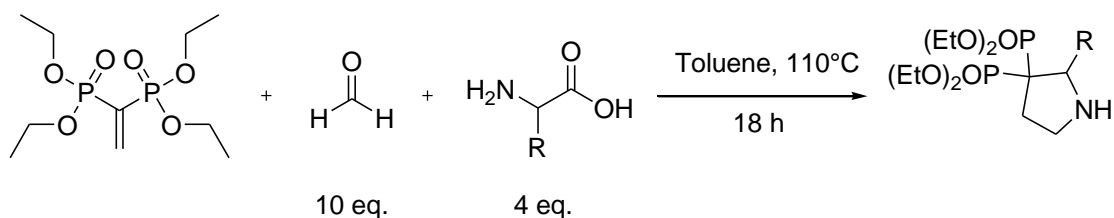
Scheme 29: 1,3 cycloaddition between VBP, formaldehyde and different amino acids.

	Amino Acid	Product		Yield (%)
1	(glycine structure)	(EtO)$_2$OP, (EtO)$_2$OP pyrrolidine NH	**GLY1**	>98[ab]
2	(alanine structure)	(EtO)$_2$OP, (EtO)$_2$OP methyl pyrrolidine NH	**ALA1**	27[c]
3	(valine structure)	(EtO)$_2$OP, (EtO)$_2$OP isopropyl pyrrolidine NH	**VAL1**	26[c]
4	(glutamic acid structure)	(EtO)$_2$OP, (EtO)$_2$OP CH$_2$COOH pyrrolidine NH	**GLU1**	0
5	(isoleucine structure)	(EtO)$_2$OP, (EtO)$_2$OP sec-butyl pyrrolidine NH	**ISO1**	0
6	(proline structure)	(EtO)$_2$OP, (EtO)$_2$OP bicyclic N	**PRO1**	0
7	(phenylalanine structure)	(EtO)$_2$OP, (EtO)$_2$OP benzyl pyrrolidine NH	**PHA1**	0
8	(sarcosine structure)	(EtO)$_2$OP, (EtO)$_2$OP pyrrolidine N-CH$_3$	**SAR1**	>98[ab]

Table 19: 1,3 cycloaddition between VBP, formaldehyde and different amino acids.
Reaction conditions: 0.65 mmol VBP, 2.5 mmol amino acid, 6.5 mmol of paraformaldehyde in 25 mL of toluene, T=110°C, t=18 h. [a] Isolated yield, [b] t=5 h, [c]= ^{31}P-NMR yield.

Reaction between VBP, paraformaldehyde and different amino acids was studied observing excellent yield of the corresponding pyrrolidine BP product when unsubstituted amino acids like glycine was used (**Table 19, entry 1**). N-substituted amino acid like sarcosine (**Table 19, entry 8**) resulted in high activity giving quantitative reaction yields. Similarly to glycine, sarcosine cycloaddition to VBP gave quantitative yield in only 5 hours (**Table 19, entries 1 and 8**). Use of substituted amino acids showed that the reaction is higly influenced by the R group of the reagent: while alanine (**Table 19, entry 2**) and valine (**Table 19, entry 3**) resulted in a significant reduction in reaction yields, with amino acids bearing more branched and longer substituents gave untreatable mixtures of by-products (**Table 19, entries 4-7**). It is worth noting that, when chiral enantiopure L-alanine or L-valine were used, the corresponding pyrrolidine BP products retained the presence of a stereocenter on the C-2 carbon atom. This is confirmed by the ^{31}P NMR spectra of the products that shows two diasterotopic ^{31}P resonances due to the asymmetry of the molecules (**Figure 35**). Although starting from a natural enantiopure substrate, the BP products were

obtained as a racemic mixture. This is due to the loss of the original stereocenter in the decarboxylation step of the reaction leading to the formation of the 1,3-dipole. [227]
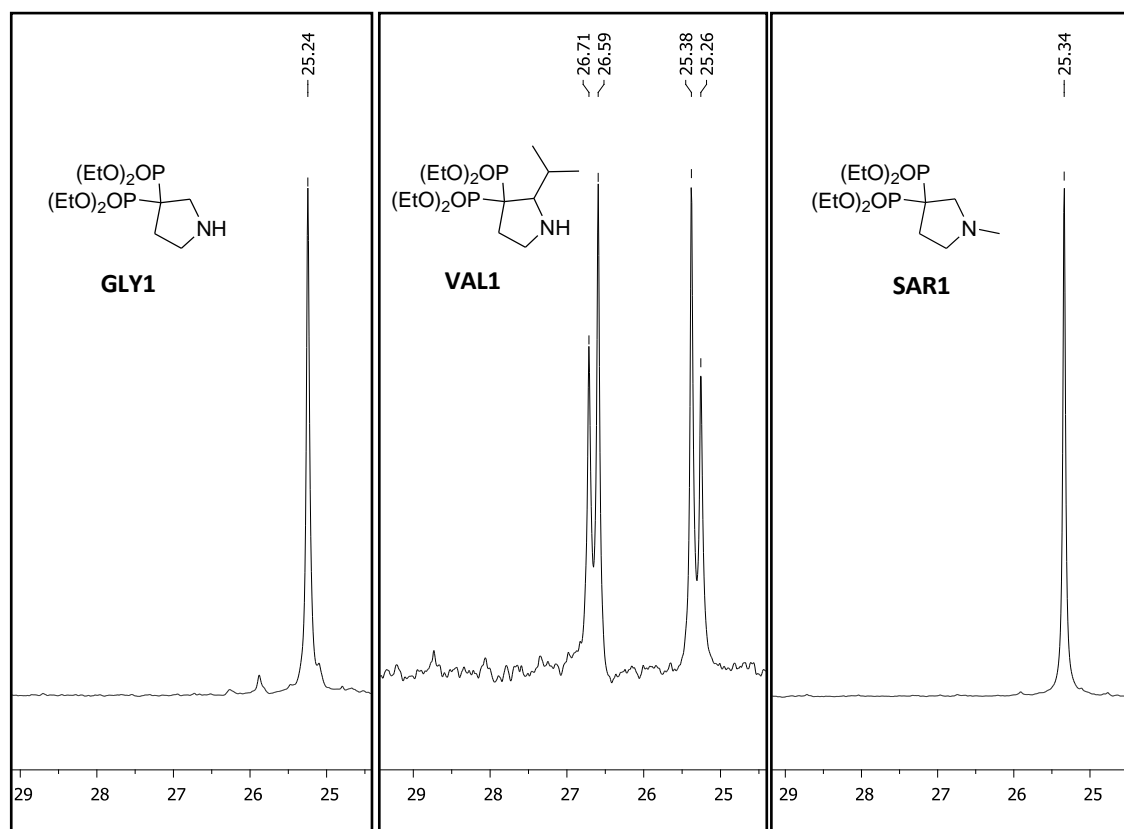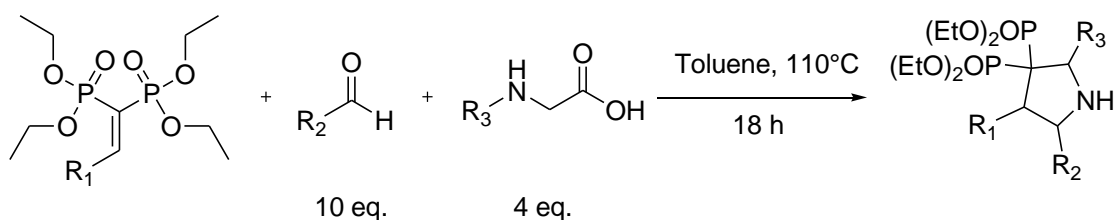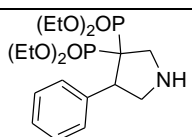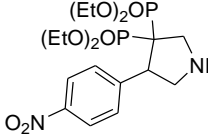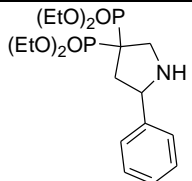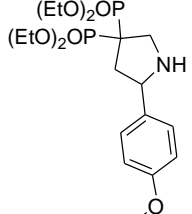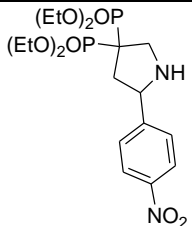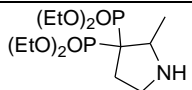

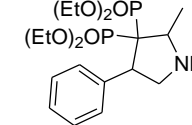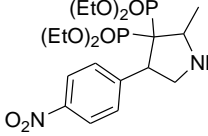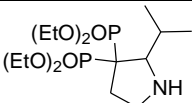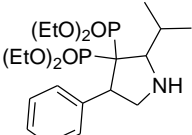Figure 35: ^{31}P {^{1}H}-NMR of achiral GLY1, chiral VAL1 and achiral SAR1.

Substituted VBP precursors bearing aromatic units were used in the same reaction in combination with different aminoacids and aldehydes in order to obtain multisubstituted pyrrolidine BP products (**Scheme 30, Table 20**).

Scheme 30: 1,3 cycloaddition between BP precursors, different aldehydes and amino acids.

	R_1	R_2	R_3	Product	Yield (%)
1	Ph	H	H	**GLY2**	42[a]
2	p-NO$_2$Ph	H	H	**GLY3**	48[a]
3	H	Ph	H	**GLY4**	0
4	H	p-OMePh	H	**GLY5**	0
5	H	p-NO$_2$Ph	H	**GLY6**	35[a]
6	H	H	Me	**ALA1**	27[b]
7	Ph	H	Me	**ALA2**	0
8	p-NO$_2$Ph	H	Me	**ALA3**	25[b]
9	H	H	Isopropyl	**VAL1**	26[b]
10	Ph	H	Isopropyl	**VAL2**	0
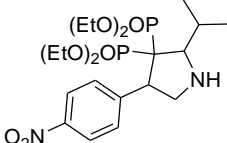
| 11 | p-NO$_2$Ph | H | Isopropyl | (EtO)$_2$OP, (EtO)$_2$OP structure with NH pyrrolidine, O$_2$N phenyl | **VAL3** | 0 |

Table 20: 1,3 cycloaddition between aromatic substituted BP precursors, different aldehydes and amino acids.

Reaction conditions: 0.65 mmol VBP, 2.5 mmol amino acid, 6.5 mmol of paraformaldehyde in 25 mL of toluene, T=110°C, t=18 h. [a] Isolated yield, [b]= ^{31}P-NMR yield.

Initially PPH and PPNO$_2$ precursors were used as dipolarophiles in 1,3 cycloaddition with glycine, showing a decrease in reaction yields compared to VBP (**Table 20, entries 1-2**). While these substituted BP precursors did not lead to the corresponding cyloaddition products in combination with valine (**Table 20, entries 9-11**), the reaction with alanine led to moderate product formation only with PPNO$_2$ (**Table 20, entries 6-8**). Similarly to the reaction with glycine (**Table 20, entries 1-2**) the use of BP precursors like PPNO$_2$ bearing an EWG gave better reaction yields probably due to the high electrophilicity of the electron-poor double-bond that makes them better dipolarophiles. These results show that steric hindrance plays a fundamental role in this reaction. Several attempts of cycloaddition made with the less bulky amino acid glycine with different types of aromatic aldehydes occurred successfully only with highly electron-poor p-NO$_2$ benzaldehyde in moderate yields, while the use of simple benzaldehyde or p-OMe substituted benzaldehyde (**Table 20, entries 3 and 4**) resulted in numerous inseparable byproducts. In general, the obtained products were difficult to purify by TLC or column chromatography, probably because of the presence of residual polar non-BP reagents used in the reaction. Best results in product formation and purification were obtained using the N-substituted amino acid sarcosine as reagent, as reported below.
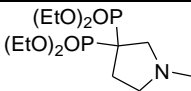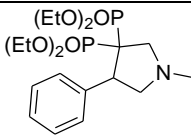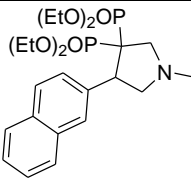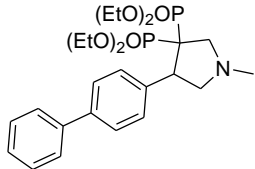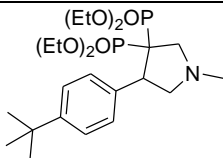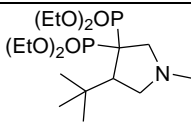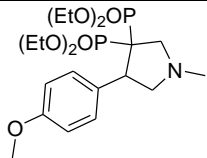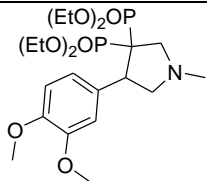
Similarly to what reported for other amino acids, the reaction between sarcosine and paraformaldehyde was extended to the use of substituted VBP precursors in order to investigate the formation of 1-methylpyrrolidine containing BPs with aromatic substituents in position 4 (**Scheme 31, Table 21**).
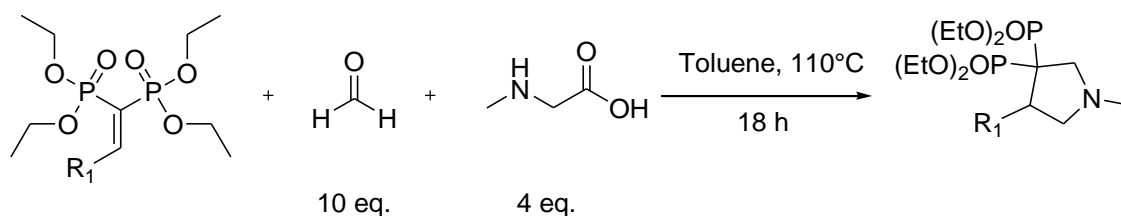
Scheme 31: Synthesis of 4-substituted 1-methylpyrrolidine containing BP.

In all cases the corresponding 1-methylpyrrolidine 4-substituted BPs were obtained in good to moderate yields depending on the electronic and steric properties of the prochiral VBP substrate. In fact, as reported in **Table 21**, the reaction led to 45% yield when

using PPH (**Table 21, entry 2**), while with more sterically demanding P2PH, P2NAP and POBr derivatives, the yields were lower (**Table 21, entries 3, 4, 11**) and with the *p*-t-Bu aliphatic BP derivative no product was detected (**Table 21, entry 6**). Similarly, with electron donating substituents on the aromatic moiety the reaction was less efficient as in the cases of t-Bu, methoxy or 3,4 dimethoxy substituents (**Table 21, entries 5, 7, 8**). Only the PPNO$_2$ precursor led to good product formation (68% yield) while the PPF derivative showed only limited activity with 11% yield (**Table 21, entries 10, 12**).

	R$_1$	Product		Yield [a] (%)
1	H		SAR1	>98
2	Ph		SAR2	45
3	2NAP		SAR3	30
4	2Ph		SAR4	21
5	p-t-Bu Ph		SAR5	33
6	t-But		SAR6	0
7	p-OMe Ph		SAR7	20
8	3,4 OMe Ph		SAR8	34
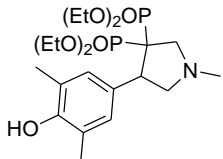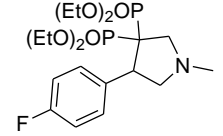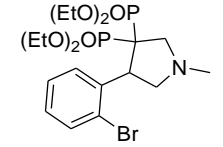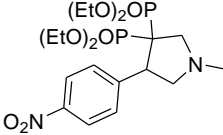
9	4OH-3,5Me		**SAR9**	0
10	p-F Ph		**SAR10**	11
11	o-Br Ph		**SAR11**	7
12	p-NO$_2$ Ph		**SAR12**	68

Table 21: Synthesis of the 4-substituted 1-methylpyrrolidine containing BP.
Reaction conditions: 0.65 mmol VBP, 2.5 mmol amino acid, 6.5 mmol of paraformaldehyde in 25 mL of toluene, T=110°C, t=18 h. [a]= Isolated yield.

The isolated products were characterized by ^{1}H, ^{31}P, ^{13}C NMR spectroscopy and GC-MS. In **Figure 36** a typical characterization for SAR3 is reported. The ^{31}P {^{1}H}-NMR spectrum of SAR3 shows two distinct resonances for the diastereotopic P atoms because of the presence of a stereogenic center in the molecule in position 4. Similar resonances resulted also in the other pyrrolidine BP derived products. Due to the proximity in chemical shift of the pyrrolidine ring resonances and their extended reciprocal coupling, the ^{1}H-NMR spectrum of SAR3 shows numerous overlapped multiplets, as further evidenced in the 2D-NMR COSY (**Figure 37**).
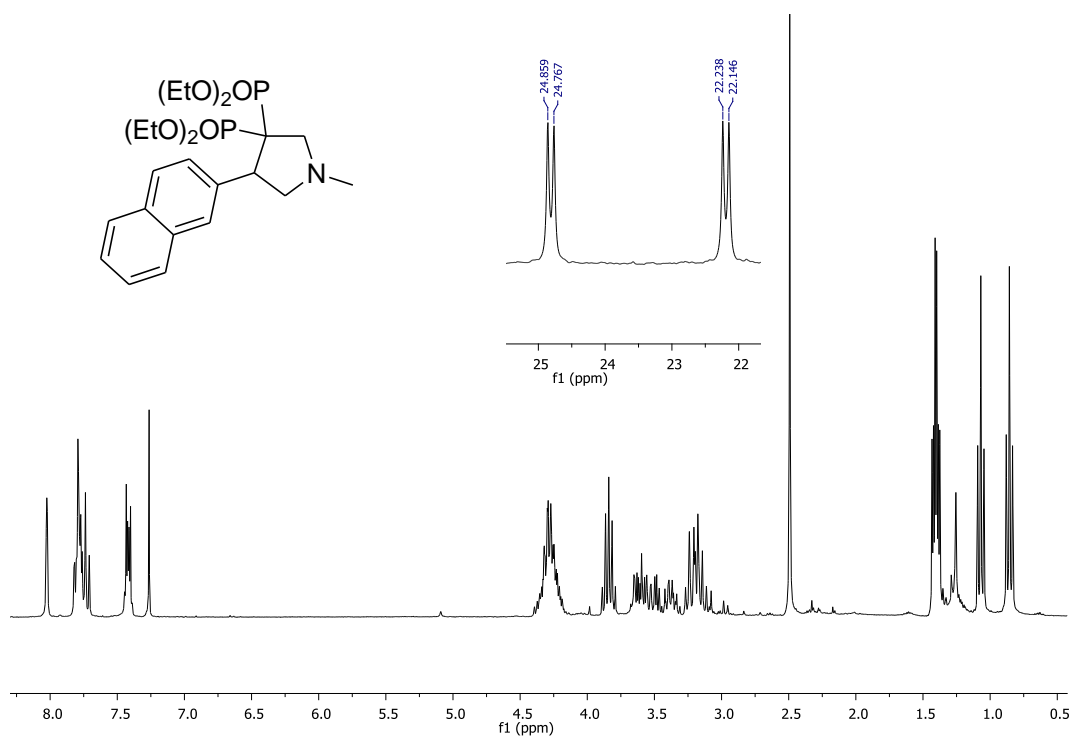
Figure 36: ^{1}H-NMR and ^{31}P {^{1}H}-NMR of SAR3.
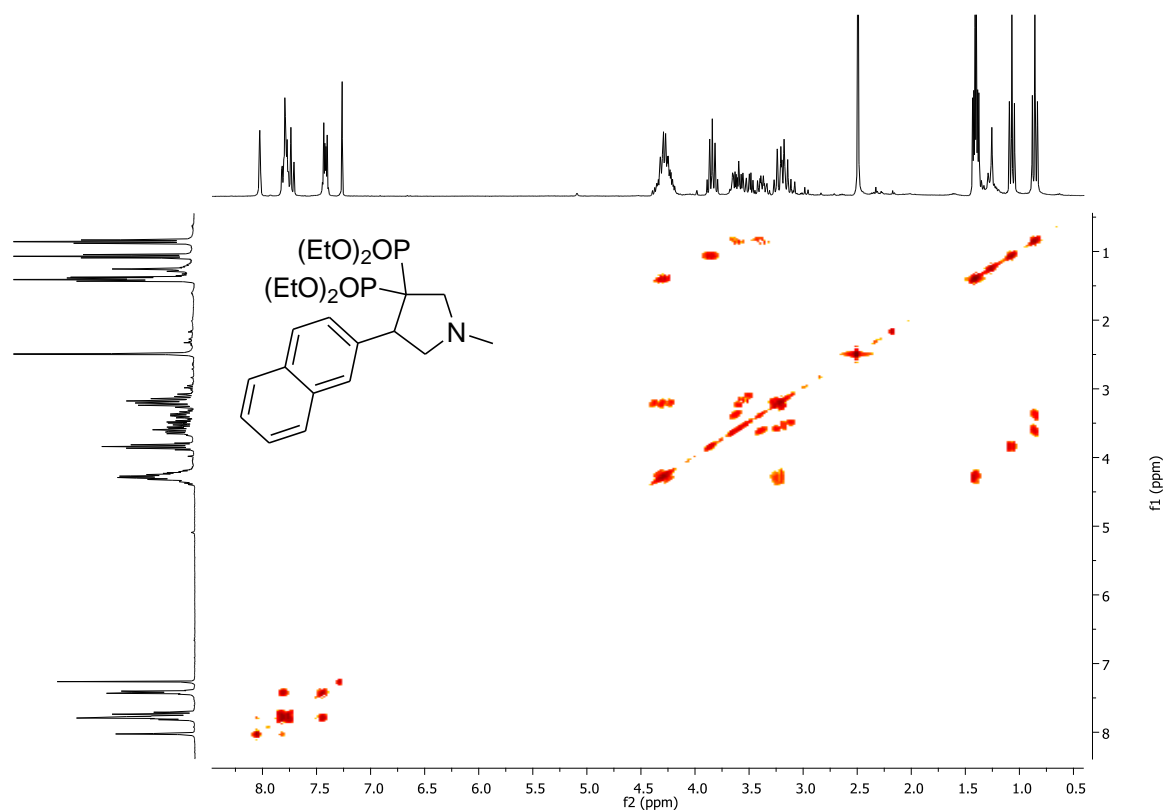
Figure 37: 2D-NMR COSY of SAR3.

2D-NMR NOESY (**Figure 38**) experiments revealed intense NOE cross-couplings between naphtyl protons and $H_{b,c}$ protons as well as with H_a proton. Determination of the *trans* or

cis geometry of the product was not tackled due to the facile pyramidal inversion occurring at the nitrogen atom of the five membered ring. [230]
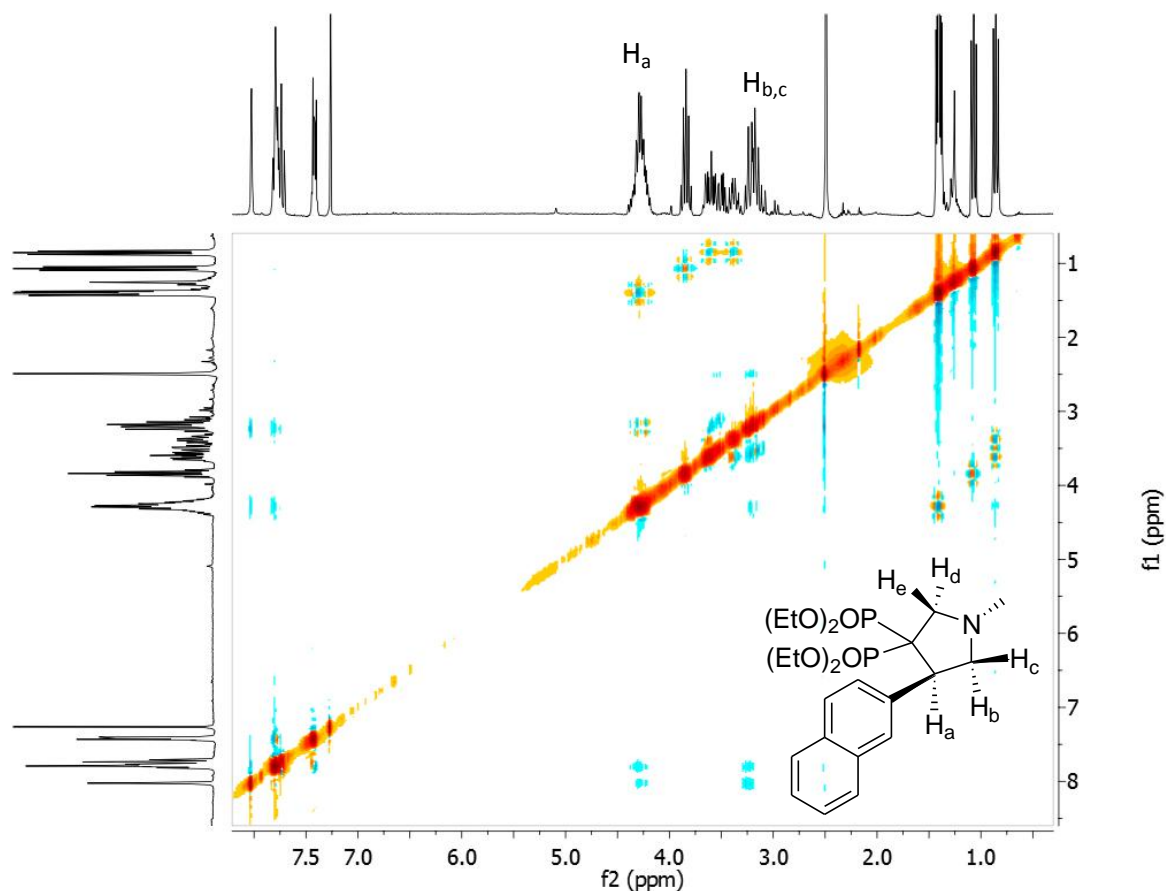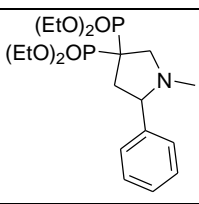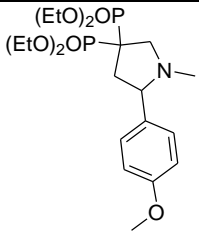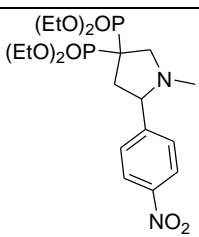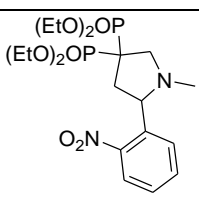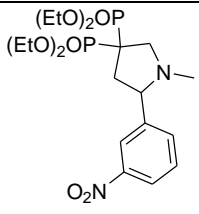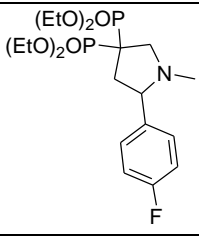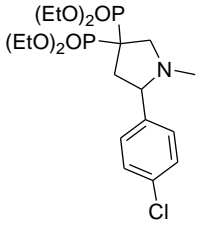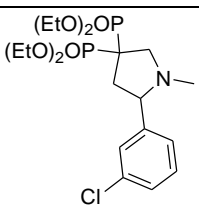
Figure 38: 2D-NMR NOESY of SAR3.

The pyrrolidine BP synthesis was further successfully extended to the use of aromatic aldehydes in place of paraformaldehyde together with sarcosine in order to obtain 5 substituted 1-methylpyrrolidine BPs derivatives (**Scheme 32**).
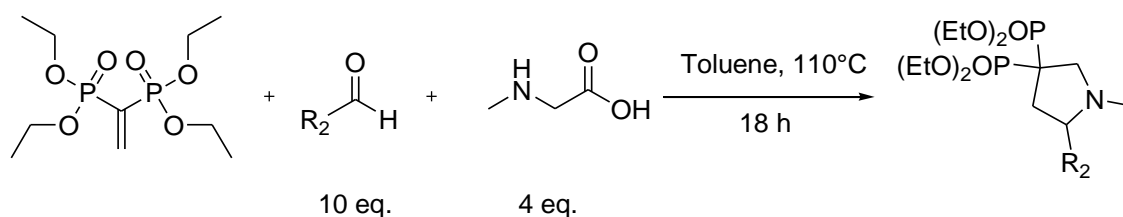
Scheme 32: Synthesis of the 5-substituted 1-methylpyrrolidine containing BP by reaction between sarcosine, VBP and different aromatic aldehydes

	R$_2$	Product		Yield (%)
1	Ph		SAR13	0
2	p-OMe Ph		SAR14	0
3	p-NO$_2$ Ph		SAR15	73[a]
4	o-NO$_2$ Ph		SAR16	0
5	m-NO$_2$ Ph		SAR17	0
6	p-F Ph		SAR18	64[b]
7	p-Cl Ph		SAR19	68[b]
8	m-Cl Ph		SAR20	0
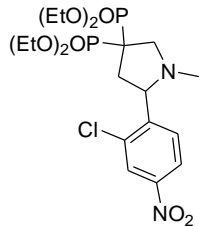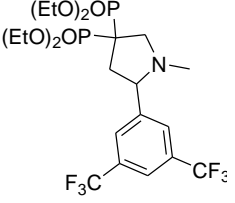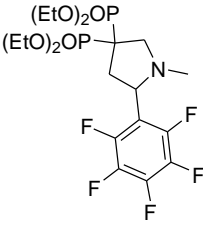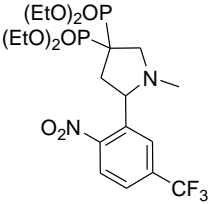
9	2Cl,4 NO$_2$ Ph		SAR21	80[a]

10	3,5 CF$_3$ Ph		SAR22	18[b]

11	5F Ph		SAR23	0

12	2NO$_2$, 5CF$_3$ Ph		SAR25	0

Table 22: Synthesis of the 5-substituted 1-methylpyrrolidine containing BPs.
Reaction conditions: 0.65 mmol VBP, 2.5 mmol amino acid, 6.5 mmol of paraformaldehyde in 25 mL of toluene, T=110°C, t=18 h. [a] Isolated yield, [b]= ^{31}P-NMR yield.

The reaction turned out to be very sensitive to the electronic properties of the aromatic aldehydes. In fact, benzaldehydes and *p*-methoxybenzaldehyde did not show formation of the desired product (**Table 22, entries 1 and 2**), while electron-poor aldehydes like *p*-chlorobenzaldehyde, *p*-fluorobenzaldehyde and *p*-nitrobenzaldehyde provided the corresponding products in 68, 64 and 73% yield, respectively (**Table 22, entries 3, 6, and 7**). Even the position of the substituent group on the ring affected the reaction, showing product formation only when EWG in para position on benzaldehyde were present (**Table 22, entries 3, 6, 7, 9**). Meta or ortho EWG substituents led to moderate yields of reaction (**Table 22, entry 10**) or did not react at all (**Table 22, entries 4, 5, 8**). Other aldehydes like pentafluoro benzaldehyde (**Table 22, entry 11**) or 2-nitro-5 trifluoromethyl benzaldehyde (**Table 22, entry 12**), even if electron poor, did not provide the corresponding cycloadducts with VBP.

It is worth to notice that coupling sarcosine with isatin, a reagent bearing a particularly activated carbonyl group, it was possible to obtain the corresponding cycloaddtion spiro-compound product bearing an isatin residue (**Scheme 33**).
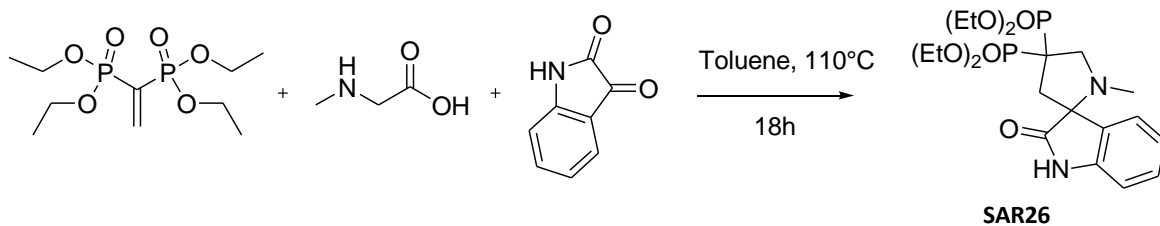
Scheme 33: Synthesis of the SAR26 by reaction between sarcosine, VBP and isatin.

The reaction gave tetraethyl 1'-methyl-2-oxospiro[indolyn-3,2'-pyrrolidin]-4',4'diildiphosphonate (SAR26, **Figure 39**) with 51% yield in 18 hours. Formation of by-products as shown by the ^{31}P-NMR spectrum of the crude did not prevent the isolation by TLC using a 1:1 mixture of acetone and ethyl acetate
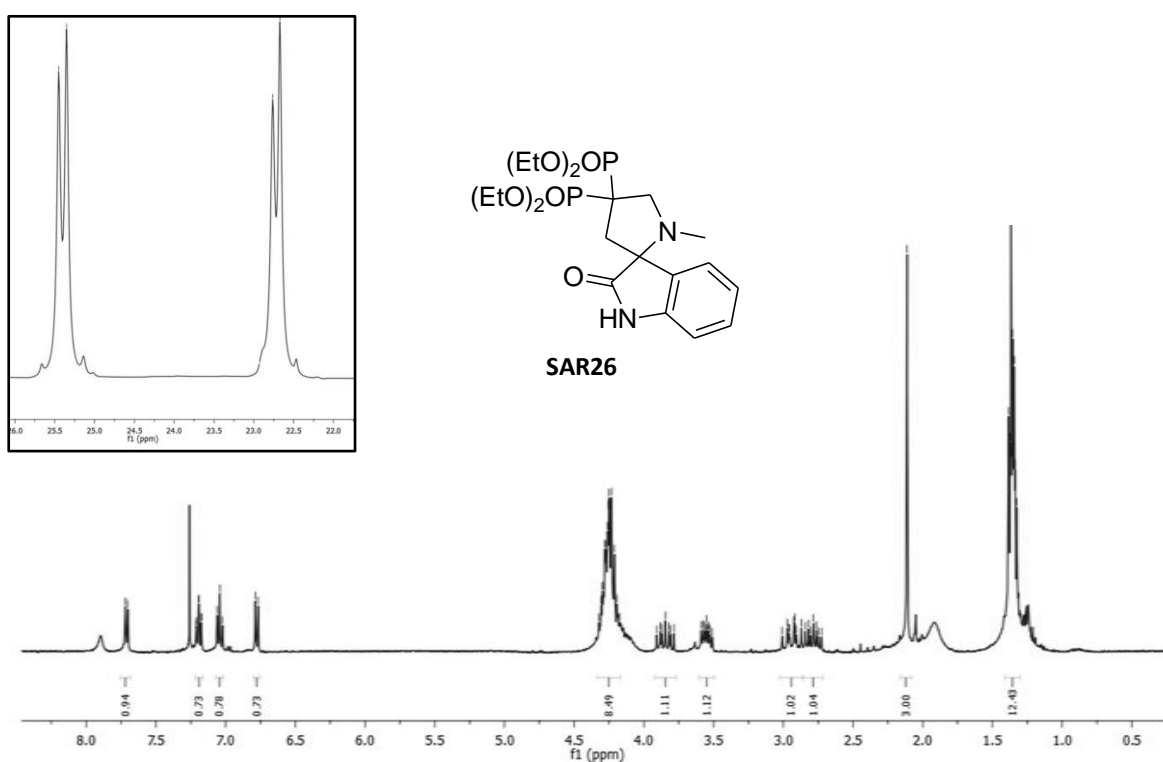
Figure 39 : ^{1}H-NMR and ^{31}P {^{1}H}-NMR of SAR26

SAR1 was subjected to subsequent deprotection of the phosphonate ester moiety by treatment with trimethylbromosilane [139] followed by hydrolysis with the water/methanol solution (9:1) (**Scheme 34**) in order to obtain the corresponding bisphosphonic acid compound.
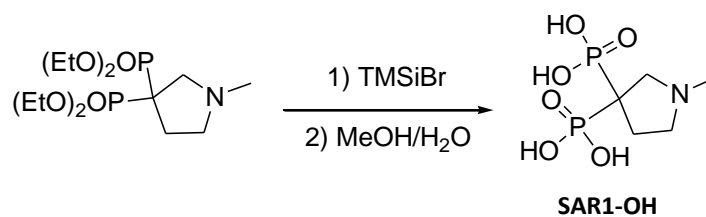
Scheme 34: SAR1 deprotection step.

The corresponding bisphosphonic acids SAR1-OH was isolated in good yield and wascharacterized by ^{1}H and ^{31}P-NMR spectroscopy in D_2O. ^{1}H-NMR spectroscopy in D_2O of SAR1-OH indicated aggregation phenomena, resulting in broad signals. ^{31}P-NMR in D_2O showed two singlets (**Figure 40**), indicating that the molecule could be present in a zwitterionic form with nitrogen protonation and formation of a stereocenter in the structure.
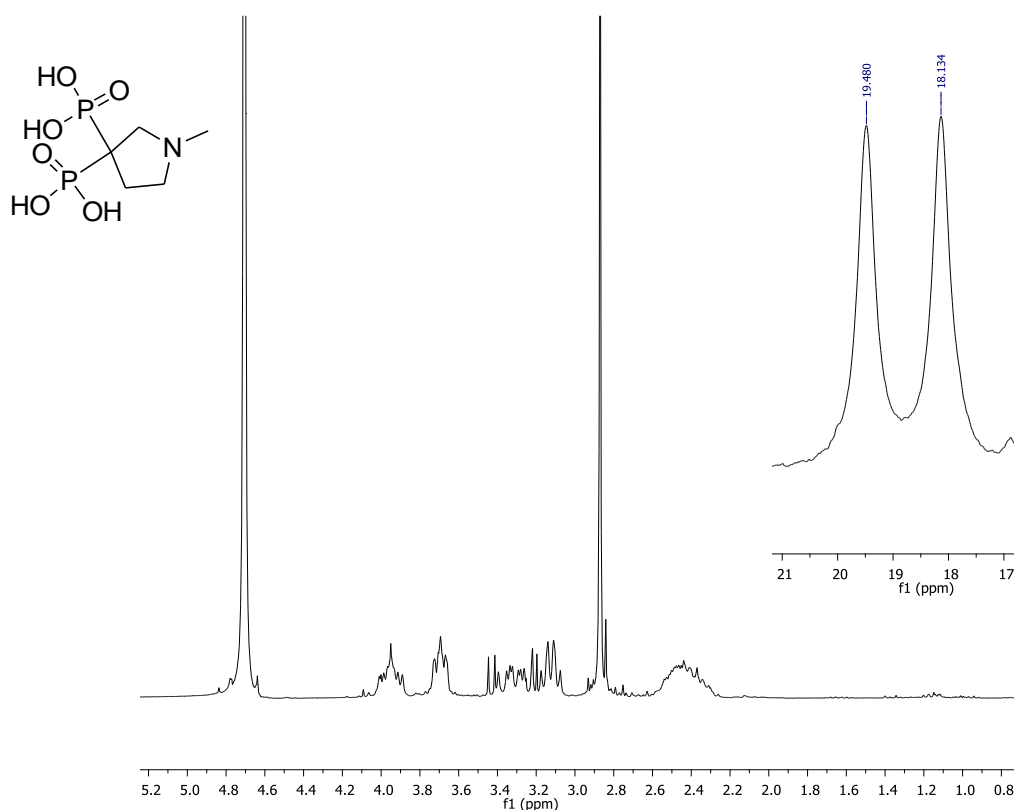
Figure 40: D_2O ^{1}H-NMR and ^{31}P {^{1}H}-NMR of SAR1-OH.

3.11   AZOLE BPS: ISONITRILE ADDITION

Isonitriles (also called isocyanides or carbylamines) are organic compounds bearing the functional group -N≡C. They are isomers of cyanides (also called nitriles, -C≡N), hence they are designated by prefix iso.[231] They are used as privileged synthons for the synthesis of other organic heterocyclic compounds, frequently via multicomponent reactions (MCRs) namely isonitrile multicomponent reactions (IMCRs) such as Passerini [232] or Ugi [233,234] reactions. IMCRs are possible in the presence of catalysts [235] or under catalyst free conditions like in the microwaves [236], ultrasound [237] or mechanochemical [238] version. Isonitriles are neutral compounds that can act both as nucleophiles and electrophiles. Usually they are represented by the linear zwitterionic form, but it has been shown that their behavoiur is better described by the carbenic formula (**Scheme 35**).[239]
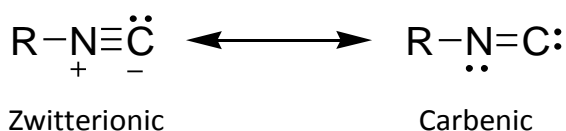
Scheme 35: resonance representation of isonitriles.

The zwitterionic structure of isonitriles describes their nucleophilic character, while the carbenic one supports its electrophilic character. Despite the huge potentialities of isonitrile chemistry, this class of molecules was paid limited attention by the academic community. This reluctance is undoubtedly related to the extremely distressing odor of isonitriles, which has also led to their proposed use as non-lethal weapons.[240]

Michael addition products of isonitriles were described in Van Leusen's works, [241] that reported the one-pot synthesis of pyrroles by the reaction of tosylmethylisonitrile (TosMIC) with Michael-acceptors in the presence of sodium hydride as base. Recently the reaction of isonitriles with various 1,3-dicarbonyl compounds catalyzed by piperidine (**Scheme 36**) was described. [242]
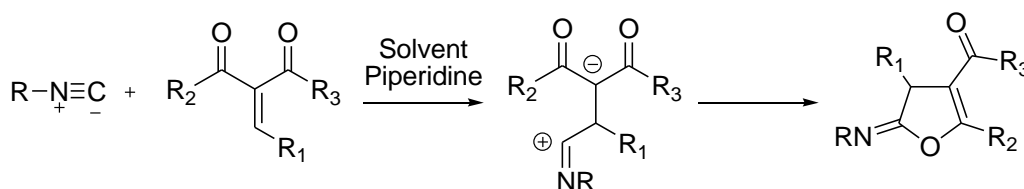
Scheme 36: reaction of isonitriles with various 1,3-dicarbonyl compounds catalyzed by piperidine in a facile and efficient synthesis of 5-hydroxy-2H-pyrrol-2-one derivatives. [242]

Among isonitriles, isocyanoacetates occupy an important place in the field of synthetic application due to their particular reactivity. Schöllkopf et al [243] reported in 1973 the first synthesis of Michael-adducts resulting from the reaction between the enolate form

of this particular class of isonitriles and a activated olefin under basic conditions (**Scheme 37**).
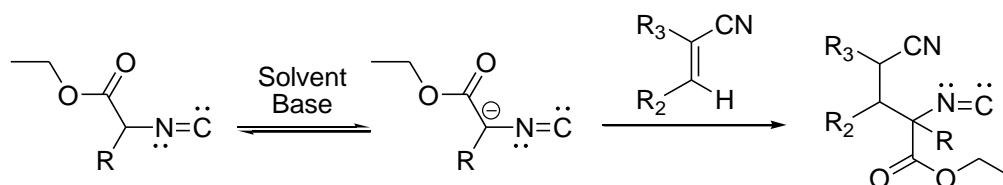
Scheme 37: Michael addition of isocyanoacetates to activated olefins. [243]

The analogy between BP precursors and 1,3-dicarbonyl compounds spurred the development of procedures for the addition of isonitriles and isocyanoacetates to BPs.
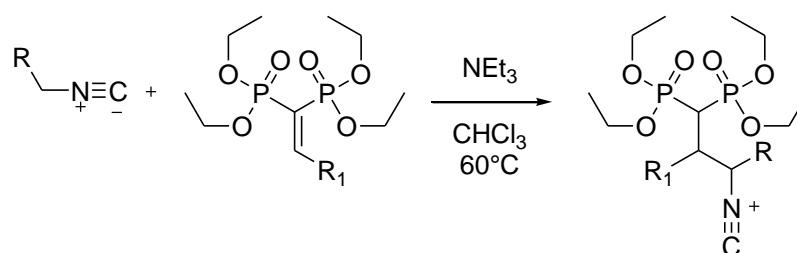
Scheme 38: Base catalyzed addition of isocyanides to BP precursors

BPs precursors were tested under mild basic condition in the presence of various isonitriles and isocyanoacetates aiming at forming the structurs reported in (**Scheme 38**). At variance with what reported in literature, [243] no α-isonitrile products were obtained but some amide-BPs were found in moderate to good yields as reported in **Table 23**.

	BP precursor	Isonitrile	Product		Isolated yield (%)
1	**VBP**	$^-C\equiv N^+$ COOEt		**NCET**	5[ab] 53
2	**VBP**	$^-C\equiv N^+$ COOMe		**NCMe**	57
3	**VBP**	$^-C\equiv N^+$ Ph		**NCPh**	0
4	**VBP**	$^-C\equiv N^+$		**NCTBut**	0

5	**PCOOEt**	$^-C\equiv N^+$ COOEt	(EtO)$_2$OP PO(OEt)$_2$ COOEt COOEt structure	**AG2Et**	36
6	**PPH**	$^-C\equiv N^+$ COOEt	phosphonate phenyl amide COOEt structure	**NCPPH**	0
7	**BPHEt**	$^-C\equiv N^+$ COOEt	(EtO)$_2$OP (EtO)$_2$OP COOEt NH COOEt structure	**NCBPHEt**	0

Table 23: Base catalyzed addition of isonitriles to BP precursors.
Reaction conditions: 0.2 mmol BP precursor, 0.2 mmol isonitrile, 0.2 mmol NEt$_3$ in 2 mL of CHCl$_3$, T=60°C, t=12h. [a] ^{31}P-NMR yield, [b] r.t.

VBP was tested with different isonitriles leading to the formation of the reported products under mild temperature condition (**Table 23, entry 1**) only when using activated isonitriles like ethyl or methyl isocyanoacetates (**Table 23, entries 1-4**).

A plausible mechanism that could explain the formation of the amide-BPs is reported in **Scheme** 39 where nucleophilic addition of the carbenic form of the isonitrile to the β carbon atom of VBP takes place. The presence of non anhydrous conditions leads to further hydrolysis forming the resulting amide-BP.
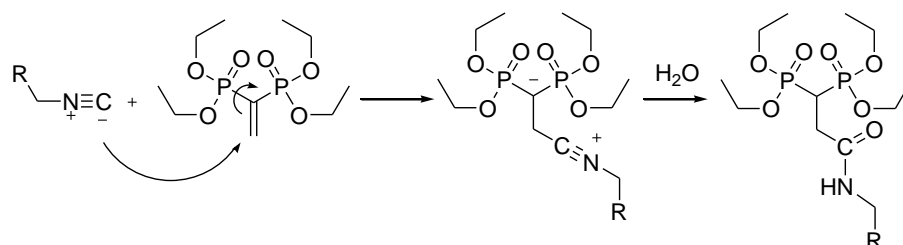
Scheme 39: Proposed mechanism for the isonitriles addition to VBP.

Notably, a small amount of an interesting by-product was observed in the reactions between VBP and isocyanoacetates (**Table 23, entries 1 and 2**). These by-products showed in the ^{31}P-NMR the presence of two different phosphorous atoms, indicating the formation of possible chiral products. Methyl and ethyl Isocyanoacetates were tested with a variety of BPs precursors showing no reactivity with di-substituted BP precursors (**Table 23, entry 7**) as well as with aromatic mono-substituted BP (**Table 23, entry 6**) probably because of steric hindrance. Electron poor non aromatic mono-substituted BP precursors like PCOOEt showed the unsual formation of a cyclic compound in moderate yield (**Table 23, entry 5**) confirmed by GC-MS analysis, ^{1}H MNR spectroscopy and ^{31}P NMR spectra, the latter showing the presence of an unusual singlet. 2D-NMR COSY (**Figure 41**) and 2D-NMR HSQC

(**Figure 42**) of NCEt allowed to confirm the structure of the synthesized amide-BP product NCEt.
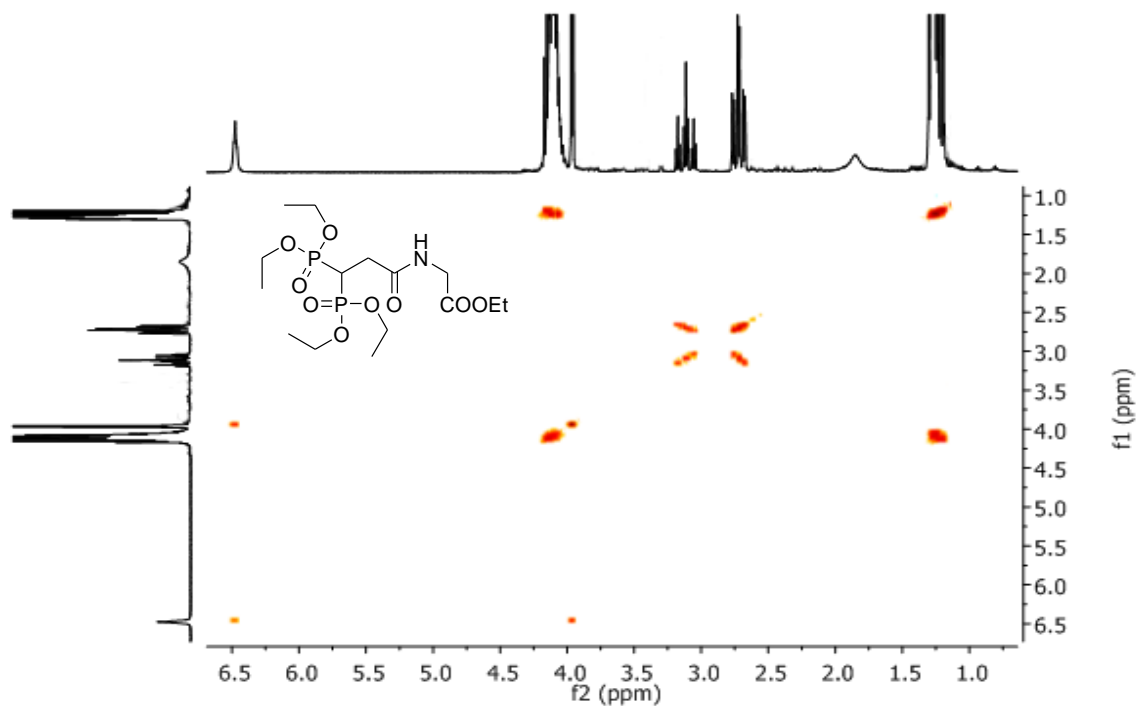
Figure 41: 2D-NMR COSY of NCEt.
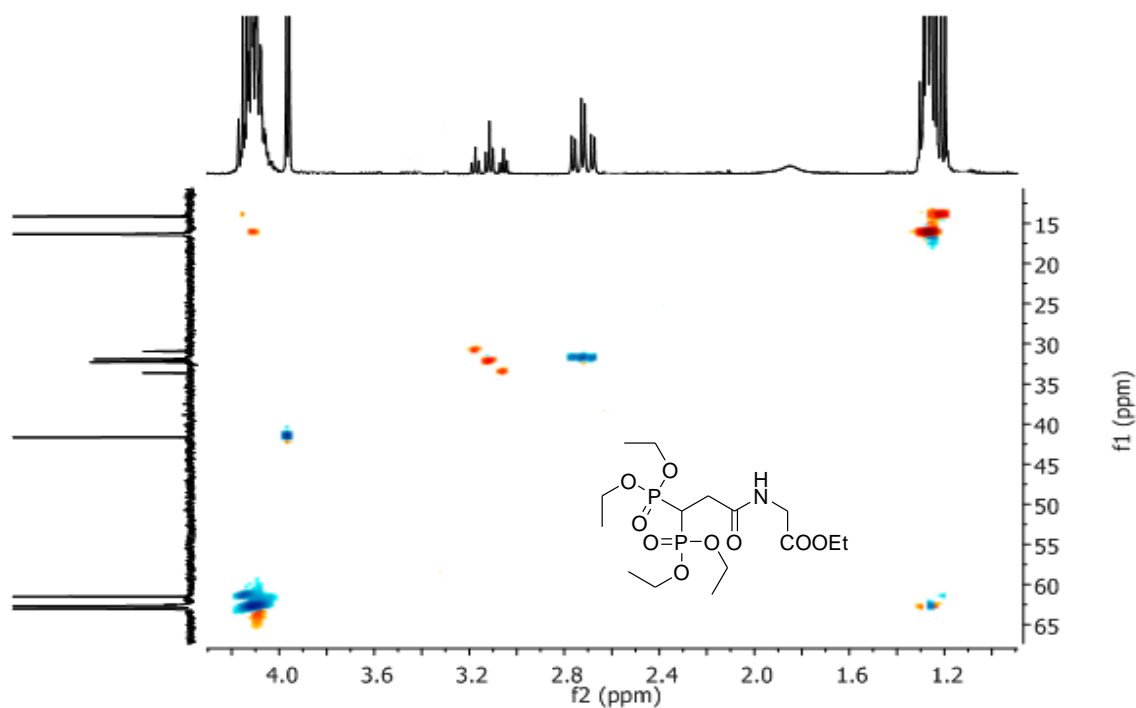
Figure 42: 2D-NMR HSQC of NCEt.

In the literature, the formation of heterocyclic compounds in the isonitrile reactions with activated olefins is not unusual and often catalyzed by metals such as Mg(II) [244] or more frequently by Ag salts.[245, 246] Grigg et al. [247] reported that silver acetate was

an efficient catalyst for the cycloaddition of methyl isocyanoacetate with Michael-acceptors under mild conditions giving pyrrolines in good yields (**Scheme 40**). More recently the combination of silver with an organocatalyst was used in a cascade sequence involving isocyanoacetates and α,β-unsaturated ketones for the enantioselective synthesis of 2,3-dihydropyrroles.[248]
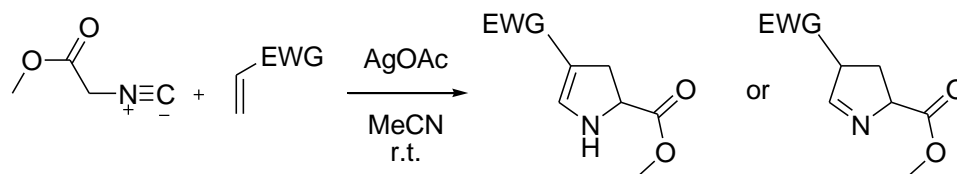
Scheme 40: silver acetate cycloaddition of methyl isocyanoacetate with Michael-acceptors.

This type of reactions could give the oppotunity to obtain cyclic BP products bearing a nitrogen atom and the asymmetric version of the reaction could be also explored.
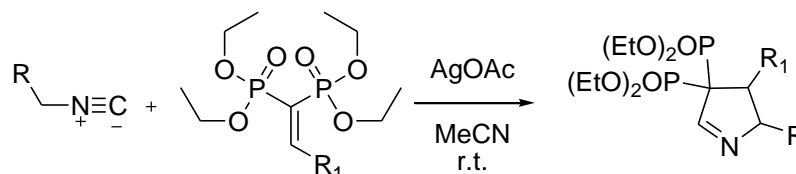
Scheme 41: : AgOAc catalyzed addition of isonitriles to BP precursors.

BPs precursors were tested under Grigg's [247] optimized AgOAc catalyzed cycloaddition condition in the presence of isocyanoacetates (**Scheme 41**). The results obtained are reported in **Table 24**.

	BP precursor	Isonitrile	product		Yield [a] (%)
1	**VBP**	$^-C{\equiv}N^+$ COOEt		**AG1Et**	89 90[b]
2	**VBP**	$^-C{\equiv}N^+$ COOMe		**AG1Me**	85
3	**VBP**	$^-C{\equiv}N^+$ Ph		**AG1Ph**	0
4	**PCOOEt**	$^-C{\equiv}N^+$ COOEt		**AG2Et**	>98

#	Catalyst	Isonitrile	Product structure	Product	Yield
5	**PPH**	⁻C≡N⁺–COOEt	(EtO)₂OP PO(OEt)₂ ... COOEt (phenyl)	**AG3Et**	>98
6	**BPHEt**	⁻C≡N⁺–COOEt	(EtO)₂OP (EtO)₂OP ... COOEt, COOEt (phenyl)	**AG4Et**	0
7	**PPOMe**	⁻C≡N⁺–COOEt	(EtO)₂OP PO(OEt)₂ ... COOEt (4-OMe phenyl)	**AG5Et**	55
8	**PPOMe**	⁻C≡N⁺–COOMe	(EtO)₂OP PO(OEt)₂ ... COOMe (4-OMe phenyl)	**AG5Me**	62
9	**PPNO₂**	⁻C≡N⁺–COOEt	(EtO)₂OP PO(OEt)₂ ... COOEt (4-NO₂ phenyl)	**AG6Et**	>98
10	**PPNO₂**	⁻C≡N⁺–COOMe	(EtO)₂OP PO(OEt)₂ ... COOMe (4-NO₂ phenyl)	**AG6Me**	>98
11	**P2NAP**	⁻C≡N⁺–COOEt	(EtO)₂OP PO(OEt)₂ ... COOEt (naphthyl)	**AG7Et**	72
12	**P2NAP**	⁻C≡N⁺–COOMe	(EtO)₂OP PO(OEt)₂ ... COOMe (naphthyl)	**AG7Me**	90
13	**PtBut**	⁻C≡N⁺–COOEt	(EtO)₂OP PO(OEt)₂ ... COOEt (tBu)	**AG8Et**	0
14	**PtBut**	⁻C≡N⁺–COOMe	(EtO)₂OP PO(OEt)₂ ... COOMe (tBu)	**AG8Me**	0

Table 24: AgOAc catalyzed addition of isonitriles to BP precursors.
Reaction conditions: 0.2 mmol BP precursor, 0.2 mmol isonitrile, 10 mol% of AgOAc in 2 mL of MeCN, T=r.t., t=12h. [a] Isolated yield, [b] T= 60°C.

VBP was tested in the reaction with different isonitriles, showing excellent reactivity only with activated isonitriles like ethyl or methyl isocyanoacetates (**Table 24, entries 1-2**). Use of electron rich isonitriles like α-methylbenzyl isonitrile did not lead to formation of the desired products (**Table 24, entry 3**). The reaction was little influenced by increasing the temperature (**Table 24, entry 1**) giving comparable yields to what found at room

temperature. ^{31}P NMR spectra showed that AG1Et and AG1Me are the corresponding byproducts in the same base catalyzed reactions (**Table 23**). Application of these reaction condition to substituted BP precursor showed that the reaction is intrisically influenced by the steric and electronic properties of the reagents. While monosubstituted BP precursors gave excellent yields (**Table 24, entries 4-7, 9, 11**), di-substituted BPs (**Table 24, entry 6**) did not lead to any azole-based BP probably because of the steric hindrance on the β-carbon atom of the precursor. BP precursors bearing electron-donating group like PPOMe showed less reactivity than those bearing electron-withdrawing groups like PPNO$_2$ (**Table 24, entries 7 and 9**) likely because electron poor alkene favor the addition of isocyanides (**Scheme 42**). A Sterically hindered β position led to decrease in reaction yields (**Table 24, entry 11**) that turned out into complete loss of reactivity in the case of the t-Bu substituted derivative (**Table 24, entries 13**). When the reaction did not lead to quantitative yields (**Table 24, entries 7, 8, 11, 12**) the steric properties of the isocyanoacetate reagent were involved as better results with less hindered methyl rather than ethyl isocyanoacetate were observed.
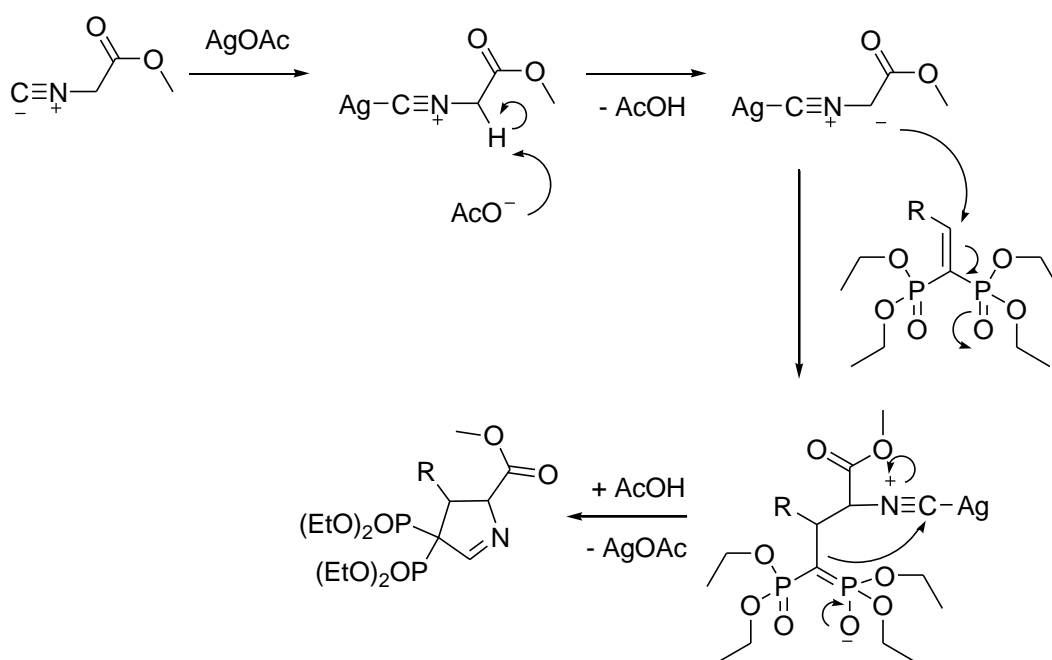
Scheme 42: Proposed mechanism for the AgOAc catalyzed isocyanoacetates cycloaddition to BP precursors.

Adaptation of the mechanism proposed by Grigg [247] to BP precursors could explain the formation of the obtained azole-BPs (**Scheme 42**). Based on this mechanism, α-deprotonation of metallated isonitrile by the acetate anion is suggested. The generated anionic nucleophile undergoes conjugate addition to the VBP as a Michael acceptor, giving an enolate-like species that further reacts through a ring closure giving the expected addition product. In **Figure 43** a comparison is reported between the traditional ^{1}H-NMR spectrum of AG6Me and the phosphorous decoupled ^{1}H {^{31}P}-NMR spectrum (B) in order to underline the presence of [1]H-^{31}P couplings. ^{31}P {^{1}H}-NMR of AG6Me showed

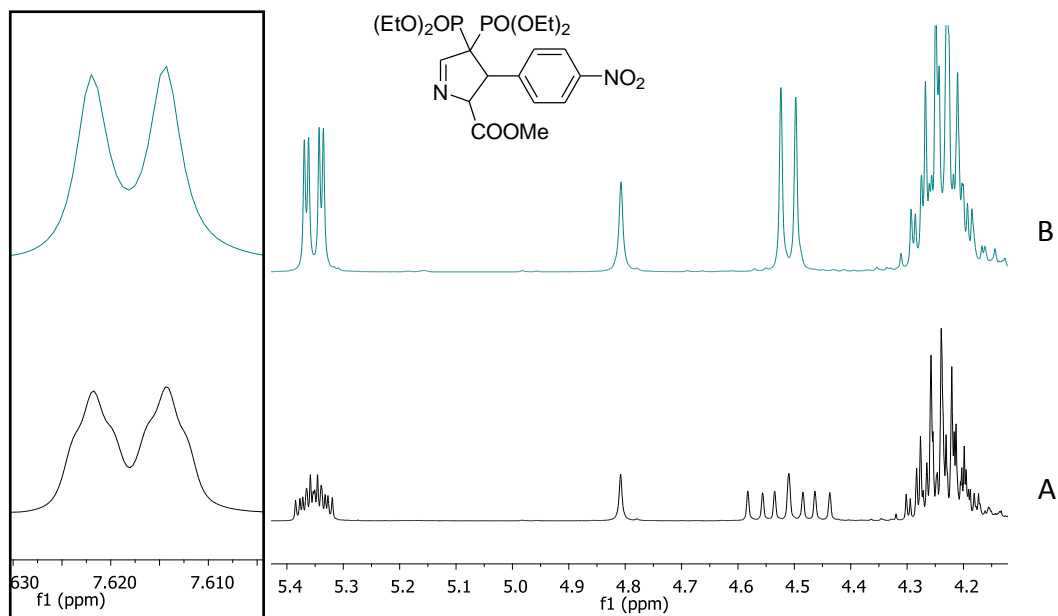the formation of two doublets shifted from PPNO$_2$ with a small coupling constant of 6.0 Hz (**Figure 44**).

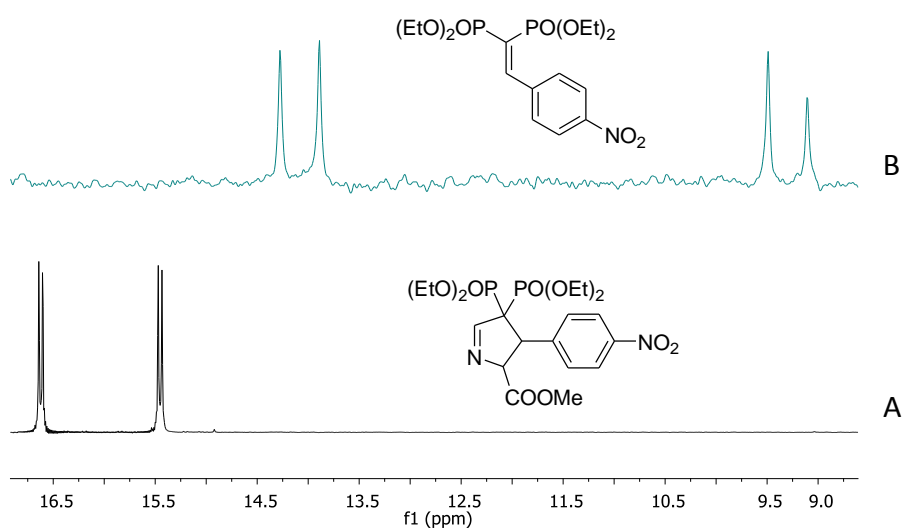Figure 43: (A) ^{1}H-NMR and (B) ^{1}H {^{31}P}-NMR of AG6Me.

Figure 44: (A) ^{31}P {^{1}H}-NMR of AG6Me and (B) ^{31}P {^{1}H}-NMR of PPNO$_2$.
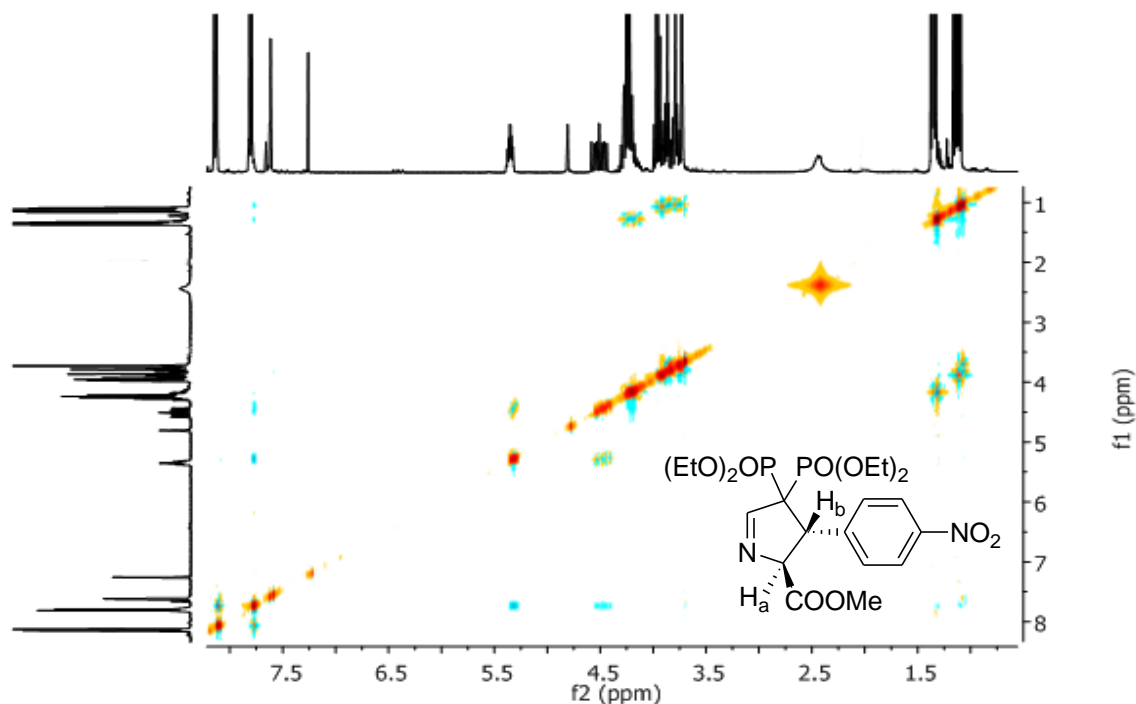
Figure 45: 2D-NMR NOESY of AG6Me.

The 2D-NMR NOESY (**Figure 45**) experiment revealed an intense cross-peak between *o*-phenyl protons and the H_a proton, indicating the formation of only the *trans* diastereoisomer. The observed $^3J_{Ha}\text{-}J_{Hb}$ coupling costants of 10.5 Hz are in agreement with what reported in the literature [249] for analogous compounds as a further confirmation of the *trans* geometry of the molecule (**Figure 46**).

trans $J_a\text{-}J_b$ = 10.5 Hz

trans $J_a\text{-}J_b$ = 10.6 Hz

Del Fiandra et al. [249]

cis $J_a\text{-}J_b$ = 7.7 Hz

Dehnel et al. [250]

Figure 46: Comparison between $^3J_{Ha\text{-}Hb}$ of AG6Me and examples of *trans-* and *cis*-azoles.

AgOAc catalyzed addition of isocyanoacetates to mono-substituted VBP precursors coupled with asymmetric ligands will be the subject of future studies in order to obtain a new class of enantio-enriched nitrogen BPs as potential new anti-resorptive drugs.

3.12 CHIRAL ISATIN CONTAINING BISPHOSPHONATES

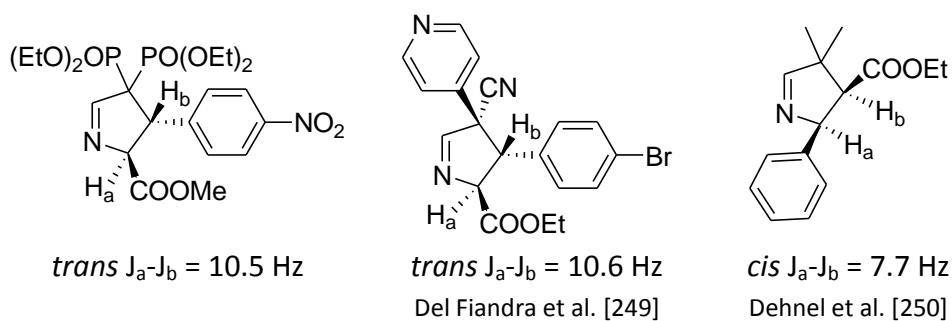Isatin is a simple molecule found in some plants as well as in humans as it is a metabolic derivative of adrenaline [251] but it is commonly employed also for the manufacture of dyes, pigments, flavors, pharmaceuticals, flame-proofing agents, corrosion inhibitors, dry bleaches, disinfectants, and sanitizing agents. It is a highly versatile starting material for the synthesis of natural products, heterocyclic, and non-cyclic compounds.[252] This molecule and its derivatives showed a broad spectrum of biological activities [253] like anti HIV, [254] antibacterial, antifungal, [255] antiviral, [256] properties to name a few. Asymmetric catalysis on isatin derivatives has recently received great attention leading to a series of highly enantioselective reactions, [257] also for the preparation of biologically active spirooxindoles.[258]

Since isatin is an example of rather nucleophilic amide derivative suitable for Michael reactions, [259] the reaction between isatin and VBP was initially investigated observing the formation of the corresponding tetraethyl [2-(2,3-dioxo-2,3-dihydro-1*H*-indol-1-yl)ethane-1,1-diyl]bis(phosphonate) (IST1) as Michael addition BP product in 86% isolated yield after 18 h at 60°C (**Scheme 43**).
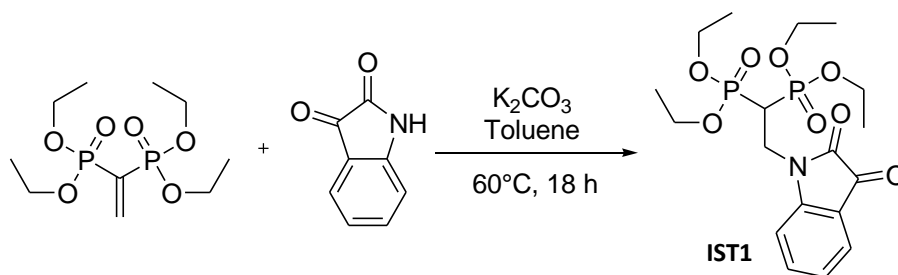
Scheme 43: Synthesis of tetraethyl IST1 by Michael addition of Isatin to VBP.

While Michael addition to VBP proceeded with excellent yields, attempts of isatin addition to monosubstituted VBP precursors led to decomposition of the BP precursors probably because of limited stability under basic condition.

IST1 was subjected to subsequent deprotection of the phosphonate ester moiety by treatment with trimethylbromosilane [139] followed by hydrolysis with the water/methanol solution (9:1) (**Scheme 44**).
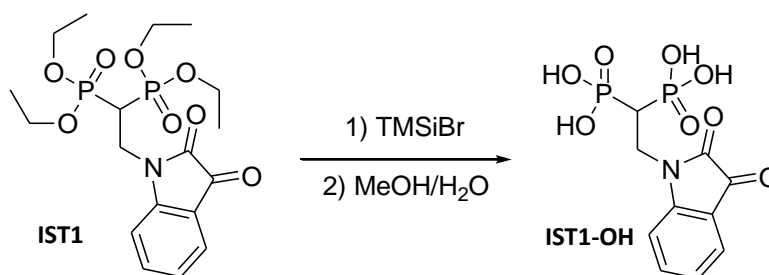
Scheme 44: IST1 deprotection step.

The corresponding bisphosphonic acids IST1-OH was isolated in good yield without any decomposition of the product. IST1 and IST1-OH were characterized by ^{1}H and ^{31}P-NMR spectroscopy in CDCl$_3$ and D$_2$O respectively (**Figure 47**) showing in the latter case no aggregation phenomena (**Figure 48**).
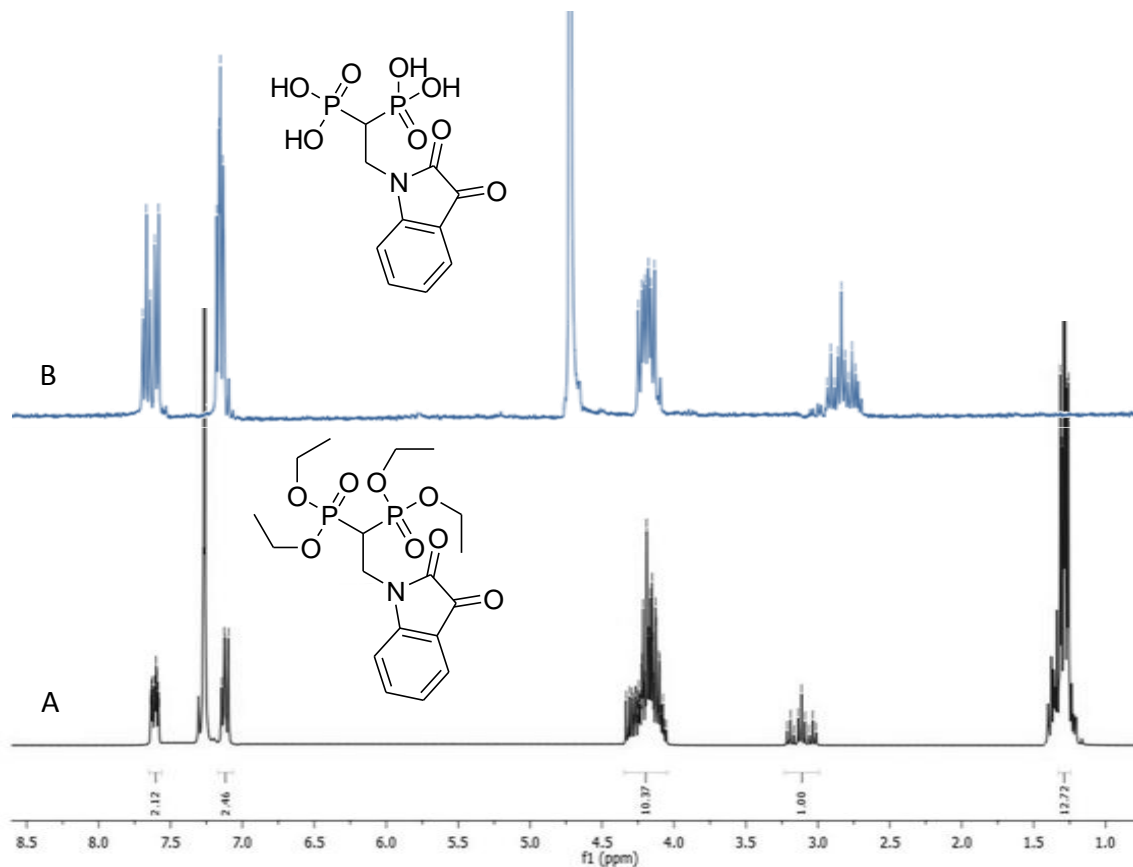

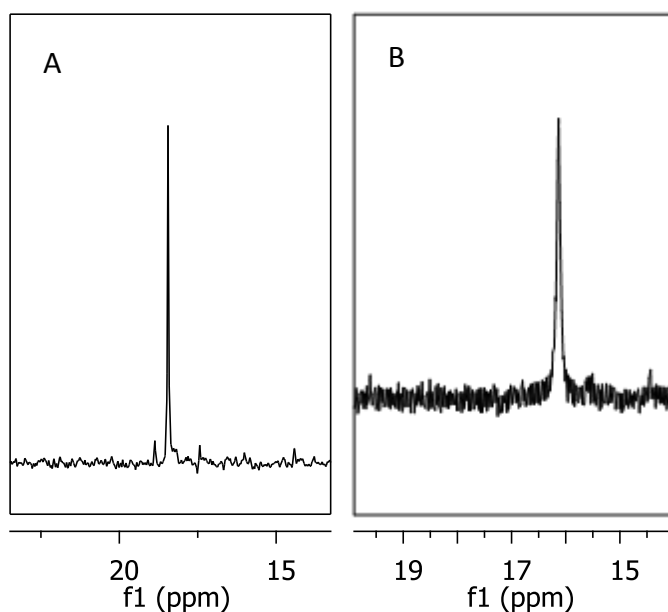Figure 47: CDCl$_3$ ^{1}H-NMR of IST1 (A) and D$_2$O ^{1}H-NMR IST1-OH (B).

Figure 48: CDCl$_3$ ^{31}P {^{1}H}-NMR of IST1 (A) and D$_2$O ^{31}P {^{1}H}-NMR IST1-OH (B).

The carbonyl group in position 3 of the isatin moiety is an extremely important electrophilic unit that can be further functionalized. In particular, several aldol condensation reactions have been reported [260] on isatin derivatives that turned out to be extremely stereoselective when using amine based chiral organocatalysts like proline derivatives, [261] enantiopure 1,2-cyclohexanediamine species [262] or Cinchona alkaloid amine derivatives.[263] Alternatively, good stereoseletivities were observed also with chiral thiourea catalyst bearing Cinchona units [264] or [2.2]paracyclophane-based derivatives.[265]

In the following section, the highly stereoselective synthesis of isatin containing BPs obtained by organocatalyzed aldol condensation on IST1 is described (**Scheme 45**).
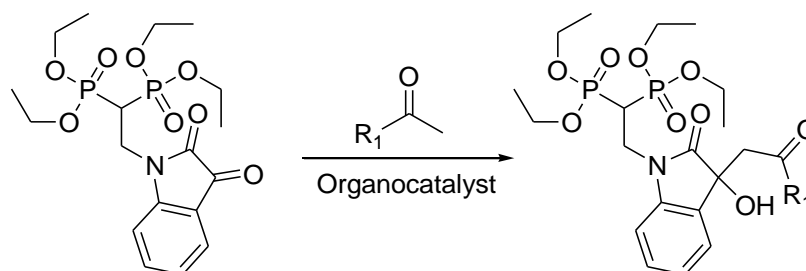
Scheme 45: Organocatalyzed aldol condensation of carbonyl compounds to IST1.
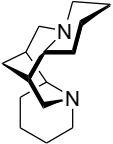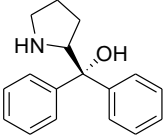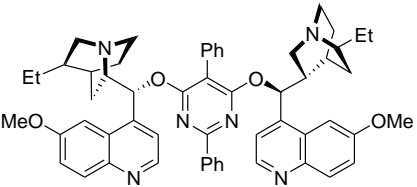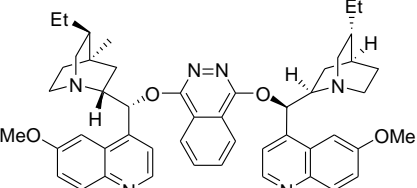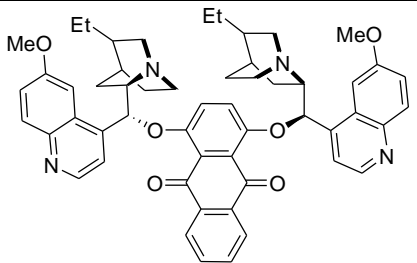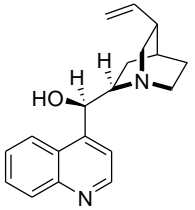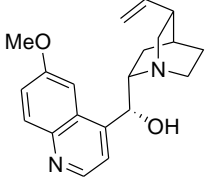
The aldol condensation between IST1 and acetone used both as reagent and solvent awas studied (**Scheme 46**) leading to the corresponding chiral tertiary alcohol. A series of organocatalysts were investigated in order to optimize the yield and stereoselectivityof the reaction.
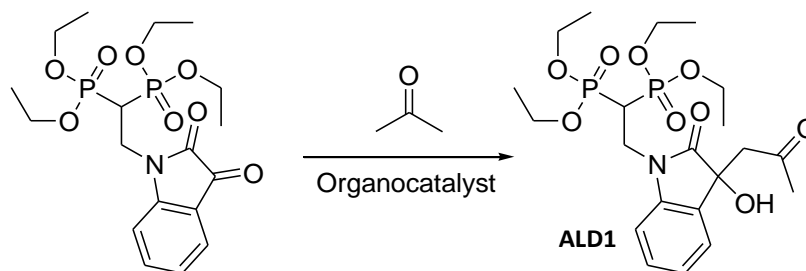
Scheme 46:Organocatalyzed aldol condensation of acetone to IST1.

As reported in **Table 25**, the reaction with (-)-sparteine was completely inefficient (**Table 25, entry 1**), while using (R)-diphenyl(pyrrolidin-2-yl) as organocatalyst, the expected product ALD1 was formed in 84% yield after 48h at room temperature, but unfortunately in the racemic form (**Table 25, entry 2**). A series of dimeric conjugates of cinchona alkaloids were tested (**Table 25, entries 3-5**) observing in all cases yields from 9 to 48% but with no or minimal asymmetric induction on the products. Among other alkaloids, Cinchonidine led to the formation of the desired product in 50% yield and 10% e.e. (**Table 25, entry 6**), while higher yields were observed with Quinine and Quinidine (63% and 73% respectively) with low enantioselectivity (3 and 12% e.e., respectively) (**Table 25, entries 7 and 8**). A marked

increase in catalytic activity was observed with the thiourea derivatives of Quinine TioQN and Quinidine TioQD [194] that allowed good product formation in 85 and 80% yield respectively in 18h at room temperature with low to moderate asymmetric induction (3 and 34 % e.e. respectively, **Table 25, entries 9 and 10**).

	Organocatalyst	Yield [a] (%)	e.e. [b] (%)
1	(-)-spartein	0	-
2	(R)-diphenyl (pyrrolidin-2-yl) methanol	84	0
3	(DHQ)$_2$Pyr	9	0
4	(DHQ)$_2$PHAL	48	-7
5	(DHQ)$_2$AQN	18	-10
6	Cinchonidine	50	-10
7	Quinine	63	-3

8		Quinidine	73	-12
9		TioQN[c]	85	3
10		TioQD[c]	80	-34

Table 25: Organocatalyzed aldol condensation between IST1 and acetone.
Reaction conditions: 0.12 mmol of IST1, solvent: 3 mL acetone, 25 mol% of organocatalyst, rt, 42 h.
[a] Isolated yield, [b] e.e. was expressed by elution order in chromatogram: positive value if the enrichment was in the first enantiomer and viceversa, [c] 18h.

It is noteworthy that chiral organocatalyst bearing free hydroxyl group (**Table 25, entries 2, 6-8**) showed high activity. This means that the hydroxyl group could play an important role in the activation, probably by hydrogen bonding of the electrophylic carbonyl moiety of isatin that undergoes nucleophilic attack by the base formed enolate derived from ketone. Excellent activity of thiourea-chincona derivatives (**Table 25, entries 9 and 10**) could be explained also by the spatial proximity between the H-bonding with the thiourea unit activated isatin and the nearby deprotonated ketone (**Figure 49**) that could enhance the reaction rate as reported by Cong-Gui and co-workers for other Isatin stereoselective ketone additions.[266]
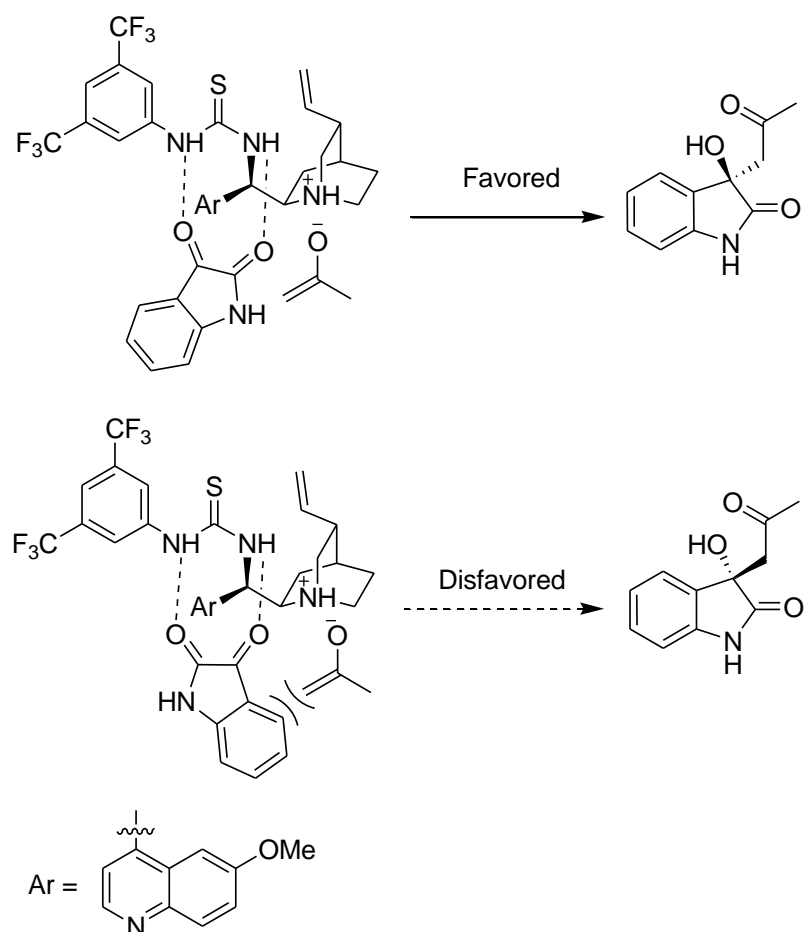
Figure 49: Plausible activation mechanism of isatin by thiourea-chincona derivatives organocatalyst.

The increased organocatalytic activity and moderate stereoselectivity observed with Quinidine-thiourea derivative spurred the investigation of the solvent effect on the reaction (**Scheme 47**).
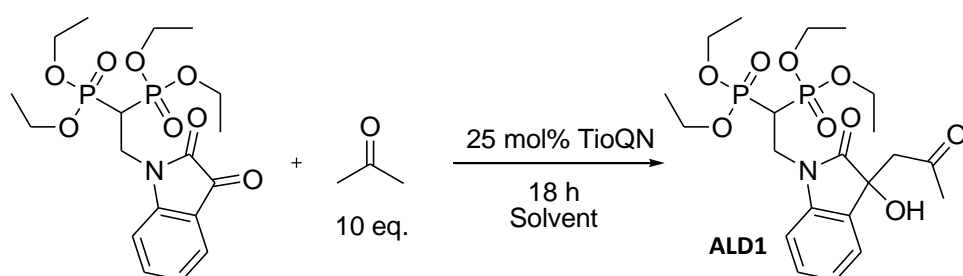
Scheme 47: Aldol condensation of acetone to IST1 under different solvent and temperature reaction conditions.

The aldol condensations between IST1 and 10 equivalents of acetone in apolar solvents like toluene, THF and acetonitrile were repeated, observing after 18 hours decreased yields in the condensation product (18, 21 and 32%, respectively) but positively increased enantioselectivity up to 48% e.e. when acetonitrile was used as the solvent (**Table 26,**

entries 5-7). Reactions with TioQN or TioQD organocatalysts carried out at -10°C instead of room temperature showed only a decrease in product yields without increase in the enantioselectivity of the reaction (3% and 36% e.e. respectively) similar to what obtained at room temperature (**Table 26, entries 1-4**).

	Organocatalyst	Solvent	Temperature (°C)	Yield [a] (%)	e.e. [b] (%)
1	TioQN	Acetone	r.t.	85	3
2	TioQN	Acetone	-10	50	3
3	TioQD	Acetone	r.t.	80	-34
4	TioQD	Acetone	-10	35	-36
5	TioQD	Toluene	r.t.	16[c]	-3
6	TioQD	THF	r.t.	20[c]	-23
7	TioQD	Acetonitrile	r.t.	31[c]	-48

Table 26: Aldol condensation of acetone to IST1 under different solvent and temperature reaction conditions.
Reaction conditions: 0.12 mmol of IST1, 1 mL of the solvent, 25 mol% of organocatalyst, 18 h.
[a] Isolated yield, [b] e.e. was expressed by elution order in chromatogram: positive value if the enrichment was in the first enantiomer and viceversa, [c] 10 eq. of acetone, 18h.
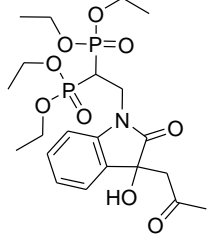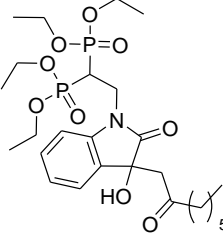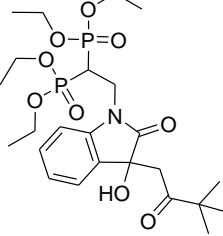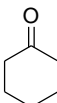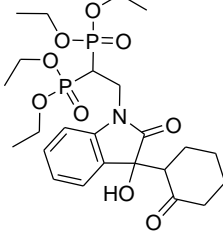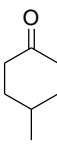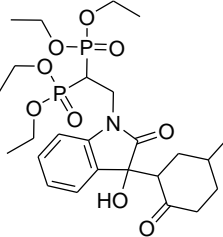
In order to investigate the scope of the reaction, IST1 was reacted with different aliphatic cyclic and acyclic ketones in the presence of the TioQD organocatalyst (**Scheme 48**). The ketones were used also as solvent when liquid at room temperature, while they were employed as a 1.8 M solution in acetonitrile if solid at room temperature. Results are reported in **Table 27**.
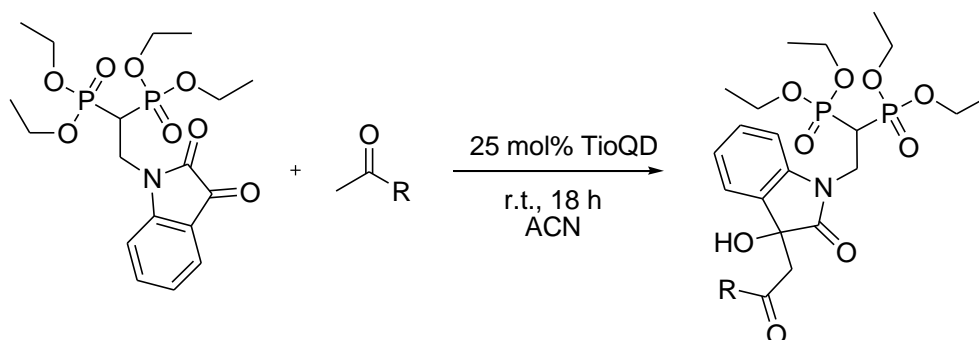
Scheme 48: Aldol condensation between IST1 with different aliphatic cyclic and acyclic ketones in the presence of the TioQD organocatalyst.

	Ketone	BP product		Yield [a] (%)	e.e. [b] (%)
1	(structure)	(structure)	**ALD1**	80	-34
2	(structure)	(structure)	**ALD2**	87[c]	-16
3	(structure)	(structure)	**ALD3**	0[c]	-
4	(structure)	(structure)	**ALD4**	>98	d.r. 67:33, e.e. -90 e.e. -82
5	(structure)	(structure)	**ALD5**	>98	-
6	(structure)	(structure)	**ALD6**	>98	-
7	(structure)	(structure)	**ALD7**	>98	-
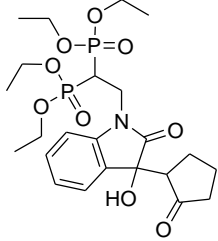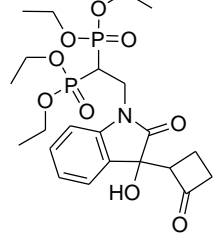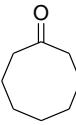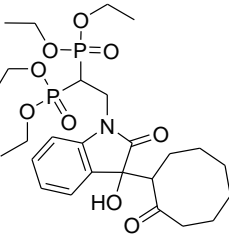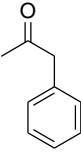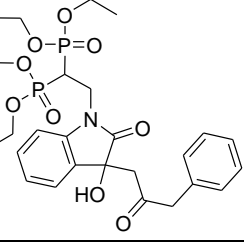
	Ketone	Product		Yield[a]	e.e.[b]
8	(cyclopentanone)	(structure)	**ALD8**	0[c]	-
9	(cyclobutanone)	(structure)	**ALD9**	78[cd]	-
10	(cyclooctanone)	(structure)	**ALD10**	0[cd]	-
11	(phenylacetone)	(structure)	**ALD11**	78	+33

Table 27: TioQD catalyzed aldol condensation of different aliphatic cyclic and acyclic ketones to IST1. Reaction conditions: 0.12 mmol of IST1, 1 mL of the ketone, 25 mol% of organocatalyst, 18 h. [a] Isolated yield, [b] e.e. was expressed by elution order in chromatogram: positive value if the enrichment was in the first enantiomer and viceversa, [c] 42 h, [d] 1.8 M solution of ketone in 1 mL of acetonitrile

With TioQD the use of a longer aliphatic ketone like 2-octanone led to a yield similar to acetone but with a decrease in enantioselectivity (16% e.e.) (**Table 27, entry 2**), while the sterically hindered 3,3,-dimethyl-2-butanone did not form the expected condensation product (**Table 27, entry 3**). Cyclic aliphatic ketones showed very different results depending on ring size (**Table 27, entries 4-10**). In fact, while cyclopentanone and cyclooctanone did not react at all (**Table 27, entries 8, 10**), cyclobutanone and cyclohexanone led to 78% and >98% yield, respectively (**Table 27, entries 4, 9**) observing the formation of two diastereoisomeric species *syn* and *anti*. While for the adduct with cyclobutanone it was not possible to separate the stereoisomers and determine d.e. and e.e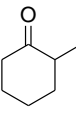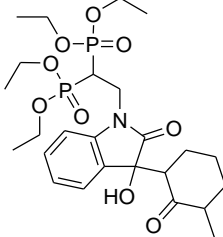., for cyclohexanone a diastereoisomeric ratio of 67:33 and 90% e.e. and 82% e.e. for the two pairs of enantiomers were observed (**Table 27, entry 4**). Other cyclohexanones bearing 2- and 4-methyl or 4-isopropyl substituents (**Table 27, entries 5-7**) on the six membered ring led to

quantitative formation of the aldol condensation products but the presence of three stereocenters on the molecule did not allow to separate the mixture of stereoisomers.

The reaction was then extended to the use of aromatic ketones as reported in **Scheme 49**. Some of the used ketones were synthesized by Au(I) catalyzed hydratation of aromatic alkyne following procedure reported by Nolan et al.[267]
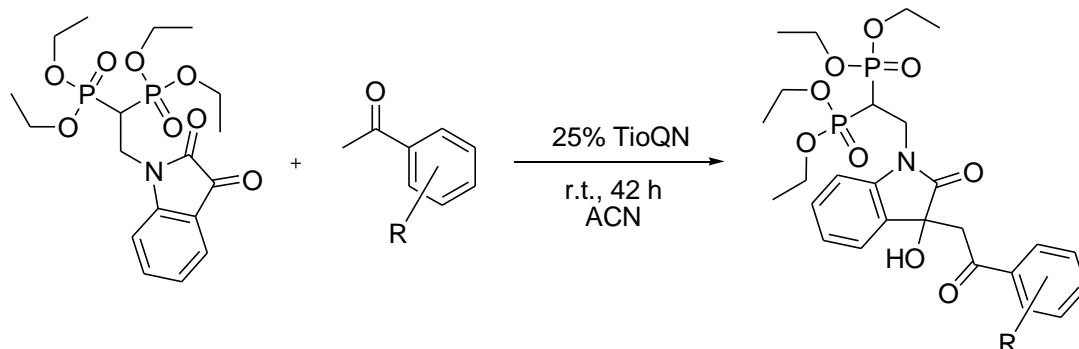
Scheme 49: Aldol condensation between IST1 with different aromatic ketones in the presence of the TioQN organocatalyst.

Ketone	BP product		Yield [a] (%)	e.e. [b] (%)
1		**ALD12**	>98	-81
2		**ALD13**	92	-96
3		**ALD14**	92[cd]	-86
4		**ALD15**	87[cd]	-16

121
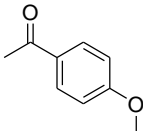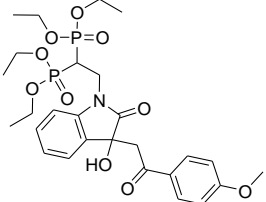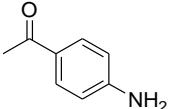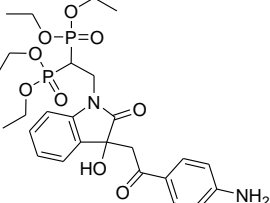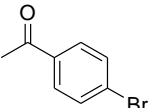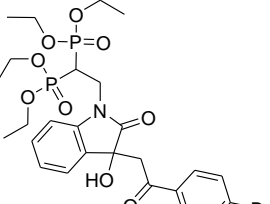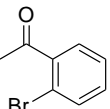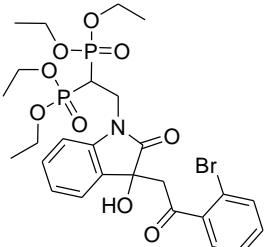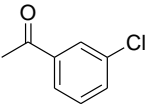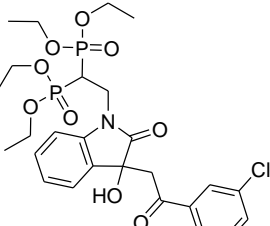
#	Ketone	Product		Yield	e.e.
5			ALD16	68[cd]	-
6			ALD17	0[cd]	-
7			ALD18	81[d]	+60
8			ALD19	>98	-6
9			ALD20	>98	+37

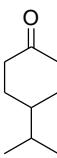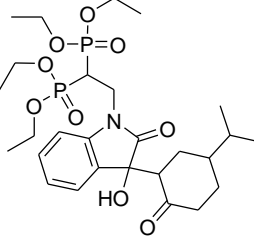Table 28: TioQD catalyzed aldol condensation of different aromatic ketones to IST1.
Reaction conditions: 0.12 mmol of IST1, 1 mL of the ketone, 25 mol% of organocatalyst, 18 h.
[a] Isolated yield, [b] e.e. was expressed by elution order in chromatogram: positive value if the enrichment was in the first enantiomer and viceversa, [c] 42 h,[d] 1.8 M solution of ketone in 1 mL of acetonitrile.

In particular acetophenone led to quantitative formation of the desired product tetraethyl 2-(3-hydroxy-2-oxo-3-(2-oxo-2-phenylethyl)indolin-1-yl) ethane -1,1-diyldiphosphonate (ALD12) with 81% e.e. (**Table 28, entry 1**). The steric and electronic effects of the acetophenone derivatives on the stereoselective aldol condensation were then investigated. This is the case of the reaction with *p*-methyl-acetophenone mediated by TioQD that provided 92% yield with 96% e.e. in favor of the more retained enantiomer (**Table 28, entry 2**) while with *p*-t-But-acetophenone yield was 92% with 86% e.e. (**Table 28,**

entry 3) for the more retained enantiomer. With *p*-pentyl-acetophenone, 87% yield was observed but with a marked decrease of enantioselectivity down to 16% e.e. (**Table 28, entry 4**). With electron donating groups like in *p*-methoxy-acetophenone the reaction was efficient with 68% yield but with no asymmetric induction (**Table 28, entry 5**) while an amino-ketone did not react at all (**Table 28, entry 6**). With electron withdrawing groups as in *p*-bromo-acetophenone the yield was 81% and 60% e.e. (**Table 28, entry 7**), while the ortho isomer led to quantitative product formation but with a dramatic loss in asymmetric induction (**Table 28, entry 8**). Similarly, *m*-chloro-acetophenone provided quantitative yield with moderate stereoselectivity (**Table 28, entry 9**).

The use of a variety of ketones with different steric and electronic properties showed that ketones bearing EWG could better stabilize the enolate intermediate giving higher reaction yields than ketones bearing EDG. Conversely, the stereoselectivity increased with electron-rich reagents probably because of π-π stacking interactions between the chiral base electron-poor aromatic ring and the aromatic ketone reagents.

The isolated products were characterized by ^{1}H, ^{31}P, ^{13}C NMR spectroscopy. ^{31}P {^{1}H}-NMR spectrum of ALD1 is reported in **Figure 50** showing two distinct resonances for the diastereotopic P atoms. Same resonances resulted also in the other isatin BP obtained products. ^{1}H-NMR spectra of ALD1 showed typical signals [268] as reported on **Figure 50**, assigning to H_a signal at 5.75 ppm and to H_b and H_c the overlapped signals at 3.25 ppm.
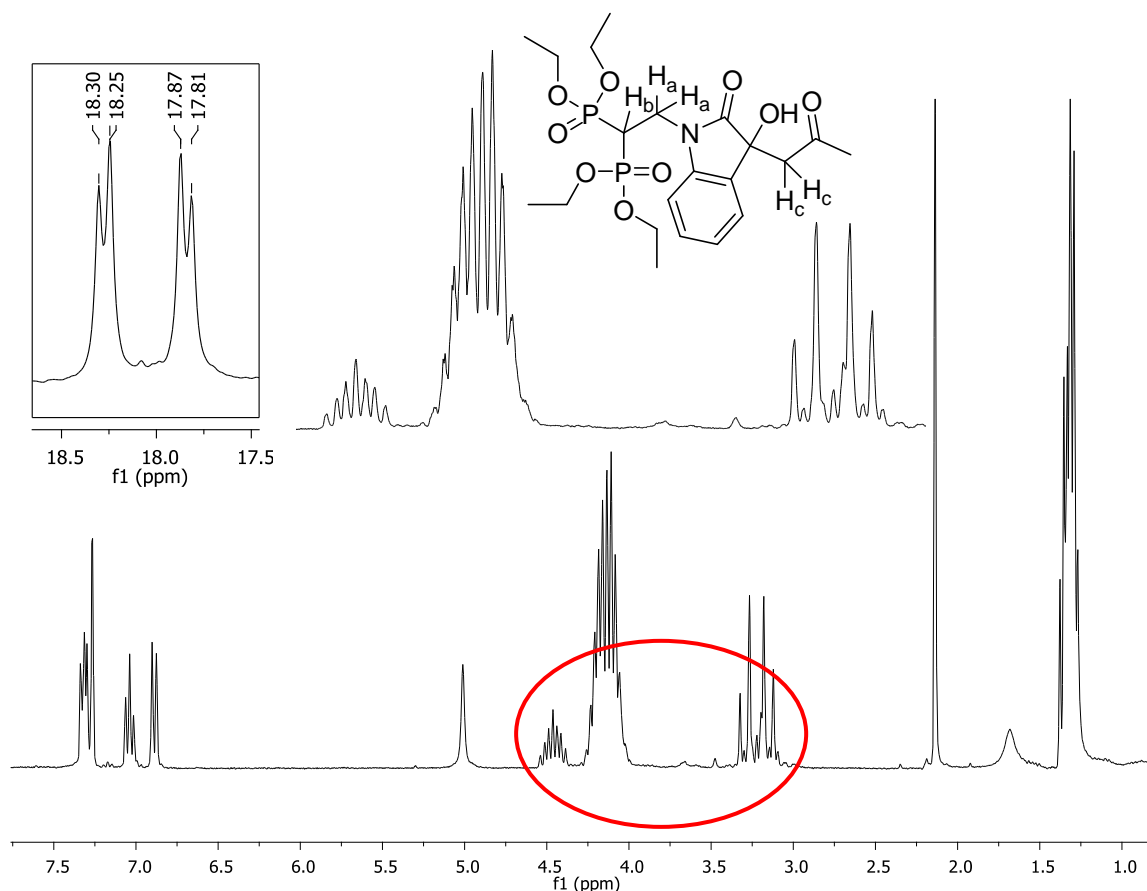
Figure 50: ^{1}H-NMR and ^{31}P {^{1}H}-NMR spectra of ALD1.

It is worth noting that even though Quinine and Quinidine derivatives are actually diastereoisomers differing for the inverted configuration at C8 and C9, often in asymmetric catalysis they behave as enantiomers leading to inversion of the product enatioselectivity and for this reason they are usually referred to as pseudo-enantiomers.[269] This property is particularly interesting in medicinal chemistry where the possibility to obtain both enantiomers in a selective manner is fundamental to assess the biological effects of separate enantiomers.
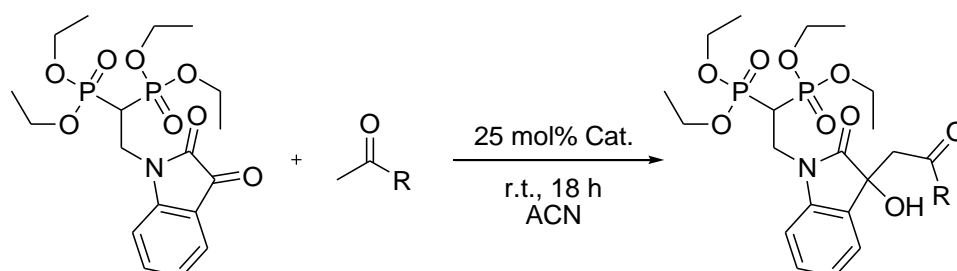
Scheme 50: TioQD and TioQN catalyzed aldol condensation of different aromatic ketones to IST1.

BP product	Catalyst	Yield [a] (%)	e.e. [b] (%)
1 **ALD4**	TioQD	>98	d.r. 67:33 e.e. -90 e.e. -82
	TioQN	70	d.r. 69:31 e.e. +62 e.e. -91
2 **ALD13**	TioQD	92	-96
	TioQN	80	+95
3 **ALD14**	TioQD	92[cd]	-86
	TioQN	76[cd]	+95

Table 29: TioQD and TioQN catalyzed aldol condensation of different aromatic ketones to IST1.
Reaction conditions: 0.12 mmol of IST1, 1 mL of the ketone, 25 mol% of organocatalyst, 18 h.
[a] Isolated yield, [b] e.e. was expressed by elution order in chromatogram: positive value if the enrichment was in the first enantiomer and viceversa, [c] 42 h,[d] 1.8 M solution of ketone in 1 mL of acetonitrile.

Selected ketones were subjected to aldol condensation with IST1 catalyzed also by TioQN in order to verify the ability of obtain both enantioenriched forms of the BP products (**Scheme 50**). The obtained results revealed a decrease in product formation when TioQN was used but confirmed the attitude of TioQN and TioQD to behave as pseudo-enantiomers (**Table 29, entries 1-3**). In fact, the two diastereoisomeric thiourea catalysts led to the formation of the corresponding aldol products in comparable yields but with opposite stereoselectivities. The excellent e.e. obtained e.g. like for ALD13 (**Table 29, entry 2**) give the opportunity to verify the different behaviors of the synthesized enantiomers on toxicity and biological activity tests.

Aldol reaction between IST1 and ketones will be the subject of future studies with other organocatalyst like chiral squaramide derivatives [270] aiming at enhancing the stereoselectivity of the reaction and seeking for suitable new enantiopure anti-resorptive drugs to be tested for the relation between stereochemistry and biological activity.

3.13   FLUORESCENT BISPHOSPHONATE PROBE

The diagnosis and treatment of bone diseases have been improved by the development of new quantitative methods of skeletal assessment and by the availability of an increasing number of therapeutic options, respectively. A number of imaging methods exist and all have advantages and disadvantages.

In vivo imaging methods have been widely used in the diagnosis of bone diseases and are based on nuclear medicine techniques using radioactive tracers as contrast agents. Commonly BP drugs are used that, by means of appropriate linkers, convey radioactive metals such as [99m]Tc [271, 272] or ^{68}Ga to the bones.[273] The administration of the same tracers can become an effective [274] therapy if the metals are [177]Lu [275], [186]Re [276] or [90]Y. [277] Laboratory experiments use this type of tracers as well as simple isotope enriched BPs [278] in pharmacokinetic and pharmacodynamic studies.

Over the past two decades optical imaging, including fluorescence, has become an attractive tool with unprecedented advantages in live cell imaging, examining and monitoring disease stages and determining therapy effectiveness in preclinical models in cells cultures as well as living tissues. Fluorescence imaging relies on the detection of light emission of specific fluorophore when excited by appropriate wavelength energy: together with the development of a vast array of fluorescent imaging probes and conjugates, it is now possible to point out several cells and trace virtually any intracellular or extracellular mechanism. Fluorogenic probes basically comprise a recognition unit (bullet) attached to a signaling unit (fluorophore) that converts molecular recognition into highly discriminative and easily detected/measured optical signals. Variation of signals are associated with changes in the photophysical properties of the probes such as fluorescence enhancement/quenching due to interaction of the probes with particular analytes: binding of a specific analyte to a fluorophore can cause either enhancement (turn-on) or quenching (turn-off) of the fluorescence intensity, coupled with a red or blue shift of the emission band or absorption band.

McKenna and co-worker were the first to report in 2008 [279] the synthesis of the fluorescent labeled conjugates of risedronate using an epoxide linker strategy that enabled conjugation of BP with a carboxyfluorescein label (**Scheme 51**).
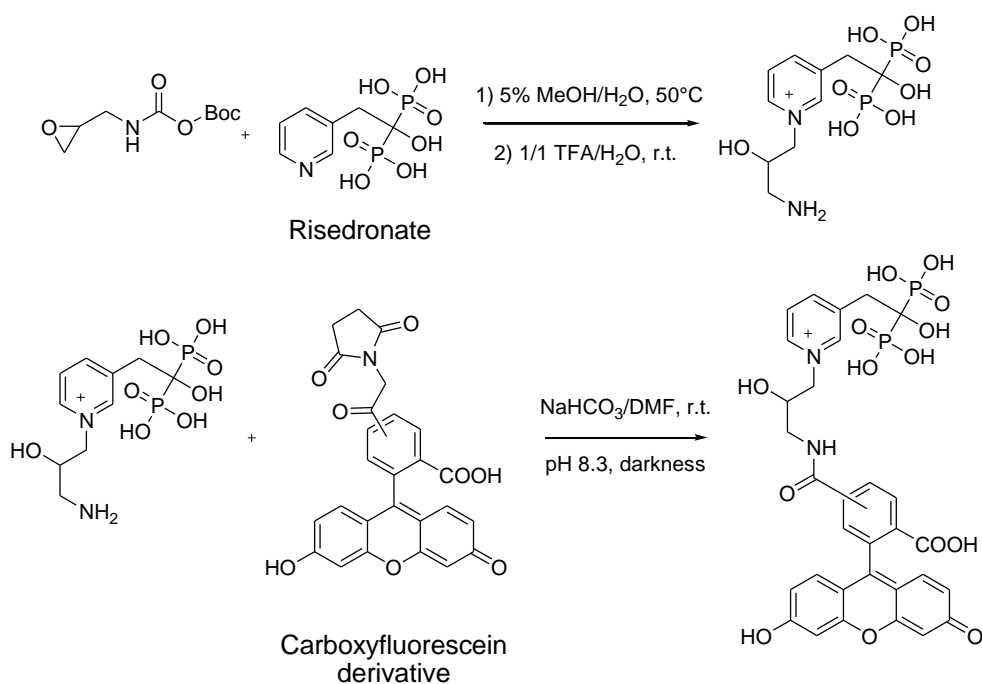
Scheme 51: "Magic Linker" strategy reported by Prof.McKenna.

These authors demonstrated also that the new linking chemistry did not hamper the ability of the BP to inhibit protein prenylation in vitro, visualizing osteoclast resorption in vitro. McKenna's group extended this method to several BP-dyes combinations [280] creating and testing a toolkit of bone imaging fluorescent probes with variable spectroscopic properties, bone mineral binding affinities and antiprenylation activities.[281] Other fluorescent probes were developed by Kikuchi et al [282] that reported a pH dependent BP-borondipyrromethene (BODIPY) probe for the detection of bone-resorbing osteoclasts *in vivo* (**Figure 51-A**). α-bis substituted fluorescent BPs [283] as well as non-gem bisphosphonate fluorescent nanoparticles [284] were also studied (**Figure 51-B and C**).

Near-infrared (NIR) fluorescence imaging is also suitable for *in vivo* studies of bone minerals and cells. Firstly introduced in 2001, [285] it requires the covalent conjugation of a bisphosphonate to an NIR fluorophore (**Figure 51-D**), creating a highly potent bifunctional molecule for biomedical imaging.[286, 287]
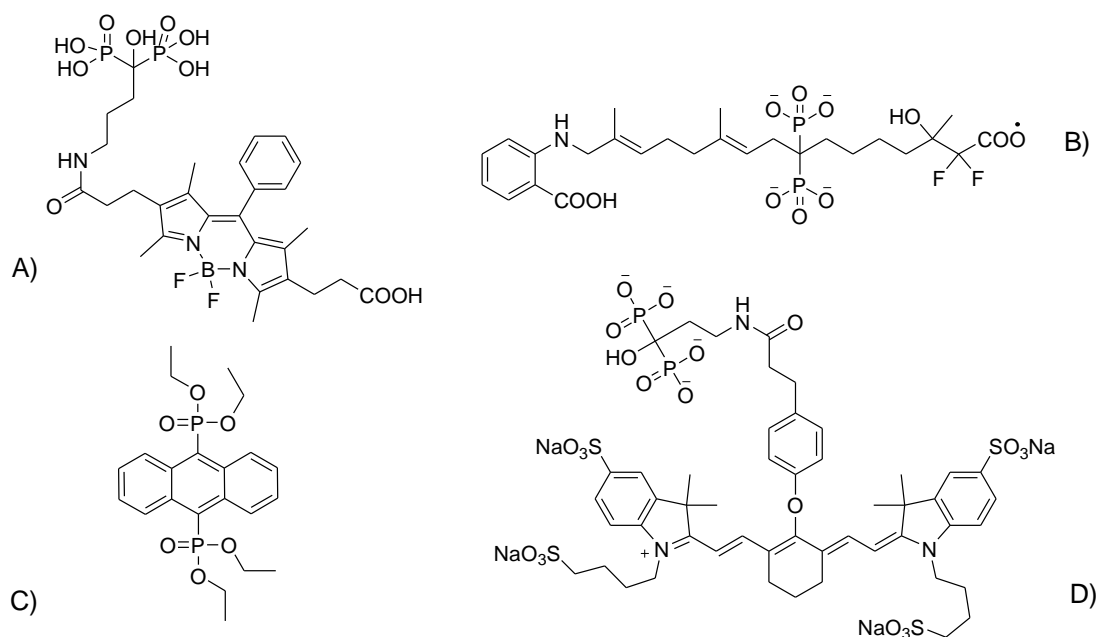
Figure 51: A) BODIPY pH sensitive BP fluorescent probe; B) α-bis substituted fluorescent BP; C) non-gem BP fluorescent nanoparticle; D) first BP conjugate to an NIR fluorophore.

All BP fluorescent probes so far synthesized use as fluorophores molecules widely used in biochemistry (**Figure 52**), such as Carboxyfluorescein (FAM), AlexaFluor 647 (AXF647), rhodamine red (RhR), carboxyRhodamine (ROX) and others. [281] To the best of our knowledge, no fluorescent BP probes have been so far synthesized with diketopyrrolopyrrole based dyes as fluorophore group.
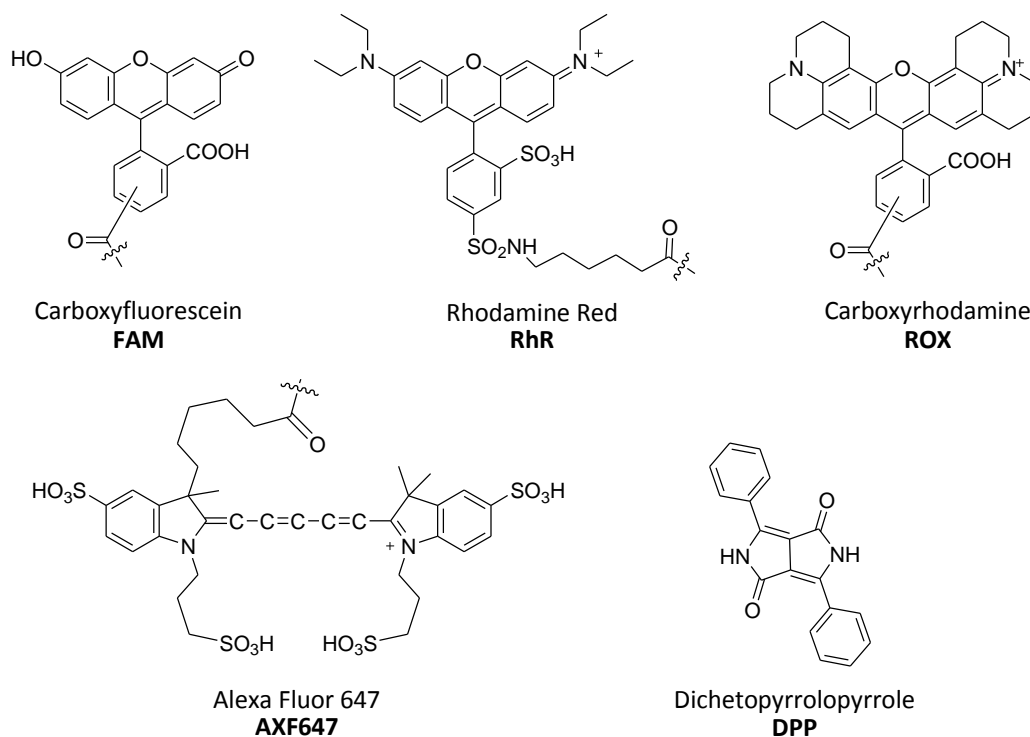
Figure 52: Common fluorophores used in biochemistry application and DPP structure.

3.13.1   *Diketopyrrolopyrrole Based Dyes*

Diketopyrrolopyrrole (DPP) was discovered and synthesized for the first time by accident in 1974 [288] in prof. Siegal studies on 2-azetinones synthesis. Nowadays DPP is synthesized by pseudo-Stobbe reaction of aromatic nitrile with dialkyl succinate (**Scheme 52**) following a procedure developed by Ciba researchers. [289]
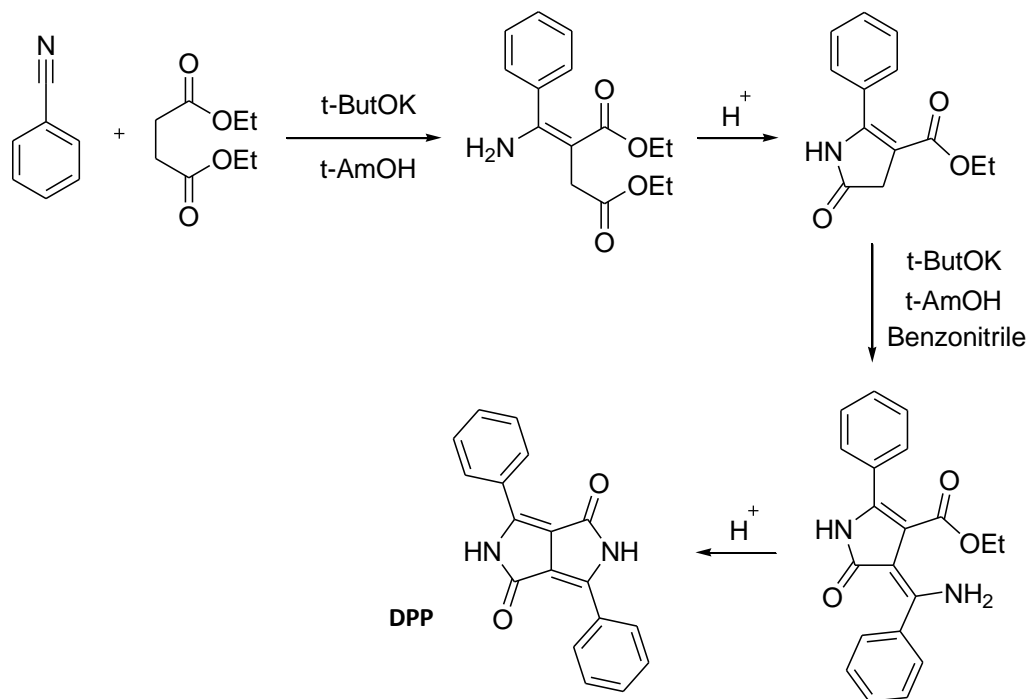
Scheme 52: Synthesis of 3,6-diphenylpyrrolo[3,4-c]pyrrole-1,4(2H,5H)-dione (DPP).

DPP attracted considerable research interest over the past few years due to its peculiar properties. DPP is a bicyclic system with high melting point (>350°C) coupled with low solubility (<110 mg/L in DMF at 25°C) giving low reactivity but outstanding physico-chemical stability. DPP has a planar structure that can induce strong intermolecular H-bonding between NH and carbonyl group as well as π-π stacking with neighboring molecules. All these properties explain its low solubility. The molecular frame of DPP has many reactive centers such as the aryl rings that undergo electrophilic or nucleophilic reactions and the bicyclic lactam chromophoric unit with three other different functional groups: double bonds, carbonyl and secondary amine groups that may potentially undergo structural modification for further derivatization.[290] DPP shows an absorption spectrum in the visible region with an absorbance peak at 504 nm in solution and 538 nm in the solid state with high molar extinction coefficient (33850 L·mol^{-1} · cm^{-1}).[291] Solid DPP is coloured in intense red, while its solutions are bright flourescent yellow. Similarly to DPP, even DPP derivatives exhibit high fluorescence and fluorescence quantum yields and possess exceptional thermal and photostability. Difference between emitted and adsorbed wavelenght (Stokes Shift) are comprised between 10 and 15 nm with average

fluorescence quantum yields of 60%. Notably changing residues at the N-position allow to enhance both solubility [292] as well as the Stokes Shift.

DPP attracted the interest of several research groups in the chemical community because of its wide application as a fluorescent probe over other organic dyes caused by its excellent photostability and quantum yields. To date, DPP-based high-performance materials have been developed, [293] while the ability of DPP to recognize biologically important species still remains relatively unexplored. DPP-based fluorescent probes for various analytes such as anions [294], cations [295], reactive oxygen species (ROS) [296], thiols [297], pH [298], CO_2 [299], and H_2 [300] are known. Fluorescent DPP derivatives as biological probes were reported by Bolze et al. [301] who synthesized a DPP-based non-ionic water-soluble Two-Photon-Excited Fluorescence (TPEF) microscopy dye (**Figure 53-A**) characterized by high phostability. These probes were explored for their application in co-focal and TPEF microscopic evaluation of tumoral HeLa cell cultures. The same group developed also a fluorescently tagged peptides [302] with useful perspective in microscopy for living cells.
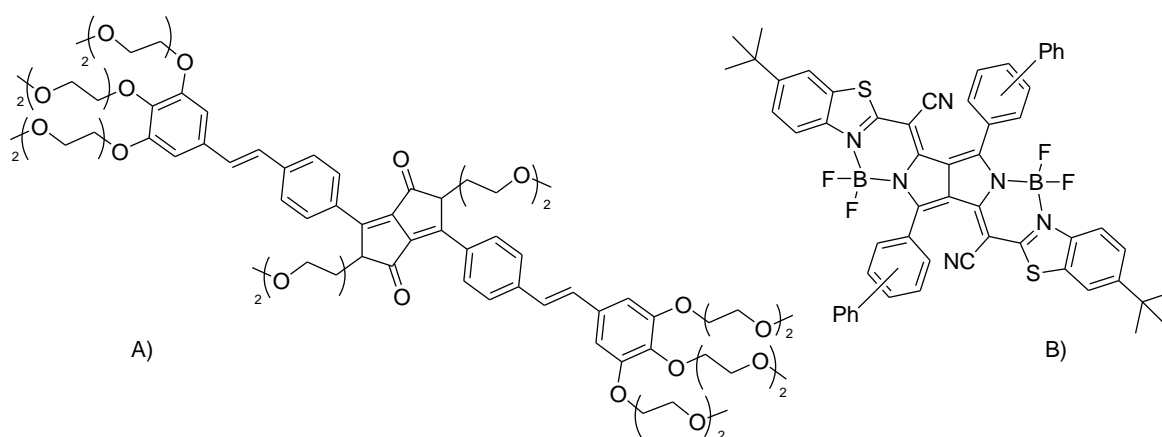
Figure 53: A) water soluble fluorescent DPP biologic probes and B) pyrrolopyrrole cyanine dyes as NIR fluorophores.

Structural modifications of the DPP unit have been carried out for the development of highly stable NIR dyes. Daltrozzo and collaborators modified the DPP core to synthesize cyaninetype NIR absorbing dyes, [303] exhibiting weak absorption in the visible spectral range, but strong and narrow absorptions in the NIR region (**Figure 53-B**). Furthermore, water-soluble pyrrolopyrrole cyanine dyes were synthesized as NIR fluorophores observing their highly photostability.[304] Live cell imaging showed the easy internalization of these dyes into mammalian cells through endocytosis processes, demonstrating their advantages for imaging applications at the cellular level confirming the DPP-based dyes intriguing properties that make them new candidate molecules for use as molecular probes in bio-imaging.

3.13.2   *Triazole Bisphosphonates: Copper Catalyzed Azide-Alkyne Cycloaddition*

As previous described, it is known that a wide range of compounds containing 1,2,3-triazole structural moiety exhibited diverse biologically properties, such as anti-HIV [201] and antimicrobial activities. [202] With respect to introducing 1,2,3-triazole groups into organic molecules, one of the most popular reactions, the copper(I)-catalyzed Azide-Alkyne Cycloaddition discovered by the groups of Sharpless and Meldal [203, 204] belongs to the *"Click Chemistry"* class. Copper-catalyzed azide-alkyne cycloaddition (CuAAC) is a metal catalyzed version of the Huisgen 1,3-dipolar cycloaddition between a terminal alkyne and an organic azide leading preferentially to the formation of 1,4-disubstituted 1,2,3-triazoles (**Scheme 53**).
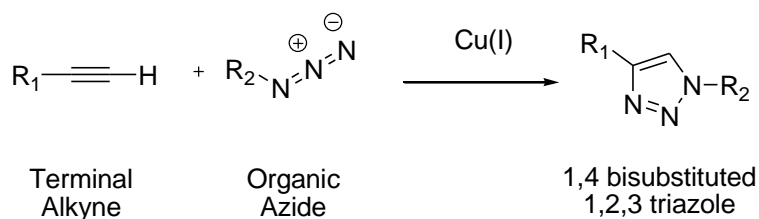
Scheme 53: Genaral copper-catalyzed azide-alkyne cycloaddition (CuAAC).

The use of Cu(I) allows the cycloaddition to occur at room temperature or under moderate heating, leading to high regioselectivity and exclusive formation of 1,4-disubstituted triazole with much shorter workup and purification steps.[305] It is worth of notice that 1,5-disubstituted triazole could be obtained by analogous ruthenium-catalyzed azide-alkyne cycloaddition (RuAAC) as reported by Fokin's group in 2005.[306] CuAAC catalyzed reaction is a virtually quantitative, very robust, general reaction, suitable even for biomolecular ligation [307] or polymerization [308] that could be performed under a wide variety of conditions and with almost any source of solvated Cu(I).[309] $CuSO_4$ is usually used as catalyst with sodium ascorbate as reducing agent in water/tert-butanol mixture in 2:1 ratio at room temperature following the conditions developed in the pioneering study by Sharpless and co-workers.[203] The product is usually formed in very high yield if the reactants do not precipitate [310] and if Cu(I) remains in the same oxidation state and does not undergo oxidation or disproportion. The common use of a Cu(II) source coupled with large excess of reducing agent maintain the Cu(I) concentration at a high level at all times during reaction. The presence of reducing agent makes the reaction much less susceptible to oxygen enabling to avoid strict air-free conditions. Except for decomposition due to substrate instability, the triazole-formation is essentially insensitive to steric bulk and electronic properties of the alkyne and azide, [305] although the rate of the reaction may differ and conditions may have to be optimized in specific cases. The triazole formed is essentially chemically inert to e.g. oxidation, reduction, and hydrolysis. [311]

The Cu(I)-catalyzed variant of Huisgen 1,3-dipolar cycloaddition of organic azide with dipolarophiles is considered to be a stepwise process involving copper in the intermediate steps.[312] Initially copper forms an acetylide via coordination to the alkyne (**Scheme 54**). The current evidence indicates that the copper acetylide species involved in catalysis requires two metal centers. [313] Following the formation of the active copper acetylide species, azide displacement of one ligand generates a copper acetylide-azide complex. Complexation of the azide makes it more susceptible to nucleophilic attack at terminal nitrogen atom by the acetylide carbon, generating a unconventional metallacycle. The intermediate then undergoes ring contraction to give copper triazolyl derivative, which upon protonolysis gives the desired 1,2,3-triazole product (**Scheme 54**). [305]
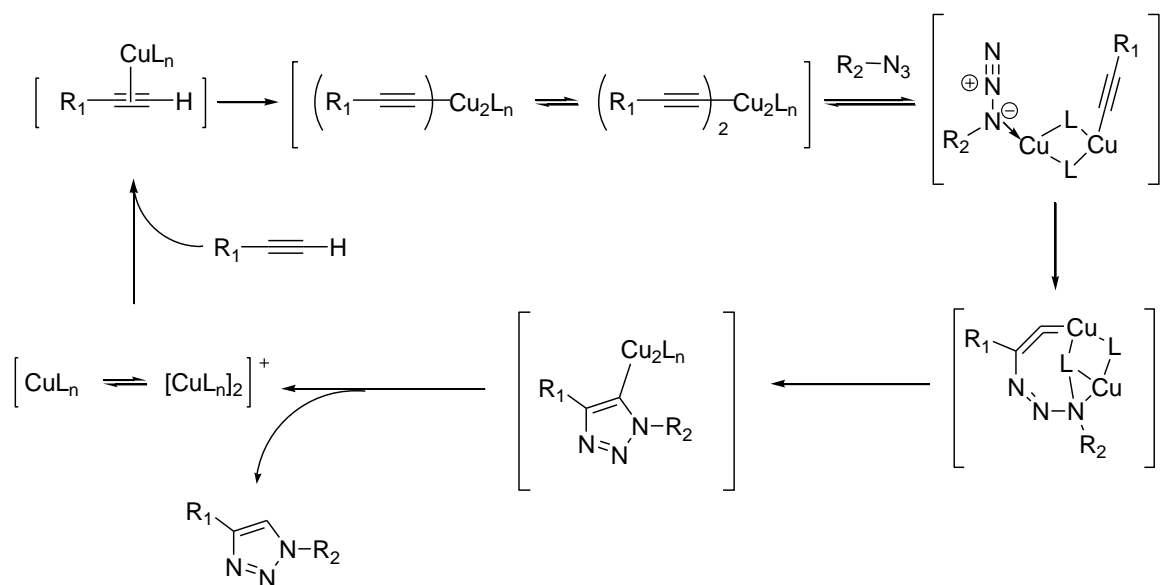
Scheme 54: Proposed mechanism for copper-catalyzed azide-alkyne cycloaddition (CuAAC).

Several application of CuAAC "Click Reaction" have been reported involving phosphonates reagents: Delain-Bioton and collaborators [314] reported the CuAAC synthesis of 1,2,3-triazolyl-alkyl phosphonates through Huisgen 1,3-dipolar cycloaddition. Either alkynyl phosphonate or azido phosphonate were used as starting materials for the cycloaddition with an azidoalkane or a substituted alkyne respectively, obtaining high yields of products in a regiospecific fashion (**Scheme 55**).
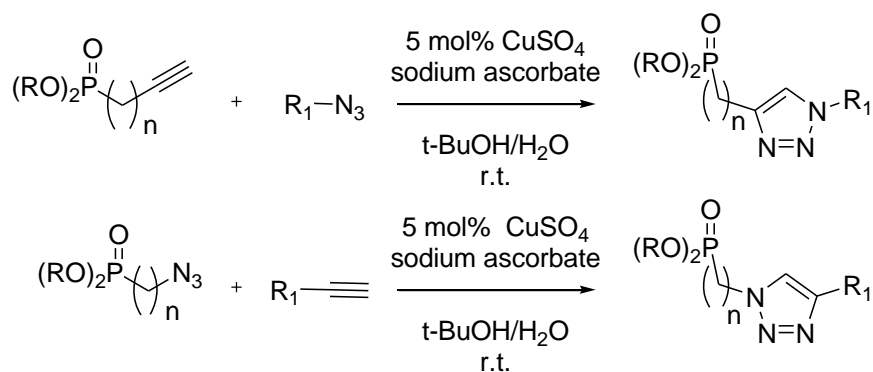
Scheme 55: Synthesis of 1,2,3 triazolyl substituted alkyl phosphonates.

Also monopropargyl-substituted phosphonocarboxylate, structurally similar to BPs, has been used to obtain via CuAAC a series of novel potentially biologically active 1,2,3-triazole-containing phosphono carboxylates (**Scheme 56**).[315]
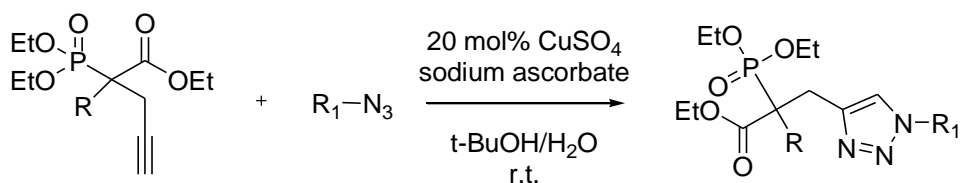
Scheme 56: Synthesis of 1,2,3 triazolyl substituted phosphono carboxylates.

Numerous CuAAC "Click" examples are reported using only alkynyl BPs [316] as starting reagents, also under ultrasound conditions, [317] coupling the former units to anticancer pharmacophore [318] or long hydrophobic tail in order to test their cytotoxicity and ability to act as inhibitor of geranylgeranyl diphosphate synthase.[319, 320]

Only the synthesis of few examples of α-azido BP [207] and γ-azido BP [208] have been reported but no Click reactions were tried with these compounds. Conversely, syntheses and reactions with β-azido BP is a highly debated topic.[209, 210] As reported in **Chapt. 4.8**, by addition of trimethylsylil azide to VBP we were able to synthesize a stable β-azido BP, reporting consistent spectroscopic data in order to support the obtained structure. Click reaction on β-azido BP is therefore an underdeveloped area of research. In order to fill this gap, β-azido BP was tested in the CuAAC with alkynyl DPP fluorescent derivatives. Conjugation by triazolynic bridge between azido-BP and a new DPP fluorophore group could originate a new fluorescent probe (**Scheme 57**) where anti resorption activity is maintained, giving the opportunity to use this new molecule as fluorescent probe on *in vitro* studies of osteoclast activity.

3.13.3 *β-N₃ BP Click Reaction*

The possibility to obtain β-azido BP as previously reported, gave the opportunity to establish a collaboration with Prof. De Lucchi and his research group at the Università Ca' Foscari di Venezia that are expanding their interest in DPP syntheses and functionalization. [292] The efforts of the two research groups joined in order to test β-azido BP on CuAAC with alkynyl DPP fluorescent derivatives.

Using reaction conditions reported by Sharpless and co-workers [203], CuAAC reaction was first run between β-N$_3$BP and tert-butyl 1,4-dioxo-3,6-diphenyl-5-(prop-2-ynyl)-4,5-dihydropyrrolo[3,4-c]pyrrole-2(1H)-carboxylate (DPPBoc) as terminal alkyne (**Scheme 57**).
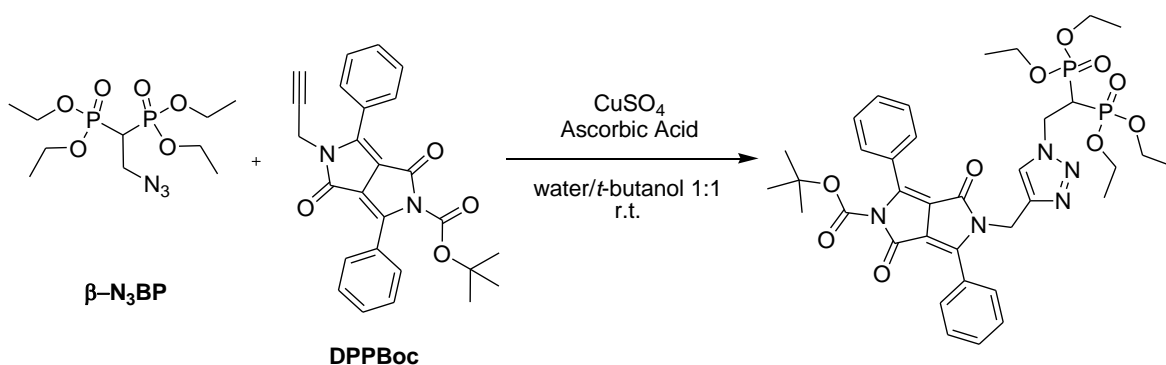
Scheme 57: CuAAC reaction between β−N$_3$BP and DPPBoc

	BP precursor	Alkyne	Catalyst	Solvent	Main product
1	β-N₃BP	DPPBoc	CuSO₄/Ascorbic acid 1 eq/2 eq	water/*t*-butanol 1/1	VBP
2	β-N₃BP-Me	DPPBoc	CuSO₄/Ascorbic acid 1 eq/2 eq	water/*t*-butanol 1/1	VBP-Me
3	VBP[a]	DPPBoc	CuSO₄/Ascorbic acid 1 eq/2 eq	water/acetic acid 1/1	
4	VBP[ab]	DPPBoc	CuSO₄/Ascorbic acid 1 eq/2 eq	water/acetic acid 1/1	Not isolated
5	VBP-Me[a]	DPPBoc	CuSO₄/Ascorbic acid 1 eq/2 eq	water/acetic acid 1/1	
6	β-N₃BP	1-Octyne	CuSO₄/Ascorbic acid 1 eq/2 eq	water/acetic acid 1/1	VBP

Table 30: CuAAC reaction on DPPBoc under different experimental conditions.

Reaction conditions: 0.09 mmol of BP, 2 mL of solvent, 1 eq of alkyne, r.t., 18 h. [a] 2 eq. of NaN₃ were used in order to form in situ azido-BP. [b] 30 min of sonication of the reaction mixture.

Use of CuSO₄/ascorbic acid (1 eq./2 eq.) catalyst coupled with water/*t*-butanol mixture as solvent resulted in degradation of the azido BP forming basically the starting VBP reagent (**Table 30, entry 1**). Even with methyl protected azido-BP the reaction did not work properly. In fact, VBP-Me was recovered as the main degradation product when β-N₃BP-Me was used as azido reagent under the same reaction conditions (**Table 30, entry 2**). Several attempts were made avoiding the use of β-N₃BP and adapting the reaction conditions reported by Chen and collaborators [209] starting from VBP with excess of NaN₃ in order to give *in situ* formation of β-N₃BP that could directly react with DPPBoc. No azido BP formation occurred despite either a change in the solvent mixture or sonication (**Table 30, entries 3 and 4**), resulting in partial formation of triazolinic-DPPBoc by-product as consequence of the CuAAc reaction between NaN₃ an DPPBoc also when used reduced steric hindrance VBP-Me precursor (**Table 30, entry 5**). CuACC was tested between β-N₃BP and a reduced steric hindrance terminal alkyne like 1-octyne resulting also in this case in decomposition of the azido reagent (**Table 30, entry 8**). Notably DPPBoc showed low solubility in the previously used reaction mixture, hence 3,6-diphenyl-2,5-di(prop-2-ynyl)pyrrolo[3,4-c]pyrrole-1,4(2H,5H)-dione (DPPProp) was choosen as DPP reagent due to its intrinsic higher solubility. Double propargyl moieties connected to the DPP core could originate a fluorescent probe with very high affinity for the bone tissue (**Scheme 58**).
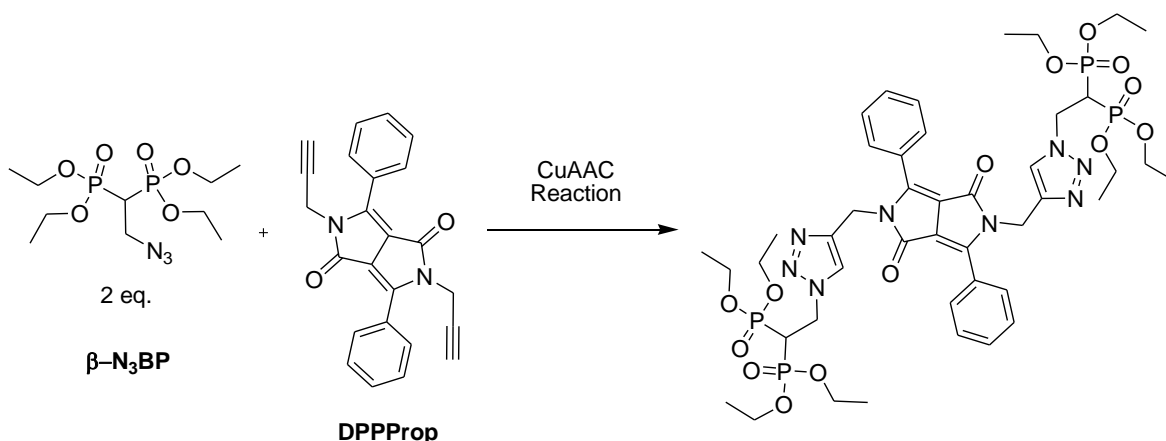
Scheme 58: CuAAC reaction between β-N₃BP and DPPProp.

	BP precursor	Alkyne	Catalyst	Solvent
1	β-N₃BP	DPPProp	CuSO₄/Ascorbic acid 2 eq/4 eq	water/acetic acid 1/1
2	β-N₃BP-Me	DPPProp	CuSO₄/Ascorbic acid 2 eq/4 eq	water/acetic acid 1/1
3	VBP[a]	DPPProp	CuSO₄/Ascorbic acid 2 eq/4 eq	water/acetic acid 1/1
4	β-N₃BP[b]	DPPProp	NHC-CuCl	CH₂Cl₂
5	β-N₃BP[b]	DPPProp	NHC-CuBF₄	CH₂Cl₂

6	β-N$_3$BP[b]	DPPProp	NHC-CuCl	NEAT
7	β-N$_3$BP[bc]	DPPProp	NHC-CuCl	NEAT

Table 31: CuAAC reaction on DPPProp under different experimental conditions.
Reaction conditions: 0.08 mmol of DPPProp, 2 mL of solvent, 1 eq of alkyne, room temperature, 18 h.
[a] 2 eq. of NaN$_3$ were used in order to form in situ azido-BP, [b] 0,5 mol% of catalyst, [c] 80°C.

DPPProp was tested on CuAAC under different reaction conditions using azido-BP as well as with VBP with NaN$_3$ excess (**Table 31, entries 1-3**). The desired product was not obtained in any of tested reactions reported in **Table 31**, recovering just the unreacted reagents. Several attempts were made with a different catalytic system since in the literature it is reported that bis(N-heterocyclic carbene) copper(I) complexes (NHC) are very active for CuAAC reactions [321, 322] even under very low catalyst amount.[323] Use of 0.5 mol% chloro[1,3-bis(2,6-diisopropylphenyl)imidazol-2-ylidene]copper(I) (NHC-CuCl) as catalyst in CuAAC reaction between β-N$_3$BP-Me and DPPProp again did not result in cycloaddition product formation even if β-N$_3$BP with bis(1,3-bis(2,6-diisopropylphenyl)imidazol-2-ylidene)copper(I) tetrafluoroborate (NHC-CuBF$_4$) was used (**Table 31, entries 4-5**). Neat conditions were also tested [324] to push the reaction, but unfortunately again no products were observed (**Table 31, entry 6**). Increase in the temperature reaction up to 80°C coupled with neat conditions (**Table 31, entry 7**) resulted in β-N$_3$BP decomposition with formation of VBPNH$_2$, VBP and 2BP (**Chapt. 4.8**) as main by-products.
Conjugation between β-N$_3$BP and DPP fluorophore was then abandoned.

3.13.4 *γ-N$_3$ BP Click Reaction*

Results presented in this chapter were obtained during a research period in Prof. C.E. McKenna's research group at University of Southern California, Los Angeles (CA), United States of America.

Despite we were not able to obtain Click Reaction between β-azido BP and DPP fluorophore, studies on this type of reaction continued in order to obtain the desired BP fluorescent probe. It was decided to elongate the side chain of BP containing the azido group, evaluating the reactivity of a γ-azido BP in CuAAC.
As a consequence of the versatility of Click reactions, there is a considerable interest in synthetic methodologies for the preparation of organic azides. One possible procedure consists in the diazo-transfer reaction that involves the conversion of a primary amine into an organic azide by the action of a powerful and difficult to handle diazo donor (most commonly a sulfonyl azide). In the following section a simple, straightforward and easily to scale up synthesis of a γ-azido BP lacking the presence of the gem hydroxyl function is described, via diazo-transfer to 3-amino-propane-1,1-bisphosphonate tetraethyl ester (γ−NH$_2$BP). The γ-azido BP was obtained using imidazole-1-sulfonyl azide hydrochloride as a more safer diazo-transfer reagent compared to the more common triflyl azide. [325]

The obtained compound has been tested in click reactions with terminal alkynes as well as the alkynyl DPP fluorophore in order to obtain a new fluorescent probe for *in vitro* study of osteoclast activity.

The reaction of nitromethane with VBP in the presence of sodium methylate (**Scheme 59-A**) gave the corresponding 3-nitro-propane-1,1-bisphosphonate tetraethyl ester (γ−NO$_2$BP) in quantitative yield on a multigram scale when a large excess of nitroalkane was used, in agreement with what reported by Winckler and collaborators.[326] The catalytic hydrogenation of the nitro group allowed to obtain the desired γ−NH$_2$BP which is a suitable reagent for the diazo-transfer reaction (**Scheme 59-B**). The hydrogenation reaction proceeded at room temperature with 1 bar of hydrogen with Pd/charcoal under vigorous stirring and required only one hour to give the corresponding amino bisphosphonate. Longer reaction time resulted in a variety of by-products probably due to dimerization or dealkylation of the ester moiety.
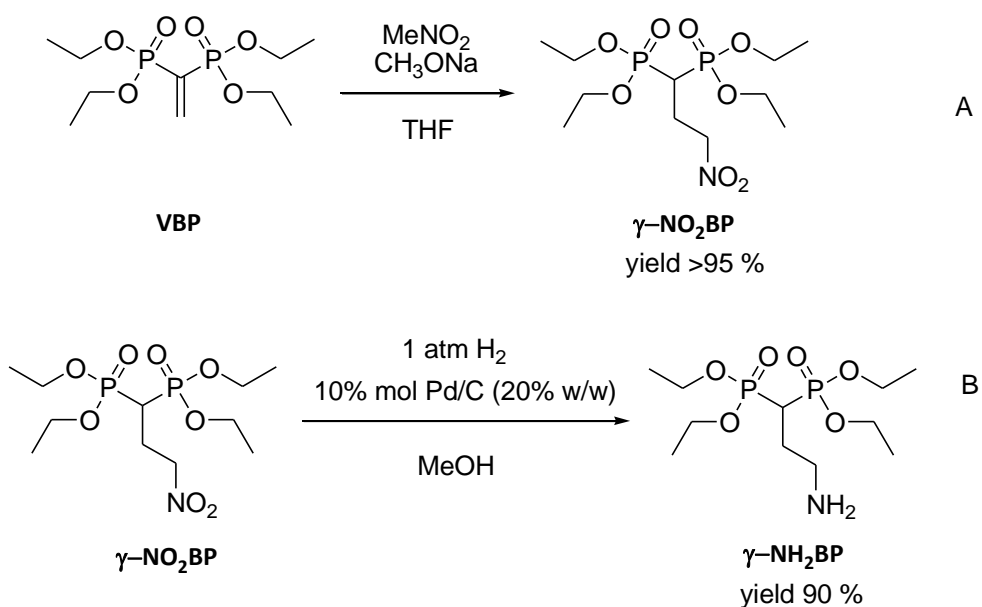
Scheme 59: Adddition of nitromethane to VBP (A) and catalytic hydrogenation of γ-NO$_2$BP (B).

This easy two-step route allowed the synthesis of γ−NH$_2$BP in a multi-gram scale without the need of any purification step. The obtained product turned out to be quite susceptible to decomposition. Therefore it could not be stored and was used right after preparation for the next diazo-transfer reaction.

Diazo-transfer reactions (**Scheme 60**) are commonly used for introducing diazo-functionality or for converting primary amines into azides.[327, 328, 329]
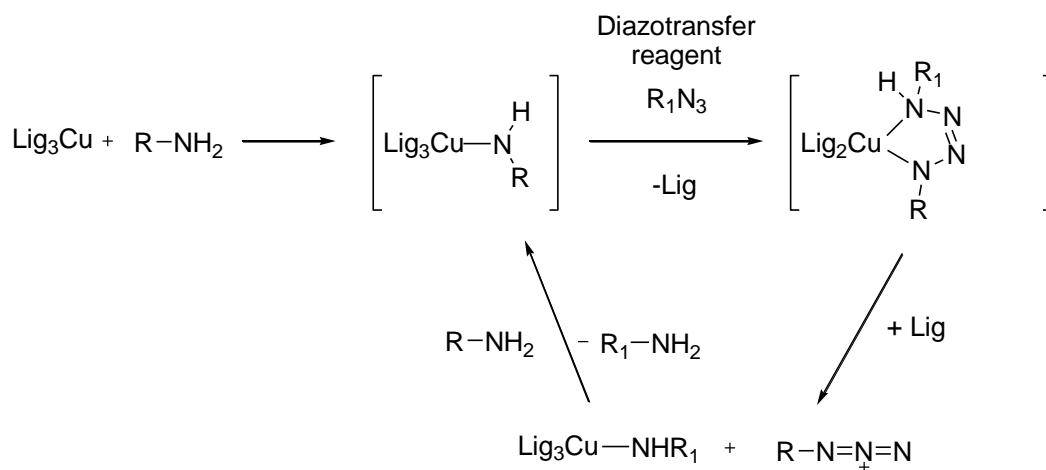
Scheme 60: Plausible mechanism of Cu catalyzed diazo transfer reaction. [330]

Zaloom and Roberts showed that triflyl azide (TfN$_3$, **Figure 54**) is excellent for converting α-amino acids to the corresponding α-azido acids. [331] The method was improved by Alper and collaborators [332] who developed a CuSO$_4$ catalyzed version of the reaction. In the past decades triflyl azide has been the reagent of choice for diazo-transfer reactions even though its standard synthetic protocol [333] has several disadvantages like the use of toxic and costly triflic anhydride, the use of an excess of sodium azide and the formation of highly explosive TfN$_3$ that, under no circumstances, should be isolated. Recent advances in the field led to the introduction of a number of new safer and economic diazotransfer reagents (**Figure 54**). [325]
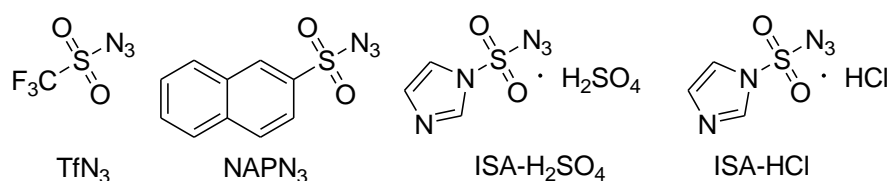
Figure 54: Structures of common sulphonyl azides.

Imidazole-1-sulfonyl azide hydrochloride (ISA-HCl) was chosen as safe and economic diazo-transfer reagent [334] to obtain the desired γ-azido bisphosphonate (γ−N$_3$BP). This diazo-donor was easily prepared by the addition of two equivalents of imidazole to chlorosulfonyl azide, preformed *in situ* by reaction of equimolar amouts of sodium azide and sulfuryl chloride in acetonitrile.[334] This one-pot reaction on a large scale allowed the synthesis of a shelf-stable crystalline ISA-HCl from inexpensive materials (**Scheme 61**). Attempts to synthesize a more stable and safer diazo-donor like imidazole-1-sulfonyl azide hydrogen sulfate (ISA-H$_2$SO$_4$) [335] resulted in a impractical viscous oil otherwise previously reported.
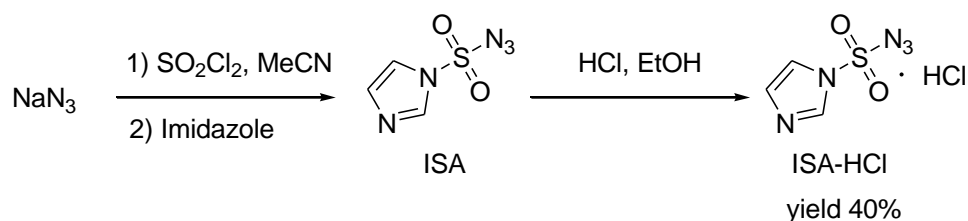
Scheme 61: Synthesis of ISA-HCl.

The diazo transfer reaction between primary amino group and organic azides can be efficiently catalyzed by CuSO$_4$ [332] and this class of catalytic reactions well tolerates the presence of water.[327] The reaction between γ–NH$_2$BP and ISA-HCl was carried out under mild basic conditions (aq. K$_2$CO$_3$, pH=8-10) at room temperature in the presence of 15 mol% of CuSO$_4$ (**Scheme 62**).
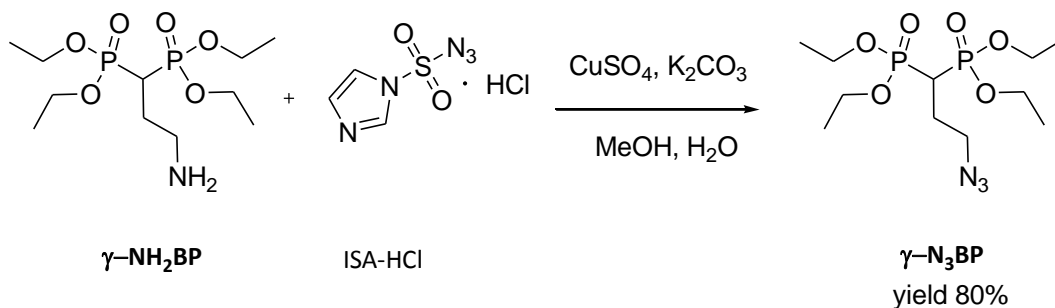
Scheme 62: Synthesis of γ–N$_3$BP.

While the use of the safest diazo-donor 2-Naphthalenesulfonyl azide (NAPN$_3$) [336] gave only the decomposition of the starting reagents, the use of ISA-HCl led to nearly quantitative yields under the previously described mild experimental conditions. The syntheses of γ–N$_3$BP could be scaled up to hundreds of milligrams without significant side effects. The γ-azido BP tetraethyl ester obtained was purified and characterized by ^{1}H and ^{31}P-NMR as well as the others γ-BP compounds. Typical signals are reported in **Figure 55**.
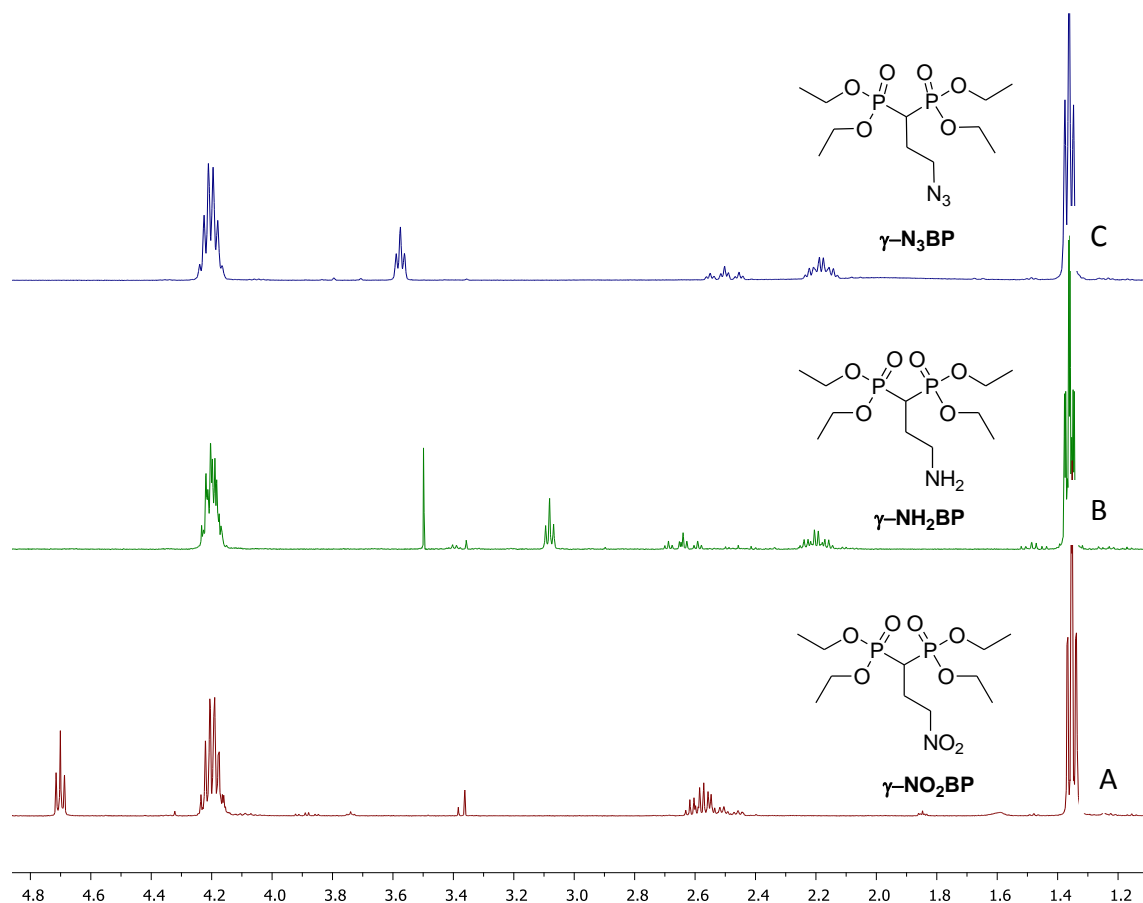
Figure 55: CDCl$_3$ ^{1}H-NMR of γ–NO$_2$BP (A), γ–NH$_2$BP (B) and γ–N$_3$BP (C).

Using the reaction conditions reported by Sharpless and co-workers [203], CuAAC reaction was first run and optimized employing as terminal alkyne 3-butyn-1-ol, a low reactivity alkyne that could mimic the behavior of the DPP fluorophores (**Scheme 63**).
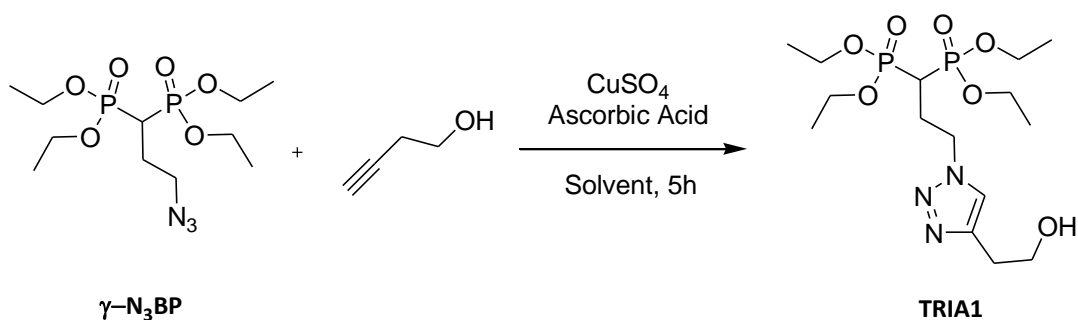
Scheme 63: CuAAC reactionbetween γ–N$_3$BP and 3-butyn-1-ol.

The use of 5 mol% CuSO$_4$ catalyst coupled to 10 mol% ascorbic acid as a reducing reagent did not catalyze the Click reaction (**Table 32, entry 1**). Changing the solvent mixture and the use of an equimolar amount of copper catalyst led to moderate yields of the desired cycloaddition product tetraethyl 3-(4-(2-hydroxyethyl)-1H-1,2,3-triazol-1-yl)propane-1,1-diyldiphosphonate (TRIA1) (**Table 32, entry 2**). The reaction was influenced by temperature, leading to good yields of the desired product TRIA1 when carried out at 50 °C even after

only 2 hours (**Table 32, entry 3**). As described above, (**Chapt. 3.13.2**) the reaction resulted in the total formation of the 1,4 disubstituted cyclic adduct as evidenced by ^{1}H-NMR analysis. Excellent reaction yields and total $\gamma-N_3BP$ consumption were obtained also by reducing the amount of the alkyne reagent as shown in **Table 32, entry 4**. It is noteworthy that the isolated yield of TRIA1 was moderate (26%). The hydroxyl group present in TRIA1 enhances its hydrophilicity, making it difficult the isolation by organic solvent extraction and purification.

	Amount of alkyne [eq.]	Catalyst	Solvent	Temperature (°C)	Yield [a] (%)
1	2	5 mol% CuSO$_4$ 10 mol% ascorbic acid	Water/t-But 2:1	r.t.	0
2	2	100 mol% CuSO$_4$ 200 mol% ascorbic acid	Water/Isopropanol 1:1	r.t.	10
3	2	100 mol% CuSO$_4$ 200 mol% ascorbic acid	Water/Isopropanol 1:1	50	78 75[b]
4	1.1	100 mol% CuSO$_4$ 200 mol% ascorbic acid	Water/Isopropanol 1:1	50	70[b]

Table 32: optimization of CuAAC reaction conditions between $\gamma-N_3BP$ and 3-butyn-1-ol.
Reaction conditions: 0.055 mmol of $\gamma-N_3BP$, 2 mL of solvent, 5 h. [a] 31P-NMR yield, [b] 2 h.

Optimized conditions were used in the Click reaction mediated by copper and ascorbic acid between $\gamma-N_3BP$ and alkynyl DPP based fluorophores like DPPBoc (**Scheme 64**) and DPPProp (**Scheme 65**).
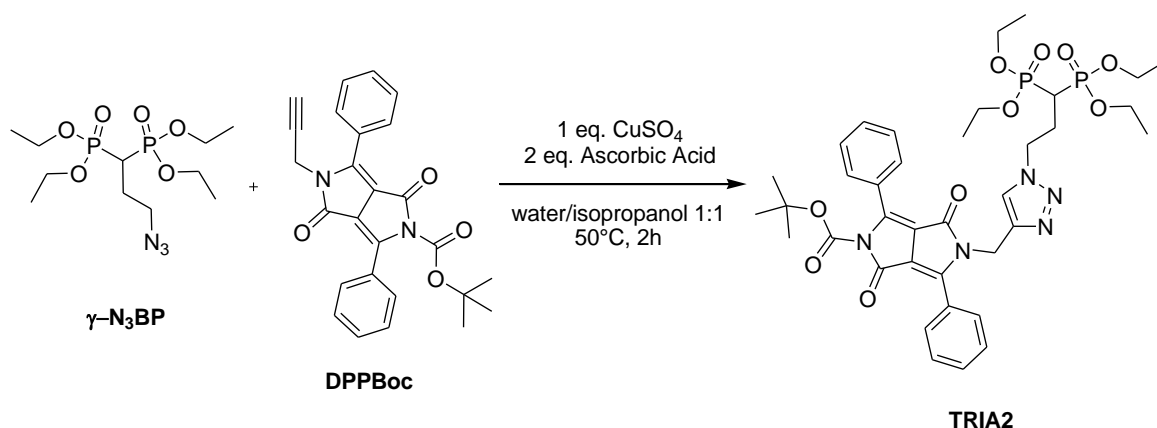
Scheme 64: CuAAC reaction between $\gamma-N_3BP$ and DPPBoc.
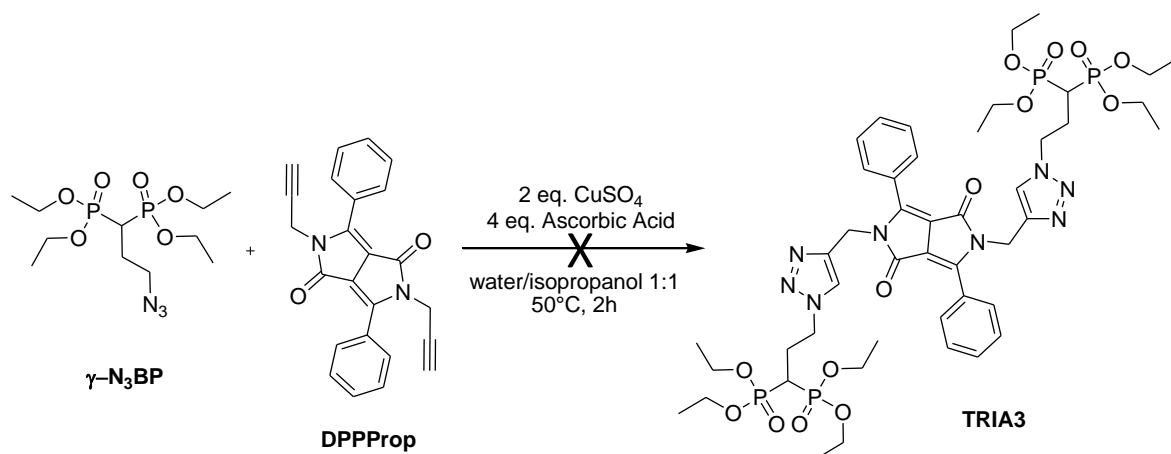
Scheme 65: CuAAC reaction between γ–N₃BP and DPPProp.

At variance with β–N₃BP, the Click reaction between γ–N₃BP and DPPBoc occurred at the first attempt to give the corresponding desired 1,4 substituted triazolic cycloadduct (TRIA2) in 85 % yield, without any difficulties even in the extraction step from the aqueous solvent. Unfortunately, the use of DPPProp having two alkynyl functionality in the Click reaction with γ–N₃BP did not lead to the desired double cycloaddition product. DPPProp showed a particularly low solubility in the reaction mixture, calling for further optimization with this type of fluorophore. Click reaction with DPPBoc was repeated in a 10 times higher scale using 120 mg of γ–N₃BP and allowing to obtain TRIA2 in 90% yield without undesired by-products. Purification by semi automated column chromatography led to the partial loss of a *tert*-butyloxycarbonyl group with consequent deprotection of the amino group of TRIA2 as demonstrated by the splitting of the 1H-NMR signals (**Figure 56**) and confirmed by ESI-MS analysis. It is worth to notice that the singlet at 7.75 ppm assigned to the triazolic proton is in agreement with the literature [317, 319] thus confirming the exclusive formation of a 1,4 substituted triazolic cycle.
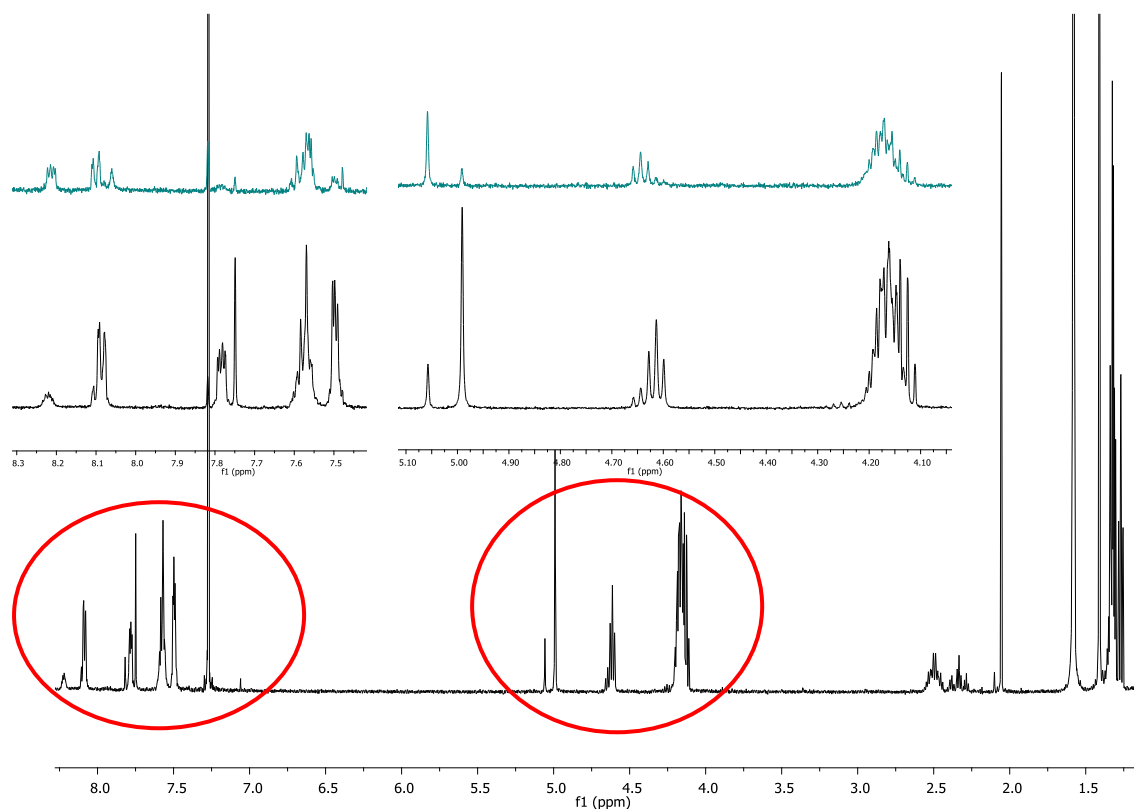
Figure 56: ^{1}H-NMR of TRIA2 revealed partial Boc deprotection.

In order to obtain the fluorescent BP probe for subsequent fluorescent and activity tests, TRIA2 was subjected to deprotection of the ethyl ester groups. The classical method [139] that makes use of TMSiBr at room temperature in dichloromethane was compared to a microwave-assisted method in acetonitrile. The latter turned out to be considerably faster, allowing the formation of the intermediate silylester in only 20 minutes reaction with 16 eq. of TMSiBr at 1200 watt power (**Scheme 66**).
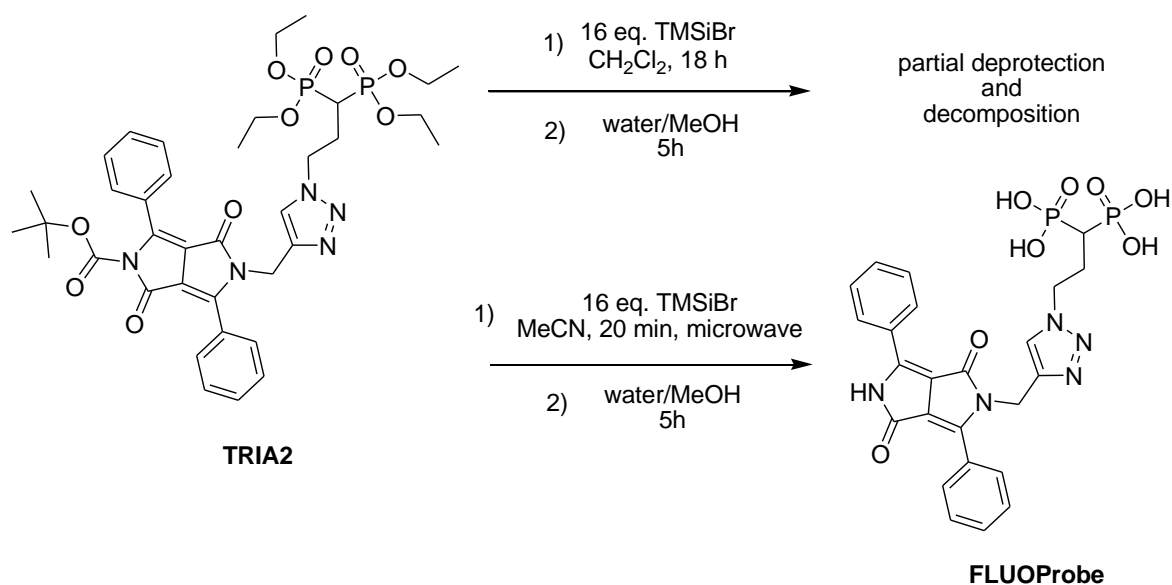
Scheme 66: Classic and microwaves assisted deprotection methods.

^{31}P-NMR analyses in DMSO-d$_6$ of TRIA2 deprotected with classical method showed formation of numerous phosphorus signals, due both to partial deprotection of the ethyl ester groups and to decomposition of the molecule. In contrast, ^{31}P-NMR analyses in DMSO-d6 of TRIA2 deprotected by the microwave assisted method showed the formation of only a sharp signal that was attributed to the corresponding 3-(4-((1,4-dioxo-3,6-diphenyl-4,5-dihydropyrrolo[3,4-c]pyrrol-2(1H)-yl)methyl)-1H-1,2,3-triazol-1-yl)propane-1,1-diyldiphosphonic acid (FLUOProbe). ^{1}H-NMR spectra (**Figure 57**) evidenced that this method ensured also the complete loss of *tert*-butoxycarbonyl group giving FLUOProbe as potential fluorescent probe for *in vitro* test of osteoclast activity.
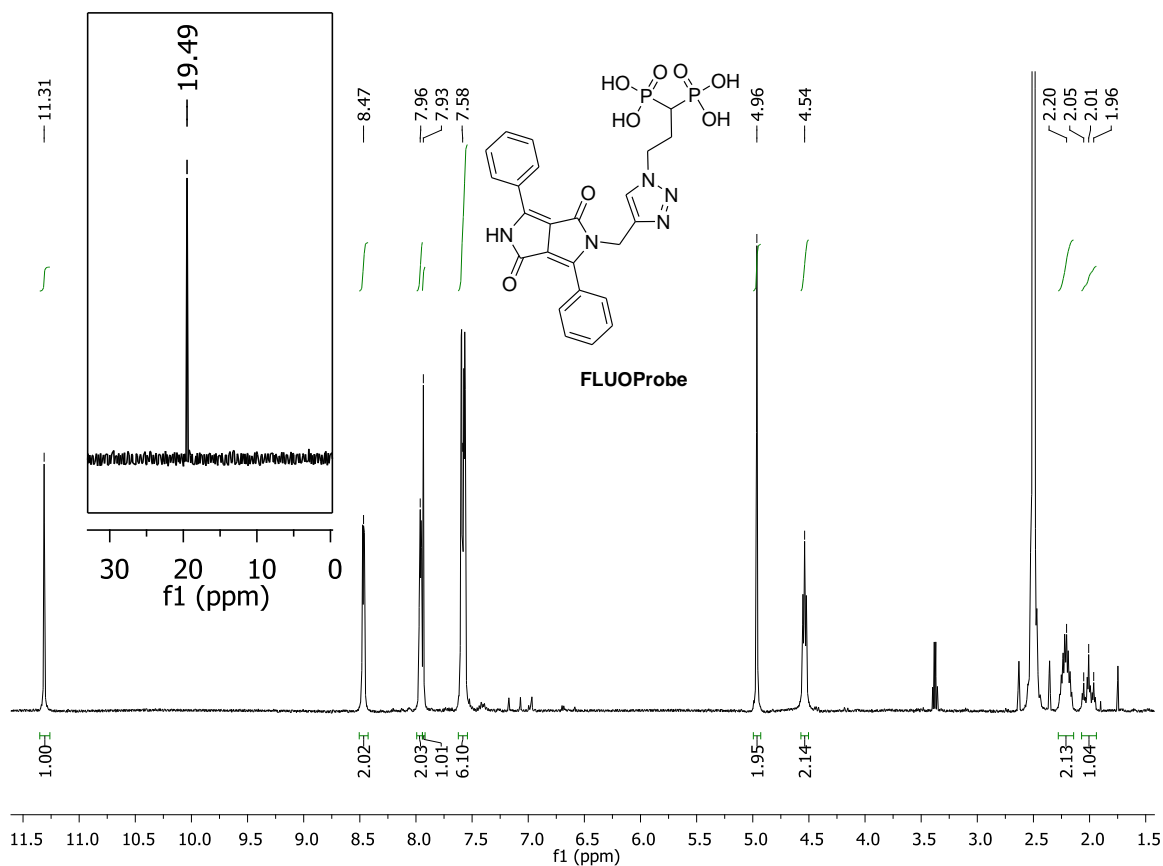
Figure 57: DMSO-d$_6$ ^{1}H-NMR and ^{31}P {^{1}H}-NMR of FLUOProbe.

FLUOProbe was washed with diethyl ether in order to eliminate the presence of HBr formed as by-product from the deprotection step and fully characterized by NMR spectroscopy and ESI-MS. Elemental analysis confirmed a good 85% purity for FLUOProbe that was then used in the activity and fluorescence tests. UV-vis spectra of water/DMSO solution of FLUOProbe were carried out showing a peak at 472 nm. Fluorescence analysis of the same solution showed an emission peak at 512 nm, resulting in a good 40 nm Stokes Shift (**Figure 58**).
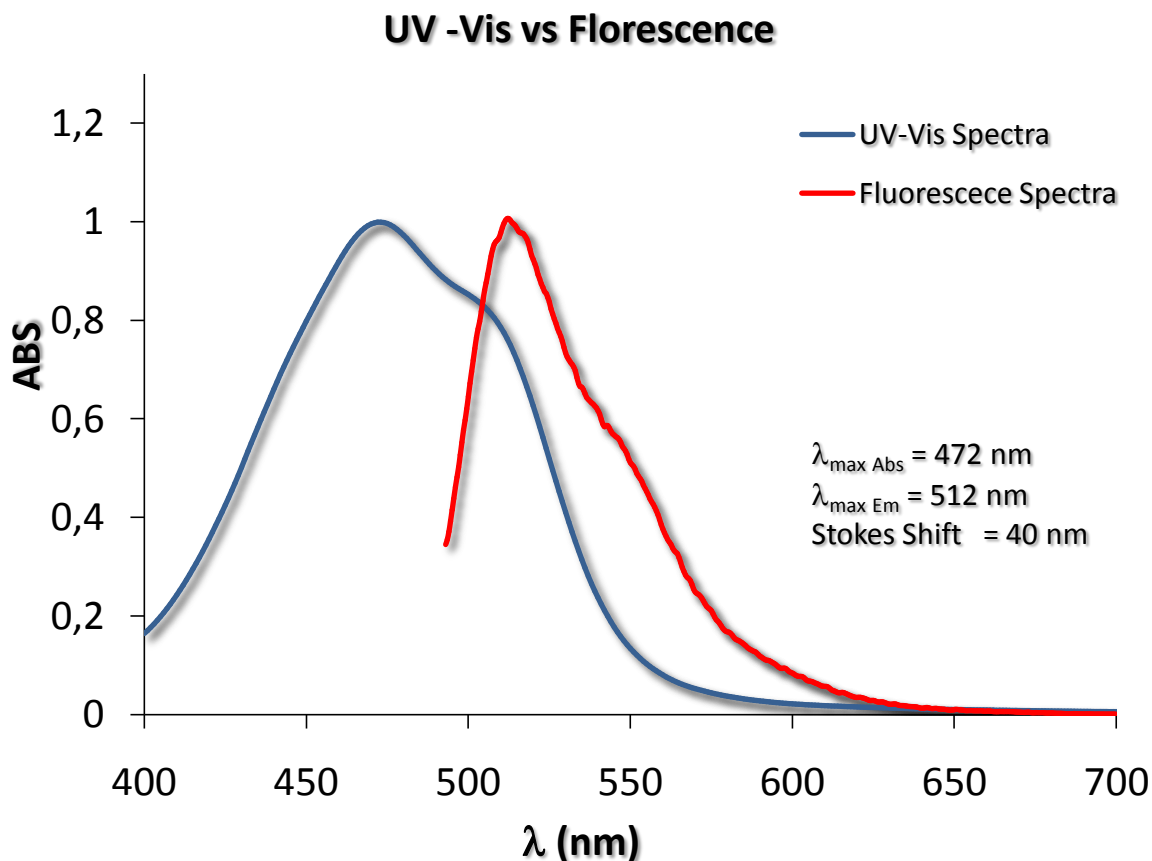
Figure 58: UV-vis and Fluorescence of water/DMSO solution of FLUOProbe.

UV turbidity detection-based method popularized by Lipinski and others [337] was choosen in order to determine the solubility of FLUOProbe. This method is affected by several shortcomings [338] like the poor reproducibility for very sparingly water soluble compounds, the apparent lack of standardization and the use of DMSO exaggerates solubility to an uncertain extent but it can provide useful information in order to assess future *in vitro* studies of the obtained fluorescent molecule. A precise measure can not be obtained using this turbidimetric approach, but it is a way to obtain a rough estimate of the solubility. The final data are reported as an estimated precipitation range.

Aqueous solubility was measured using this turbidimetric assay. Initially, a stock DMSO solution of FLUOProbe was diluted in DMSO to produce a range of solutions with different concentrations. These were then added to phosphate buffered saline solution at pH 7.4 resulting in a final concentration of 1% v/v DMSO and incubated for 2 hours at room temperature. DMSO-H_2O FLUOProbe solutions were prepared as reported in **Table 33**.

FLUOProbe Concentration (μM)	1	2	4	6	8
Average absorbance[a]	0,000375	0,000325	0,00395	0,005875	0,006875

Table 33: DMSO-H_2O FLUOProbe solutions prepared and resulting absorbance value at 620 nm. [a]: measure repeated 4 times.

UV absorbance at 620 nm was registered for each solution at different concentration [339] at the end of the incubation period. Precipitation was observed as confirmed by an increasing in absorbance due to light scattering derived by the formation of particulate material. Increased UV absorbance from light scattering was measured at 620 nm because FLUOProbe showed very low absorbance at this wavelenghts. The precipitation range was calculated from Absorbance vs FLUOProbe concentration plot as reported in **Figure 59**.

Solubility Profile
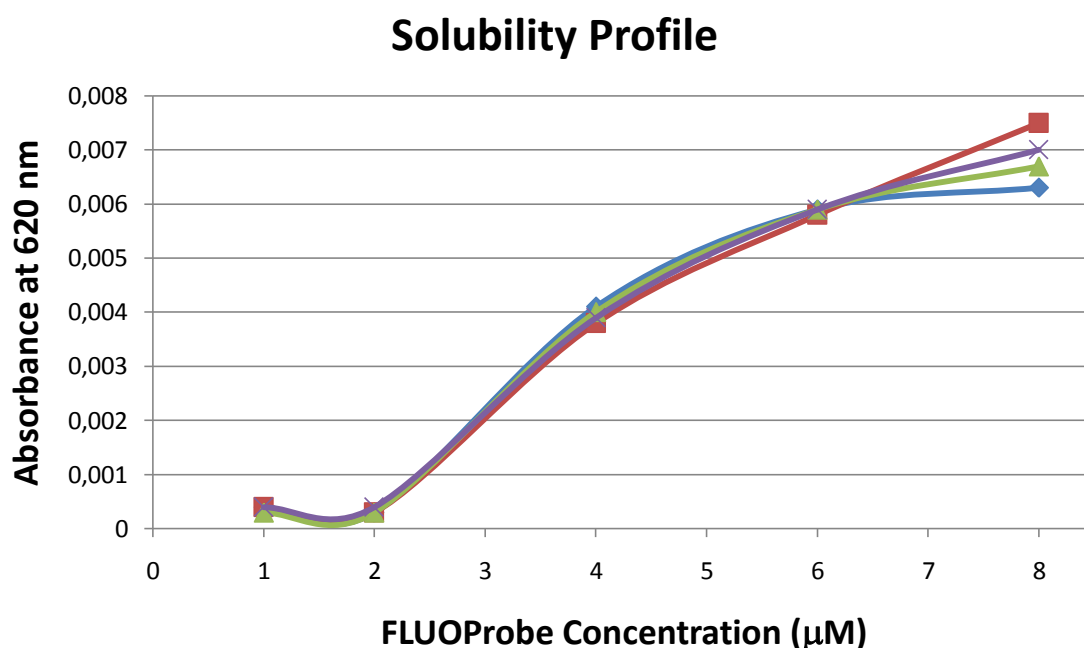
Figure 59: Solubility profile of 1% v/v DMSO/H$_2$O solutions of FLUOProbe.

As shown in **Figure 59**, analyses of 8 µM of FLUOProbe solution demonstrated low reproducibility due probably to low homogeneity of the sample. Variation of absorbance occurred indeed between 2 µM and 4 µM and this indicated that in this range of concentration, precipitation of BP probe occurred. Whit 5% v/v DMSO, the solutions resulted homogeneous up to 50 µM, while for solution with 1% v/v DMSO, the maximum solubility was calculated to be lower than 2 µM and this solvent composition was used since it is biocompatible with the next activity tests.

The fluorescent adduct between DPP and BP (FLUOProbe) was used for a series of *in vitro* tests in order to investigate the affinity of the species for the bone matrix. In particular a solution of FLUOProbe in α-MEM, (Life Technologies) was added on bovine cortical bone slice. Microscopic (Fluorescence) analyses demonstrated that the synthesized BP probe was able to bind hydroxyapatite resulting as a dark material (**Figure 60-A**). Fluorescence microscopy showed intense red areas where osteoclasts were present (**Figure 60-B**). This indicates that these cells can uptake FLUOProbe thus becoming clearly fluorescent and easily recognizable and localizable.
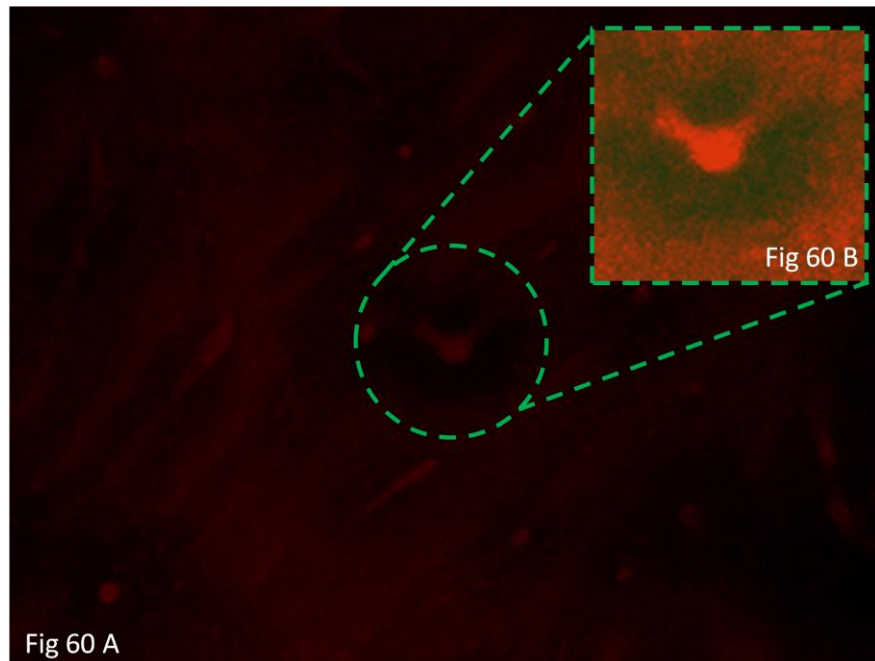
Figure 60: Fluorescence microscopy of FLUOProbe treated bovine cortical bone.

Osteoclast resorbing activity was assayed by plating the cells (cultured with α-MEM by Life Technologies) supplemented with 10% FBS and in the presence of 25 ng/ml recombinant human Macrophage Colony Stimulating Factor (rh-MCSF) plus 30 ng/ml rh-RANKL (R&D Systems) on untreated and FLUOProbe-treated hydroxyapatite. While on pure hydroxyapatite resorbance lacunae were present (**Figure 61-A**, **upper part**), no osteoclast activity was found on treated HAP (**Figure 61-B**), suggesting that FLUOProbe presents potentially anti-resorpitive properties. Further analyses will be performed in order to assess the cytotoxicity of the synthesized fluorescent probe as well as anabolic ability by treating mesenchymal stem cells during osteogenic commitment.

Figure 61: Osteoclast resorbing activity tests. Untreated (A) and FLUOProbe-treated (B) HAP.

4. <u>CONCLUSION</u>

Using methylenebisphosphonate tetraethyl ester (MBP) as main building block, a wide range of double bond containing BP precursors were synthesized. Vinyliden bisphosphonate tetraethyl ester (VBP) was synthesized as key BP precursors with unsubstituted double bond precursor while $TiCl_4$ catalyzed condensation of arom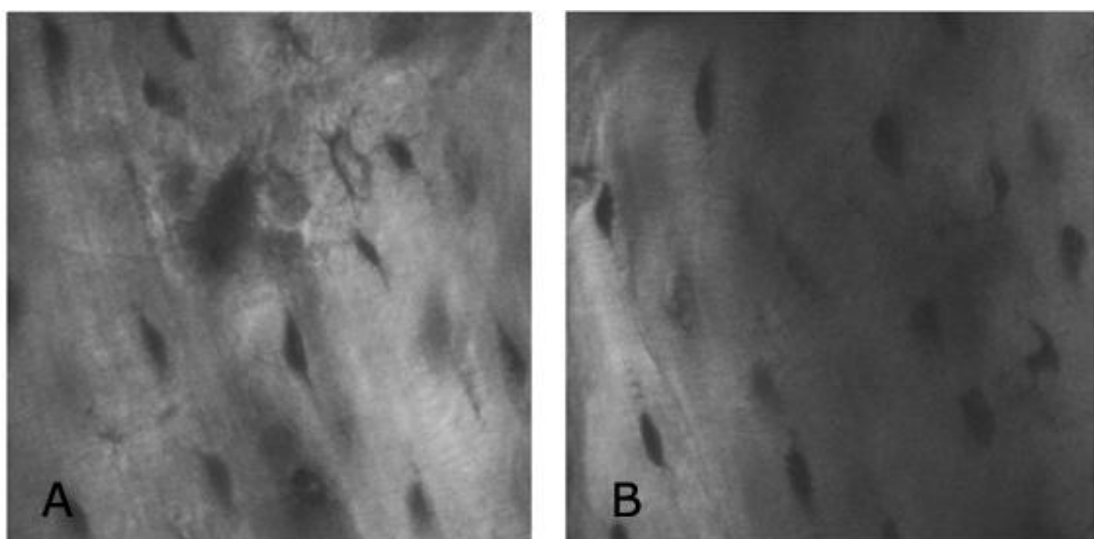atic aldehydes on MBP permitted to obtain up to 18 monosubstituted aromatic VBP precursors. Use of glyoxylate or α-keto esters coupled with a modified $TiCl_4$ catalyzed condensation gave the opportunity to synthesize a non aromatic VBP precursor as well as up to 10 previously unknown bis-substituted VBP molecules. All the obtained precursors showed different steric and electronic properties depending on the level of substitution of the double bond and were preparared on an up to 2 g scale. Key precursors were obtained also in a reduced steric hindrance form bearing a tetramethyl ester moieties as well as bisphosphonic acids. The prepared tetraethyl and tetramethyl ester VBP as well as the corresponding acids were used in collaboration with Prof. Canton's research group, in functionalization of zirconia nanoparticles resulting in outstanding changes in the material properties.

Several type of reactions, in many cases mediated by catalysts and with a wide range of reagents, were tested on BP precursors in order to obtain numerous new BP molecules.

Cu(II) mediated addition of boronic acids to VBP permitted to obtain several BP molecules with different electronic and steric properties using a less expensive and non toxic metal catalyst under milder experimental condition compared to what reported in the literature. Even though the reaction turned out to be very sensitive to steric hindrance of the BP precursor as well as the boronic reagent, several BP molecules were obtained in the final bisphosphonic acid form.

Catalyzed thio-Michael addition of ferrocenyl reagent permitted to conjugate low toxicity properties of S-containing BP with pharmacological properties of ferrocene. Multigrams scale synthesis of sulfur-containing bisphosphonic acid permitted, in collaboration with Prof. Bigi's research group, to functionalize hydroxyapatite based biomaterials. The obtained functionalized HAPs are under investigation to complete anti-osteoclast activity and toxicity tests.

In order to obtain enantioenriched BP molecules, double bond hydrogenation was run on bis-substituted BP precursors. Pd/C catalyzed hydrogenation of bis-substituted BP precursors resulted in quantitative formation of racemic mixtures that were used in optimization of chiral HPLC analyses method. Attempts to carry out asymmetric hydrogenation were made using $NaBH_4$ coupled with an organocatalyst resulting in quantitative hydrogenation but without any asymmetric induction. On the other hand the use of Rh precursors coupled with chiral ligands did not provide any useful results.

During this PhD thesis several potentially highly active nitrogen containing BPs were prepared.

Zn(II) catalyzed addition of trimethylsilyl cyanide to monosubstituted VBP precursors allowed to obtain new β-nitrile BP molecules that will be tested on nitrile group reduction reaction in order to obtain γ-amino BPs. Similarly, Pd(II) addition of trimethylsilyl azide to VBP gave the corresponding β-azido BP in excellent yield as stable final product. The reaction was influenced by temperature conditions: while quantitative formation of azido-BP was obtained at room temperature, termal N_2 elimination occurred at high temperature giving a β-amino unsaturated BP compound.

Cu(II) mediated Friedel-Crafts reaction on VBP yielded numerous N-BP molecules. It was possible to use organic solvents as well as aqueous micellar media, resulting in comparable yields of reaction. Despite the reaction turned out to be very sensitive to steric hindrance of the monosustituted VBP molecules, several indolyl-BP were obtained by Friedel-Crafts reaction on non aromatic VBP precursor. Selected molecules were deprotected and obtained in the final N-bisphosphonic acid form.

Cycloaddition reaction were also studied: 1,3 dipolar cycloaddition of azomethine-ylides derived from aminoacids and aromatic aldehydes gave the opportunity to synthesize several pyrrolidine BPs with high structural complexity depending on reagents substitutions. The reaction turned out to be very sensitive to the electronic properties of the monosubtituted VBP as well as aldehydes, giving good product formtion only when an electron withdrawing group was present on the reagents.

Use of activated isonitrile reagents led to different product formation depending on catalityc system employed. Base catalyzed reaction led to a hydrolyzed-addition product only with unsubstituted VBP. Ag(I) mediated reactions provided azole BP cycloaddition products with structural complexity depending on the starting VBP precursors. This reaction turned out to be total regioselective forming preferably the *anti* isomer as confirmed by full NMR characterization.

Aldol condensation mediated by chiral organocatalysts on isatin-BP derivative allowed to synthesize several new N-BPs. Cyclic ketones showed high reactivity but the formation of numerous stereocenters did not permitted to determine the enantiomeric excess. Aldol condensation of benzophenones mediated by chiral pseudo-enantiomers thiourea-quinine and thiourea-quinidine derivatives organocatalysts enabled the synthesis and quantification of both enantiomers of N-containing BPs with enantiomeric excess up to 96%. They will be deprotected and investigated in activity and toxicity tests.

Synthesis of azide-BPs allowed to study Cu(I) catalyzed azido-alkyne cycloaddition (*Click Reaction*). A collaboration with Prof. De Lucchi's research group was established in order to conjugate through *Click Reaction* the BP molecule with a diketopyrrolopyrrole based fluorophore and to obtain a new fluorescent BP probe for *in vitro* osteoclast activity studies. *Click reaction* carried out with β-azide BP showed that this reagent was unstable under different reaction conditions, resulting in decomposition to the starting VBP

reagent. Use of DPP fluorophore with enhanced solubility did not produce the desired product even if high activity NHC-copper catalysts were used. During the research period at University of Southern California in Prof. McKenna's research group, attempts to conjugate BP moieties with DPP fluorophore continued. γ-azide BP was synthesized by diazotransfer reaction on an γ-amino BP using a safer diazotransfer reagent compared to that usually used in the literature. Luckily C*lick reaction* between γ-azide BP and DPP fluorophore occurred smoothly, allowing to prepare the 1,4 triazolinic fluorescent BP probe in excellent yield. BP-DPP was subjected to microwave assisted deprotection that gave up to 120 mg of the final BP fluorescent probe that was fully characterized by NMR and mass spectroscopy, UV-Vis and fluorescence analyses. Range of solubility was determined by turbidimetric UV method while elemental analyses confirmed that the compound was sufficiently pure for activity and fluorescence tests. Antiresorption activity tests as well as fluorescence tests confirmed that synthesized BP-DPP probe was able to bind hydroxyapatite materials further demonstrating that it can be adsorbed into osteoclast cells. Currently, additional activity, toxicity and fluorescence tests are ongoing with the synthesized BP probe.

Overall the synthesized BP precursors were approximately 40, including a new class of bis-substituted VBP molecules. About 140 new BPs molecules were prepared, several of them, also containing N atoms in the side chain, were obtained in the bisphosphonic acids final form. In a particular case, both enantiomers of N-containing BPs were synthesized with a high enantiomeric excess giving the opportunity to investigate the different behavior of pairs of N containing bisphosphonic acid enantiomers, which is a rather unexplored issue.

5. <u>EXPERIMENTAL</u>

General.

^{1}H NMR, ^{31}P{^{1}H} NMR, ^{13}C{^{1}H} NMR spectra were run on:

Bruker Avance 300 spectrometer operating at 300, 122, 75 MHz, respectively, at 298 K.

Bruker Avance 400 spectrometer operating at 400, 162, 101 MHz, respectively, at 298 K.

Varian VNMRS 500 spectrometer operating at 500, 202 MHz, respectively, at 298 K.

δ values are reported in ppm relative to $Si(CH_3)_4$ or 85% H_3PO_4.

GC-MS analyses were performed on a GC Trace GC 2000 coupled with a quadrupole MS Thermo Finnigan Trace MS with *Full Scan* method. Experimental conditions are reported in the following table.

Experimental conditions for GC-MS analyses	
Capillary column:	HP5-MS 30 m, 0.25 mm x 0.25 μm
Initial T, °C:	80°C for 5 min
Rate, °C/min:	30°C/min
Final T, °C:	280°C for 30 min
Injector T (split), °C:	280°C
Gas carrier flow, mL/min.	0.8 mL/min
Injected volume, μL	0.8-1 μL
Solvent delay, min.	4 min.
Mass range, amu:	35-500 amu
Detector voltage, V:	350 V
Interface T, °C	280°C
Source T, °C:	200°C

Low resolution mass spectra (LRMS) were recorded on a Finningan LCQ Deca XP Max mass spectrometer coupled to electrospray ionisation source (ESI) in positive or negative mode.

Column chromatography was performed on 230-400 mesh silica, thin layer chromatography was carried out on 20 cm x 20 cm ALUGRAM® Xtra SIL G/UV$_{254}$ MACHEREY-NAGEL, automated column chromatography was performed on CombiFlash^{+} Lumen at reported conditions.

HPLC analyses were performed on a Hewlett Packard Series 1100 G1311A QuatPump at reported conditions.

Microwaves assisted deprotection step was performer on Ethos synth microwave synthesis labstation at reported conditions.

5.1 BPs PRECURSORS

5.1.1 *Methylen Bisphosphonate Tetraethyl Esters (MBP)*

The sodium ethoxide solution was prepared by addition of metal sodium (5 g, 220 mmol) in portions to ethanol (130 mL). Diethyl phosphite (220 mmol) was then added with stirring to the sodium ethoxide solution, continuing for 1 h at room temperature and the mixture was concentrated on a rotary evaporator. The residue was dissolved with 10 mL of metliylene chloride (156 mmol) and the mixture was stirred 2 weeks at room temperature. The mixture was washed with brine and the methylene chloride phase was dried with sodium sulphate and concentrated on a rotary evaporator. The residue was distilled at reduced pressure to give MBP in 54% yield.

MBP
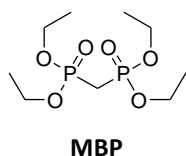
^{1}H NMR (400 MHz, CDCl$_3$)δ 4.20 – 4.00 (m, 8H), 2.39 (t, *J* = 21.0 Hz, 2H), 1.29 (t, *J* = 7.1 Hz, 12H) ppm.
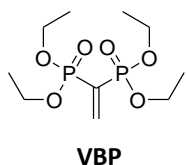
^{31}P {1H}-NMR (162 MHz, CDCl$_3$) δ 19.38 (s, 2P) ppm.

^{13}C {1H}-NMR (101 MHz, CDCl$_3$) δ 62.62 (t, *J* = 3.0 Hz), 25.43 (t, *J* = 136.9 Hz), 16.36 (d, *J* = 3.2 Hz) ppm.

GC-MS (70 eV) m/z: 288 [M]$^+$, 261 [M -CH$_2$CH$_3$]$^+$, 233 [M -2(CH$_2$CH$_3$)]$^+$, 205 [M - 3(CH$_2$CH$_3$)]$^+$.

5.1.2 *Vinyliden Bisphosphonate Tetraethyl Esters (VBP)*

Paraformaldehyde (3,18 g, 106mmol) and diethylamine (21mmol) were combined in 60 mL of methanol and the mixture was warmed until clear. The heat was removed and MBP (20mmol) was then added. The mixture was refluxed for 24 h, then was concentrated under vacuum. Toluene (30mL) was added and the solution again concentrated. This last step was repeated to ensure complete removal of methanol from the intermediate which was obtained as a clear liquid. The residue was re-dissolved in toluene (30 mL), treated with 15,2 mg of pTSA (0,09 mmol) and refluxed through a Dean-Stark trap for 18 h. The sample was concentrated in vacuo, dissolved in CH$_2$Cl$_2$, washed twice with H$_2$O, dried with NaSO$_4$, and concentrated in vacuum to give VBP higher than 90% yield.

VBP

^{1}H NMR (400 MHz, CDCl$_3$) δ 6.97 (dd, *J* = 37.8, 33.8 Hz, 2H), 4.23 – 4.03 (m, 8H), 1.33 (t, *J* = 7.1 Hz, 12H) ppm.

^{31}P {1H}-NMR (162 MHz, CDCl$_3$) δ 13.05 (s, 2P) ppm.

^{13}C {1H}-NMR (101 MHz, CDCl$_3$) δ 149.29 (s), 132.17 (t, *J* = 166.6 Hz), 62.78 (t, *J* = 2.8 Hz), 16.38 (t, *J* = 3.3 Hz) ppm.

GC-MS (70 eV) m/z: 300 [M]$^+$, 273 [M -CH$_2$CH$_3$]$^+$, 245 [M -2(CH$_2$CH$_3$)]$^+$, 217 [M - 3(CH$_2$CH$_3$)]$^+$.

5.1.3 *General procedure for synthesis of the mono-substituted alkylidene bisphosphonates*

A flame-dried 50 mL round bottom flask with magnetic stir bar was charged with TiCl$_4$ (15 mmol) and 3.9 mL of CCl$_4$ at 0 °C. 30 mL of dry THF was added dropwise to the flask and a bright yellow precipitate formed. Subsequently aldehyde (5 mmol) and tetraethyl methylenediphosphonate (5 mmol) were added. A solution of 2.3 mL of 4-Methylmorpholine (21mmol) in 5.0 mL of dry THF was then added dropwise to the stirring mixture over 1h. The reaction was allowed to warm to room temperature and stirred overnight. The reaction was quenched with water and extracted with EtOAc. The organic layer was washed with brine and dried over Na$_2$SO$_4$. Concentration in *vacuo* followed by column chromatography provided the corresponding alkylidene bisphosphonate.
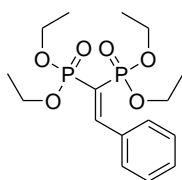
PPH

Tetraethyl 2-phenylethene-1,1-diyldiphosphonate

^{1}H NMR (400 MHz, CDCl$_3$) δ 8.26 (dd, *J* = 47.7, 29.1 Hz, 1H), 7.73 − 7.66 (m, 2H), 7.37 − 7.31 (m, 3H), 4.22 − 4.10 (m, 4H), 4.04 − 3.92 (m, 4H), 1.34 (t, *J* = 7.1 Hz, 6H), 1.10 (t, *J* = 7.1 Hz, 6H).

^{31}P {1H}-NMR (162 MHz, CDCl$_3$) δ 17.15 (d, *J* = 50.6 Hz, 1P), 11.94 (d, *J* = 50.5 Hz, 1P).

^{13}C {1H}-NMR (101 MHz, CDCl$_3$) δ 161.36 (d, *J* = 2.0 Hz), 134.59 (dd, *J* = 21.7, 8.6 Hz), 130.45 (s), 130.27 (t, *J* = 1.4 Hz), 128.00 (s), 120.96 (dd, *J* = 170.2, 165.2 Hz), 62.62 (s), 62.39 (d, *J* = 6.3 Hz), 16.28 (d, *J* = 6.6 Hz), 15.97 (d, *J* = 6.7 Hz).

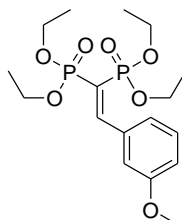GC-MS (70 eV) m/z: 376 [M]$^+$, 331 [M -OCH$_2$CH$_3$]$^+$, 239 [M$^+$ -PO(OEt)$_2$]$^+$.
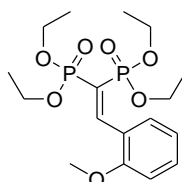
POOMe

Tetraethyl 2-(2-methoxyphenyl)ethene-1,1-diyldiphosphonate

^{1}H NMR (300 MHz, CDCl$_3$) δ 8.48 (dd, *J* = 48.2, 28.8 Hz, 1H), 7.86 (d, *J* = 7.8 Hz, 1H), 7.41 − 7.34 (m, 1H), 6.96 (t, *J* = 7.4 Hz, 1H), 6.86 (d, *J* = 8.3 Hz, 1H), 4.27 − 4.13 (m, 4H), 4.11 − 3.94 (m, 4H), 3.84 (s, 3H), 1.39 (t, *J* = 7.1 Hz, 6H), 1.14 (t, *J* = 7.1 Hz, 6H) ppm.

^{31}P {1H}-NMR (122 MHz, CDCl$_3$) δ 16.06 (d, *J* = 53.2 Hz, 1P), 11.32 (d, *J* = 53.1 Hz, 1P) ppm.
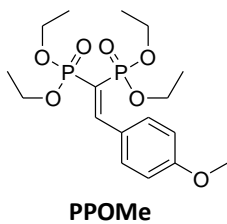
PMOMe

Tetraethyl 2-(3-methoxyphenyl)ethene-1,1-diyldiphosphonate

^{1}H NMR (300 MHz, CDCl$_3$) δ 8.29 (dd, *J* = 47.6, 29.1 Hz, 1H), 7.46 (s, 1H), 7.31 − 7.26 (m, 2H), 6.98 − 6.93 (m, 1H), 4.27 − 4.15 (m, 4H), 4.11 − 3.97 (m, 4H), 3.84 (s, 3H), 1.38 (t, *J* = 7.1 Hz, 6H), 1.17 (t, *J* = 7.1 Hz, 6H) ppm.

^{31}P {1H}-NMR (122 MHz, CDCl$_3$) δ 18.53 (d, *J* = 50.0 Hz, 1P), 13.35 (d, *J* = 50.0 Hz, 1P) ppm.
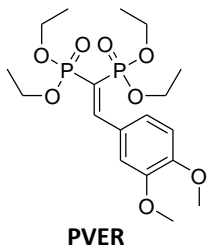
Tetraethyl 2-(4-methoxyphenyl)ethene-1,1-diyldiphosphonate

^{1}H NMR (300 MHz, CDCl$_3$) δ 8.23 (dd, J = 48.0, 29.5 Hz, 1H), 7.85 (d, J = 8.9 Hz, 2H), 6.91 (d, J = 8.9 Hz, 2H), 4.25 − 4.12 (m, 4H), 4.12 − 4.01 (m, 4H), 3.85 (s, 3H), 1.37 (t, J = 7.1 Hz, 6H), 1.21 (t, J = 7.1 Hz, 6H) ppm.

^{31}P {1H}-NMR (122 MHz, CDCl$_3$) δ 19.86 (d, J = 49.8 Hz, 1P), 14.40 (d, J = 49.8 Hz, 1P) ppm.

GC-MS, (70 eV) m/z: 406 [M]$^+$, 391 [M -Me]$^+$, 361 [M -OEt]$^+$, 269 [M -PO(OEt)$_2$]$^+$.

Tetraethyl 2-(3,4-dimethoxyphenyl)ethene-1,1-diyldiphosphonate

^{1}H NMR (300 MHz, CDCl$_3$) δ 8.22 (dd, J = 47.9, 29.6 Hz, 1H), 7.84 (d, J = 2.1 Hz, 1H), 7.33 (dd, J = 8.4, 2.1 Hz, 1H), 6.87 (d, J = 8.4 Hz, 4H), 4.25 − 4.12 (m, 4H), 4.11 − 3.99 (m, 4H), 3.93 (d, J = 1.3 Hz, 6H), 1.37 (t, J = 7.1 Hz, 6H), 1.21 (t, J = 7.1 Hz, 6H) ppm.

^{31}P {1H}-NMR (122 MHz, CDCl$_3$) δ 17.43 (d, J = 49.1 Hz, 1P), 12.06 (d, J = 49.1 Hz, 1P) ppm.
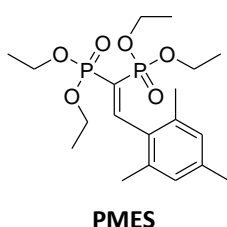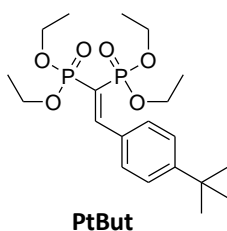
Tetraethyl 2-mesitylethene-1,1-diyldiphosphonate

^{1}H NMR (300 MHz, CDCl$_3$) δ 8.29 (dd, J = 48.7, 27.7 Hz, 1H), 6.84 (s, 2H), 4.31 − 4.14 (m, 2H), 4.00 − 3.85 (m, 2H), 3.81 − 3.64 (m, 2H), 2.26 (s, 3H), 2.19 (s, 6H), 1.40 (t, J = 7.1 Hz, 6H), 1.12 (t, J = 7.1 Hz, 6H) ppm.

^{31}P {1H}-NMR (122 MHz, CDCl$_3$) δ 14.32 (d, J = 55.0 Hz, 1P), 9.98 (d, J = 55.0 Hz, 1P) ppm.

GC-MS, (70 eV) m/z: 418 [M]$^+$, 403 [M -Me]$^+$, 373 [M -OEt]$^+$, 281 [M -PO(OEt)$_2$]$^+$.
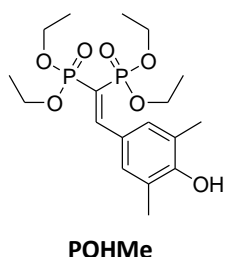
Tetraethyl 2-(4-tert-butylphenyl)ethene-1,1-diyldiphosphonate

^{1}H NMR (300 MHz, CDCl$_3$) δ 8.28 (dd, J = 47.9, 29.2 Hz, 1H), 7.72 (d, J = 8.4 Hz, 2H), 7.41 (d, J = 8.5 Hz, 2H), 4.28 − 4.11 (m, 4H), 4.11 − 3.96 (m, 4H), 1.37 (t, J = 7.1 Hz, 6H), 1.31 (s, 9H), 1.15 (t, J = 7.1 Hz, 6H) ppm.

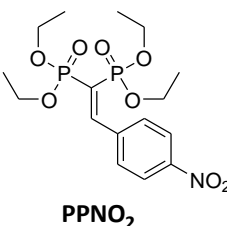^{31}P {1H}-NMR (122 MHz, CDCl$_3$) δ 16.58 (d, J = 50.8 Hz, 1P), 11.19 (d, J = 50.8 Hz, 1P) ppm.

GC-MS, (70 eV) m/z: 432 [M]$^+$, 295 [M -PO(OEt)$_2$]$^+$, 239 [M -PO(OEt)$_2$ –tBut +H]$^+$.

Tetraethyl 2-(4-hydroxy-3,5-dimethylphenyl)ethene-1,1-diyldiphosphonate

^{1}H NMR (300 MHz, CDCl$_3$) δ 8.12 (dd, J = 48.6, 29.7 Hz, 1H), 7.46 (s, 1H), 7.34 (s, 1H), 4.15 − 4.05 (m, 8H), 2.17 (s, 6H), 1.33 (t, J = 7.2 Hz, 6H), 1.22 (t, J = 7.2 Hz, 6H) ppm.

^{31}P {1H}-NMR (122 MHz, CDCl$_3$) δ 17.93 (d, J = 49.8 Hz, 1P), 12.45 (d, J = 49.8 Hz, 1P) ppm.
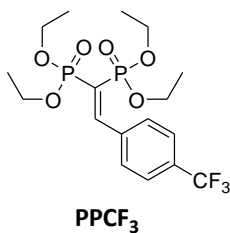
Tetraethyl 2-(4-nitrophenyl)ethene-1,1-diyldiphosphonate

^{1}H NMR (300 MHz, CDCl$_3$) δ 8.31 (dd, J = 46.7, 28.5 Hz, 1H), 8.24 (d, J = 8.8 Hz, 2H), 7.84 (d, J = 8.8 Hz, 2H), 4.31 − 4.15 (m, 4H), 4.14 − 3.99 (m, 4H), 1.40 (t, J = 7.1 Hz, 6H), 1.19 (t, J = 7.1 Hz, 6H) ppm.

^{31}P {1H}-NMR (122 MHz, CDCl$_3$) δ 16.61 (d, J = 46.8 Hz, 1P), 11.83 (d, J = 46.8 Hz, 1P) ppm.

GC-MS, (70 eV) m/z: 421 [M]$^+$, 376 [M -OEt]$^+$, 284 [M -PO(OEt)$_2$]$^+$.

PPOMe

PVER

PMES

PtBut

POHMe

PPNO$_2$

Tetraethyl 2-(4-(trifluoromethyl)phenyl)ethene-1,1-diyldiphosphonate

^{1}H NMR (300 MHz, CDCl$_3$) δ 8.31 (dd, J = 47.1, 28.9 Hz, 1H), 7.80 (d, J = 8.2 Hz, 2H), 7.64 (d, J = 8.3 Hz, 2H), 4.30 − 4.13 (m, 4H), 4.13 − 3.93 (m, 4H), 1.39 (t, J = 7.1 Hz, 6H), 1.16 (t, J = 7.1 Hz, 6H) ppm.

^{31}P {1H}-NMR (122 MHz, CDCl$_3$) δ 17.26 (d, J = 48.4 Hz, 1P), 12.28 (d, J = 48.3 Hz, 1P) ppm.
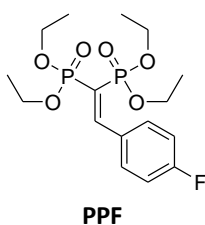
PPCF$_3$
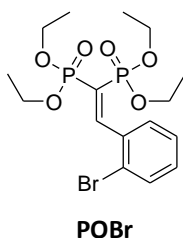
Tetraethyl 2-(2-bromophenyl)ethene-1,1-diyldiphosphonate

^{1}H NMR (300 MHz, CDCl$_3$) δ 8.25 (dd, J = 46.7, 27.7 Hz, 1H), 7.70 (dd, J = 7.7, 1.6 Hz, 1H), 7.56 (dd, J = 7.9, 1.1 Hz, 1H), 7.32 (td, J = 7.6, 1.1 Hz, 1H), 7.22 (td, J = 7.7, 1.6 Hz, 1H), 4.29 − 4.15 (m, 4H), 4.03 − 3.86 (m, 4H), 1.38 (t, J = 7.1 Hz, 6H), 1.10 (t, J = 7.1 Hz, 6H) ppm.

^{31}P {1H}-NMR (122 MHz, CDCl$_3$) δ 14.15 (d, J = 50.3 Hz, 1P), 9.53 (d, J = 50.3 Hz, 1P) ppm.

GC-MS, (70 eV) m/z: 454 [M, Cluster Br] [+], 375 [M -Br] [+], 317 [M -PO(OEt)$_2$] [+].
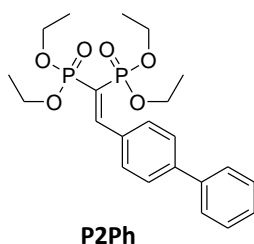
POBr

Tetraethyl 2-(4-fluorophenyl)ethene-1,1-diyldiphosphonate

^{1}H NMR (300 MHz, CDCl$_3$) δ 8.21 (dd, J = 47.6, 29.1 Hz, 1H), 7.77 (dd, J = 8.7, 5.4 Hz, 2H), 7.03 (t, J = 8.7 Hz, 2H), 4.24 − 4.09 (m, 4H), 4.10 − 3.92 (m, 4H), 1.33 (t, J = 7.1 Hz, 6H), 1.14 (t, J = 7.1 Hz, 6H) ppm.

^{31}P {1H}-NMR (122 MHz, CDCl$_3$) δ 15.96 (d, J = 48.7 Hz, 1P), 10.72 (d, J = 48.7 Hz, 1P) ppm.

GC-MS, (70 eV) m/z: 394 [M] [+], 349 [M -OEt] [+], 257 [M -PO(OEt)$_2$] [+].
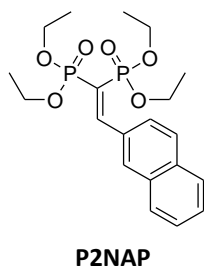
PPF

Tetraethyl 2-(biphenyl-4-yl)ethene-1,1-diyldiphosphonate

^{1}H NMR (300 MHz, CDCl$_3$) δ 8.34 (dd, J = 47.7, 29.2 Hz, 1H), 7.87 (d, J = 8.3 Hz, 2H), 7.67 − 7.57 (m, 4H), 7.50 − 7.42 (m, 2H), 7.42 − 7.34 (m, 1H), 4.31 − 4.15 (m, 4H), 4.13 − 4.00 (m, 4H), 1.39 (t, J = 7.1 Hz, 6H), 1.19 (t, J = 7.1 Hz, 6H) ppm.

^{31}P {1H}-NMR (122 MHz, CDCl$_3$) δ 16.00 (d, J = 50.3 Hz, 1P), 10.76 (d, J = 50.3 Hz, 1P) ppm.

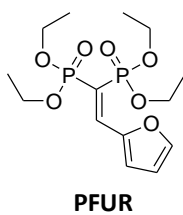GC-MS, (70 eV) m/z: 452 [M] [+], 315 [M -PO(OEt)$_2$] [+].

P2Ph

Tetraethyl 2-(naphthalen-2-yl)ethene-1,1-diyldiphosphonate

^{1}H NMR (300 MHz, CDCl$_3$) δ 8.47 (dd, J = 47.7, 29.2 Hz, 1H), 8.28 (s, 1H), 7.86 (dd, J = 18.1, 8.3 Hz, 4H), 7.57 − 7.47 (m, 2H), 4.32 − 4.15 (m, 4H), 4.12 − 3.97 (m, 4H), 1.41 (t, J = 7.1 Hz, 6H), 1.13 (t, J = 7.1 Hz, 6H) ppm.

^{31}P {1H}-NMR (122 MHz, CDCl$_3$) δ 16.16 (d, J = 50.1 Hz, 1P), 11.00 (d, J = 50.1 Hz, 1P) ppm.
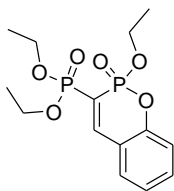
GC-MS, (70 eV) m/z: 426 [M] [+], 411 [M -Me] [+], 381 [M -OEt] [+], 289 [M -PO(OEt)$_2$] [+].

P2NAP

Tetraethyl 2-(furan-2-yl)ethene-1,1-diyldiphosphonate

^{1}H NMR (300 MHz, CDCl$_3$) δ 8.04 (dd, J = 45.5, 29.5 Hz, 1H), 7.62 (s, J = 0.7 Hz, 1H), 7.54 (d, J = 3.6 Hz, 1H), 6.55 (dd, J = 3.6, 1.7 Hz, 1H), 4.23 − 4.09 (m, 8H), 1.36 (t, J = 7.3 Hz, 6H), 1.31 (t, J = 7.1 Hz, 6H) ppm.

^{31}P {1H}-NMR(122 MHz, CDCl$_3$) δ 19.40 (d, J = 45.2 Hz, 1P), 13.72 (d, J = 45.3 Hz, 1P) ppm.
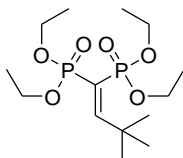
PFUR

PSAL

^{1}H NMR (300 MHz, CDCl$_3$) δ 8.11 (dd, *J* = 40.1, 24.3 Hz, 1H), 7.51 − 7.41 (m, 2H), 7.19 (dd, *J* = 12.8, 7.9 Hz, 2H), 4.38 − 4.16 (m, 6H), 1.41 − 1.34 (m, 9H) ppm.

^{31}P {1H}-NMR (122 MHz, CDCl$_3$) δ 11.80 (d, *J* = 42.4 Hz, 1P), 3.18 (d, *J* = 42.5 Hz, 1P) ppm.

GC-MS, (70 eV) m/z: 346 [M] $^+$, 209 [M -PO(OEt)$_2$] $^+$.

PtBut

Tetraethyl 3,3-dimethylbut-1-ene-1,1-diyldiphosphonate

^{1}H NMR (400 MHz, CDCl$_3$) δ 7.54 (dd, *J* = 52.2, 32.7 Hz, 1H), 4.16 − 3.98 (m, 8H), 1.30-1.25 (m, 12H), 1.25 (s, 9H) ppm.

^{31}P NMR (162 MHz, CDCl$_3$) δ 18.84 (d, *J* = 53.0 Hz, 1P), 12.51 (d, *J* = 52.9 Hz, 1P) ppm.

5.1.4 *General procedure for synthesis of the bi-substituted alkylidene bisphosphonates*

A flame-dried 50 mL round bottom flask with magnetic stir bar was charged with MBP (3 mmol), 40 mL of CH_2Cl_2 and 3 mmol of glyoxylate. 12 mmol of NEt_3 was added to the solution under inert atmosphere and then cooled down to 0°C. 3 mmol of $TiCl_4$ was added dropwise to the flask and the reaction was allowed to warm to room temperature and stirred overnight. The reaction was concentrated under vacuum and the formed oily solid was partially dissolved with ethyl acetate. The organic phase was filtered on silica bed, concentrated under reduced pressure and purified by column chromatography using 95/5 ethyl acetate/acetone mixture as eluent.

for the synthesis of **BPHEt**, commercially available ethyl phenyl glyoxylate was used.
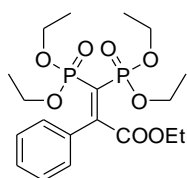
BPHEt

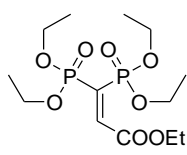Ethyl 3,3-bis(diethoxyphosphoryl)-2-phenylacrylate
^{1}H NMR (400 MHz, CDCl$_3$) δ 7.48 – 7.44 (m, 2H), 7.38 – 7.33 (m, 3H), 4.29 – 4.18 (m, 6H), 3.97 – 3.88 (m, 2H), 3.85 – 3.75 (m, 2H), 1.37 (t, *J* = 7.1 Hz, 6H), 1.25 (t, *J* = 7.2 Hz, 3H), 1.07 (t, *J* = 7.1 Hz, 6H) ppm.
^{31}P {^{1}H}-NMR (162 MHz, CDCl$_3$) δ 12.61 (d, *J* = 44.7 Hz, 1P), 11.49 (d, *J* = 44.7 Hz, 1P) ppm.
^{13}C {^{1}H}-NMR (101 MHz, CDCl$_3$) δ 167.62 (dd, *J* = 26.9, 12.3 Hz), 163.78 (s), 135.88 (dd, *J* = 19.7, 9.5 Hz), 129.63 (s), 128.07 (s), 127.79 (s), 122.29 (dd, *J* = 167.7, 159.9 Hz), 62.97 (d, *J* = 5.2 Hz), 62.45 (d, *J* = 6.4 Hz), 62.23 (s), 16.27 (d, *J* = 6.4 Hz), 16.00 (d, *J* = 6.6 Hz), 13.83 (s) ppm.
GC-MS, (70 eV) m/z: 448 [M] [+], 403 [M-OEt] [+], 375 [M -COOEt] [+], 311 [M - PO(OEt)$_2$][+], 267 [M -PO(OEt)$_2$–OEt+H] [+], 239 [M-PO(OEt)$_2$–COOEt+H] [+].

For the synthesis of **PCOOEt** commercially available ethyl glyoxylate was used.

PCOOEt

Ethyl 3,3-bis(diethoxyphosphoryl)acrylate
^{1}H NMR (400 MHz, CDCl$_3$) δ 7.43 (dd, *J* = 44.4, 27.7 Hz, 1H), 4.28 (q, *J* = 7.2 Hz, 2H), 4.23 – 4.04 (m, 8H), 1.37 – 1.29 (m, 15H) ppm.
^{31}P {^{1}H}-NMR (162 MHz, CDCl$_3$) δ 13.01 (d, *J* = 42.1 Hz, 1P), 9.22 (d, *J* = 42.2 Hz, 1P) ppm.
^{13}C {^{1}H}-NMR(101 MHz, CDCl$_3$) δ 165.34 (dd, *J* = 27.1, 11.3 Hz), 150.21 (s), 129.01 (dd, *J* = 164.4, 162.1 Hz), 63.20 (d, *J* = 5.9 Hz), 63.06 (d, *J* = 5.6 Hz), 62.07 (s), 16.35 (t, *J* = 6.0 Hz), 14.05 (s) ppm.
GC-MS, (70 eV) m/z: 327 [M -OCH$_2$CH$_3$] [+], 299 [M-COOEt] [+], 271 [M-CH$_2$CH$_3$- CH$_2$CH$_3$+H] [+], 235 [M -PO(OEt)$_2$] [+].
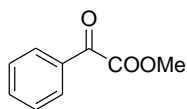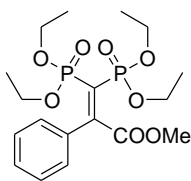
Methyl 2-oxo-2-phenylacetate
^{1}H NMR (300 MHz, CDCl$_3$) δ 8.05 – 7.99 (m, 2H), 7.67 (m, 1H), 7.56 – 7.47 (m, 2H), 3.98 (s, 3H) ppm.
^{13}C {^{1}H}-NMR (75 MHz, CDCl$_3$) δ186.18 (s), 164.1 (s), 135.0 (s), 132.4 (s), 130.1 (s), 128.9 (s), 52.8 (s) ppm.
GC-MS, (70 eV) m/z: 164 [M] [+], 106 [M -COOMe] [+].

Methyl 3,3-bis(diethoxyphosphoryl)-2-phenylacrylate

^{1}H NMR (400 MHz, CDCl$_3$) δ 7.50 − 7.45 (m, 2H), 7.39 − 7.36 (m, 3H), 4.31 − 4.18 (m, 6H), 4.00 − 3.74 (m, 2H), 3.80 (s, 3H), 1.39 (t, *J* = 7.0 Hz, 6H), 1.08 (t, *J* = 7.0 Hz, 6H) ppm.

^{31}P {^{1}H}- NMR (122 MHz, CDCl$_3$) δ 11.23 (d, *J* = 44.1 Hz, 1P), 9.89 (d, *J* = 44.1 Hz, 1P) ppm.

^{13}C {^{1}H}- NMR (75 MHz, CDCl$_3$) δ 168.54 (dd, *J* = 25.8, 13.2 Hz), 163.99 (s), 136.74 − 135.48 (m), 130.16 (s, *J* = 8.4 Hz), 128.54 (s), 128.23 (s), 123.25 (t, *J* = 164.5 Hz), 63.45 (d, *J* = 1.5 Hz), 62.89 (d, *J* = 3.0 Hz), 53.46 (s), 16.68 (d, *J* = 4.1 Hz), 16.40 (d, *J* = 3.4 Hz) ppm.

GC-MS, (70 eV) m/z: 434 [M]$^+$, 403 [M -OMe]$^+$, 375 [M -COOMe]$^+$, 297 [M - PO(OEt)$_2$]$^+$, 239 [M -COOMe-PO(OEt)$_2$]$^+$.
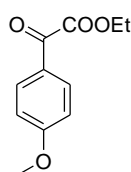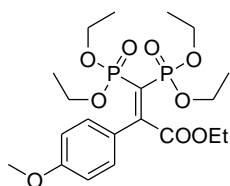
Ethyl 2-(4-methoxyphenyl)-2-oxoacetate

^{1}H NMR (300 MHz, CDCl$_3$) δ 8.01 (d, *J* = 8.9 Hz, 2H), 6.98 (d, *J* = 8.9 Hz, 2H), 4.43 (q, *J* = 7.1 Hz, 2H), 3.90 (s, 3H), 1.42 (t, *J* = 7.1 Hz, 3H) ppm.

^{13}C {^{1}H}- NMR (75 MHz, CDCl$_3$) δ 184.8 (s), 164.9 (s), 164.0 (s), 132.3 (s), 125.2 (s), 114.1 (s), 61.9 (s), 55.4 (s), 13.9 (s) ppm.

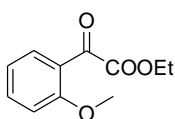GC-MS, (70 eV) m/z: 208 [M]$^+$, 135 [M -COOEt]$^+$.

Ethyl 3,3-bis(diethoxyphosphoryl)-2-(4-methoxyphenyl)acrylate

^{1}H NMR (400 MHz, CDCl$_3$) δ 7.46 (d, *J* = 8.8 Hz, 2H), 6.89 (d, *J* = 8.7 Hz, 2H), 4.32 − 4.18 (m, 6H), 4.01 − 3.83 (m, 4H), 3.82 (s, *J* = 4.7 Hz, 3H), 1.38 (t, *J* = 7.0 Hz, 6H), 1.27 (t, *J* = 7.1 Hz, 3H), 1.11 (t, *J* = 7.0 Hz, 6H) ppm.

^{31}P {^{1}H}-NMR (122 MHz, CDCl$_3$): δ 11.80 (d, *J* = 44.3 Hz, 1P), 10.71 (d, *J* = 44.0 Hz, 1P) ppm.

^{13}C {^{1}H}-NMR (75 MHz, CDCl$_3$) δ 167.82 (dd, *J* = 26.7, 12.3 Hz), 163.67 (s), 160.92 (s), 129.78 (s), 127.89 (dd, *J* = 20.0, 9.8 Hz), 120.53 (dd, *J* = 167.7, 160.8 Hz), 113.40 (s), 62.73 (d, *J* = 5.1 Hz), 62.33 (d, *J* = 6.3 Hz), 62.06 (s), 55.19 (s), 16.15 (d, *J* = 6.4 Hz), 15.91 (d, *J* = 6.5 Hz), 13.74 (s) ppm.

GC-MS, (70 eV) m/z: 478 [M]$^+$, 433 [M -OEt]$^+$, 405 [M -COOEt]$^+$, 341 [M - PO(OEt)$_2$]$^+$, 297 [M -PO(OEt)$_2$–OEt-H]$^+$, 269 [M -PO(OEt)$_2$–COOEt-H]$^+$.

Ethyl 2-(2-methoxyphenyl)-2-oxoacetate

^{1}H NMR (300 MHz, CDCl$_3$) δ 7.82 (dd, *J* = 7.8, 1.8 Hz, 1H), 7.58 − 7.49 (m, 1H), 7.02 (td, *J* = 7.8, 0.8 Hz, 1H), 6.95 (d, *J* = 8.4 Hz, 1H), 4.34 (q, *J* = 7.1 Hz, 2H), 1.34 (t, *J* = 7.1 Hz, 3H) ppm.

^{13}C {^{1}H}-NMR(76 MHz, CDCl$_3$) δ 187.06 (s, *J* = 66.7 Hz), 165.75 (s, *J* = 44.4 Hz), 160.73 (s, *J* = 56.6 Hz), 136.83 (s), 131.08 (s), 123.15 (s, *J* = 14.1 Hz), 121.70 (s), 112.51 (s), 62.18 (s), 56.42 (s), 14.55 (s) ppm.

GC-MS, (70 eV) m/z: 208 [M]$^+$, 135 [M -COOEt]$^+$.

159
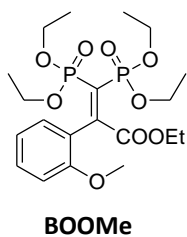
Ethyl 3,3-bis(diethoxyphosphoryl)-2-(2-methoxyphenyl)acrylate

^{1}H NMR (400 MHz, CDCl$_3$) δ 7.51 (dd, J = 7.6, 1.7 Hz, 1H), 7.38 (ddd, J = 8.3, 7.5, 1.7 Hz, 1H), 7.00 (td, J = 7.5, 1.0 Hz, 1H), 6.88 (dd, J = 8.3, 0.7 Hz, 1H), 4.35 − 4.21 (m, 6H), 4.14 − 4.04 (m, 1H), 4.03 − 3.95 (m, 1H), 3.94 − 3.83 (m, 1H), 3.81 (s, 3H), 3.73 − 3.59 (m, 1H), 1.41 (t, J = 7.1 Hz, 6H), 1.32 (t, J = 7.2 Hz, 3H), 1.26 − 1.15 (broad signal, 3H), 1.02 (broad signal, 3H) ppm.

^{31}P {^{1}H}-NMR(162 MHz, CDCl$_3$) δ 12.45 (d, J = 46.3 Hz, 1P), 11.99 (d, J = 46.3 Hz, 1P) ppm.

^{13}C {^{1}H}-NMR (76 MHz, CDCl$_3$) δ 167.75 (d, J = 38.5 Hz), 161.37 (s, J = 11.2 Hz), 156.99 (d, J = 6.2 Hz), 132.15 (s), 131.92 (s), 126.72 − 126.19 (m), 128.11 − 123.39 (m), 120.88 (s, J = 21.8 Hz), 111.04 (s, J = 18.2 Hz), 63.46 (s), 62.90 (d, J = 23.9 Hz), 62.33 (s, J = 8.0 Hz), 56.01 (s, J = 16.7 Hz), 16.78 − 16.56 (m), 16.43 (s), 14.30 (s) ppm.

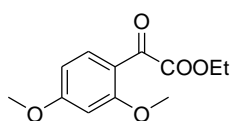GC-MS, (70 eV) m/z: 478 [M] $^+$, 447 [M -OMe] $^+$, 433 [M -OEt] $^+$, 405 [M -COOEt] $^+$.
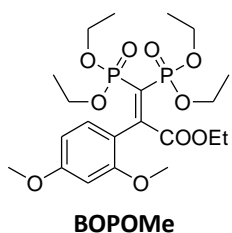
Ethyl 2-(2,4-dimethoxyphenyl)-2-oxoacetate

^{1}H NMR (300 MHz, CDCl$_3$) δ 7.91 (d, J = 8.8 Hz, 1H), 6.60 (dd, J = 8.8, 2.2 Hz, 1H), 6.43 (d, J = 2.2 Hz, 1H), 4.37 (q, J = 7.1 Hz, 2H), 3.88 (s, 3H), 3.84 (s, 3H), 1.38 (t, J = 7.1 Hz, 4H) ppm.

^{13}C {^{1}H}-NMR (75 MHz, CDCl$_3$) δ 185.48 (s), 167.18 (s), 166.38 (s), 162.77 (s), 133.29 (s), 116.37 (s), 107.22 (s), 98.61 (s), 61.97 (s), 56.39 (s), 56.16 (s), 14.58 (s) ppm.

GC-MS, (70 eV) m/z: 238 [M] $^+$, 165 [M -COOEt] $^+$.

Ethyl 3,3-bis(diethoxyphosphoryl)-2-(2,4-dimethoxyphenyl)acrylate

^{1}H NMR (400 MHz, CDCl$_3$) δ 7.52 (d, J = 8.5 Hz, 1H), 6.51 (dd, J = 8.5, 2.3 Hz, 1H), 6.40 (d, J = 2.3 Hz, 1H), 4.33 − 4.17 (m, 7H), 4.15 − 3.93 (m, 3H), 3.81 (s, J = 4.5 Hz, 3H), 3.75 (s, 3H), 1.37 (t, J = 7.1 Hz, 6H), 1.30 (t, J = 7.2 Hz, 3H), 1.22 − 0.99 (m, 6H) ppm.

^{31}P {^{1}H}-NMR (162 MHz, CDCl$_3$) δ 13.02 (d, J = 46.7 Hz, 1P), 12.67 (d, J = 46.5 Hz, 1P) ppm.

^{13}C {^{1}H}-NMR (101 MHz, CDCl$_3$) δ 167.72 (dd, J = 23.4, 14.6 Hz), 163.11 (s), 160.91 (s), 158.15 (s), 133.64 (s), 123.84 (dd, J = 168.0, 163.0 Hz), 118.87 (dd, J = 17.6, 11.4 Hz), 104.28 (s), 98.44 (s), 62.96 (d, J = 4.5 Hz), 62.52 (s), 61.91 (s), 55.51 (d, J = 7.1 Hz), 16.28 (d, J = 5.2 Hz), 16.04 (s), 13.93 (s) ppm.

GC-MS, (70 eV) m/z: 508 [M] $^+$, 477 [M -OMe] $^+$, 463 [M -OEt] $^+$, 435 [M -COOEt] $^+$.
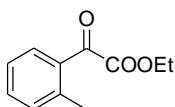
Ethyl 2-oxo-2-o-tolylacetate

^{1}H NMR (300 MHz, CDCl3) δ 7.72 − 7.67 (m, 1H), 7.53 − 7.45 (m, 1H), 7.36 − 7.28 (m, 2H), 4.44 (q, J = 7.1 Hz, 2H), 2.61 (s, 3H), 1.42 (t, J = 7.1 Hz, 3H) ppm.

^{13}C {1H}-NMR (75 MHz, CDCl3) δ 189.22 (s), 165.06 (s), 141.74 (s), 134.07 (s), 132.78 (s, J = 5.0 Hz), 132.67 (s), 131.1 (s), 126.34 (s), 62.67 (s), 21.85 (s, J = 10.3 Hz), 14.51 (s, J = 62.3 Hz) ppm.

GC-MS, (70 eV) m/z: 192 [M] $^+$, 119[M -COOEt] $^+$, 91 [M -COCOOEt] $^+$.
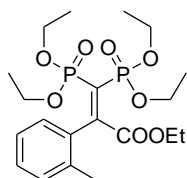
Ethyl 3,3-bis(diethoxyphosphoryl)-2-o-tolylacrylate

^{1}H NMR (400 MHz, CDCl$_3$) δ 7.25 − 7.20 (m, 1H), 7.20 − 7.14 (m, 1H), 4.31 − 4.17 (m, 6H), 3.96 − 3.83 (m, 2H), 3.83 − 3.70 (m, 1H), 3.67 − 3.56 (m, 1H), 2.39 (s, 3H), 1.39 (t, J = 7.1 Hz, 4H), 1.25 (t, J = 7.1 Hz, 3H), 1.16 − 1.07 (m, 6H).

^{31}P {^{1}H}-NMR (162 MHz, CDCl$_3$) δ 12.00 (d, J = 46.4 Hz, 1P), 11.13 (d, J = 46.6 Hz, 1P) ppm.

^{13}C {^{1}H}-NMR (101 MHz, CDCl$_3$) δ 167.19 (dd, J = 27.3, 12.3 Hz), 164.01 (s), 135.63 (dd, J = 17.8, 10.2 Hz), 135.59 (s), 130.01 (s), 128.83 (s), 127.93 (t, J = 1.6 Hz), 125.26 (s), 124.23 (dd, J = 168.9, 157.9 Hz), 63.02 (d, J = 5.2 Hz), 62.92 (d, J = 5.0 Hz), 62.40 (d, J = 6.5 Hz), 62.32 (d, J = 6.4 Hz), 62.06 (s), 19.89 (s), 16.31 (d, J = 3.3 Hz), 16.25 (d, J = 3.4 Hz), 16.15 (d, J = 6.1 Hz), 13.82 (s) ppm.

GC-MS, (70 eV) m/z: 462 [M]$^+$, 447 [M -Me]$^+$, 417 [M -OEt]$^+$, 389 [M -COOEt]$^+$, 325 [M -PO(OEt)$_2$]$^+$.

BOMe

For the synthesis of **BPNO$_2$** commercially available p-nitrophenyl glyoxylate was used.

Ethyl 3,3-bis(diethoxyphosphoryl)-2-(4-nitrophenyl)acrylate

^{1}H NMR (400 MHz, CDCl$_3$) δ 8.24 (d, J = 8.9 Hz, 2H), 7.63 (d, J = 8.9 Hz, 2H), 4.31 − 4.20 (m, 6H), 4.03 − 3.87 (m, 4H), 1.42 − 1.38 (m, 6H), 1.27 (t, J = 7.2 Hz, 3H), 1.16 (t, J = 7.1 Hz, 6H) ppm.

^{31}P {^{1}H}-NMR (162 MHz, CDCl$_3$) δ 11.26 (d, J = 40.9 Hz, 1P), 10.52 (d, J = 40.9 Hz, 1P) ppm.

^{13}C {^{1}H}-NMR (75 MHz, CDCl$_3$) δ 167.05 (dd, J = 25.9, 12.7 Hz), 161.40 (s), 148.66 (s), 142.74 (dd, J = 19.8, 10.0 Hz), 129.24 (s), 125.30 (dd, J = 165.0, 160.0 Hz), 123.64 (s), 63.65 (d, J = 5.2 Hz), 63.21 (d, J = 6.3 Hz), 63.14 (s), 16.70 (d, J = 6.1 Hz), 16.55 (d, J = 6.1 Hz), 14.22 (s) ppm.

GC-MS, (70 eV) m/z: 493[M]$^+$, 448 [M-OEt]$^+$, 420 [M-COOEt]$^+$, 392 [M-COOEt − Et+H]$^+$, 356 [M-PO(OEt)$_2$]$^+$, 284 [M-COOEt -PO(OEt)$_2$]$^+$.

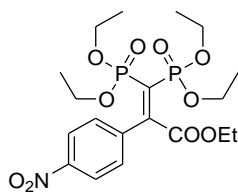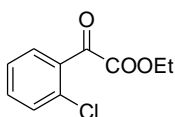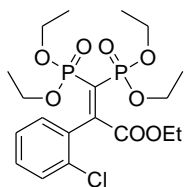**BPNO$_2$**

Ethyl 2-(2-chlorophenyl)-2-oxoacetate

^{1}H NMR (300 MHz, CDCl$_3$) δ 7.77 (dd, J = 7.7, 1.7 Hz, 1H), 7.57 − 7.48 (m, 1H), 7.47 − 7.37 (m, 2H), 4.42 (q, J = 7.1 Hz, 2H), 1.40 (t, J = 7.2 Hz, 3H) ppm.

^{13}C {^{1}H}-NMR(75 MHz, CDCl$_3$) δ 186.60 (d, J = 13.3 Hz), 163.20 (s), 134.39 (s), 131.72 (s), 130.66 (s), 127.58 − 127.09 (m), 62.90 (s), 13.96 (s) ppm.

GC-MS, (70 eV) m/z: 212 [M, Cluster 1 Chloro]$^+$, 139 [M -COOEt, Cluster 1Chloro]$^+$, 111 [M -COCOOEt, Cluster 1 Chloro]$^+$.

Ethyl 2-(2-chlorophenyl)-3,3-bis(diethoxyphosphoryl)acrylate

^{1}H NMR (400 MHz, CDCl$_3$) δ 7.42 − 7.34 (m, 1H), 7.33 − 7.27 (m, 1H), 4.32 − 4.19 (m, 6H), 4.09 − 3.98 (m, 2H), 3.95 − 3.87 (m, 1H), 3.74 − 3.64 (m, 1H), 1.39 (td, J = 6.9, 1.8 Hz, 6H), 1.28 (t, J = 7.2 Hz, 3H), 1.21 (t, J = 7.1 Hz, 3H), 1.09 (t, J = 7.0 Hz, 3H).

^{31}P {^{1}H}-NMR (162 MHz, CDCl$_3$) δ 11.37 (d, J = 43.8 Hz, 1P), 10.64 (d, J = 43.8 Hz, 1P) ppm.

^{13}C {^{1}H}-NMR (101 MHz, CDCl$_3$) δ 166.26 (dd, J = 26.2, 12.1 Hz), 160.28 (d, J = 2.2 Hz), 135.35 (dd, J = 19.7, 9.7 Hz), 131.95 (s), 130.63 (s), 130.26 (s), 129.35 (s), 126.59 (dd, J = 166.3, 158.1 Hz), 126.45 (s), 63.21 (t, J = 5.2 Hz), 62.90 (d, J = 6.2 Hz), 62.39 (d, J = 6.4 Hz), 62.33 (s), 16.28 (d, J = 6.3 Hz), 16.18 (d, J = 6.3 Hz), 16.06 (d, J = 6.2 Hz), 13.79 (s) ppm.

BOCl
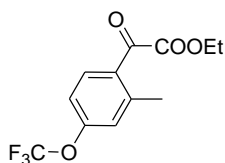
Ethyl 2-(2-methyl-4-(trifluoromethoxy)phenyl)-2-oxoacetate

^{1}H NMR (300 MHz, CDCl$_3$) δ 7.77 (dd, J = 7.8, 1.3 Hz, 1H), 7.18 – 7.11 (m, 2H), 4.44 (q, J = 7.1 Hz, 2H), 2.62 (s, 3H), 1.42 (t, J = 7.2 Hz, 3H) ppm.

^{13}C {^{1}H}-NMR (75 MHz, CDCl$_3$) δ 187.28 (s), 164.08 (s), 152.54 (s), 144.43 (s), 134.29 (s), 129.71 (s), 123.73 (s), 120.33 (q, J = 259.2 Hz), 117.33 (s), 62.54 (s), 21.51 (s), 14.03 (s) ppm.

GC-MS, (70 eV) m/z: 276 [M] $^+$, 203 [M -COOEt] $^+$, 191 [M -OCF$_3$] $^+$, 175 [M COCOOEt]$^+$.
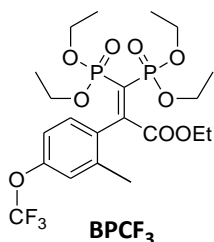
## Ethyl 3,3-bis(diethoxyphosphoryl)-2-(2-methyl-4-(trifluoromethoxy)phenyl)acrylate

^{1}H NMR (400 MHz, CDCl$_3$) δ 7.26 – 7.22 (m, 1H), 7.03 (d, J = 7.0 Hz, 2H), 4.29 – 4.17 (m, 6H), 3.98 – 3.86 (m, 2H), 3.86 – 3.75 (m, 1H), 3.74 – 3.65 (m, 1H), 2.41 (s, 3H), 1.39 (t, J = 7.1 Hz, 6H), 1.26 (t, J = 7.2 Hz, 3H), 1.12 (dt, J = 8.7, 7.1 Hz, 6H) ppm.

^{31}P {^{1}H}-NMR (162 MHz, CDCl$_3$) δ 11.49 (d, J = 45.3 Hz, 1P), 10.80 (d, J = 45.3 Hz, 1P) ppm.

^{13}C {^{1}H}-NMR (101 MHz, CDCl$_3$) δ 166.88 (dd, J = 26.8, 12.4 Hz), 162.32 (s), 149.37 (d, J = 1.8 Hz), 138.32 (s), 134.22 (dd, J = 19.2, 9.6 Hz), 129.47 (s), 125.32 (dd, J = 168.0, 158.2 Hz), 122.22 (s), 120.41 (q, J = 257.4 Hz), 117.62 (s), 63.12 (d, J = 5.2 Hz), 63.02 (d, J = 5.1 Hz), 62.54 (d, J = 6.6 Hz), 62.47 (d, J = 6.5 Hz), 62.26 (s), 20.02 (s), 16.29 (d, J = 3.4 Hz), 16.23 (d, J = 3.6 Hz), 16.06 (d, J = 5.8 Hz), 13.79 (s) ppm.

^{19}F {^{1}H}-NMR (376 MHz, CDCl$_3$) δ -57.71 (s, 3F) ppm.

GC-MS, (70 eV) m/z: 546 [M] $^+$, 501 [M -OEt] $^+$, 473 [M -COOEt] $^+$, 461 [M -OCF$_3$] $^+$, 409 [M -PO(OEt)$_2$]$^+$.
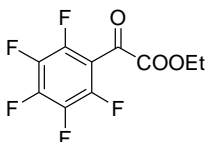
Ethyl 2-oxo-2-(perfluorophenyl)acetate

^{1}H NMR (300 MHz, CDCl$_3$) δ 4.44 (q, J = 7.1 Hz, 2H), 1.41 (t, J = 7.1 Hz, 3H) ppm.

^{13}C {^{1}H}-NMR (75 MHz, CDCl$_3$) δ 178.14 (s), 160.56 (s), 147.99 – 147.39 (m), 146.63 – 146.01 (m), 144.56 – 143.87 (m), 143.15 – 142.42 (m), 139.90 – 139.17 (m), 136.48 – 135.74 (m), 110.85 (t, J = 16.2 Hz), 63.77 (s), 13.85 (s) ppm.

GC-MS, (70 eV) m/z: 268 [M] $^+$, 195 [M -COOEt] $^+$, 167 [M -COCOOEt] $^+$.
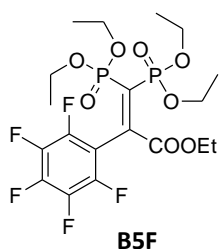
Ethyl 3,3-bis(diethoxyphosphoryl)-2-(perfluorophenyl)acrylate

^{1}H NMR (400 MHz, CDCl$_3$) δ 4.26 – 4.11 (m, 6H), 4.09 – 3.95 (m, 4H), 1.32 (t, J = 7.1 Hz, 6H), 1.27 – 1.19 (m, 9H) ppm.

^{31}P {^{1}H}-NMR (162 MHz, CDCl$_3$) δ 9.12 (t, J = 36.3 Hz, 2P) ppm.

^{13}C {^{1}H}-NMR (101 MHz, CDCl$_3$) δ 165.00 (dd, J = 20.3, 16.0 Hz), 148.09 (s), 144.68 (s), 142.63 – 141.78 (m), 140.50 (s), 139.12 – 138.39 (m), 136.70 – 135.77 (m), 131.60 (t, J = 158.2 Hz), 63.58 – 63.41 (m), 63.28 – 63.07 (m), 62.92 (s), 16.31 – 16.03 (m), 13.74 (s) ppm.

^{19}F {^{1}H}-NMR (376 MHz, CDCl$_3$) δ -137.98 – -138.53 (m), -152.17 (t, J = 20.9 Hz), -161.64 – -162.06 (m) ppm.

GC-MS, (70 eV) m/z: 538 [M] $^+$, 493 [M -OEt] $^+$, 465 [M -COOEt] $^+$.
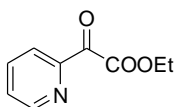
Ethyl 2-oxo-2-(pyridin-2-yl)acetate

^{1}H NMR (300 MHz, CDCl$_3$) δ 8.74 (d, J = 4.7 Hz, 1H), 8.10 (d, J = 7.8 Hz, 1H), 7.90 (td, J = 7.7, 1.7 Hz, 1H), 7.54 (ddd, J = 7.6, 4.8, 1.2 Hz, 1H), 4.48 (q, J = 7.2 Hz, 2H), 1.41 (t, J = 7.2 Hz, 3H) ppm.

^{13}C {^{1}H}-NMR (75 MHz, CDCl$_3$) δ 187.79 (s), 165.41 (s), 150.36 (s), 149.90 (s), 137.33 (s), 128.36 (s), 123.45 (s), 62.27 (s), 14.16 (s) ppm.

GC-MS, (70 eV) m/z: 179 [M]$^+$, 150 [M -Et]$^+$, 106 [M -COOEt]$^+$, 78 [M -COCOOEt]$^+$.
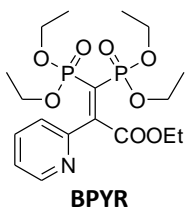
Ethyl 3,3-bis(diethoxyphosphoryl)-2-(pyridin-2-yl)acrylate

^{1}H NMR (400 MHz, CDCl$_3$) δ 8.62 (dt, J = 4.8, 1.4 Hz, 1H), 7.74 – 7.70 (m, 2H), 7.31 – 7.26 (m, 4H), 4.34 – 4.20 (m, 6H), 4.18 – 4.04 (m, 2H), 4.03 – 3.89 (m, 4H), 1.40 – 1.35 (m, 6H), 1.29 (t, J = 7.2 Hz, 3H), 1.10 (td, J = 7.1, 0.5 Hz, 6H) ppm.

^{31}P {^{1}H}-NMR (162 MHz, CDCl$_3$) δ 12.09 (d, J = 42.1 Hz, 1P), 11.09 (d, J = 42.2 Hz, 1P) ppm.

^{13}C {^{1}H}-NMR (101 MHz, CDCl$_3$) δ 166.78 (dd, J = 26.4, 12.4 Hz), 161.36 (s), 154.44 (dd, J = 22.1, 10.4 Hz), 149.13 (s), 136.20 (s), 125.03 (s), 124.33 (dd, J = 164.9, 159.4 Hz), 124.01 (s), 63.15 (d, J = 5.3 Hz), 62.75 (d, J = 6.4 Hz), 62.45 (s), 16.27 (d, J = 6.6 Hz), 16.01 (d, J = 6.7 Hz), 13.81 (s) ppm.

GC-MS, (70 eV) m/z: 449 [M]$^+$, 434 [M -Me]$^+$, 404 [M -OEt]$^+$, 376 [M -COOEt]$^+$, 312 [M -PO(OEt)$_2$]$^+$.

5.1.5 *Methylen Bisphosphonate Tetramethyl Esters (MBP-Me)*

In a round bottom flask equipped with magnetic stirring bar, 3.5 mmol of MBP and 10 mL of dichloromethane were added. To the solution 42 mmol (12 eq.) of $(CH_3)_3SiBr$ was added, leaving stirring overnight at r.t. under inert atmosphere. The solvent was removed under vacuum and to the crude was added 10 ml $MeOH/H_2O$. After 4 hours reaction, the solvent was removed under vacuum giving the corresponding methylen bisphosphonic acid MBP-OH. In a round bottom flask equipped with magnetic stirring bar and condenser, 3 mmol of MBP-OH and 60 mmol (20 eq.) of trimethyl orthoformate were added. The solution was heated to reflux and stirred overnight under inert atmosphere, then the crude was concentrated in vacuo to give the corresponding methylen bisphosphonate tetramethyl esters.
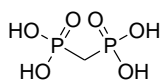
MBP-OH

Methylenediphosphonic acid
^{1}H NMR (300 MHz, D_2O) δ 2.29 (t, J = 20.5 Hz, 2H) ppm.
^{31}P {^{1}H}-NMR (122 MHz, D_2O) δ 16.33 (s, 2P) ppm.
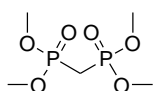
MBP-Me

Tetramethyl methylenediphosphonate
^{1}H NMR (300 MHz, $CDCl_3$) δ 3.84 (s, 6H), 3.80 (s, 6H), 2.46 (t, J = 21.1 Hz, 2H).
^{31}P {^{1}H}-NMR (122 MHz, $CDCl_3$) δ 20.69 (s, 2P) ppm.
GC-MS, (70 eV) m/z: 232 [M]$^+$, 201 [M -OMe]$^+$, 124 [M -PO(OMe)$_2$ +H]$^+$.

5.1.6 *Vinyliden Bisphosphonate Tetramethyl Esters (VBP-Me)*

For the synthesis of VBP-Me was followed the procedure reported by Degenhardt et al [120]. As phosphorous reagent, MBP-Me was used.
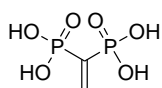
VBP-OH

Ethene-1,1-diyldiphosphonic acid
^{1}H NMR (300 MHz, D_2O) δ 6.55 (dd, J = 37.4, 34.3 Hz, 2H) ppm.
^{31}P {^{1}H}-NMR (122 MHz, D_2O) δ 9.96 (s, 2P).
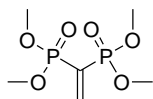
VBP-Me

Tetramethyl ethene-1,1-diyldiphosphonate
^{1}H NMR (300 MHz, $CDCl_3$) δ 7.03 (dd, J = 37.5, 34.3 Hz, 2H), 3.84 − 3.75 (m, 12H) ppm.
^{31}P {^{1}H}-NMR (122 MHz, $CDCl_3$) δ 14.31 (s, 2P) ppm.
GC/MS, (70 eV) m/z: 244 [M]$^+$, 229 [M -Me]$^+$, 213 [M -OMe]$^+$, 135 [M -PO(OMe)$_2$]$^+$.

5.1.7 *General procedure for synthesis of tetramethyl ester mono-substituted alkylidene bisphosphonates*

In a round bottom flask equipped with magnetic stirring bar, 1.3 mmol of aromatic mono-substituted VBP precursor and 5 mL of dichloromethane were added. To the solution 15.6 mmol (12 eq.) of $(CH_3)_3SiBr$ was added, leaving stirring overnight at r.t. under inert atmosphere. The solvent was removed under vacuum and to the crude was added 5 ml $MeOH/H_2O$. After 4 hours reaction, the solvent was removed under vacuum giving the corresponding bisphosphonic acid.

In a round bottom flask equipped with magnetic stirring bar and condenser, 1 mmol of aromatic mono-substituted bisphosphonic acid and 20 mmol of trimethyl orthoformate were added. The solution was heated to reflux and stirred overnight under inert atmosphere, then the crude was concentrated in vacuo to give the corresponding tetramethyl esters VBP precursor.


PPH-OH

2-phenylethene-1,1-diyldiphosphonic acid
^{1}H NMR (300 MHz, D_2O) δ 7.98 (dd, *J* = 46.3, 28.8 Hz, 1H), 7.65 − 7.48 (m, 2H), 7.45–7.27 (m, 3H) ppm.
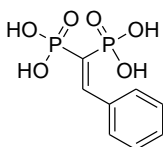^{31}P {^{1}H}-NMR (122 MHz, D_2O) δ 13.64 (d, *J* = 54.0 Hz, 1P), 8.07 (d, *J* = 54.0 Hz, 1P) ppm.
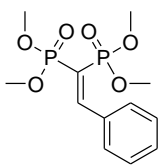
PPH-Me

Tetramethyl 2-phenylethene-1,1-diyldiphosphonate
^{1}H NMR (300 MHz, $CDCl_3$) δ 8.34 (dd, *J* = 48.1, 29.1 Hz, 1H), 7.78 − 7.70 (m, 2H), 7.44 − 7.37 (m, 3H), 3.85 (d, *J* = 11.3 Hz, 6H), 3.66 (d, *J* = 11.4 Hz, 6H) ppm.
^{31}P {^{1}H}-NMR(122 MHz, $CDCl_3$) δ 18.85 (d, *J* = 51.1 Hz, 1P), 13.43 (d, *J* = 51.1 Hz, 1P) ppm.
GC-MS, (70 eV) m/z: 320 [M] [+], 211 [M -PO(OMe)$_2$] [+], 109 [PO(OMe)$_2$] [+].
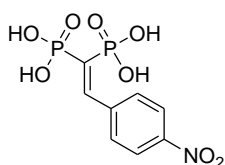
PPNO$_2$-OH

2-(4-nitrophenyl)ethene-1,1-diyldiphosphonic acid
^{1}H NMR (300 MHz, D_2O) δ 8.14 (d, J = 8.8 Hz, 2H), 7.97 (dd, J = 44.8 Hz, 28.2 Hz, 1H), 7.67 (d, J = 8.7 Hz, 2H) ppm.
^{31}P {^{1}H}-NMR (122 MHz, D_2O) δ 12.01 (d, *J* = 46.0 Hz, 1P), 6.51 (d, *J* = 46.0 Hz, 1P) ppm.
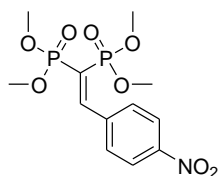
PPNO$_2$-Me

Tetramethyl 2-(4-nitrophenyl)ethene-1,1-diyldiphosphonate
^{1}H NMR (300 MHz, $CDCl_3$) δ 8.34 (dd, *J* = 47.0, 28.5 Hz, 1H), 8.26 (d, J= 8.7 Hz, 2H), 7.82 (d, J= 8.7 Hz, 2H), 3.88 (d, J= 11.4 Hz, 6H), 3.68 (d, J= 11.4 Hz, 6H), ppm.
^{31}P {^{1}H}-NMR(122 MHz, $CDCl_3$) δ 16.80 (d, *J* = 47.8 Hz, 1P), 11.83 (d, *J* = 47.8 Hz, 1P) ppm.
GC-MS, (70 eV) m/z: 365 [M] [+], 350 [M -Me] [+], 256 [M -PO(OMe)$_2$] [+], 109 [PO(OMe)$_2$] [+].

PPOME-OH
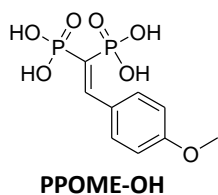
2-(4-methoxyphenyl)ethene-1,1-diyldiphosphonic acid

^{1}H NMR (300 MHz, D$_2$O) δ 7.85 (dd, J = 45.9 Hz, 29.0 Hz, 1H), 7.67 (d, J = 7.5 Hz, 2H), 6.92 (d, J = 7.2 Hz, 2H), 3.55 (s, 3H) ppm.

^{31}P {^{1}H}-NMR (122 MHz, D$_2$O) δ 14.97 (d, J = 33.0 Hz, 1P), 8.48 (d, J = 33.0 Hz, 1P) ppm.

PPOMe-Me
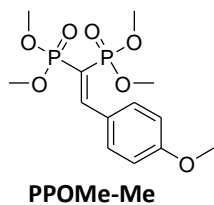
Tetramethyl 2-(4-methoxyphenyl)ethene-1,1-diyldiphosphonate

^{1}H NMR (300 MHz, CDCl$_3$) δ 8.34 (dd, *J* = 48.1, 29.2 Hz, 1H), 7.78–7.67 (m, 2H), 7.47–7.37 (m, 2H), 3.85 (d, *J* = 11.3 Hz, 6H), 3.66 (d, *J* = 11.4 Hz, 6H), 3.49 (s, 3H) ppm.

^{31}P {^{1}H}-NMR(122 MHz, CDCl$_3$) δ 18.84 (d, *J* = 51.3 Hz, 1P), 13.44 (d, *J* = 51.3 Hz, 1P) ppm.

GC-MS, (70 eV) m/z: 350 [M]$^+$, 319 [M -OMe]$^+$, 241 [M -PO(OMe)$_2$]$^+$, 109 [PO(OMe)$_2$]$^+$.

5.2 NON NITROGEN BPs

5.2.1 *General Procedure for the Cu(II) Catalyzed Addition of Boronic Acids to VBP*

In a vial equipped with magnetic stirring bar 100 mg of VBP (0.33 mmol), 2 mL of anhydrous toluene, 12 mg of Cu(OTf)$_2$ (10 mol% with respect to VBP) were added followed by 1.5 equivalents of boronic acid with respect to VBP. The vial was thermostatted at 70°C for 18h under vigorous stirring. Subsequently, the mixture was diluted with 5 mL of dichloromethane, the organic phase was extracted with a saturated aqueous solution of EDTA and washed with water. The product of the reaction was isolated by means of preparative TLC with 6:4 n-hexane:acetone eluent and was characterized with ^{1}H, ^{31}P NMR analysis.
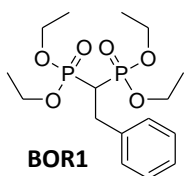
BOR1

Tetraethyl 2-phenylethane-1,1-diyldiphosphonate
^{1}H-NMR (300 MHz, CDCl$_3$): δ1.21-1.31 (m, 12H), 2.65 (tt, J = 24.0, 6.3 Hz, 1H), 3.24 (td, J = 16.5, 6.3 Hz, 2H), 3.97-4.21 (m, 8H), 7.15-7.28 (m, 5H) ppm.
^{31}P {1H}-NMR (122 MHz, CDCl$_3$): δ 24.20 (s, 2P) ppm.
GC-MS, (70 eV) m/z: 378 [M]$^{+}$, 241 [M -PO(OCH$_2$CH$_3$)$_2$]$^{+}$, 185 [241-2(CH$_2$CH$_2$)]$^{+}$.
Elemental Analysis C$_{16}$H$_{28}$O$_6$P$_2$: Calculated C, 50.79; H, 7.46; Found: C, 50.77; H, 7.49; %

BOR2
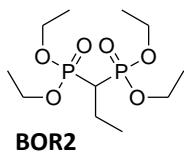
Tetraethyl propane-1,1-diyldiphosphonate
^{1}H-NMR (300 MHz, CDCl$_3$): δ 1.16 (t, J = 7.5 Hz, 3H), 1.20-1.31 (m, 12H), 2.69 (tt, J = 24.0, 6.0 Hz, 1H), 3.89 (m, 2H), 4.02-4.22 (m, 8H) ppm.
^{31}P {1H}-NMR (122 MHz, CDCl$_3$): δ 22.71 (s, 2P) ppm.
Elemental Analysis C$_{11}$H$_{26}$O$_6$P$_2$: Calculated C, 41.77; H, 8.29; Found: C, 41.79; H, 8.31; %

BOR3
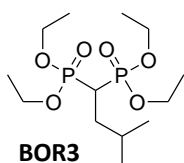
Tetraethyl 3-methylbutane-1,1-diyldiphosphonate
^{1}H-NMR (300 MHz, CDCl$_3$): δ 1.16 (d, J = 6.1 Hz, 6H), 1.21-1.29 (m, 12H), 1.61 (m, 1H), 2.64 (tt, J = 24.0, 6.0 Hz, 1H), 3.92 (m, 2H), 4.00-4.21 (m, 8H) ppm.
^{31}P {1H}-NMR (122 MHz, CDCl$_3$): δ 19,97 (s, 2P) ppm.
Elemental Analysis C$_{13}$H$_{30}$O$_6$P$_2$: Calculated C, 45.35; H, 8.78; Found: C, 45.33; H, 8.80; %

BOR4
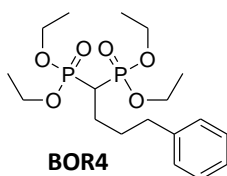
Tetraethyl 4-phenylbutane-1,1-diyldiphosphonate
^{1}H-NMR (300 MHz, CDCl$_3$): δ 1.21-1.32 (m, 14H), 2.67 (t, J=24.0, Hz, 1H), 2.87 (m, 2H), 3.86 (td, J=16.0, 6.0 Hz, 2H), 4.01-4.25 (m, 8H), 7.30-7.50 (m, 5H) ppm.
^{31}P {1H}-NMR (122 MHz, CDCl$_3$): δ 20.00 (s, 2P) ppm.
Elemental Analysis C$_{18}$H$_{32}$O$_6$P$_2$: Calculated C, 53.20; H, 7.94; Found: C, 53.16; H, 7.95; %
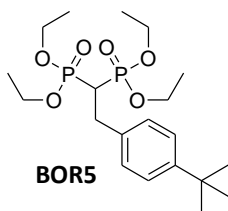
Tetraethyl 2-(4-tert-butylphenyl)ethane-1,1-diyldiphosphonate

^{1}H-NMR (300 MHz, CDCl$_3$): δ 1.05 (s, 9H), 1.18-1.27 (m, 12H), 2.64 (tt, J = 23.4, 6.3 Hz, 1H), 3.21 (td, J = 16.5, 6.3 Hz, 2H), 3.96 – 4.18 (m, 8H), 7.19 (d, J = 7.50 Hz, 2H), 7.29 (d, J = 7.50 Hz, 2H) ppm.

^{31}P {1H}-NMR (122 MHz, CDCl$_3$): δ 21.70 (s, 2P) ppm.

GC-MS, (70 eV) m/z: 434 [M]$^+$, 297 [M -PO(OCH$_2$CH$_3$)$_2$]$^+$, 269 [297-CH$_2$CH$_2$]$^+$, 241 [269-CH$_2$CH$_2$]$^+$, 185 [241-C$_4$H$_9$]$^+$.

Elemental Analysis C$_{20}$H$_{36}$O$_6$P$_2$: Calculated C, 55.29; H, 8.35; Found: C, 55.31; H, 8.33; %
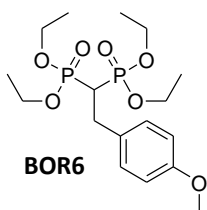
**Tetraethyl 2-(4-methoxyphenyl)ethane-1,1-diyldiphosphonate**

^{1}H-NMR (300 MHz, CDCl$_3$): δ 1.28 (m, 12H), 2.59 (tt, J = 23.7, 6.0 Hz, 1H), 3.19 (td, J = 16.5, 6.0 Hz, 2H), 3.78 (s, 3H), 4.02 – 4.19 (m, 8H), 6.81 (d, J = 8.7 Hz, 2H), 7.19 (d, J = 8.7 Hz, 2H) ppm.

^{31}P {1H}-NMR (122 MHz, CDCl$_3$): δ 24.33 (s, 2P) ppm.

GC-MS, (70 eV) m/z: 408 [M]$^+$, 363 [M -OEt]$^+$, 271 [M -PO(OEt)$_2$]$^+$.

Elemental Analysis C$_{17}$H$_{30}$O$_7$P$_2$: Calculated C, 50.00; H, 7.40; Found: C, 49.97; H, 7.44; %

Tetraethyl 2-(2,3-dimethoxyphenyl)ethane-1,1-diyldiphosphonate

^{1}H-NMR (300 MHz, CDCl$_3$): δ 1.21-1.27 (m, 12H), 3.04 (tt, J = 23.2, 7.1 Hz, 1H), 3.24 (td, J = 15.8, 7.1 Hz, 2H), 3.85 (s, 6H), 4.01 – 4.13 (m, 8H), 6.77-6.99 (m, 3H) ppm.

^{31}P {1H}-NMR (122 MHz, CDCl$_3$): δ 21.81 (s, 2P) ppm.

Elemental Analysis C$_{18}$H$_{32}$O$_8$P$_2$: Calculated C, 49.32; H, 7.36; Found: C, 49.36; H, 7.37; %
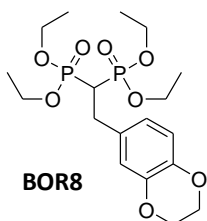
Tetraethyl 2-(2,3-dihydrobenzo[b][1,4]dioxin-6-yl)ethane-1,1-diyldiphosphonate

^{1}H-NMR (300 MHz, CDCl$_3$): δ 1.24-1.33 (m, 12H), 2.57 (tt, J = 23.7, 6.0 Hz, 1H), 3.13 (td, J = 16.5, 6.0 Hz, 2H), 4.02 – 4.19 (m, 8H), 4.22 (s, 4H), 6.70 – 6.75 (m, 3H) ppm.

^{31}P {1H}-NMR (122 MHz, CDCl$_3$): δ 24.26 (s, 2P) ppm.

GC-MS, (70 eV) m/z: 436 [M]$^+$, 391 [M -OEt]$^+$, 299 [M -PO(OEt)$_2$]$^+$.

Elemental Analysis C$_{18}$H$_{30}$O$_8$P$_2$: Calculated C, 49.54; H, 6.93; Found: C, 49.57; H, 6.95; %
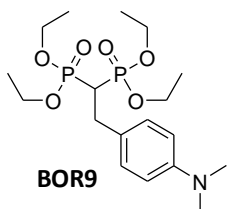
Tetraethyl 2-(4-(dimethylamino)phenyl)ethane-1,1-diyldiphosphonate

^{1}H-NMR (300 MHz, CDCl$_3$): δ 1.28 (m, 12H), 2.59 (tt, J = 23.7, 6.0 Hz, 1H), 2.90 (s, 6H), 3.16 (td, J = 16.7, 6.0 Hz, 2H), 4.00 – 4.30 (m, 8H), 6.67 (d, J = 8.7 Hz, 2H), 7.14 (d, J = 8.7 Hz, 2H) ppm.

^{31}P {1H}-NMR (122 MHz, CDCl$_3$): δ 24.59 (s, 2P) ppm.

GC-MS, (70 eV) m/z: 421 [M]$^+$, 376 [M -OEt]$^+$, 284 [M -PO(OEt)$_2$]$^+$.

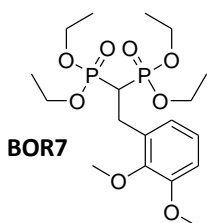Elemental Analysis C$_{18}$H$_{33}$NO$_6$P$_2$: Calculated C, 51.30; H, 7.89; N, 3.32; Found: C, 51.31; H, 7.87; N, 3.31; %
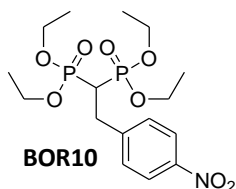
Tetraethyl 2-(4-nitrophenyl)ethane-1,1-diyldiphosphonate

^{1}H-NMR (300 MHz, CDCl$_3$): δ 1.27 (m, 12H), 2.62 (tt, J = 23.7, 6.3 Hz, 1H), 3.33 (td, J = 16.5, 6.3 Hz, 2H), 4.00 – 4.20 (m, 8H), 7.45 (d, J = 8.7 Hz, 2H), 8.14 (d, J = 8.7 Hz, 2H) ppm.

^{31}P {1H}-NMR (122 MHz, CDCl$_3$): δ 23.38 (s, 2P) ppm.

GC-MS, (70 eV) m/z: 423 [M]$^+$, 378 [M -OEt]$^+$, 286 [M -PO(OEt)$_2$]$^+$.

Elemental Analysis C$_{16}$H$_{27}$NO$_8$P$_2$: Calculated C, 45.39; H, 6.43; N, 3.31; Found: C, 45.36; H, 6.40; N, 3.34;%

BOR10

Tetraethyl 2-(4-bromophenyl)ethane-1,1-diyldiphosphonate

^{1}H-NMR (300 MHz, CDCl$_3$): δ 1.27 (m, 12H), 2.57 (tt, J = 23.7, 6.3 Hz, 1H), 3.19 (td, J = 16.5, 6.3 Hz, 2H), 4.00 – 4.21 (m, 8H), 7.15 (d, J = 8.4 Hz, 2H), 7.39 (d, J = 8.4 Hz, 2H) ppm.

^{31}P {1H}-NMR (122 MHz, CDCl$_3$): δ 23.89 (s, 2P) ppm.

GC-MS, (70 eV) m/z: 456 [M, Cluster Br]$^+$, 411 [M -OEt, Cluster Br]$^+$, 319 [M -PO(OEt)$_2$, Cluster Br]$^+$.

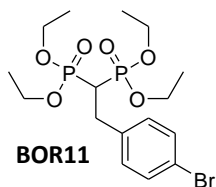Elemental Analysis C$_{16}$H$_{27}$BrO$_6$P$_2$: Calculated C, 42.03; H, 5.95; Found: C, 42.00; H, 5.97; %

BOR11
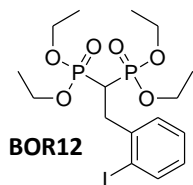
Tetraethyl 2-(2-iodophenyl)ethane-1,1-diyldiphosphonate

^{1}H-NMR (300 MHz, CDCl$_3$): δ 1.18-1.27 (m, 12H), 3.10 (tt, J = 23.0, 7.6 Hz, 1H), 3.36 (td, J= 16.2, 7.6 Hz, 2H), 3.96 – 4.18 (m, 8H), 6.90 (dt, J = 7.7, 1.6 Hz, 1H), 7.26 (dt, J = 7.7, 1.6 Hz, 1H), 7.39 (dd, J = 7.8, 1.3 Hz, 1H), 7.8 (dd, J = 7.8, 1.3 Hz, 1H) ppm.

^{31}P {1H}-NMR (122 MHz, CDCl$_3$): δ 20.68 (s, 2P) ppm.

GC-MS, (70eV) m/z: 504 [M]$^+$, 459 [M -OCH$_2$CH$_3$]$^+$, 377 [M -I]$^+$, 367 [M -PO(OEt)$_2$]$^+$.

Elemental Analysis C$_{16}$H$_{27}$IO$_6$P$_2$: Calculated C, 38.11; H, 5.40; Found: C, 38.15; H, 5.43; %

BOR12
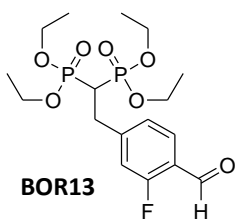
Tetraethyl 2-(3-fluoro-4-formylphenyl)ethane-1,1-diyldiphosphonate

^{1}H-NMR (300 MHz, CDCl$_3$): δ 1.20-1.33 (m, 12H), 2.65 (tt, J = 24.0, 6.0, 1H), 3.27 (td, J = 15.0, 6.0, 2H), 3.98-4.22 (m, 8H), 7.10-7.20 (m, 2H), 7.78 (t, J=6.0 Hz, 1H), 10.31 (s, 1H) ppm.

^{31}P {1H}-NMR (122 MHz, CDCl$_3$): δ 20.50 (s, 2P) ppm.

GC-MS, (70 eV) m/z: 424 [M]$^+$, 379 [M -OEt]$^+$, 287 [M -PO(OEt)$_2$]$^+$.

Elemental Analysis C$_{17}$H$_{27}$FO$_7$P$_2$: Calculated C, 48.12; H, 6.41; Found: C, 48.10; H, 6.38; %
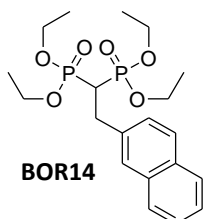
BOR13

Tetraethyl 2-(naphthalen-2-yl)ethane-1,1-diyldiphosphonate

^{1}H-NMR (300 MHz, CDCl$_3$): δ 1.23 (m, 12H), 2.75 (tt, J = 24.0, 6.3 Hz, 1H), 3.41 (td, J = 16.5, 6.3 Hz, 2H), 4.00-4.22 (m, 8H), 7.36 – 7.48 (m, 3H), 7.69-7.82 (m, 4H) ppm.

^{31}P {1H}-NMR (122 MHz, CDCl$_3$): δ 24.21 (s, 2P) ppm.

GC-MS, (70 eV) m/z: 428 [M]$^+$, 383 [M -OEt]$^+$, 291 [M -PO(OEt)$_2$]$^+$.

Elemental Analysis C$_{20}$H$_{30}$O$_6$P$_2$: Calculated C, 56.07; H, 7.06; Found: C, 56.04; H, 7.07; %

BOR14

Tetraethyl 2-(4-methylnaphthalen-1-yl)ethane-1,1-diyldiphosphonate

^{1}H-NMR (300 MHz, CDCl$_3$): δ 1.16-1.28 (m, 12H), 2.66 (s, 3H), 2.87 (tt, J = 23.4, 6.6 Hz, 1H), 3.70 (td, J = 15.9, 6.6 Hz, 2H), 3.94 – 4.24 (m, 8H), 7.22 (d, J = 7.2 Hz, 1H), 7.38 (d, J = 7.2 Hz, 1H), 7.50 – 7.55 (m, 2H), 8.01 (d, J= 9.0 Hz, 1H), 8.13 (d, J= 9.0 Hz, 1H) ppm.

^{31}P {1H}-NMR (122 MHz, CDCl$_3$): δ 24.21 (s, 2P) ppm.

GC-MS, (70 eV) m/z: 442 [M]$^+$, 397 [M -OEt]$^+$, 305 [M -PO(OEt)$_2$]$^+$.

Elemental Analysis C$_{21}$H$_{32}$O$_6$P$_2$: Calculated C, 57.01; H, 7.29; Found: C, 56.97; H, 7.32; %
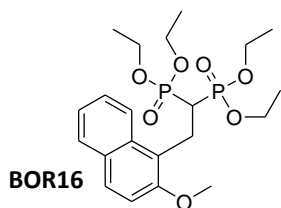
Tetraethyl 2-(2-methoxynaphthalen-1-yl)ethane-1,1-diyldiphosphonate

^{1}H-NMR (300 MHz, CDCl$_3$): δ 1.08-1.23 (m, 12H), 3.12 (tt, J = 23.7, 6.9 Hz, 1H), 3.73 (td, J = 15.3, 6.9 Hz, 2H), 3.96 (s, 3H), 4.00-4.24 (m, 8H), 7.21 (d, J = 7.90Hz, 1H), 7.34 (t, J = 6.9Hz, 1H), 7.45 (t, J = 6.9 Hz, 1H), 7.76 (m, 3H) ppm.

^{31}P {1H}-NMR (122 MHz, CDCl$_3$): δ 22.04 (s, 2P) ppm.

Elemental Analysis C$_{21}$H$_{32}$O$_7$P$_2$: Calculated C, 55.02; H, 7.04; Found: C, 55.04; H, 7.05; %
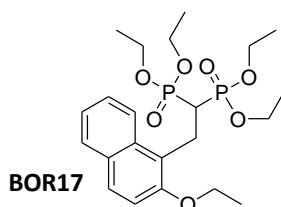
Tetraethyl 2-(2-ethoxynaphthalen-1-yl)ethane-1,1-diyldiphosphonate

^{1}H-NMR (300 MHz, CDCl$_3$): δ 1.14 (m, 12H), 1.49 (t, J = 6.9 Hz, 3H), 3.18 (tt, J = 23.4, 6.9 Hz, 1H), 3.73 (td, J= 15.8, 6.9 Hz, 2H), 3.87-4.10 (m, 8H), 4.19 (q, J = 7.2 Hz, 2H), 7.21 (d, J = 9.0 Hz, 1H), 7.34-7.27 (m, 1H), 7.51-7.42 (m, 1H), 7.73 (m, 2H), 8.17 (d, J = 8.4 Hz, 1H) ppm.

^{31}P { 1H}-NMR (122 MHz, CDCl$_3$): δ 24.70 (s, 2P) ppm.

GC-MS, (70 eV) m/z: 472 [M]$^+$, 427 [M -OEt]$^+$, 335 [M -PO(OEt)$_2$]$^+$.

Elemental Analysis C$_{22}$H$_{34}$O$_7$P$_2$: Calculated C, 55.93; H, 7.25; Found: C, 55.95; H, 7.23; %
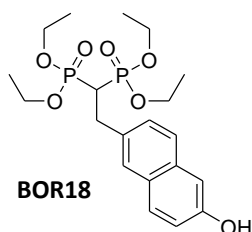
Tetraethyl 2-(6-hydroxynaphthalen-2-yl)ethane-1,1-diyldiphosphonate

^{1}H-NMR (300 MHz, CDCl$_3$): δ 1.25 (m, 12H), 2.77 (tt, J = 24.0, 6.3 Hz, 1H), 3.38 (td, J = 16.5, 6.3 Hz, 2H), 4.00 – 4.24 (m, 8H), 6.97-7.08 (m, 2H), 7.29 (d, J = 9.6 Hz, 1H), 7.48 (d, J = 8.4 Hz, 1H), 7.52 (d, J = 8.7 Hz, 1H), 7.61 (s, 1H) ppm.

^{31}P {1H}-NMR (122 MHz, CDCl$_3$): δ 24.66 (s, 2P) ppm.

GC-MS, (70 eV) m/z: 444 [M]$^+$, 307 [M -PO(OEt)$_2$]$^+$.

Elemental Analysis C$_{20}$H$_{30}$O$_7$P$_2$: Calculated C, 54.05; H, 6.80; Found: C, 54.08; H, 6.83; %
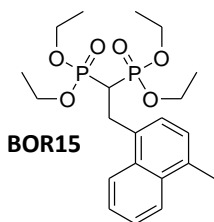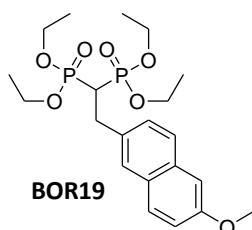
Tetraethyl 2-(6-methoxynaphthalen-2-yl)ethane-1,1-diyldiphosphonate

^{1}H-NMR (300 MHz, CDCl$_3$): δ 1.23 (m, 12H), 2.72 (tt, J = 23.7, 6.3 Hz, 1H), 3.37 (td, J = 16.5, 6.3 Hz, 2H), 3.90 (s, 3H), 4.02 – 4.18 (m, 8H), 7.07– 7.15 (m, 2H), 7.33 – 7.38 (m, 1H), 7.63-7.70 (m, 3H) ppm.

^{31}P {1H}-NMR (122 MHz, CDCl$_3$): δ 24.29 (s, 2P) ppm.

GC-MS, (70 eV) m/z: 458 [M]$^+$, 413 [M -OEt]$^+$, 321 [M -PO(OEt)$_2$]$^+$.

Elemental Analysis C$_{21}$H$_{32}$O$_7$P$_2$: Calculated C, 55.02; H, 7.04; Found: C, 55.00; H, 7.01; %

BOR15

BOR16

BOR17

BOR18

BOR19

BOR20
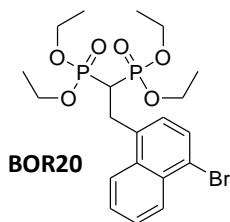
Tetraethyl 2-(4-bromonaphthalen-1-yl)ethane-1,1-diyldiphosphonate
^{1}H-NMR (300 MHz, CDCl$_3$): δ 1.15-1.40 (m, 12H), 2.85 (tt, J = 23.1, 6.9 Hz, 1H), 3.70 (td, J = 15.6, 6.9 Hz, 2H), 3.98-4.26 (m, 8H), 7.10-8.30 (m, 6H) ppm.
^{31}P {1H}-NMR (122 MHz, CDCl$_3$): δ 21.29 (s, 2P) ppm.
GC-MS, (70 eV) m/z: 506 [M]$^+$, 369 [M -PO(OCH$_2$CH$_3$)$_2$]$^+$, 341 [369 -(CH$_2$CH$_2$)]$^+$, 313 [341 -(CH$_2$CH$_2$)]$^+$, 233 [313 -Br]$^+$.
Elemental Analysis C$_{20}$H$_{29}$BrO$_6$P$_2$: Calculated C, 47.35; H, 5.76; Found: C, 47.33; H, 5.80; %

BOR21
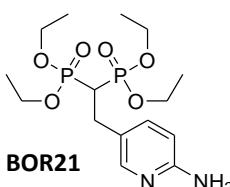
Tetraethyl 2-(6-aminopyridin-3-yl)ethane-1,1-diyldiphosphonate
^{1}H-NMR (300 MHz, CDCl$_3$): δ 1.18-1.30 (m, 12H), 2.81 (tt, J = 23.1, 6.3 Hz, 1H), 3.30 (td, J = 14.8, 6.3 Hz 2H), 4.06 – 4.28 (m, 8H), 6.42 (d, J = 6.40 Hz, 1H), 7.74 (d, J = 6.6 Hz, 1H), 8.46 (s, 1H) ppm.
^{31}P {1H}-NMR (122 MHz, CDCl$_3$): δ 20.47 (s, 2P) ppm.
Elemental Analysis C$_{15}$H$_{28}$N$_2$O$_6$P$_2$: Calculated C, 45.69; H, 7.16; N, 7.10; Found: C, 45.71; H, 7.12; N, 7.13; %

BOR22
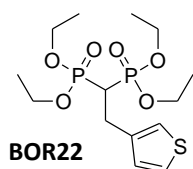
Tetraethyl 2-(thiophen-3-yl)ethane-1,1-diyldiphosphonate
^{1}H-NMR (300 MHz, CDCl$_3$): δ 1.28 (m, 12H), 2.61 (tt, J = 23.7, 6.0 Hz, 1H), 3.27 (td, J = 16.5, 6.0 Hz, 2H), 4.04-4.20 (m, 8H), 7.01 (d, J = 4.9 Hz, 1H), 7.10 (s, 1H), 7.23 (d, J = 4.9 Hz, 1H) ppm.
^{31}P {1H}-NMR (122 MHz, CDCl$_3$): δ 24.10 (s, 2P) ppm.
GC-MS, (70 eV) m/z: 384 [M]$^+$, 339 [M -OEt]$^+$, 247 [M -PO(OEt)$_2$]$^+$.
Elemental Analysis C$_{14}$H$_{26}$O$_6$P$_2$S: Calculated C, 43.75; H, 6.82; Found: C, 43.78; H, 6.84; %

BOR23
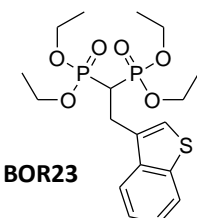
Tetraethyl 2-(benzo[b]thiophen-3-yl)ethane-1,1-diyldiphosphonate
^{1}H-NMR (300 MHz, CDCl$_3$): δ 1.20-1.31 (m, 12H), 2.80 (tt, J = 23.7, 6.3 Hz, 1H), 3.51 (td, J = 16.1, 6.3 Hz, 2H), 4.00-4.22 (m, 8H), 7.31 (s, 1H), 7.33-7.42 (m, 2H), 7.81-7.90 (m, 2H) ppm.
^{31}P {1H}-NMR (122 MHz, CDCl$_3$): δ 23.99 (s, 2P) ppm.
GC-MS, (70 eV) m/z: 434 [M]$^+$, 389 [M -OEt]$^+$, 297 [M -PO(OEt)$_2$]$^+$.
Elemental Analysis C$_{18}$H$_{28}$O$_6$P$_2$S: Calculated C, 49.77; H, 6.50; Found: C, 49.79; H, 6.54; %

BOR24
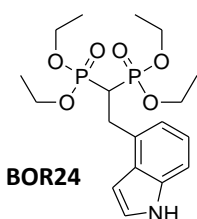
Tetraethyl 2-(1H-indol-4-yl)ethane-1,1-diyldiphosphonate
^{1}H-NMR (300 MHz, CDCl$_3$): δ 1.19-1.30 (m, 12H), 2.97 (tt, J = 23.5, 6.2 Hz, 1H), 4.05 – 4.19 (m, 8H), 4.74 (td, J = 14.1, 6.2 Hz, 2H), 6.44 (d, J = 3.2 Hz, 1H), 7.10 (t, J = 7.0 Hz, 1H), 7.21 (s, 1H), 7.44 (d, J= 7.6 Hz, 1H), 7.60 (d, J= 7.6 Hz, 1H) ppm.
^{31}P {1H}-NMR (122 MHz, CDCl$_3$): δ 19.29 (s, 2P) ppm.
Elemental Analysis C$_{18}$H$_{29}$NO$_6$P$_2$: Calculated C, 51.80; H, 7.00; N, 3.36; Found: C, 51.84; H, 6.98; N, 3.35; %
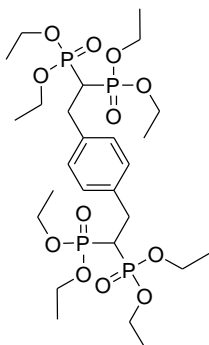
Octaethyl 2,2'-(1,4-phenylene)bis(ethane-2,1,1-triyl)tetraphosphonate

^{1}H-NMR (300 MHz, CDCl$_3$): δ 1.28 (m, 24 H), 2.59 (tt, J = 23.4, 6.3 Hz, 2H), 3.20 (td, J = 15.0, 6.3 Hz, 4H), 4.00 - 4.22 (m, 16H), 7.18 (s, 4H) ppm.

^{31}P {1H}-NMR (122 MHz, CDCl$_3$): δ 24.32 (s, 4P) ppm.

GC-MS, (70 eV) m/z: 678 [M]$^+$, 633 [M -OEt]$^+$, 541 [M -PO(OEt)$_2$]$^+$, 404 [M - 2PO(OEt)$_2$]$^+$.

Elemental Analysis C$_{26}$H$_{50}$O$_{12}$P$_4$: Calculated C, 46.02; H, 7.43; Found: C, 46.06; H, 7.45; %

BOR25
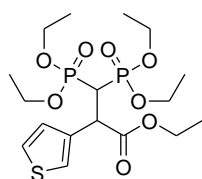
Ethyl 3,3-bis(diethoxyphosphoryl)-2-(thiophen-3-yl)propanoate

^{1}H NMR (400 MHz, CDCl$_3$) δ 7.30 (dd, *J* = 3.0, 1.2 Hz, 1H), 7.19 (dd, *J* = 5.0, 3.0 Hz, 1H), 7.14 (dd, *J* = 5.0, 1.3 Hz, 1H), 4.33 (dd, *J* = 20.1, 9.9 Hz, 1H), 4.24–4.10 (m, 6H), 4.03–3.87 (m, 3H), 3.82–3.72 (m, 1H), 3.50 (td, *J* = 23.4, 9.6 Hz, 1H), 1.33 (td, *J* = 7.1, 4.6 Hz, 6H), 1.24–1.14 (m, 9H) ppm.

^{31}P {1H}-NMR (162 MHz, CDCl$_3$) δ 21.48 (d, *J* = 2.4 Hz, 1P), 20.24 (d, *J* = 2.4 Hz, 1P) ppm.

^{13}C {1H}-NMR (101 MHz, CDCl$_3$) δ 171.75 (dd, *J* = 15.5, 5.3 Hz), 135.38 (dd, *J* = 13.5, 4.7 Hz), 128.91 (s), 125.08 (s), 124.34 (s), 63.08 (d, *J* = 6.7 Hz), 62.68 (d, *J* = 6.6 Hz), 62.48 (d, *J* = 6.8 Hz), 62.09 (d, *J* = 6.7 Hz), 61.50 (s), 44.54 (t, *J* = 3.0 Hz), 40.75 (dd, *J* = 136.0, 128.9 Hz), 16.32 (t, *J* = 6.1 Hz), 16.21 (d, *J* = 0.5 Hz), 16.14 (d, *J* = 0.9 Hz), 13.94 (s) ppm.

GC-MS, (70 eV) m/z: 456 [M]$^+$, 410 [M -OEt-H]$^+$, 382 [M -COOEt-H]$^+$, 319 [M - PO(OEt)$_2$]$^+$.

BOR26

5.2.2 2-(6-(ferrocenyl)hexanethio)ethane-1,1-diyldiphosphonic acid (VBPFHT-OH)

In a vial equipped with magnetic stirring bar 500 mg of VBP (1.67 mmol), 2 mL of $CHCl_3$, 1.70 mmol of 2-mercaptoethanol and 5 mol% of NEt_3 with respect to VBP) were added. The system was left overnight under stirring at 70°C after which the solvent is removed under vacuum. The crude was diluted with 10 mL of CH_2Cl_2 and washed twice with 25 mL of water. The organic phase was dried with $NaSO_4$, filtered, concentrated under reduced pressure and purified by column chromatography using 1:1 ethyl acetate/acetone as eluent. The resulting pale yellow oil (VBPTIO) was used in the next deprotection step.

In a round bottom flask equipped with magnetic stirring bar, 250 mg of VBPTIO (0.93 mmol) and 5 mL of 1-2 dichloroethane were added. To the solution, 11.3 mmol (12 eq.) of $(CH_3)_3SiBr$ was added, leaving the mixture under stirring at 70°C under inert atmosphere for 1.5 hours after which the solvent was removed under vacuum. To the crude, 5 mL of $MeOH/H_2O$ were added. After 4 hours reaction, the solvent was removed under vacuum giving VBPTIO-OH as a pale green oil.

VBPFHT
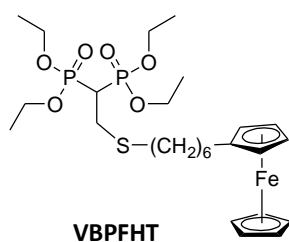
Tetraethyl 2-(6-(ferrocenyl)hexanethio)ethane-1,1-diyldiphosphonate
^{1}H NMR (300 MHz, $CDCl_3$) δ 4.26 − 4.12 (m, 8H), 4.08 (s, 5H), 4.03 (s, 5H), 3.04 (td, J = 16.3, 5.9 Hz, 2H), 2.69 − 2.47 (m, 3H), 2.31 (t, J = 8.0 Hz, 2H), 1.67 − 1.40 (m, 8H), 1.35 (t, J = 7.1 Hz, 12H) ppm.
^{31}P {1H}-NMR (122 MHz, $CDCl_3$) δ 20.47 (s, 2P) ppm.

VBPFHT-OH
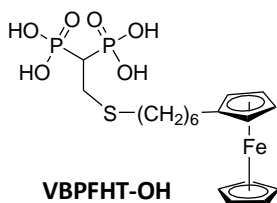
2-(6-(ferrocenyl)hexanethio)ethane-1,1-diyldiphosphonic acid
^{31}P {1H}-NMR (122 MHz, DMSO) δ 17.60 (s, 2P) ppm.
ESI, m/z: 491 [M]⁻

5.2.3 2-(2-hydroxyethylthio)ethane-1,1-diyldiphosphonic acid (VBPTIO-OH)

In a vial equipped with magnetic stirring bar 500 mg of VBP (1.67 mmol), 2 mL of $CHCl_3$, 1.70 mmol of 2-mercaptoethanol and 5mol% of NEt_3 with respect to VBP) were added. The system is left overnight under stirring at 70 ° C after which the solvent is removed under vacuum. The crude was diluted with 10 ml of CH_2Cl_2 and washed twice with 25 mL of water. The organic phase was dried with $NaSO_4$, filtered and concentrated under reduced pressure. The crude was purified by column chromatography using 1:1 ethyl acetate/acetone as eluent. The resulting pale yellow oil (VBPTIO) was used in the next deprotection step.

In a round bottom flask equipped with magnetic stirring bar, 250 mg of VBPTIO (0.93 mmol), and 5 mL of 1-2 dichloroethane were added. To the solution, 11.3 mmol (12 eq.)

of (CH$_3$)$_3$SiBr was added, leaving stirring at 70 ° C under inert atmosphere for 1.5 hours after which the solvent is removed under vacuum. To the crude was added 5 ml MeOH/H$_2$O. After 4 hours reaction, the solvent was removed under vacuum giving VBPTIO-OH as a pale yellow oil.
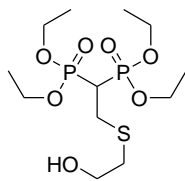
VBPTIO

Tetraethyl 2-(2-hydroxyethylthio)ethane-1,1-diyldiphosphonate
^{1}H NMR (300 MHz, CDCl$_3$) δ 4.28 – 4.11 (m, 8H), 3.78 (t, J = 5.5 Hz, 2H), 3.12 (td, J = 16.7, 6.0 Hz, 2H), 2.77 (t, J = 5.5 Hz, 2H), 2.70 (tt, 24.0, 5.9 Hz), 1.36 (t, J = 7.1 Hz, 12H) ppm.
^{31}P {1H}-NMR (122 MHz, CDCl$_3$) δ 20.52 (s, 2P) ppm.
GC-MS, (70 eV) m/z: 378 [M]$^+$, 360 [M-H$_2$O]$^+$, 333 [M -CH$_2$CH$_2$OH]$^+$, 241 [M - PO(OEt)$_2$]$^+$, 223 [M -PO(OEt)$_2$ –H$_2$O]$^+$.
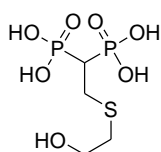
VBPTIO-OH

2-(2-hydroxyethylthio)ethane-1,1-diyldiphosphonic acid
^{1}H NMR (300 MHz, D$_2$O) δ 3.68 (t, J = 6.2 Hz, 2H), 2.97 (td, J = 15.9, 6.4 Hz, 2H), 2.70 (t, J = 6.2 Hz, 2H), 2.44 (tt, J = 23.0, 6.4 Hz, 1H) ppm.
^{31}P {1H}-NMR (122 MHz, D$_2$O) δ 18.19 (s, 2P) ppm.
ESI, m/z: 265 [M-H]$^-$, 284 [M+H$_2$O]$^-$.

5.2.4 *General Procedure for Pd/C Hydrogenation of Bi-Substituted VBP Precursors.*

In a vial equipped with magnetic stirring bar 100 mg of bi-substituted VBP precursor, 5 mL of non anhydrous MeOH and 20% mol of Pd (with respect to VBP precursor) of Pd/C 5% w/w catalyst were added.

The system was closed under inert atmosphere and H_2 (1 atm) was bubbled overnight. The solutionwas filtered and the solvent removed under reduced pressure. The crude was purified by TLC chromatography using 8:2 ethyl acetate/acetone as eluent.

The purified raceme product was eluted by cellulose-2 chiral HPLC in isocratic condition in order to optimize a enantiomeric separation method. Eluition times of enantiomer are reported (in parenhesis eluition time of non hydogenated VBP precursor).
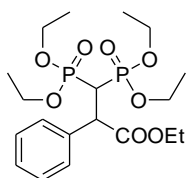
H2BPHEt

Ethyl 3,3-bis(diethoxyphosphoryl)-2-phenylpropanoate

^{1}H NMR (400 MHz, CDCl$_3$) δ 7.43 – 7.37 (m, 2H), 7.30 – 7.22 (m, 3H), 4.29 – 4.05 (m, 7H), 3.96 – 3.74 (m, 3H), 3.61 – 3.45 (m, 2H), 1.34 (td, *J* = 7.1, 3.2 Hz, 6H), 1.19 – 1.10 (m, 6H), 1.06 (t, *J* = 7.1 Hz, 3H) ppm.

^{31}P {^{1}H}-NMR (162 MHz, CDCl$_3$) δ 21.84 (d, *J* = 2.5 Hz, 1P), 20.20 (d, *J* = 2.5 Hz, 1P) ppm.

^{13}C {^{1}H}-NMR (101 MHz, CDCl$_3$) δ 172.17 (dd, *J* = 18.5, 3.0 Hz), 135.55 (dd, *J* = 14.3, 4.0 Hz), 129.90 (s), 127.95 (s), 127.80 (s), 63.20 (d, *J* = 6.6 Hz), 62.68 (d, *J* = 6.7 Hz), 62.34 (d, *J* = 6.9 Hz), 61.97 (d, *J* = 6.7 Hz), 61.40 (s), 49.60 – 49.07 (m), 40.72 (dd, *J* = 136.1, 127.8 Hz), 16.45 – 16.23 (m), 16.13 (d, *J* = 0.9 Hz), 16.07 (d, *J* = 1.4 Hz), 13.88 (s) ppm.

GC/MS, (70 eV) m/z: 450 [M] [+], 405 [M -OEt] [+], 376 [M -COOEt-H] [+], 313 [M -PO(OEt)$_2$] [+], 269 [M -PO(OEt)$_2$-OEt] [+], 241 [M -PO(OEt)$_2$-COOEt] [+].

Eluition time: 23'-31'(11'), isopropanol/n-hexane 2/8

H2BPHMe
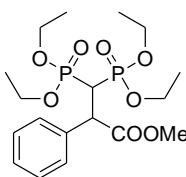
Methyl 3,3-bis(diethoxyphosphoryl)-2-phenylpropanoate

^{1}H NMR (400 MHz, CDCl$_3$) δ 7.34 (dd, *J* = 7.8, 1.7 Hz, 2H), 7.22 – 7.19 (m, 3H), 4.20 – 4.04 (m, 5H), 3.90 – 3.77 (m, 2H), 3.75 – 3.64 (m, 1H), 3.60 (s, 3H), 3.56 – 3.38 (m, 2H), 1.28 (td, *J* = 7.1, 2.0 Hz, 6H), 1.07 (t, *J* = 7.1 Hz, 3H), 1.00 (t, *J* = 7.1 Hz, 3H) ppm.

^{31}P {^{1}H}-NMR (162 MHz, CDCl$_3$) δ 21.74 (d, *J* = 3.2 Hz, 1P), 20.05 (d, *J* = 3.2 Hz, 1P) ppm.

^{13}C {^{1}H}-NMR (101 MHz, CDCl$_3$) δ 172.91 (dd, *J* = 18.7, 3.0 Hz), 135.52 (dd, *J* = 14.2, 4.0 Hz), 130.00 (s), 128.14 (s), 128.01 (s), 63.36 (d, *J* = 6.6 Hz), 62.80 (d, *J* = 6.6 Hz), 62.46 (d, *J* = 6.9 Hz), 62.07 (d, *J* = 6.7 Hz), 52.71 (s), 49.50 – 49.19 (m), 40.96 (dd, *J* = 136.3, 127.7 Hz), 16.50 (d, *J* = 6.2 Hz), 16.41 (d, *J* = 5.7 Hz), 16.22 (d, *J* = 6.4 Hz) ppm.

GC-MS, (70 eV) m/z: 436 [M] [+], 405 [M -OMe] [+], 404 [M -Ome-H] [+], 377 [M -COOMe] [+], 299 [M -PO(OEt)$_2$] [+], 268 [M -PO(OEt)$_2$–OMe-H] [+].

Eluition time: 102', 116'(40'), isopropanol/n-hexane 2/8
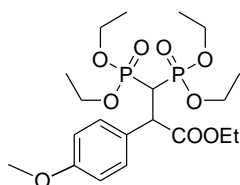
Ethyl 3,3-bis(diethoxyphosphoryl)-2-(4-methoxyphenyl)propanoate

^{1}H NMR (400 MHz, CDCl$_3$) δ 7.32 (d, J = 8.8 Hz, 2H), 6.81 (d, J = 8.8 Hz, 2H), 4.26 – 4.05 (m, 7H), 3.98 – 3.78 (m, 3H), 3.77 (s, 3H), 3.65 – 3.43 (m, 2H), 1.34 (td, J = 7.1, 3.2 Hz, 6H), 1.19 – 1.13 (m, 6H), 1.10 (q, J = 7.0 Hz, 3H) ppm.

^{31}P {^{1}H}-NMR (162 MHz, CDCl$_3$): δ 21.89 (d, J = 2.9 Hz, 1P), 20.35 (d, J = 2.9 Hz, 1P) ppm.

^{13}C {^{1}H}-NMR (101 MHz, CDCl$_3$) δ 172.49 (dd, J = 18.3, 3.1 Hz), 159.37 (s), 131.14 (s), 127.64 (dd, J = 14.4, 4.1 Hz), 113.45 (s), 63.26 (d, J = 6.6 Hz), 62.76 (d, J = 6.7 Hz), 62.46 (d, J = 6.9 Hz), 62.13 (d, J = 6.7 Hz), 61.47 (s), 55.36 (s), 48.69 (t, J = 2.9 Hz), 40.85 (dd, J = 136.2, 127.6 Hz), 16.63 – 16.34 (m), 16.27 (d, J = 6.5 Hz), 14.05 (s) ppm.

GC-MS, (70 eV) m/z: 480 [M] $^+$, 435 [M-OEt] $^+$, 407 [M -COOEt] $^+$, 343 [M - PO(OEt)$_2$]$^+$, 298 [M -PO(OEt)$_2$–OEt-H] $^+$, 270 [M-PO(OEt)$_2$–COOEt-H] $^+$.

Eluition time: 68', 79' (40'), isopropanol/n-hexane 2/8
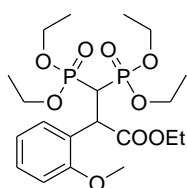
Ethyl 3,3-bis(diethoxyphosphoryl)-2-(2-methoxyphenyl)propanoate

^{1}H NMR (400 MHz, CDCl$_3$) δ 7.30 (dd, J = 7.7, 1.7 Hz, 1H), 7.15 (ddd, J = 8.2, 7.5, 1.7 Hz, 1H), 6.82 (td, J = 7.5, 1.0 Hz, 1H), 6.78 (d, J = 8.3 Hz, 1H), 4.67 (ddd, J = 14.1, 9.8, 6.1 Hz, 1H), 4.21 – 3.99 (m, 6H), 3.89 – 3.79 (m, 3H), 3.78 (s, 3H), 3.72 – 3.63 (m, 1H), 3.56 (td, J = 23.8, 9.9 Hz, 1H), 1.26 (td, J = 7.1, 3.0 Hz, 6H), 1.13 – 1.05 (m, 9H) ppm.

^{31}P {^{1}H}-NMR (122 MHz, CDCl$_3$) δ 21.03 (d, J = 0.8 Hz, 1P), 19.60 (d, J = 0.8 Hz, 1P) ppm.

^{13}C {^{1}H}-NMR (101 MHz, CDCl$_3$) δ 172.19 (dd, J = 16.3, 2.7 Hz), 157.49 (s), 130.69 (s), 128.89 (s), 124.20 (dd, J = 12.4, 5.1 Hz), 120.00 (s), 110.73 (s), 63.15 (d, J = 6.5 Hz), 62.54 (d, J = 6.7 Hz), 62.23 (d, J = 6.7 Hz), 61.18 (s), 55.68 (s), 41.42 (t, J = 2.7 Hz), 39.64 (dd, J = 135.6, 129.2 Hz), 16.47 – 16.01 (m), 13.95 (s).

GC-MS, (70 eV) m/z: 480 [M] $^+$, 343 [M -PO(OEt)$_2$] $^+$, 407 [M -COOEt] $^+$.

Eluition time: 26', 53' (18'), isopropanol/n-hexane 2/8
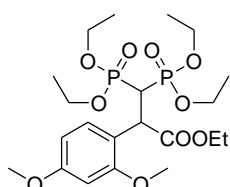
Ethyl 3,3-bis(diethoxyphosphoryl)-2-(2,4-dimethoxyphenyl)propanoate

^{1}H NMR (400 MHz, CDCl$_3$) δ 7.24 (s, 1H), 6.41 – 6.34 (m, 2H), 4.61 (ddd, J = 13.9, 9.9, 6.0 Hz, 1H), 4.26 – 4.02 (m, 6H), 3.96 – 3.81 (m, 4H), 3.79 (s, J = 8.4 Hz, 3H), 3.75 (s, 3H), 3.60 (td, J = 23.6, 9.7 Hz, 1H), 1.29 (t, J = 7.0 Hz, 6H), 1.17 – 1.10 (m, 9H) ppm.

^{31}P {^{1}H}-NMR (162 MHz, CDCl$_3$) δ 22.48 (s. 1P), 21.07 (s, 1P) ppm.

^{13}C {^{1}H}-NMR (101 MHz, CDCl$_3$) δ 172.32 (dd, J = 16.4, 2.5 Hz), 160.40 (s), 158.46 (s), 131.31 (s), 116.52 (dd, J = 12.8, 5.1 Hz), 103.97 (s), 98.31 (s), 63.20 (d, J = 6.2 Hz), 62.60 (d, J = 6.6 Hz), 62.36 (d, J = 6.4 Hz), 61.12 (s), 55.65 (s), 55.30 (s), 40.88 (s), 39.57 (dd, J = 128.3, 121.5 Hz), 29.70 (s), 16.51 – 16.06 (m), 13.99 (s) ppm.

GC-MS, (70 eV) m/z: 510 [M] $^+$, 464 [M -OEt-H] $^+$, 373 [M -PO(OEt)$_2$] $^+$.

Eluition time: 27', 40' (21'), isopropanol/n-hexane 2/8

176
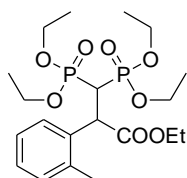
Ethyl 3,3-bis(diethoxyphosphoryl)-2-o-tolylpropanoate

^{1}H NMR (400 MHz, CDCl$_3$) δ 7.41 − 7.35 (m, 1H), 7.16 − 7.08 (m, 3H), 4.42 (td, J = 11.1, 3.6 Hz, 1H), 4.31 − 4.15 (m, 4H), 4.14 − 4.01 (m, 2H), 3.99 − 3.84 (m, 2H), 3.75 − 3.65 (m, 1H), 3.57 (td, J = 22.6, 11.5 Hz, 1H), 3.44 − 3.31 (m, 1H), 2.51 (s, 3H), 1.36 (td, J = 7.1, 1.6 Hz, 6H), 1.15 (q, J = 7.3 Hz, 6H), 1.03 (t, J = 7.1 Hz, 3H).

^{31}P {^{1}H}-NMR (162 MHz, CDCl$_3$) δ 22.25 (d, J = 4.0 Hz, 1P), 20.90 (d, J = 4.0 Hz, 1P) ppm.

^{13}C {^{1}H}-NMR (101 MHz, CDCl$_3$) δ 172.75 (dd, J = 20.0, 1.5 Hz), 137.71 (s), 134.13 (dd, J = 14.8, 4.0 Hz), 130.50 (s), 129.01 (s), 127.66 (s), 125.56 (s), 63.34 (d, J = 6.5 Hz), 62.75 (d, J = 6.7 Hz), 62.48 (d, J = 6.9 Hz), 62.01 (d, J = 6.7 Hz), 61.39 (s), 44.08 (t, J = 2.8 Hz), 40.41 (dd, J = 137.0, 127.1 Hz), 20.28 (s), 16.55 (d, J = 6.1 Hz), 16.44 (d, J = 6.2 Hz), 16.30 (d, J = 2.9 Hz), 16.24 (d, J = 2.6 Hz), 13.99 (s) ppm.

GC-MS, (70 eV) m/z: 464 [M][+], 419 [M-OEt][+], 391 [M -COOEt][+], 327 [M -PO(OEt)$_2$][+].

Eluition time: 21', 27' (8'), isopropanol/n-hexane 2/8
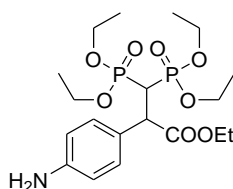
Ethyl 2-(4-aminophenyl)-3,3-bis(diethoxyphosphoryl)propanoate

^{1}H NMR (400 MHz, CDCl$_3$) δ 7.16 (d, J = 8.4 Hz, 2H), 6.58 (d, J = 8.4 Hz, 2H), 4.25 − 4.05 (m, 7H), 4.03 − 3.79 (m, 3H), 3.66 − 3.39 (m, 2H), 1.33 (td, J = 6.9, 3.5 Hz, 6H), 1.16 (t, J = 7.1 Hz, 6H), 1.11 (t, J = 7.1 Hz, 3H) ppm.

^{31}P {^{1}H}-NMR (162 MHz, CDCl$_3$): δ 22.05 (d, J = 2.5 Hz, 1P), 20.49 (d, J = 2.5 Hz, 1P) ppm.

^{13}C {^{1}H}-NMR (101 MHz, CDCl$_3$) δ 172.63 (dd, J = 18.7, 2.7 Hz), 146.17 (s), 130.92 (s), 125.50 − 125.05 (m), 114.66 (s), 111.93 (s), 63.19 (d, J = 6.6 Hz), 62.68 (d, J = 6.6 Hz), 62.37 (d, J = 6.8 Hz), 62.11 (d, J = 6.7 Hz), 61.33 (s), 48.86 − 48.47 (m), 40.83 (dd, J = 136.4, 127.0 Hz), 16.46 (t, J = 6.6 Hz), 16.31 (d, J = 2.3 Hz), 16.25 (d, J = 2.6 Hz), 14.04 (s) ppm.

GC-MS, (70 eV) m/z: 465 [M] [+], 419 [M-OEt-H] [+], 391 [M-COOEt-H] [+], 328 [M-PO(OEt)$_2$] [+], 283 [M-PO(OEt)$_2$–OEt-H] [+], 255 [M-PO(OEt)$_2$–COOEt-H] [+].

Eluition time: 118', 141' (15'), isopropanol/n-hexane 2/8
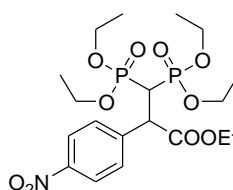
Ethyl 3,3-bis(diethoxyphosphoryl)-2-(4-nitrophenyl)propanoate

Not isolated as pure compound.

^{31}P {^{1}H}-NMR (122 MHz, CDCl$_3$) δ 20.79 (d, J = 2.6 Hz, 1P), 19.22 (d, J = 2.6 Hz, 1P) ppm.

GC-MS, (70 eV) m/z: 465 [M] [+], 419 [M-OEt-H] [+], 391 [M-COOEt-H] [+], 328 [M-PO(OEt)$_2$] [+], 283 [M-PO(OEt)$_2$–OEt-H] [+], 255 [M-PO(OEt)$_2$–COOEt-H] [+].
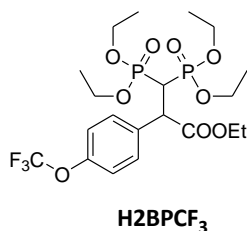
Ethyl 3,3-bis(diethoxyphosphoryl)-2-(4-(trifluoromethoxy)phenyl)propanoate

H2BPCF$_3$

^{1}H NMR (400 MHz, CDCl$_3$) δ 7.42 (d, J = 8.5 Hz, 1H), 7.02 – 6.94 (m, 2H), 4.40 (td, J = 11.0, 3.9 Hz, 1H), 4.30 – 4.16 (m, 4H), 4.15 – 4.05 (m, 2H), 4.01 – 3.87 (m, 2H), 3.79 – 3.68 (m, 1H), 3.61 – 3.39 (m, 2H), 2.53 (s, 3H), 1.36 (t, J = 7.1 Hz, 6H), 1.20 – 1.12 (m, 6H), 1.04 (t, J = 7.1 Hz, 3H) ppm.

^{31}P {^{1}H}-NMR (162 MHz, CDCl$_3$) δ 21.81 (d, J = 3.6 Hz, 1P), 20.68 (d, J = 3.6 Hz, 1P) ppm.

^{13}C {^{1}H}-NMR (101 MHz, CDCl$_3$) δ 172.40 (dd, J = 19.5, 1.7 Hz), 148.45 (dd, J = 3.3, 1.6 Hz), 140.12 (s), 133.02 (dd, J = 14.9, 4.1 Hz), 130.59 (s), 122.59 (s), 120.61 (d, J = 256.9 Hz), 117.83 (s), 63.46 (d, J = 6.6 Hz), 62.83 (t, J = 6.5 Hz), 62.05 (d, J= 6.8 Hz), 61.62 (s), 43.72 (t, J = 2.5 Hz), 40.41 (dd, J = 137.0, 127.5 Hz), 20.40 (s), 16.54 (d, J = 6.0 Hz), 16.43 (d, J = 6.2 Hz), 16.26 (d, J = 6.2 Hz), 16.14 (d, J = 6.1 Hz), 13.99 (s) ppm.

^{19}F {^{1}H}-NMR (376 MHz, CDCl$_3$) δ -57.73 (s) ppm.

GC-MS, (70 eV) m/z: 548 [M]$^+$, 503 [M -OEt]$^+$, 475 [M -COOEt]$^+$, 411 [M - PO(OEt)$_2$]$^+$.

Eluition time: 6', 8' (4'), isopropanol/n-hexane 2/8
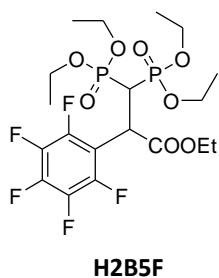
Ethyl 3,3-bis(diethoxyphosphoryl)-2-(perfluorophenyl)propanoate

H2B5F

^{1}H NMR (400 MHz, CDCl$_3$) δ 4.53 (ddd, J = 13.8, 10.5, 3.1 Hz, 1H), 4.30 – 4.13 (m, 6H), 4.08 – 3.94 (m, 4H), 3.72 (td, J = 23.0, 10.5 Hz, 1H), 1.36 (td, J = 7.0, 4.9 Hz, 6H), 1.25 – 1.17 (m, 9H) ppm.

^{31}P {^{1}H}-NMR (162 MHz, CDCl$_3$) δ 20.86 (d, J = 6.8 Hz, 1P), 19.09 (d, J = 6.8 Hz, 1P) ppm.

^{13}C {^{1}H}-NMR (101 MHz, CDCl$_3$) δ 168.88 (d, J = 15.9 Hz), 147.72 – 147.22 (m), 145.26 – 144.73 (m), 142.72 – 142.22 (m), 139.18 – 138.09 (m), 136.44 – 135.82 (m), 63.71 (d, J = 6.6 Hz), 63.10 (dd, J = 8.0, 6.8 Hz), 62.87 (d, J = 6.7 Hz), 62.42 (s), 38.13 (s), 37.44 (dd, J = 134.0, 129.5 Hz), 16.51 (d, J = 6.0 Hz), 16.41 (d, J = 6.2 Hz), 16.07 (t, J = 6.0 Hz), 14.01 (s) ppm.

^{19}F {^{1}H}-NMR (376 MHz, CDCl$_3$) δ -138.01 – -138.22 (m), -152.25 (t, J = 20.9 Hz), -161.69 – -161.89 (m) ppm.

GC-MS, (70 eV) m/z: 540 [M]$^+$, 495 [M -OEt]$^+$, 467 [M -COOEt]$^+$, 403 [M -PO(OEt)$_2$]$^+$.
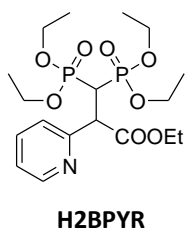
Ethyl 3,3-bis(diethoxyphosphoryl)-2-(pyridin-2-yl)propanoate

H2BPYR

^{1}H NMR (400 MHz, CDCl$_3$) δ 8.56 (ddd, J = 4.8, 1.8, 0.8 Hz, 1H), 7.63 (td, J = 7.7, 1.8 Hz, 1H), 7.42 (d, J = 7.9 Hz, 1H), 7.18 (ddd, J = 7.5, 4.8, 1.1 Hz, 1H), 4.37 (ddd, J = 11.6, 10.0, 7.6 Hz, 1H), 4.27 – 4.13 (m, 6H), 4.08 – 3.98 (m, 1H), 3.96 – 3.88 (m, 1H), 3.87 – 3.71 (m, 3H), 1.36 – 1.29 (m, 6H), 1.22 – 1.09 (m, 9H) ppm.

^{31}P {^{1}H}-NMR (162 MHz, CDCl$_3$) δ 21.63 (d, J = 3.2 Hz, 1P), 20.44 (d, J = 3.2 Hz, 1P) ppm.

^{13}C {^{1}H}-NMR (101 MHz, CDCl$_3$) δ 170.90 (dd, J = 18.0, 6.1 Hz), 148.95 (s), 136.22 (s), 125.09 (s), 122.51 (s), 63.11 (d, J = 6.5 Hz), 62.77 – 62.51 (m), 62.09 (d, J = 6.9 Hz), 61.51 (s), 16.37 (d, J = 6.1 Hz), 16.28 (d, J = 6.2 Hz), 16.12 (dd, J = 6.3, 4.8 Hz), 13.95 (s) ppm.

GC-MS, (70 eV) m/z: 451 [M]$^+$, 406 [M -OEt]$^+$, 378 [M -COOEt]$^+$, 314 [M -PO(OEt)$_2$]$^+$.

5.3 NITROGEN BPs

5.3.1 *General procedure for synthesis of β-nitrile bisphosphonates*

Catalytic tests

In a vial equipped with magnetic stirring bar 0.07 mmol of VBP precursors, 2 mL of anhydrous 1,2-dichloroethane was added followed by 5 mol% with respect to VBP precursors of Zn(OTf)$_2$ and 5 equivalents TMSiCN. The vial was thermostatted at 70°C for 18h under vigorous stirring. Subsequently, the mixture was diluted with 5 mL of dichloromethane, the organic phase was extracted with a saturated aqueous solution of EDTA and washed with water. The organic phase was anhydrified with Na$_2$SO$_4$ and the solvent was removed under reduced pressure. The product of the reaction was isolated by means of preparative and was characterized with ^{1}H, ^{31}P and MS analyses. Selected purified raceme product was eluted by chiral HPLC in isocratic condition in order to optimize a enantiomeric separation method. Eluition times of enantiomer are reported.

General procedure for the ester deprotection of the nitrile BPs

The tetraethyl ester of the bisphosphonic acid (0.07 mmol) was introduced in a vial under anhydrous condition. To this 12 equivalents of bromotrimethylsilane (2.4 mmol) were added. The vial was stirred under inert atmosphere at rt for 18 h. The crude mixture was concentrated under reduced pressure, diluted with a 9:1 solution of methanol and water, stirred for 4 h at room temperature and dried. The free bisphosphonic acid was obtained in quantitative yield and was characterized by ^{1}H and ^{31}P NMR and ESI-MS on negative mode.

CNVBP
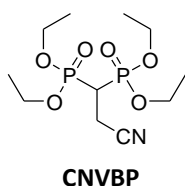
Tetraethyl 2-cyanoethane-1,1-diyldiphosphonate
^{1}HNMR (300 MHz, CDCl$_3$): δ 1.35 – 1.39 (m, 12H),2.61 (tt, *J* = 22.9, 6.2 Hz, 1H), 2.93 (td, *J* = 15.5, 6.4 Hz, 2H), 4.19 – 4.28 (m, 8H) ppm.
^{31}P { ^{1}H }-NMR (122 MHz, CDCl$_3$): δ 17.7 (s, 2P) ppm.
GC-MS, (70 eV) m/z: 327 [M] [+], 298 [M -Et] [+], 282 [M -OEt] [+], 190 [M -PO(OEt)$_2$] [+].

CNVBP-OH
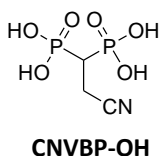
2-cyanoethane-1,1-diyldiphosphonic acid
^{1}H NMR (300 MHz, D$_2$O): δ 2.74 (tt, *J* = 23.2, 5.8 Hz, 1H), 3.65 (td, *J* = 16.6, 5.8 Hz, 2H) ppm.
^{31}P {^{1}H}-NMR (122 MHz, D$_2$O): δ 19.9 (s, broad, 2P) ppm.

CNPPH
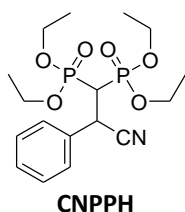
Tetraethyl 2-cyano-2-phenylethane-1,1-diyldiphosphonate
^{1}H NMR (300 MHz, CDCl$_3$): δ 1.12 (t, *J* = 7.10 Hz, 3H), 1.29 (t, *J* = 7.10 Hz, 3H), 1.35– 1.42 (m, 6H), 2.89 (td, *J* = 24.5, 3.10 Hz, 1H), 4.09-4.34 (m, 8H), 4.74 (ddd, *J* = 27.9, 12.9, 3.1 Hz, 1H), 7.29-7.41 (m, 3H), 7.43-7.50 (m, 2H) ppm.
^{31}P {^{1}H}-NMR (122 MHz, CDCl$_3$): δ 16.1 (s, 1P), 17.6 (s, 1P) ppm.
Eluition time: cellulose-2, 29', 30', isopropanol/n-hexane 11/89.
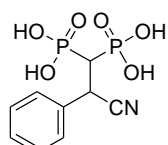
CNPPH-OH

2-cyano-2-phenylethane-1,1-diyldiphosphonic acid

^{1}H NMR (300 MHz, D$_2$O): δ 3.14 (s,broad, 1H), 4.70 (s, broad, 1H), 7.26 (d, *J* = 5.40 Hz, 3H), 7.38 (d, *J* = 6,00 Hz, 2H) ppm.

^{31}P { ^{1}H } -NMR (121.5 MHz, D$_2$O): δ 16.9 (s, broad, 2P).

MS ESI, m/z: 290.88 [M] $^-$, 308.84 [M+H$_2$O]$^-$, 322.79 [M+CH$_3$OH]$^-$.
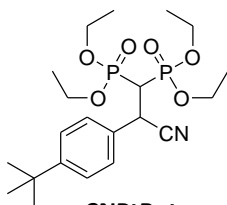
CNPtBut

Tetraethyl 2-(4-tert-butylphenyl)-2-cyanoethane-1,1-diyldiphosphonate

^{1}H NMR (300 MHz, CDCl$_3$): δ 1.10 (t, *J* = 7.0 Hz, 3H), 1.23-1.44 (m, 18H), 2.88 (td, *J* = 24.5 Hz, 3.3 Hz, 1H), 4.11-4.33 (m, 8H), 4.71 (ddd, *J* = 27.7 Hz, 12.9, 3.3 Hz, 1H), 7.40 (s, 4H) ppm.

^{31}P {^{1}H}-NMR (122 MHz, CDCl$_3$): δ 16.2 (s, 1P); 17.7 (s, 1P) ppm.

GC-MS, (70 eV) m/z: 459 [M] $^+$, 414 [M -OEt] $^+$, 322 [M -PO(OEt)$_2$] $^+$, 266 [M - PO(OEt)$_2$ –tBut +H] $^+$.

Eluition time: cellulose-2,**25**', 27', isopropanol/n-hexane 13/87.
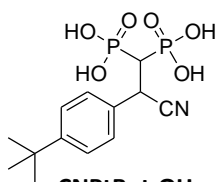
CNPtBut-OH

2-(4-tert-butylphenyl)-2-cyanoethane-1,1-diyldiphosphonic acid

^{1}H NMR (300 MHz, D$_2$O): δ 1.17 (s, 9H), 3.22 (broad, 1H); 4.67 (broad, 1H), 7.28-7.36 (m, 4H) ppm.

^{31}P {^{1}H}-NMR (122 MHz, D$_2$O): δ 17.7 (s, broad, 2P) ppm.
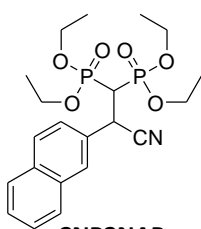
CNP2NAP

Tetraethyl 2-cyano-2-(naphthalen-2-yl)ethane-1,1-diyldiphosphonate

^{1}H NMR (300 MHz, CDCl$_3$): δ 1.01 (t, *J* = 7.07 Hz, 3H), 1.41-1.51 (m, 9 H), 4.30-4.45 (m, 8H), 3.10 (td, *J* = 24.5, 2.86 Hz, 1H), 5.47 (ddd, *J* = 30.3, 11.6, 2.79 Hz, 1H), 7.49-7.62 (m, 3H), 7.85-8.02 (m, 4H) ppm.

^{31}P {^{1}H}-NMR (122 MHz, CDCl$_3$): δ 15.9 (s, 1P), 18.2 (s, 1P) ppm.

GC-MS, (70 eV) m/z: 453 [M] $^+$, 316 [M -PO(OEt)$_2$] $^+$.

Eluition time: cellulose-4, 39', 42', isopropanol/n-hexane 13/87.
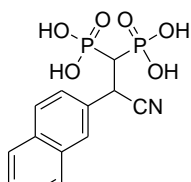
CNP2NAP-OH

2-cyano-2-(naphthalen-2-yl)ethane-1,1-diyldiphosphonic acid

^{1}HNMR (300 MHz, D$_2$O): δ 3.33 (m , 1H), 5.06 (m, 1H), 7.38-7.53 (m, 1H), 7.54-7.62 (m, 3H), 7.63-7.70 (m, 1H), 7.78 (d, *J* = 7.4 Hz, 1H), 7.89 (d, *J* = 8.2 Hz, 1H) ppm.

^{31}P {^{1}H}-NMR (122 MHz, D$_2$O): δ 16.3 (s, broad, 2P) ppm.

MS ESI, m/z: 340.9 [M] $^-$, 358.8 [M+H$_2$O]$^-$, 372.8 [M+CH$_3$OH]$^-$.
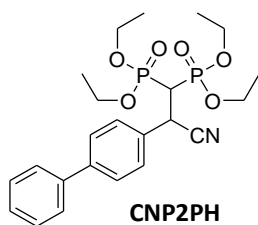
CNP2PH

Tetraethyl 2-(biphenyl-4-yl)-2-cyanoethane-1,1-diyldiphosphonate

^{1}H NMR (300 MHz, CDCl$_3$): δ 1.14 (t, J = 7.07 Hz, 3H), 1.31 (t, J = 7.06 Hz, 3H), 1.40 (m, 6H), 2.93 (td, *J*= 24.6, 3.22 Hz, 1H), 3.92–4.36 (m, 8H), 4.79 (ddd, *J* = 27.4, 12.9, 2.78 Hz, 1H), 7.34–7.48 (m, 3 H), 7.53–7.62 (m, 6H) ppm.

^{31}P {^{1}H}-NMR (122 MHz, CDCl$_3$): δ 16.2 (s, 1P), 17.6 (s, 1P) ppm.

GC-MS, (70 eV) m/z: 479 [M] $^+$, 434 [M -OEt] $^+$, 342 [M -PO(OEt)$_2$] $^+$.

Eluition time: cellulose-4, 48', 64', isopropanol/n-hexane 13/87.
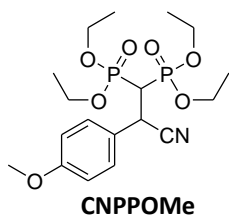
Tetraethyl 2-cyano-2-(4-methoxyphenyl)ethane-1,1-diyldiphosphonate

^{1}H NMR (300 MHz, CDCl$_3$): 1.15-1.42 (m, 12H), 2.83 (td, J = 24.6, 3.2, 1H), 3.80 (s, 3H), 4.14-4.30 (m, 8H), 4.69 (ddd, J = 25.7, 14.6, 3.00 Hz, 1H); 6.88 (d, J = 8.8 Hz, 2H), 7.39 (d, J = 8.8 Hz, 2H) ppm.

^{31}P {^{1}H}-NMR (122 MHz, CDCl$_3$): 17.7 (s, 1P); 16.3 (s, 1P) ppm.

CNPPOMe
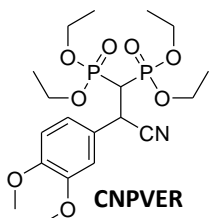
Tetraethyl 2-cyano-2-(3,4-dimethoxyphenyl)ethane-1,1-diyldiphosphonate

^{1}H NMR (300 MHz, CDCl$_3$): δ 1.18 (t, J = 7.1 Hz, 3H), 1.31 (t, J = 7.2, 3H), 1.35–1.42 (m, 6H), 2.86 (td, J = 24.6, 3.1 Hz, 1H); 3.88 (s, 3H); 3.90 (s, 3H); 4.01–4.33 (m, 8H); 4.70 (ddd, J = 27.0, 13.6, 3.1 Hz, 1H); 6.84 (m, 1H); 7.00–7.05 (m, 2H) ppm.

^{31}P {^{1}H}-NMR (122 MHz, CDCl$_3$): δ 16.4 (s, 1P), 17.7 (s, 1P) ppm.
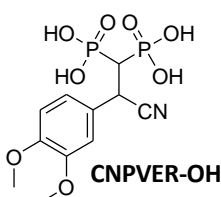
CNPVER

2-cyano-2-(3,4-dimethoxyphenyl)ethane-1,1-diyldiphosphonic acid

^{1}H NMR (300 MHz, D$_2$O): δ 3.22 (broad, 1H),3.74 (d, J = 4.5 Hz, 6H),4.68 (broad, 1H),6.88 (d, J = 8.0 Hz, 1H),6.95 (d, J = 8.4 Hz, 1H),7.03 (s, 1H) ppm.

^{31}P {^{1}H}-NMR (122 MHz, D$_2$O): δ 16.4 (s, broad, 2P) ppm.

CNPVER-OH
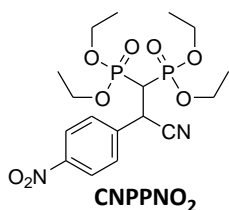
Tetraethyl 2-cyano-2-(4-nitrophenyl)ethane-1,1-diyldiphosphonate

^{1}H NMR (300 MHz, CDCl$_3$): δ 1.20 (t, J = 7.1 Hz, 3H), 1.30 (t, J = 7.1 Hz, 3H), 1.38 (t, J = 7.2 Hz, 3H), 1.42 (t, J = 7.2 Hz, 3H), 2.87 (td, J = 24.3, 3 Hz, 1H), 4.01-4.36 (m, 8H), 4.83 (ddd, J = 26.8, 13.5, 3.00 Hz, 1H), 7.70 (d, J = 8.6 Hz, 2H), 8.25 (d, J = 8.9 Hz, 2H) ppm.

^{31}P {^{1}H}-NMR (122 MHz, CDCl$_3$): δ 15.7 (s, 1P), 16.8 (s, 1P) ppm.
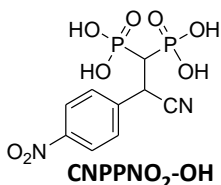
CNPPNO$_2$

2-cyano-2-(4-nitrophenyl)ethane-1,1-diyldiphosphonic acid

^{1}H NMR (300 MHz, D$_2$O): δ 2.90 (td, broad, 1H), 4.70 (ddd, broad, 1H), 7.65 (m, 2H), 8.14 (m, 2H) ppm.

^{31}P {^{1}H}-NMR (122 MHz, D$_2$O): δ 15.2 (s,broad, 2P) ppm.

MS ESI, m/z: 335.9 [M] [-], 353.7 [M+H$_2$O][-].

CNPPNO$_2$-OH
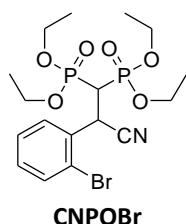
Tetraethyl 2-(2-bromophenyl)-2-cyanoethane-1,1-diyldiphosphonate

^{1}H NMR (300 MHz, CDCl$_3$): δ 1.03 (t, J = 7.1 Hz, 3H), 1.28 (t, J = 7.1 Hz, 3H), 1.42 (t, J = 7.1 Hz, 6H), 3.26 (ddd, J = 25.3, 23.2, 4.1 Hz, 1H), 3.80-4.41 (m, 8H), 5.03 (ddd, J = 30.5, 8.6, 4.0 Hz, 1H), 7.23 (td, overlapped, J = 7.5, 1.5, 1H), 7.38 (td, J = 7.6, 1.2, 1H), 7.56 (dd, J = 8.0, 1.2 Hz, 1H), 7.87 (dd, J = 7.8, 1.6 Hz, 1H) ppm.

^{31}P {^{1}H}-NMR (122 MHz, CDCl$_3$): δ 15.87 (s, 1P), 17.14 (s, 1P) ppm.

GC-MS, (70 eV) m/z: 481 [M, Cluster Br] [+], 452 [M -Et, Cluster Br] [+], 436 [M -OEt, Cluster Br] [+], 402 [M -Br] [+].

CNPOBr

CNPPF
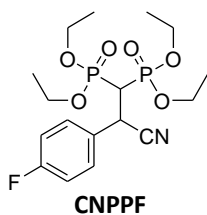
Tetraethyl 2-cyano-2-(4-fluorophenyl)ethane-1,1-diyldiphosphonate

^{1}HNMR (300 MHz, CDCl$_3$): δ 1.31 (t, *J* = 7.1 Hz, 4H), 1.35-1.42 (m, 8H), 2.83 (td, *J* = 24.5, 3.2 Hz, 1H), 4.14-4.33 (m, 8H), 4.73 (ddd, *J* = 27.0, 13.5, 3.2 Hz, 1H), 7.06 (m, 2H), 7.45-7.49 (s, 2H) ppm.

^{31}P {^{1}H}-NMR (122 MHz, CDCl$_3$): δ 16.1 (s, 1P), 17.3 (s, 1P) ppm.

GC-MS, (70 eV) m/z: 421 [M] $^+$, 376 [M -OEt] $^+$, 284 [M -PO(OEt)$_2$] $^+$.

Eluition time: cellulose-2, 20',24', isopropanol/n-hexane 13/87.
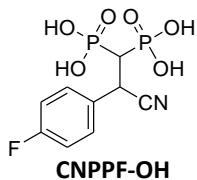
CNPPF-OH

2-cyano-2-(4-fluorophenyl)ethane-1,1-diyldiphosphonic acid

^{1}HNMR (300 MHz, D$_2$O): δ 3.22 (broad, 1H), 4.68 (broad, 1H), 6.98 (t, *J* = 8.6 Hz, 2H), 7.34-7.38 (m, 2H) ppm.

^{31}P {^{1}H}-NMR (122 MHz, D$_2$O): δ 18.6 (s, broad, 2P) ppm.

MS ESI, m/z: 308.9 [M] $^-$, 326.8 [M+H$_2$O]$^-$, 340.8 [M+CH$_3$OH]$^-$.

5.3.2 General procedure for catalytic addition TMSIN$_3$ to VBP

In a vial equipped with magnetic stirring bar 0.07 mmol of VBP and 2 mL of solvent was added followed by 5 mol% with respect to VBP precursors of catalyst and 5 equivalents of TMSiN$_3$. The vial was thermostatted at reported temperature for 18h under vigorous stirring. Subsequently, the mixture was diluted with 5 mL of dichloromethane, the organic phase was extracted with a saturated aqueous solution of EDTA and washed with water. The organic phase was anhydrified with Na$_2$SO$_4$ and the solvent was removed under reduced pressure. Amino-BP product was isolated by means of preparative TLC and was characterized with ^{1}H, ^{31}P and GC-MS analyses.

β-N$_3$BP
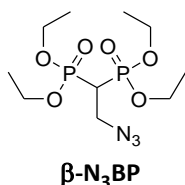
Tetraethyl 2-azidoethane-1,1-diyldiphosphonate
^{1}H NMR (300 MHz, CDCl$_3$) δ 4.29–4.13 (m, 8H), 3.82 (td, J = 16.0, 5.8 Hz, 2H), 2.58 (tt, J = 23.6, 5.8 Hz, 1H), 1.36 (t, J = 7.1 Hz, 12H) ppm.
^{31}P {1H}-NMR (122 MHz, CDCl$_3$) δ 18.88 (s, 2P) ppm.

PPHNH$_2$
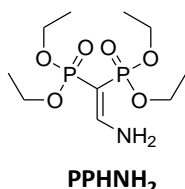
Tetraethyl 2-aminoethene-1,1-diyldiphosphonate
^{1}H NMR (300 MHz, CDCl$_3$) δ 5.87 (d, J = 22.4 Hz, broad, 2H), 4.62 (dd, J = 20.2, 13.2 Hz, 1H), 4.24–3.98 (m, 8H), 1.34 (dt, J = 12.7, 7.1 Hz, 12H) ppm.
^{31}P {1H}-NMR (122 MHz, CDCl$_3$) δ 20.53 (d, J = 87.0 Hz, 1P), 10.16 (d, J = 87.0 Hz, 1P) ppm.
GC-MS, (70 eV) m/z: 315 [M]$^+$, 271 [M -COOEt +H]$^+$, 178 [M -PO(OEt)$_2$]$^+$.

β-N$_3$BP-Me
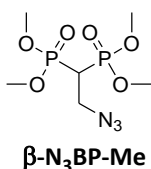
Tetramethyl 2-azidoethane-1,1-diyldiphosphonate
^{1}H NMR (300 MHz, CDCl$_3$) δ 3.88 (d, J = 2.7 Hz, 4H), 3.84 (d, J = 2.1 Hz, 4H), 3.83–3.77 (m, overlapped, 2H), 2.64 (tt, J = 23.1, 5.8 Hz, 1H) ppm.
^{31}P {1H}-NMR (122 MHz, CDCl$_3$) δ 21.38 (s, 2P) ppm.

VBPNH$_2$-Me
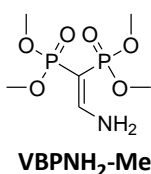
Tetramethyl 2-aminoethene-1,1-diyldiphosphonate
^{1}H NMR (300 MHz, CDCl$_3$) δ 4.32 (dd, J = 19.8, 13.9 Hz, 1H), 3.68 (d, J = 11.1 Hz, 6H), 3.55 (d, J = 11.3 Hz, 6H) ppm.
^{31}P {1H}-NMR (122 MHz, CDCl$_3$) δ 23.35 (d, J = 87.4 Hz, 1P), 12.40 (d, J = 87.4 Hz, 1P) ppm.
GC-MS, (70 eV) m/z: 259 [M]$^+$, 228 [M -OMe]$^+$, 150 [M -PO(OMe)$_2$]$^+$, 109 [M - NH$_2$CHCPO(OMe)$_2$]$^+$.

N$_3$PPH
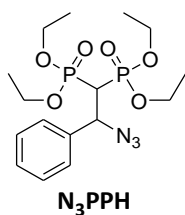
Tetraethyl 2-azido-2-phenylethane-1,1-diyldiphosphonate
Not isolated as pure compound

^{1}H NMR (300 MHz, CDCl$_3$) δ 7.76–7.71 (m, 2H), 7.46–7.34 (m, 3H), 5.30 (ddd, J= 23.0, 13.4, 3.7 Hz, 1H), 4.27–3.95 (m, 8H), 2.97 (td, J = 24.7, 3.7 Hz, 1H), 1.38 (t, J = 7.1 Hz, 6H), 1.14 (t, J = 7.1 Hz, 6H) ppm.
^{31}P {1H}-NMR (122 MHz, CDCl$_3$) δ 19.09 (s, 1P), 17.32 (s, 1P) ppm.

PPHNH₂
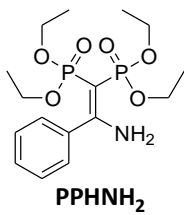
Tetraethyl 2-amino-2-phenylethene-1,1-diyldiphosphonate

^{1}H NMR (300 MHz, CDCl$_3$) δ 7.29–7.21 (m, 5H), 6.47 (d, J = 24.5 Hz, 2H), 4.07–3.93 (m, 4H), 3.92–3.79 (m, 4H), 1.22 (t, J = 7.1 Hz, 6H), 1.16 (t, J = 7.1 Hz, 6H) ppm.

^{31}P {1H}-NMR (122 MHz, CDCl$_3$) δ 19.76 (d, J = 90.0 Hz, 1P), 10.58 (d, J = 90.0 Hz, 1P) ppm.

GC-MS, (70 eV) m/z: 391 [M] [+], 362 [M -Et] [+], 346 [M -COOEt] [+], 254 [M -PO(OEt)$_2$] [+].

5.3.3 General procedure for catalytic addition of indoles to VBP

Catalytic tests in organic solvent

In a vial equipped with magnetic stirring bar 100 mg of VBP (0.33 mmol), 2 mL of anhydrous 1,2-dichloroethane was added followed by 12 mg of Cu(OTf)$_2$ (10 mol% with respect to VBP) and 1.5 equivalents of indole with respect to VBP. The vial was thermostatted at 70°C for 18h under vigorous stirring. Subsequently, the mixture was diluted with 5 mL of dichloromethane, the organic phase was extracted with a saturated aqueous solution of EDTA and washed with water. The product of the reaction was isolated by means of preparative TLC with 6:4 n-hexane:acetone eluent and was characterized with ^{1}H, ^{31}P and GC-MS analyses.

Catalytic tests in water

In a vial equipped with magnetic stirring bar 100 mg of VBP (0.3 mmol), 2 mL of distilled water, 100 mg of sodium dodecylsulfate (SDS) were added followed by 12 mg of Cu(OTf)$_2$ (10 mol% with respect to VBP) and 1.5 equivalents of indole with respect to VBP. The vial was thermostatted at 70°C for 18h under vigorous stirring. Subsequently, the mixture was diluted with 5 mL of ethyl acetate and the organic phase was extracted with a saturated aqueous solution of EDTA and washed with water. The product of the reaction was isolated by means of preparative TLC with 6:4 n-hexane:acetone eluent and was characterized with ^{1}H, ^{31}P and GC-MS analyses.

General procedure for the ester deprotection of the indolyl BP

The tetraethyl ester of the bisphosphonic acid (0.2 mmol) was introduced in a vial under anhydrous condition. To this 12 equivalents of bromotrimethylsilane (2.4 mmol) were added. The vial was stirred under inert atmosphere at rt for 18 h. The crude mixture was concentrated under reduced pressure, diluted with a 9:1 solution of methanol and water, stirred for 4 h at room temperature and dried. The free bisphosphonic acid was obtained in quantitative yield and was characterized by ^{1}H and ^{31}P NMR.

IND1
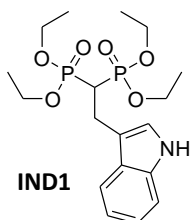
Tetraethyl 2-(1H-indol-3-yl)ethane-1,1-diyldiphosphonate
^{1}H NMR (300 MHz, CDCl$_3$): δ 1.19-1.31 (m, 12H), 2.78 (tt, J = 24.0, 6.3 Hz, 1H), 3.43 (td, J = 16.5, 6.3Hz, 2H), 3.99-4.28 (m, 8H), 7.07-7.22 (m, 3H), 7.35 (d, J = 8.10, 1H), 7.67 (d, J = 8.06, 1H) ppm.
^{31}P {1H}-NMR (122 MHz, CDCl$_3$): δ 22.14 (s, 2P) ppm.
GC-MS,(70 eV) m/z: 417 [M][+], 280 [M-PO(OCH$_2$CH$_3$)$_2$][+], 252[280-CH$_2$CH$_2$][+], 224 [252-CH$_2$CH$_2$][+], 143 [(C$_{10}$H$_9$N)][+], 130 [143-CH][+].
Elemental Analysis C$_{18}$H$_{29}$NO$_6$P$_2$: Calculated C, 51.80; H, 7.00; N, 3.36; Found: C, 51.83; H, 7.02; N, 3.35; %

IND1-OH
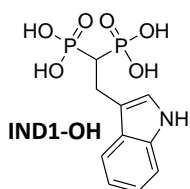
2-(1H-indol-3-yl)ethane-1,1-diyldiphosphonic acid
^{1}HNMR (300 MHz, D$_2$O): δ 2.62 (tt, *J* = 23.4, 6.3 Hz, 1H), 3.27 (dt, *J* =16.0, 6.3 Hz, 2H), 6.98-7.68(m, 5H) ppm.
^{31}P {1H}-NMR (122 MHz, D$_2$O): δ 20.47 (s, 2P) ppm.

IND2
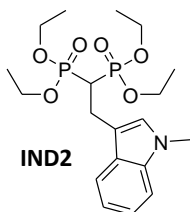
Tetraethyl 2-(1-methyl-1H-indol-3-yl)ethane-1,1-diyldiphosphonate
^{1}HNMR (300 MHz, CDCl$_3$): δ1.22-1.31 (m, 12H), 2.74 (tt, *J* = 24.0, 5.9 Hz, 1H), 3.41 (td, *J* = 16.5, 5.9Hz, 2H), 3.73 (s, 3H), 4.00-4.75 (m, 8H), 7.06 (m, 2H), 7.21 (t, *J*=8.10, 1H), 7.31 (d, *J*= 8.2 Hz, 1H), 7.66 (d, *J*= 8.2, 1H) ppm.
^{31}P {1H}-NMR (122 MHz, CDCl$_3$): δ 22.22 (s, 2P) ppm.
Elemental Analysis C$_{19}$H$_{31}$NO$_6$P$_2$: Calculated C, 52.90; H, 7.24; N, 3.25; Found: C, 52.87; H, 7.26; N, 3.22; %

IND2-OH
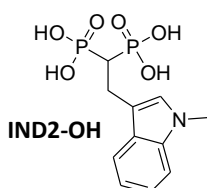
2-(1-methyl-1H-indol-3-yl)ethane-1,1-diyldiphosphonic acid
^{1}H NMR (300 MHz, D$_2$O): δ 2.29 (s, 3H); 2.57 (tt, *J* = 22.7 Hz, 6.1 Hz, 1H); 3.24 (dt, *J*= 16.0 Hz, 6.1 Hz,2H); 3.54 (s, 3H); 6.98 – 7.13 (m, 2H); 7.30 (d, *J*= 8.1 Hz, 1H); 7.54 (d, *J* = 7.8 Hz, 1H) ppm.
^{31}P {1H}-NMR (122 MHz, D$_2$O): δ 20.4 (s, 2P) ppm.

IND3
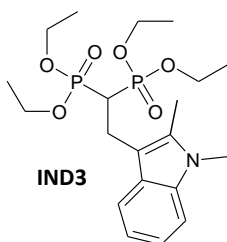
Tetraethyl 2-(1,2-dimethyl-1H-indol-3-yl)ethane-1,1-diyldiphosphonate
^{1}HNMR (300 MHz, CDCl$_3$): δ 1.14-1.30 (m, 12H), 2.40 (s, 3H), 2.79 (tt, *J*= 23.7, 6.4 Hz, 1H), 3.40 (td, *J*= 15.6, 6.4 Hz, 2H), 3,64 (s, 3H), 3.93-4.19 (m, 8H), 7.05 (t, *J*=6.9, 1H), 7.14 (t, *J*=6.9, 1H), 7.23 (d, *J* = 8.1,1H), 7.57 (d, *J* = 7.8, 1H) ppm.
^{31}P {1H}-NMR (122 MHz, CDCl$_3$): δ 22.20 (s, 2P) ppm.
GC-MS, (70 eV) m/z: 445 [M] [+], 308 [M-PO(OCH$_2$CH$_3$)$_2$] [+], 158 [308-CHPO(OCH$_2$CH$_3$)] [+].
Elemental Analysis C$_{20}$H$_{33}$NO$_6$P$_2$: Calculated C, 53.93; H, 7.47; N, 3.14; Found: C, 53.90; H, 7.45; N, 3.11; %

IND4
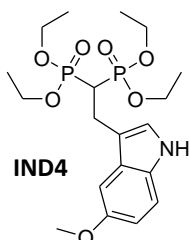
Tetraethyl 2-(5-methoxy-1H-indol-3-yl)ethane-1,1-diyldiphosphonate
^{1}H NMR (300 MHz, CDCl$_3$): δ 1.23-1.40 (m, 12H), 2.73 (tt, *J*=23.0, 6.0 Hz, 1H), 3.42 (td, *J* = 16.2, 6.0 Hz,2H), 3.93 (s, 3H), 4.05-4.30 (m, 8H), 7.20-7.31 (m, 4H) ppm.
^{31}P {1H}-NMR (122 MHz, CDCl$_3$): δ 22.10 (s, 2P) ppm.
Elemental Analysis C$_{19}$H$_{31}$NO$_7$P$_2$: Calculated C, 51.01; H, 6.98; N, 3.13; Found: C, 51.03; H, 6.95; N, 3.16; %

IND5
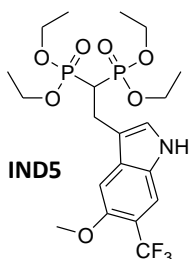
Tetraethyl 2-(5-methoxy-6-(trifluoromethyl)-1H-indol-3-yl)ethane-1,1-diyldiphosphonate
^{1}H NMR (300 MHz, CDCl3): δ 1.21-1.35 (m, 12H), 2.74 (tt, *J* = 23.8, 6.0 Hz, 1 H), 3.42 (td, *J* = 15.0, 6.0Hz, 2H), 3.95 (s, 3 H), 4.04 - 4.2 (m, 8H); 7.28 (s, 1H), 7.34 (s, 1H), 7.58 (s, 1H) ppm.
^{31}P {1H}-NMR (122 MHz, CDCl$_3$): δ 22.10 (s, 2P) ppm.
GC-MS, (70 eV) m/z: 515 [M-H2] [+], 378 [M-PO(OEt)$_2$] [+], 350 [378-(CH$_2$CH$_2$)] [+], 322 [350-(CH$_2$CH$_2$)] [+].
Elemental Analysis C$_{20}$H$_{30}$F$_3$NO$_7$P$_2$: Calculated C, 46.61; H, 5.87; N, 2.72; Found: C, 46.58; H, 5.85; N, 2.72; %
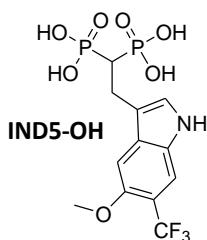
2-(5-methoxy-6-(trifluoromethyl)-1H-indol-3-yl)ethane-1,1-diyldiphosphonic acid
^{1}H NMR (300 MHz, D$_2$O): δ 2.81 (tt, J = 23.5, 5.9 Hz, 1H), 3.72 (td, J = 16.7, 5.9 Hz, 2H), 3.87 (s, 3H),7.33-7.39 (m, 2H), 7.67 (s, 1H) ppm.
^{31}P {1H}-NMR (122 MHz, D$_2$O): δ 20.1 (s, 2P) ppm.
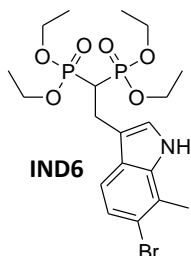
Tetraethyl 2-(6-bromo-7-methyl-1H-indol-3-yl)ethane-1,1-diyldiphosphonate
^{1}HNMR (300 MHz, CDCl$_3$): δ 1.24 − 1.31 (m, 12 H), 2.50 (s, 3H), 2.72 (tt, J = 23.8, 6.1 Hz, 1H), 3.39 (td,J = 15.0, 6.1 Hz, 2H), 4.05 − 4.21 (m, 8 H), 7.15 (s, 1H), 7.28 (d, J=8.5 Hz, 1H), 7.38 (d, J = 8.5 Hz, 1H) ppm.
^{31}P {1H}–NMR (122 MHz, CDCl$_3$): δ 21.9 (s, 2P) ppm.
GC-MS, (70 eV) m/z: 511 [M] [+], 372 [511-PHOH(OEt)$_2$] [+], 237 [372-PO(OEt)$_2$] [+], 224 [237-CH$_3$] [+].
Elemental Analysis C$_{19}$H$_{30}$BrNO$_6$P$_2$: Calculated C, 44.72; H, 5.93; N, 2.74; Found: C, 44.75; H, 5.90; N, 2.75; %
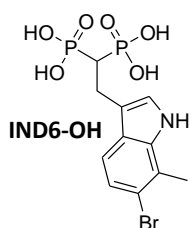
2-(6-bromo-7-methyl-1H-indol-3-yl)ethane-1,1-diyldiphosphonic acid
^{1}HNMR (300 MHz, D$_2$O): δ 1.96 (s, 3H), 2.67 (tt, J = 21.0, 6.0 Hz, 1H), 3.70 (td, J = 5.0, 6.0 Hz, 2H),7.18 (s, 1H), 7.22 (d, J = 8.7 Hz, 1H), 7.35 (d, J = 8.5 Hz, 1H) ppm.
^{31}P {1H}-NMR (122 MHz, D$_2$O): δ 15.9 (s, 2P) ppm.
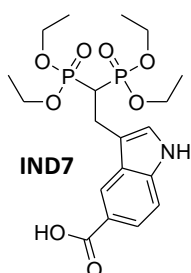
3-(2,2-bis(diethoxyphosphoryl)ethyl)-1H-indole-5-carboxylic acid
^{1}HNMR (300 MHz, CDCl$_3$): δ 1.20-1.28 (m, 12H), 2.79 (tt, J = 24.61, 6.1 Hz, 1H), 3.45 (td, J = 16.2, 6.1Hz, 2H), 4.02-4.26 (m, 8H), 7.20-7.32 (m, 2H), 7.34 (d, J=7.8, 1H),7.91 (d, J=7.8, 1H) ppm.
^{31}P {1H}-NMR (122 MHz, CDCl$_3$): δ 21.87 (s, 2P) ppm.
Elemental Analysis C$_{19}$H$_{29}$NO$_8$P$_2$: Calculated C, 49.46; H, 6.34; N, 3.04; Found: C, 49.45; H, 6.30; N, 3.01; %
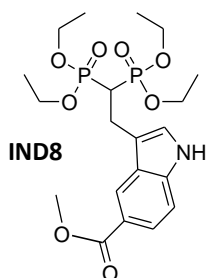
Methyl 3-(2,2-bis(diethoxyphosphoryl)ethyl)-1H-indole-5-carboxylate
^{1}HNMR (300 MHz, CDCl$_3$): δ 1.21-1.40 (m, 12H), 2.78 (tt, J = 23.4, 6.3 Hz, 1H), 3.43 (td, J = 16.2, 6.3Hz, 2H), 3.9 (s, 3H), 4.04-4.27 (m, 8H), 7.22 (m, 1H), 7.42 (d, J = 8.6 Hz, 1H), 7.90 (d, J = 8.6 Hz, 1H), 8.42 (s, 1H)ppm.
^{31}P {1H}-NMR (122 MHz, CDCl$_3$): δ 21.86 (s, 2P) ppm.
GC-MS, (70 eV) m/z: 475 [M-H$_2$] [+], 338 [M-PO(OEt)$_2$] [+], 306 [338-CH$_3$OH] [+], 278 [306-CO] [+], 250 [278-CH$_2$CH$_2$] [+].
Elemental Analysis C$_{20}$H$_{31}$NO$_8$P$_2$: Calculated C, 50.53; H, 6.57; N, 2.95; Found: C, 50.55; H, 6.60; N, 2.93; %
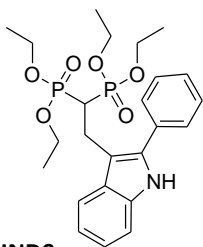
IND9

Tetraethyl 2-(2-phenyl-1H-indol-3-yl)ethane-1,1-diyldiphosphonate

^{1}HNMR (300 MHz, CDCl$_3$): δ 1.01-1.26 (m, 12H), 2.92 (tt, J=23.4, 6.5 Hz, 1H), 3.66 (td, J = 16.2, 6.5 Hz,2H), 4.80-4.04 (m, 8H), 7.11-7.76 (m, 9H) ppm.

^{31}P {1H}-NMR (122 MHz, CDCl$_3$): δ 21.74 (s, 2P) ppm.

Elemental Analysis C$_{24}$H$_{33}$NO$_6$P$_2$: Calculated C, 58.41; H, 6.74; N, 2.84; Found: C, 58.38; H, 6.71; N, 2.82; %
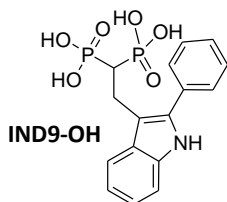
IND9-OH

2-(2-phenyl-1H-indol-3-yl)ethane-1,1-diyldiphosphonic acid

^{1}HNMR (300 MHz, D$_2$O): δ 2.63 (tt, J = 23.0, 6.2 Hz, 1H), 3.47 (dt, J = 15.6, 6.2 Hz, 2H), 7.06 - 7.13 (m,2H), 7.28 – 7.41 (m, 3H), 7.44 (d, J = 7.4 Hz, 2H), 7.57 (d, J = 7.5 Hz, 2H) ppm.

^{31}P {1H}-NMR (122 MHz, D$_2$O): δ 20.3 (s, 2P) ppm.
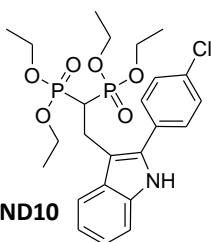
IND10

Tetraethyl 2-(2-(4-chlorophenyl)-1H-indol-3-yl)ethane-1,1-diyldiphosphonate

^{1}H NMR (300 MHz, CDCl$_3$): δ 1.10 –1.19 (m, 12 H), 2.89 (tt, J = 23.6, 6.8 Hz, 1H), 3.61 (td, J = 15.5, 6.8Hz, 2H), 3.88– 4.05(m, 8H), 7.11 – 7.22 (m, 2H), 7.35 (d, J = 7.7 Hz, 1H), 7.46 – 7.40 (m, 2H), 7.63 – 7.56(m, 2H), 7.70 (d, J = 7.7 Hz, 1H) ppm.

^{31}P {1H}-NMR (122 MHz, CDCl$_3$): δ 21.6 (s, 2P) ppm.

Elemental Analysis C$_{24}$H$_{32}$ClNO$_6$P$_2$: Calculated C, 54.60; H, 6.11; N, 2.65; Found: C, 54.64; H, 6.11; N, 2.64; %
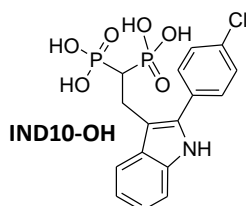
IND10-OH

2-(2-(4-chlorophenyl)-1H-indol-3-yl)ethane-1,1-diyldiphosphonic acid

^{1}H NMR (300 MHz, D$_2$O): δ 2.68 (tt, J = 21.0, 6.1 Hz, 1H), 3.71 (td, J = 16.0, 6.1 Hz, 2H), 7.09 (d, J = 6.9Hz, 1H), 7.16 (d, J = 7.0 Hz, 1H), 7.40 (d, J = 7.0 Hz, 1H), 7.45 (d, J = 8.5 Hz, 2H), 7.58 (d, J = 8.5 Hz, 2H),7.68 (d, J = 7.9 Hz, 1H) ppm.

^{31}P {1H}-NMR (122 MHz, D$_2$O): 20.2 (s, 2P) ppm.

5.3.4 General procedure for catalytic addition of indoles to substituted VBP

Catalytic tests in organic solvent

In a vial equipped with magnetic stirring bar 0.3 mmol of substituted VBP, 2 mL of anhydrous 1,2-dichloroethane was added followed by 12 mg of Cu(OTf)$_2$ (10 mol% with respect to BP) and 1.5 equivalents of indole with respect to BP. The vial was thermostatted at 70°C for 18h under vigorous stirring. Subsequently, the mixture was diluted with 5 mL of dichloromethane, the organic phase was extracted with a saturated aqueous solution of EDTA and washed with water. The product of the reaction was isolated by means of preparative TLC (conditions reported for each compounds) and characterized with ^{1}H, ^{31}P ^{13}C and GC-MS analyses.
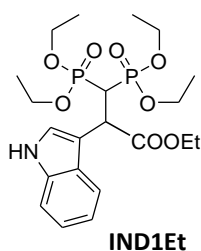
IND1Et

Ethyl 3,3-bis(diethoxyphosphoryl)-2-(1H-indol-3-yl)propanoate
^{1}H NMR (400 MHz, CDCl$_3$) δ 8.68 (s, 1H), 7.75 (d, J = 7.6 Hz, 1H), 7.33 (d, J = 7.8 Hz, 1H), 7.28 (s, 1H), 7.17–7.05 (m, 2H), 4.51 (ddd, J = 11.6, 10.0, 7.8 Hz, 1H), 4.28–4.07 (m, 6H), 3.96–3.86 (m, 1H), 3.84–3.74 (m, 2H), 3.72–3.64 (m, 1H), 3.48–3.37 (m, 1H), 1.32 (t, J = 7.0 Hz, 6H), 1.16 (t, J = 7.1 Hz, 3H), 1.05 (t, J = 7.0 Hz, 3H), 0.85 (t, J = 7.0 Hz, 3H) ppm.
^{31}P {^{1}H}-NMR (121.5 MHz, CDCl$_3$): δ 20.70 (d, J = 2.4 Hz, 1P), 19.42 (d, J = 2.4 Hz, 1P) ppm.
^{13}C {^{1}H}-NMR (75 MHz, CDCl$_3$): δ 172.22 (dd, J = 16.8, 3.2 Hz), 136.32 (s), 126.92 (s), 126.07 (s), 121.48 (s), 119.93 (s), 119.25 (s), 111.43 (s), 108.84 (dd, J = 14.3, 4.9 Hz), 63.09 (d, J = 6.6 Hz), 62.73 (d, J = 6.7 Hz), 62.60 (d, J = 7.0 Hz), 62.02 (d, J = 6.9 Hz), 61.34 (s), 41.41 (s), 40.11 (dd, J = 137.3, 127.9 Hz), 16.37 (t, J = 5.6 Hz), 16.07 (d, J = 6.5 Hz), 15.67 (d, J = 6.7 Hz), 14.01 (s) ppm.
GC-MS, (70 eV) m/z: 489 [M]$^+$, 444 [M-OEt]$^+$, 306 [M-PO(OEt)$_2$–Oet-H]$^+$, 278 [M-PO(OEt)$_2$–COOEt-H]$^+$.
Eluition condition: Ethyl Acetate/Acetone 8/2
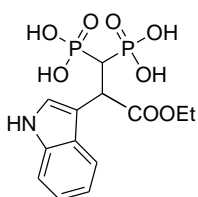
IND1Et-OH

3-ethoxy-2-(1H-indol-3-yl)-3-oxopropane-1,1-diyldiphosphonic acid
^{1}H NMR (300 MHz, D$_2$O): δ 7.73 (d, J = 7.8 Hz, 1H), 7.40 (d, J = 8.0 Hz, 1H), 7.33 (s, 1H), 7.11 (dt, J = 14.8, 7.0 Hz, 2H), 4.37 (broad signal, 1H), 4.11 − 3.92 (m, 2H), 3.46 (td, J = 21.2, 10.4 Hz, 1H), 1.07 (t, J = 7.1 Hz, 3H) ppm.
^{31}P {^{1}H}-NMR (122 MHz, D$_2$O): δ 17.90 (s. Broad signal, 2P) ppm.
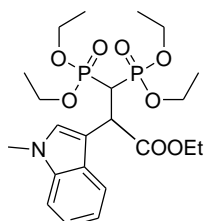
IND2Et

Ethyl 3,3-bis(diethoxyphosphoryl)-2-(1-methyl-1H-indol-3-yl)propanoate
^{1}H NMR (400 MHz, CDCl$_3$) δ 7.74 (d, J = 8.0 Hz, 1H), 7.24 (s, 1H), 7.20–7.15 (m, 1H), 7.12–7.07 (m, 1H), 4.48 (ddd, J = 11.5, 9.9, 7.9 Hz, 1H), 4.28–4.05 (m, 7H), 3.93–3.82 (m, 1H), 3.75 (s, 3H), 3.82–3.61 (m, 3H), 3.49–3.38 (m, 1H), 1.31 (td, J = 7.1, 2.9 Hz, 6H), 1.21–1.16 (m, 3H), 1.03 (dd, J = 8.8, 5.3 Hz, 3H), 0.91–0.83 (m, 3H) ppm.
^{31}P {^{1}H}-NMR (162 MHz, CDCl$_3$) δ 22.03 (d, J = 2.0 Hz, 1P), 20.80 (d, J = 2.1 Hz, 1P) ppm.
^{13}C {^{1}H}-NMR (101 MHz, CDCl$_3$) δ 172.39 (dd, J = 16.2, 3.7 Hz), 136.85 (s), 129.99 (s), 127.72 (s), 121.54 (s), 120.33 (s), 119.27 (s), 109.13 (s), 108.42 (dd, J = 14.0, 4.8 Hz), 63.13 (d, J = 6.6 Hz), 62.69 (d, J = 6.6 Hz), 62.39 (d, J = 6.9 Hz),

61.94 (d, J = 6.7 Hz), 61.45 (s), 41.10 (t, J = 3.0 Hz), 40.54 (dd, J = 136.7, 127.6 Hz), 32.94 (s), 29.84 (s), 16.44 (t, J = 6.2 Hz), 16.10 (d, J = 6.6 Hz), 15.88 (d, J = 6.6 Hz), 14.13 (s) ppm.

GC-MS, (70 eV) m/z: 503 [M] [+], 458 [M-OEt-H] [+], 430 [M-COOEt] [+], 366 [M-PO(OEt)$_2$] [+], 321 [M-PO(OEt)$_2$–Oet-H] [+], 293 [M-PO(OEt)$_2$-COOEt-H] [+].

Eluition condition: Ethyl Acetate/Acetone 1/1

IND3Et
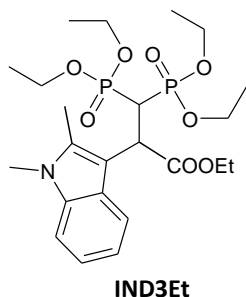
Ethyl 3,3-bis(diethoxyphosphoryl)-2-(1,2-dimethyl-1H-indol-3-yl)propanoate

^{1}H NMR (400 MHz, CDCl$_3$) δ 7.71 (d, J = 7.8 Hz, 1H), 7.19 (d, J = 8.0 Hz, 1H), 7.09 (td, J = 78.1, 1.1, 1H), 7.03 (td, J = 78.1, 1.1, 1H), 4.41 (td, J = 11.6, 2.6, 1H), 4.33–4.19 (m, 4H), 4.17–4.08 (m, 1H), 4.05–3.96 (m, 1H), 3.94–3.71 (m, 3H), 3.64 (s, 3H), 3.50–3.38 (m, 1H), 3.02 (d, J = 5.9 Hz, 1H), 2.48 (s, 3H), 1.38 (td, J = 7.1, 3.2 Hz, 6H), 1.14 (t, J = 7.1 Hz, 3H), 0.99 (t, J = 7.1 Hz, 3H), 0.62 (t, J = 6.9 Hz, 3H) ppm.

^{31}P {^{1}H}-NMR (122 MHz, CDCl$_3$): δ 22.66 (d, J = 2.0 Hz, 1P), 20.97 (d, J = 2.0 Hz, 1P) ppm.

^{13}C {^{1}H}-NMR (101 MHz, CDCl$_3$) δ 171.87 (d, J = 19.8 Hz), 136.81 (s), 136.47 (s), 127.26 (s), 120.53 (s), 120.16 (s), 119.24 (s), 108.48 (s), 104.89 (dd, J = 16.8, 4.4 Hz), 63.25 (d, J = 6.6 Hz), 62.68 (d, J = 6.6 Hz), 62.41 (d, J = 6.9 Hz), 61.66 (d, J = 7.0 Hz), 61.25 (s), 41.27 (s), 39.04 (dd, J = 138.6, 125.6 Hz), 29.81 (s), 16.54 (dd, J = 9.5, 6.1 Hz), 16.06 (d, J = 6.5 Hz), 15.61 (d, J = 6.6 Hz), 14.14 (s), 10.99 (s) ppm.

GC-MS, (70 eV) m/z: 517 [M][+], 472 [M-OEt][+], 444 [M-COOEt][+], 380 [M-PO(OEt)$_2$][+].

Eluition condition: Ethyl Acetate/Acetone 1/1

IND6Et
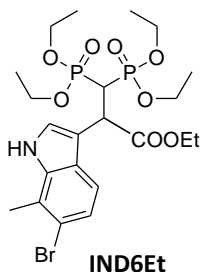
Ethyl 2-(6-bromo-7-methyl-1H-indol-3-yl)-3,3-bis(diethoxyphosphoryl) propanoate

^{1}H NMR (300 MHz, CDCl$_3$) δ 8.79 (s, 1H), 7.46 (d, J = 8.6 Hz, 1H), 7.32–7.16 (m, 2H), 4.45 (ddd, J = 11.7, 9.8, 8.2 Hz, 1H), 4.28–4.08 (m, 6H), 3.98–3.48 (m, 5H), 2.50 (s, 3H), 1.32 (t, J = 6.9 Hz, 6H), 1.16 (t, J = 7.1 Hz, 3H), 1.09 (t, J = 7.1 Hz, 3H), 0.91 (t, J = 7.1 Hz, 3H) ppm.

^{31}P {^{1}H}-NMR (162 MHz, CDCl$_3$) δ 21.81 (d, J = 2.7 Hz, 1P), 20.56 (d, J = 2.7 Hz, 1P) ppm.

^{13}C {^{1}H}-NMR (75 MHz, CDCl$_3$) δ 172.37 (dd, J = 17.3, 5.8 Hz), 134.70 (s), 128.55 (s), 127.42 (s), 125.73 (s), 122.50 (s), 119.98 (s), 112.55 (s), 109.98 (dd, J = 14.6, 3.5 Hz), 63.44 (d, J = 6.6 Hz), 63.12 (d, J = 6.6 Hz), 62.89 (d, J = 6.9 Hz), 62.48 (d, J = 6.7 Hz), 61.90 (s), 41.46 – 41.29 (m), 40.58 (dd, J = 136.7, 128.7 Hz), 30.13 (s), 16.73 (t, J = 6.6 Hz), 16.41 (d, J = 6.6 Hz), 16.19 (d, J = 6.7 Hz), 14.41 (s) ppm.

GC-MS, (70 eV) m/z: 535 [M-OEt-H] [+], 444 [M-PO(OEt)$_2$] [+], 400 [M-PO(OEt)$_2$-OEt][+], 372 [M-PO(OEt)$_2$-COOEt] [+].

Eluition condition: Ethyl Acetate/Acetone 1/1
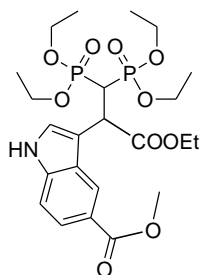
Methyl 3-(1,1-bis(diethoxyphosphoryl)-3-ethoxy-3-oxopropan-2-yl)-1H-indole-5-carboxylate

IND8Et

^{1}H NMR (400 MHz, CDCl$_3$) δ 8.91 (s, 1H), 8.52–8.50 (m, 1H), 7.87 (dd, *J* = 8.6, 1.6 Hz, 1H), 7.38–7.32 (m, 2H), 4.53 (dt, *J* = 11.6, 9.5 Hz, 1H), 4.26–4.09 (m, 6H), 3.93 (s, 3H), 3.96–3.88 (m, 1H), 3.84–3.73 (m, 3H), 3.69–3.60 (m, 1H), 1.35 (t, *J* = 7.1 Hz, 3H), 1.28 (t, *J* = 7.1 Hz, 3H), 1.19 (t, *J* = 7.1 Hz, 3H), 1.05 (t, *J* = 7.1 Hz, 3H), 0.94 (t, *J* = 7.1 Hz, 3H) ppm.

^{31}P {^{1}H}-NMR (122 MHz, CDCl$_3$) δ 20.19 (d, *J* = 2.0 Hz, 1P), 19.22 (d, *J* = 2.0 Hz, 1P) ppm.

^{13}C {^{1}H}-NMR (75 MHz, CDCl$_3$) δ 171.00 (dd, *J* = 14.6, 5.1 Hz), 167.31 (s), 137.71 (s), 126.10 (s), 126.05 (s), 122.49 (s), 122.11 (s), 121.01 (s), 110.81 (dd, *J* = 12.7, 4.9 Hz), 110.00 (s), 62.15 (d, *J* = 6.6 Hz), 61.85 (d, *J* = 6.6 Hz), 61.59 (d, *J* = 6.8 Hz), 61.30 (d, *J* = 6.6 Hz), 60.60 (s), 50.87 (s), 40.09 (t, *J* = 3.3 Hz), 39.85 (dd, *J* = 136.2, 129.6 Hz), 28.85 (s), 15.48 (d, *J* = 6.2 Hz), 15.35 (d, *J* = 6.1 Hz), 15.06 (dd, *J* = 8.4, 6.5 Hz), 13.10 (s) ppm.

GC-MS, (70 eV) m/z: 547 [M] $^+$, 473 [M-COOEt-H] $^+$, 410 [M-PO(OEt)$_2$] $^+$.

Eluition condition: Ethyl Acetate/Acetone 1/1
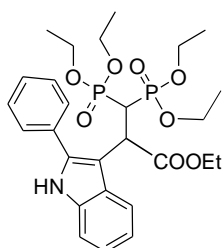
Ethyl 3,3-bis(diethoxyphosphoryl)-2-(2-phenyl-1H-indol-3-yl)propanoate

IND9Et

^{1}H NMR (300 MHz, CDCl$_3$) δ 8.12 (s, 1H), 7.96–7.77 (m, 3H), 7.50 (t, *J* = 7.4 Hz, 2H), 7.45–7.28 (m, 2H), 7.21–7.04 (m, 2H), 4.62 (ddd, *J* = 12.4, 10.0, 2.7 Hz, 1H), 4.26–4.06 (m, 6H), 3.95 (td, *J* = 22.5, 12.0 Hz, 1H), 3.79–3.64 (m, 1H), 3.63–3.45 (m, 2H), 3.16–3.02 (m, 1H), 1.32 (dt, *J* = 20.5, 7.1 Hz, 6H), 1.16 (t, *J* = 7.1 Hz, 3H), 0.81 (t, *J* = 7.0 Hz, 3H), 0.60 (t, *J* = 7.1 Hz, 3H) ppm.

^{31}P {^{1}H}-NMR (122 MHz) δ 21.13 (d, *J* = 2.8 Hz, 1P), 19.38 (d, *J* = 2.8 Hz, 1P) ppm.

^{13}C {^{1}H}-NMR (75 MHz, CDCl$_3$) δ 171.70 (d, *J* = 18.0 Hz), 137.86 (s), 135.93 (s), 132.83 (s), 129.29 (s), 128.99 (s), 128.32 (s), 122.13 (d, *J* = 9.0 Hz), 122.02 (s), 120.04 (s), 110.75 (s), 62.58 (dd, *J* = 77.9, 37.9 Hz), 61.33 (s), 41.19 (s), 29.83 (s), 16.48 (s), 15.72 (s), 14.10 (s) ppm.

GC-MS, (70 eV) m/z: 519 [M-OEt-H] $^+$, 474 [M-(OEt)$_2$] $^+$, 428 [M-PO(OEt)$_2$] $^+$.

Eluition condition: Ethyl Acetate/Acetone 1/1
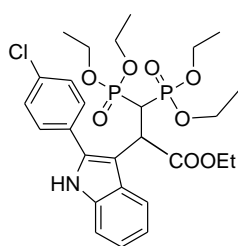
Ethyl 2-(2-(4-chlorophenyl)-1H-indol-3-yl)-3,3-bis(diethoxyphosphoryl)propanoate

IND10Et

^{1}H NMR (300 MHz, CDCl$_3$) δ 8.07 (s, 1H), 7.87 (d, *J* = 7.7 Hz, 1H), 7.82 (d, *J* = 8.4 Hz, 2H), 7.47 (d, *J* = 8.3 Hz, 2H), 7.32 (d, *J* = 7.9 Hz, 1H), 7.14 (dt, *J* = 15.1, 7.0 Hz, 2H), 4.58–4.48 (m, 1H), 4.25–4.05 (m, 4H), 3.95 (dd, *J* = 22.5, 10.5 Hz, 2H), 3.87–3.74 (m, 1H), 3.72–3.57 (m, 2H), 3.53–3.43 (m, 1H), 3.07–2.96 (m, 1H), 1.34 (dt, *J* = 16.9, 7.1 Hz, 6H), 1.14 (t, *J* = 7.1 Hz, 3H), 0.90 (t, *J* = 7.1 Hz, 3H), 0.59 (t, *J* = 7.1 Hz, 3H) ppm.

^{31}P {^{1}H}-NMR (162 MHz, CDCl$_3$) δ 22.28 (d, *J* = 2.5 Hz, 1P), 20.74 (d, *J* = 2.5 Hz, 1P) ppm.

^{13}C {^{1}H}-NMR (75 MHz, CDCl$_3$) δ 136.89 (s), 136.25 (s), 134.76 (s), 131.52 (s), 130.91 (s), 129.48 (s), 128.47 (s), 122.77 (s), 122.38 (s), 120.50 (s), 111.07 (s), 63.70 (d, *J* = 6.4 Hz), 63.05 (d, *J* = 6.7 Hz), 62.70 (d, *J* = 7.1 Hz), 62.03 (d, *J* = 6.9 Hz), 61.68 (s), 41.49 (s), 32.36 (s), 30.12 (s), 29.79 (s), 23.12 (s), 16.77 (t, *J* = 5.7 Hz), 16.20 (d, *J* = 6.7 Hz), 15.88 (d, *J* = 6.2 Hz), 14.37 (s) ppm.

GC-MS, (70 eV) m/z: 526 [M-COOEt]$^+$, 462 [M-PO(OEt)$_2$]$^+$, 418 [M-PO(OEt)$_2$-OEt]$^+$.

Eluition condition: Ethyl Acetate/Acetone 1/1

IND11Et
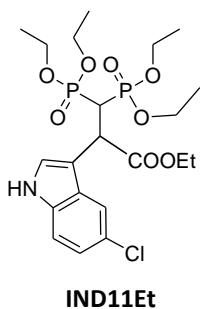
Ethyl 2-(5-chloro-1H-indol-3-yl)-3,3-bis(diethoxyphosphoryl)propanoate

^{1}H NMR (400 MHz, CDCl$_3$) δ 8.47 (s, 1H), 7.73 (d, J = 2.0 Hz, 1H), 7.33 (d, J = 2.6 Hz, 1H), 7.24 (d, J = 8.9 Hz, 1H), 7.11 (dd, J = 8.6, 2.0 Hz, 1H), 4.49–4.40 (m, 1H), 4.27–4.09 (m, 6H), 3.97–3.86 (m, 1H), 3.84–3.56 (m, 4H), 1.36–1.28 (m, 6H), 1.19 (t, J = 7.1 Hz, 3H), 1.06 (t, J = 7.1 Hz, 3H), 0.95 (t, J = 7.1 Hz, 3H) ppm.

^{31}P {^{1}H}-NMR (162 MHz, CDCl$_3$) δ 21.70 (d, J = 2.2 Hz, 1P), 20.51 (d, J = 2.2 Hz, 1P) ppm.

^{13}C {^{1}H}-NMR (75 MHz, CDCl$_3$) δ 172.09 (dd, J = 17.3, 5.8 Hz), 134.43 (s), 128.28 (s), 127.14 (s), 125.45 (s), 122.23 (s), 119.71 (s), 112.28 (s), 63.17 (d, J = 6.6 Hz), 62.84 (d, J = 6.6 Hz), 62.61 (d, J = 6.9 Hz), 62.21 (d, J = 6.7 Hz), 61.62 (s), 41.23 − 40.96 (m), 40.30 (dd, J = 136.7, 128.7 Hz), 29.85 (s), 16.45 (t, J = 6.6 Hz), 16.13 (d, J = 6.6 Hz), 15.92 (d, J = 6.7 Hz), 14.13 (s) ppm.

GC-MS, (70 eV) m/z: 523 [M] $^+$, 477 [M-OEt-H] $^+$, 449 [M-COOEt-H] $^+$, 386 [M-PO(OEt)$_2$] $^+$, 342 [M-PO(OEt)$_2$-OEt] $^+$, 314 [M-PO(OEt)$_2$-COOEt)] $^+$.

Eluition condition: Ethyl Acetate/Acetone 1/1

5.3.5 *General procedure for syntheses of BP containing pirrolydine*

In a round bottom flask equipped with condenser and magnetic stirring bar, 0.65 mmol of BP precursor and 25 mL of toluene were added followed by 2.5 mmol of amino acid (4 Eq.) and 6.5 mmol of aldehyde (10 Eq.). The mixture was refluxed for 18 h under vigorous stirring. Solvent was removed under reduced pressure and the product of the reaction was isolated by means of preparative TLC with 1:1 acetone/ethyl acetate as eluent and characterized with ^{1}H, ^{31}P ^{13}C and GC-MS analyses.

GLY1
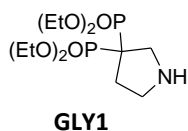
Tetraethyl pyrrolidine-3,3-diyldiphosphonate
^{1}H NMR (300 MHz, CDCl$_3$) δ 4.26–4.11 (m, 8H), 3.37 (t, *J* = 15.6 Hz, 2H), 2.97 (t, *J* = 6.6 Hz, 2H), 2.37-2.13 (m, 2H), 1.38–1.28 (m, 12H) ppm.
^{31}P {^{1}H}-NMR (122 MHz, CDCl$_3$) δ 25.24 (s, 1P) ppm.
GC-MS (70 eV), m/z: 343 [M]$^+$, 298 [M -OEt]$^+$, 206 [M -PO(OEt)$_2$]$^+$.

GLY2
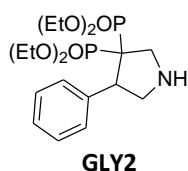
Tetraethyl 4-phenylpyrrolidine-3,3-diyldiphosphonate
^{1}H NMR (300 MHz, CDCl$_3$) δ 7.57 (d, *J* = 7.1 Hz, 2H), 7.38–7.10 (m, 3H), 4.40–4.15 (m, 4H), 4.00–3.78 (m, 3H), 3.78–3.60 (m, 3H), 3.55–3.44 (m, 1H), 3.44–3.25 (m, 2H), 1.38 (td, *J* = 7.1, 1.7 Hz, 6H), 1.17 (t, *J* = 7.1 Hz, 3H), 1.01 (t, *J* = 7.1 Hz, 3H) ppm.
^{31}P {^{1}H}-NMR (122 MHz, CDCl$_3$) δ 26.03 (d, *J* = 11.4 Hz, 1P), 22.16 (d, *J* = 11.4 Hz, 1P) ppm.
GC-MS (70 eV), m/z:419 [M]$^+$, 390 [M -Et]$^+$, 374 [M -OEt]$^+$, 282 [M -PO(OEt)$_2$]$^+$.

GLY3
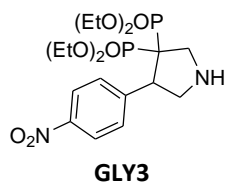
Tetraethyl 4-(4-nitrophenyl)pyrrolidine-3,3-diyldiphosphonate
^{1}H NMR (300 MHz, CDCl$_3$) δ 8.11 (d, *J* = 8.9 Hz, 2H), 7.78 (d, *J* = 8.8 Hz, 2H), 4.33–4.15 (m, 4H), 3.99–3.84 (m, 3H), 3.82–3.58 (m, 3H), 3.51–3.33 (m, 2H), 2.87 (ddd, *J* = 18.7, 12.2, 5.7 Hz, 1H), 1.38 (td, *J* = 7.1, 3.2 Hz, 6H), 1.15 (t, *J* = 7.1 Hz, 3H), 1.07 (t, *J* = 7.1 Hz, 3H) ppm.
^{31}P {^{1}H}-NMR (122 MHz, CDCl$_3$) δ 23.77 (d, *J* = 11.5 Hz, 1P), 21.29 (d, *J* = 11.5 Hz, 1P) ppm.
GC-MS (70 eV), m/z:464 [M]$^+$, 435 [M -Et]$^+$, 419 [M -OEt]$^+$, 327 [M -PO(OEt)$_2$]$^+$.

ALA1
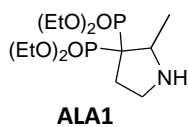
Tetraethyl (2-methylpyrrolidine-3,3-diyl)bis(phosphonate)
Not isolated as pure product

^{31}P {^{1}H}-NMR (122 MHz, CDCl$_3$) δ 27.83 (d, *J* = 13.2 Hz, 1P), 26.52 (d, *J* = 13.2 Hz, 1P) ppm.

ALA3
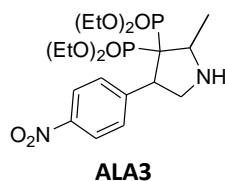
Tetraethyl (2-methyl-4-(4-nitrophenyl)pyrrolidine-3,3-diyl)bis(phosphonate)
Not isolated as pure product

^{31}P {^{1}H}-NMR (122 MHz, CDCl$_3$) δ 26.83 (d, *J* = 11.8 Hz, 1P), 22.78 (d, *J* = 11.8 Hz, 1P) ppm.
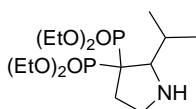
VAL1

Tetraethyl 2-isopropylpyrrolidine-3,3-diyldiphosphonate

Not isolated as pure product.

^{31}P {^{1}H}-NMR (122 MHz, CDCl$_3$) δ 26.65 (d, J = 14.9 Hz,1P), 25.32 (d, J = 14.9 Hz, 1P) ppm.

GC-MS (70 eV), m/z:385 [M]$^+$, 370 [M -Me]$^+$, 342 [M -iPr]$^+$, 248 [M -PO(OEt)$_2$]$^+$.
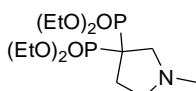
SAR1

Tetraethyl 1-methylpyrrolidine-3,3-diyldiphosphonate

^{1}H NMR (300 MHz, CDCl$_3$) δ 4.32–3.99 (m, 8H), 3.01 (t, J = 16.5 Hz, 2H), 2.64 (t, J = 6.3 Hz, 2H), 2.43–2.23 (m, 5H), 1.32 (t, J = 7.0 Hz, 12H) ppm.

^{31}P {1H}-NMR (122 MHz, CDCl3) δ 25.34 (s, 2P) ppm.

GC-MS (70 eV) m/z: 357 [M]$^+$, 342 [M -CH$_3$]$^+$, 220 [M -PO(OEt)$_2$]$^+$.
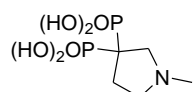
SAR1-OH

1-methylpyrrolidine-3,3-diyldiphosphonic acid

^{1}H NMR (300 MHz, D$_2$O) δ 4.03–3.87 (m, 1H), 3.75–3.63 (m, 1H), 3.27 (m, 2H), 2.87 (s, 3H), 2.56–2.30 (m, 2H) ppm.

^{31}P {^{1}H}-NMR (122 MHz, D$_2$O) δ 19.48 (s, *broad* 1P) 18.13(s, *broad* 1P) ppm.
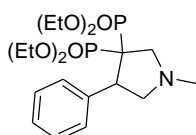
SAR2

Tetraethyl 1-methyl-4-phenylpyrrolidine-3,3-diyldiphosphonate

^{1}H NMR (300 MHz, CDCl$_3$) δ 7.61 (d, J = 7.3 Hz, 2H), 7.30–7.18 (m, 3H), 4.36–4.01 (m, 4H), 3.94–3.80 (m, 2H), 3.77–3.60 (m, 1H), 3.58–3.35 (m, 2H), 3.20–2.99 (m, 2H), 3.21–2.99 (m, 2H), 2.45 (s, 3H), 1.38 (td, J = 7.0, 1.8 Hz, 6H), 1.16 (t, J = 7.1 Hz, 3H), 1.01 (t, J = 7.1 Hz, 3H) ppm.

^{31}P {^{1}H}-NMR (122 MHz, CDCl$_3$) δ 24.78 (d, J = 10.8 Hz, 1P), 22.18 (d, J = 10.8 Hz, 1P) ppm.

^{13}C {^{1}H}-NMR (75 MHz, CDCl$_3$) δ 137.26 (s), 130.81 (s), 127.06 (d, J = 14.8 Hz), 62.93 (d, J = 7.0 Hz), 62.15 (d, J = 7.1 Hz), 42.03 (s), 16.31 (dd, J = 24.6, 4.7 Hz) ppm.

GC-MS (70 eV) m/z: 433 [M]$^+$, 418 [M -CH$_3$]$^+$, 296[M -PO(OEt)$_2$]$^+$.
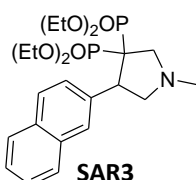
SAR3

Tetraethyl 1-methyl-4-(naphthalen-2-yl)pyrrolidine-3,3-diyldiphosphonate

^{1}H NMR (300 MHz, CDCl$_3$) δ 8.02 (s, 1H), 7.85–7.65 (m, 4H), 7.46–7.37 (m, 2H), 4.42–4.18 (m, 5H), 3.90–3.77 (m, 2H), 3.67–3.31 (m, 3H), 3.26–3.10 (m, 3H), 2.49 (s, 3H), 1.40 (td, J = 7.0, 3.4 Hz, 6H), 1.07 (t, J = 7.1 Hz, 3H), 0.86 (t, J = 7.1 Hz, 3H) ppm.

^{31}P {^{1}H}-NMR (122 MHz, CDCl$_3$) δ 24.81 (d, J = 11.2 Hz, 1P), 22.19 (d, J = 11.2 Hz, 1P) ppm.

^{13}C {^{1}H}-NMR (75 MHz, CDCl$_3$) δ 134.97–134.61 (m), 132.81 (s), 132.60 (s), 129.29 (d, J = 1.2 Hz), 127.86 (s), 127.35 (s), 126.22 (s), 125.58 (s), 125.56 (s), 63.19 (d, J = 7.0 Hz), 63.04 (d, J = 7.0 Hz), 62.21 (d, J = 2.4 Hz), 62.11 (d, J = 2.5 Hz), 60.89 (d, J = 6.4 Hz), 60.14 (t, J = 3.4 Hz), 51.61 (dd, J = 138.8, 136.0 Hz), 48.76 (t, J = 3.5 Hz), 42.08 (s), 30.93 (s), 29.70 (s), 16.60 (d, J = 1.8 Hz), 16.52 (d, J = 2.3 Hz), 16.17 (d, J = 6.2 Hz), 15.96 (d, J = 6.4 Hz) ppm.

GC-MS (70 eV) m/z: 483 [M]$^+$, 342 [M -CH$_3$]$^+$, 208 [M -2[PO(OEt)$_2$]]$^+$.
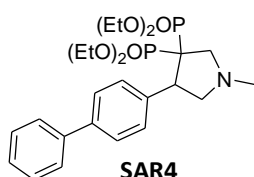
SAR4

Tetraethyl 4-(biphenyl-4-yl)-1-methylpyrrolidine-3,3-diyldiphosphonate

^{1}H NMR (300 MHz, CDCl$_3$) δ 7.70 (d, J = 8.0 Hz, 2H), 7.58 (d, J = 7.6 Hz, 2H), 7.50 (d, J = 8.0 Hz, 2H), 7.43 (t, J = 7.4 Hz, 2H), 7.33 (t, J = 7.2 Hz, 1H), 4.36 – 4.05 (m, 5H), 4.00 – 3.84 (m, 2H), 3.80 – 3.63 (m, 1H), 3.61 – 3.43 (m, 2H), 3.23 – 2.96 (m, 3H), 2.47 (s, 3H), 1.39 (td, J = 6.9, 2.8 Hz, 6H), 1.17 (t, J = 7.0 Hz, 3H),

1.01 (t, *J* = 7.0 Hz, 3H) ppm.

^{31}P {^{1}H}-NMR (122 MHz, CDCl₃) δ 24.73 (d, *J* = 10.8 Hz, 1P), 22.23 (d, *J* = 10.8 Hz, 1P) ppm.

^{13}C {^{1}H}-NMR (75 MHz, CDCl₃) δ 141.10 (s), 139.76 (s), 136.42 (dd, *J* = 5.1, 3.8 Hz), 131.22 (s), 128.71 (s), 127.10 (s), 126.97 (s), 125.79 (s), 63.11 (d, *J* = 7.1 Hz), 62.94 (s), 62.25 (s), 62.10 (s), 60.81 (d, *J* = 7.2 Hz), 60.09 (t, *J* = 3.4 Hz), 51.54 (dd, *J* = 54.4, 52.0 Hz), 48.45 (t, *J* = 3.5 Hz), 42.02 (s), 30.90 (s), 16.57 (d, *J* = 2.0 Hz), 16.50 (s), 16.27 (d, *J* = 6.1 Hz), 16.12 (d, *J* = 6.5 Hz) ppm.

GC-MS (70 eV) m/z: 509 [M] [+], 372 [M - PO(OEt)₂] [+], 234 [M -2[PO(OEt)₂]] [+].
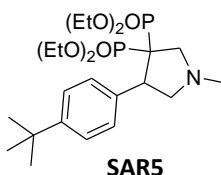
Tetraethyl 4-(4-tert-butylphenyl)-1-methylpyrrolidine-3,3-diyldiphosphonate

^{1}H NMR (300 MHz, CDCl₃) δ 7.54 (d, *J* = 8.5 Hz, 2H), 7.28 (d, *J* = 8.4 Hz, 2H), 4.33–4.16 (m, 4H), 3.89 (p, *J* = 7.2 Hz, 2H), 3.68–3.29 (m, 3H), 3.17–2.98 (m, 4H), 2.44 (s, 3H), 1.37 (td, *J* = 7.1, 3.7 Hz, 6H), 1.29 (s, 9H), 1.14 (t, *J* = 7.1 Hz, 3H), 0.96 (t, *J* = 7.1 Hz, 3H) ppm.

^{31}P {^{1}H}-NMR (122 MHz, CDCl₃) δ 24.84 (d, *J* = 10.3 Hz, 1P), 22.43 (d, *J* = 10.2 Hz, 1P) ppm.

GC-MS (70 eV) m/z: 489 [M] [+], 444 [M -OEt] [+], 352 [M -PO(OEt)₂] [+], 214 [M -2[PO(OEt)₂]] [+].
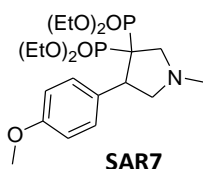
Tetraethyl 4-(4-methoxyphenyl)-1-methylpyrrolidine-3,3-diyldiphosphonate

^{1}H NMR (300 MHz, CDCl₃) δ 7.54 (d, *J* = 8.8 Hz, 2H), 6.80 (d, *J* = 8.8 Hz, 2H), 4.34–4.16 (m, 4H), 4.14–3.97 (m, 1H), 3.97–3.86 (m, 2H), 3.78 (s, 3H), 3.77–3.67 (m, 1H), 3.56–3.40 (m, 2H), 3.05 (m, 3H), 2.44 (s, 3H), 1.37 (td, *J* = 7.1, 1.7 Hz, 6H), 1.19 (t, *J* = 7.1 Hz, 3H), 1.04 (t, *J* = 7.1 Hz, 3H) ppm.

^{31}P {^{1}H}-NMR (122 MHz, CDCl₃) δ 24.91 (d, *J* = 11.2 Hz, 1P), 22.38 (d, *J* = 11.2 Hz, 1P) ppm.

GC-MS (70 eV) m/z: 463 [M] [+], 448 [M -CH₃] [+], 326 [M -PO(OEt)₂] [+], 188 [M -2[PO(OEt)₂]] [+].
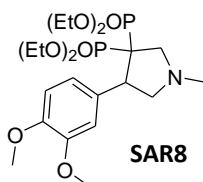
Tetraethyl 4-(3,4-dimethoxyphenyl)-1-methylpyrrolidine-3,3-diyldiphosphonate

^{1}H NMR (300 MHz, CDCl₃) δ 7.36 (d, *J* = 1.9 Hz, 1H), 7.07 (dd, *J* = 8.4, 2.0 Hz, 1H), 6.76 (d, *J* = 8.4 Hz, 1H), 4.36 – 4.14 (m, 4H), 4.13 – 3.97 (m, 1H), 3.97 – 3.87 (m, 5H), 3.85 (s, 3H), 3.77 – 3.64 (m, 1H), 3.57 – 3.40 (m, 2H), 3.16 – 2.95 (m, 3H), 2.44 (s, 3H), 1.37 (td, *J* = 7.1, 4.0 Hz, 6H), 1.17 (t, *J* = 7.1 Hz, 3H), 1.03 (t, *J* = 7.1 Hz, 3H) ppm.

^{31}P {^{1}H}-NMR (122 MHz, CDCl₃) δ 24.91 (d, *J* = 10.6 Hz, 1P), 22.55 (d, *J* = 10.6 Hz, 1P) ppm.

^{13}C {^{1}H}-NMR (75 MHz, CDCl₃) δ 148.12 (s), 147.87 (s), 129.89 (dd, *J* = 6.6, 2.3 Hz), 122.84 (s), 114.83 (s), 110.07 (s), 63.17 (d, *J* = 4.2 Hz), 63.08 (d, *J* = 4.3 Hz), 62.24 (d, *J* = 7.1 Hz), 61.21 (d, *J* = 6.5 Hz), 60.37 (t, *J* = 3.5 Hz), 56.06 (s), 56.02 (s), 51.59 (t, *J* = 2.8 Hz), 48.66 – 48.49 (m), 42.15 (s), 16.74 (d, *J* = 2.4 Hz), 16.66 (d, *J* = 2.5 Hz), 16.47 (d, *J* = 6.1 Hz), 16.32 (d, *J* = 6.4 Hz) ppm.

GC-MS (70 eV) m/z: 463 [M] [+], 448 [M -OEt] [+], 356 [M -PO(OEt)₂] [+], 218 [M -2[PO(OEt)₂]] [+].
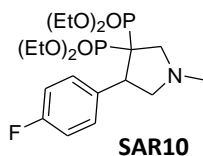
Tetraethyl 4-(4-fluorophenyl)-1-methylpyrrolidine-3,3-diyldiphosphonate

^{1}H NMR (300.15 MHz, CDCl₃) δ 7.59 (dd, *J* = 8.6, 5.6 Hz, 2H), 6.94 (t, *J* = 8.8 Hz, 2H), 4.34 – 4.16 (m, 4H), 4.02 – 3.86 (m, 3H), 3.82 – 3.67 (m, 1H), 3.61 – 3.30 (m, 2H), 3.18 – 2.97 (m, 3H), 2.44 (s, 3H), 1.37 (td, *J* = 7.0, 2.1 Hz, 6H), 1.18 (t,

J = 7.1 Hz, 3H), 1.05 (t, J = 7.1 Hz, 3H) ppm.

^{31}P {^{1}H}-NMR (122.5 MHz, CDCl$_3$) δ 24.53 (d, J = 11.0 Hz, 1 P), 22.06 (d, J = 11.0 Hz, 1P) ppm.

^{13}C {^{1}H}-NMR (75 MHz, CDCl$_3$ δ 207.10 (s), 133.10 (dd, J = 6.3, 2.7 Hz), 132.50 (d, J = 7.8 Hz), 113.95 (d, J = 20.9 Hz), 63.29 (d, J = 6.9 Hz), 63.16 (d, J = 7.0 Hz), 62.39 (d, J = 2.7 Hz), 62.29 (d, J = 2.8 Hz), 61.07 (d, J = 6.8 Hz), 60.13 (t, J = 3.6 Hz), 48.12 (t, J = 2.3 Hz), 42.12 (s, J = 21.5 Hz), 31.07 (s, J = 5.1 Hz), 16.70 (d, J = 1.8 Hz), 16.63 (d, J = 2.2 Hz), 16.43 (d, J = 6.2 Hz), 16.32 (d, J = 6.2 Hz) ppm.

GC-MS (70 eV) m/z: 451 [M] $^+$, 406 [M -OEt] $^+$, 314 [M -PO(OEt)$_2$] $^+$, 176 [M - 2[PO(OEt)$_2$]] $^+$.
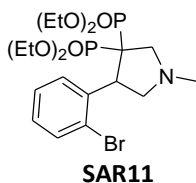
Tetraethyl 4-(2-bromophenyl)-1-methylpyrrolidine-3,3-diyldiphosphonate

^{1}H NMR (300 MHz, CDCl$_3$) δ 8.12 (dd, J = 8.0, 1.7 Hz, 1H), 7.47 (dd, J = 8.0, 1.3 Hz, 1H), 7.24–7.18 (m, 1H), 7.09–6.97 (m, 1H), 4.65–4.43 (m, 1H), 4.36–4.13 (m, 5H), 4.10–3.93 (m, 2H), 3.79–3.63 (m, 1H), 3.62–3.46 (m, 2H), 3.11–2.81 (m, 2H), 2.43 (s, 3H), 1.36 (td, J = 7.1, 4.2 Hz, 6H), 1.17 (t, J = 7.1 Hz, 3H), 1.06 (t, J = 7.1 Hz, 3H) ppm.

^{31}P {^{1}H}-NMR (122 MHz, CDCl$_3$) δ 24.99 (d, J = 5.9 Hz, 1P), 21.58 (d, J = 5.9 Hz, 1P) ppm.

GC-MS (70 eV) m/z: 512 [M] $^+$, 466 [M -OEt] $^+$, 432 [M -Br] $^+$, 374 [M -PO(OEt)$_2$] $^+$, 294 [M -PO(OEt)$_2$ -Br] $^+$, 236 [M -2[PO(OEt)$_2$]] $^+$.
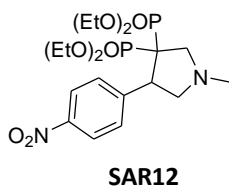
Tetraethyl 1-methyl-4-(4-nitrophenyl)pyrrolidine-3,3-diyldiphosphonate

^{1}H NMR (300.15 MHz, CDCl$_3$) δ 8.11 (d, J = 8.9 Hz, 2H), 7.80 (d, J = 8.8 Hz, 2H), 4.36 – 4.18 (m, 4H), 4.10 (m, 1H), 4.00 – 3.86 (m, 2H), 3.85 – 3.73 (m, 1H), 3.74 – 3.58 (m, 1H), 3.43 (dt, J = 18.1, 10.2 Hz, 1H), 3.09 (dq, J = 10.7, 7.8 Hz, 3H), 2.46 (s, 3H), 1.39 (td, J = 7.1, 3.7 Hz, 6H), 1.16 (t, J = 7.1 Hz, 3H), 1.06 (t, J = 7.1 Hz, 3H) ppm.

^{31}P {^{1}H}-NMR (122.5 MHz, CDCl$_3$) δ 24.04 (d, J = 11.3 Hz, 1 P), 21.46 (d, J = 11.4 Hz, 1P) ppm.

^{13}C {^{1}H}-NMR (75 MHz, CDCl$_3$) δ 147.00 (s), 145.91 (dd, J = 6.7, 2.9 Hz), 131.74 (s), 122.25 (s), 63.48 (t, J = 7.0 Hz), 62.66 (d, J = 3.9 Hz), 62.56 (d, J = 3.6 Hz), 60.82 (d, J = 5.9 Hz), 60.06 (d, J = 3.8 Hz), 51.69 (dd, J = 138.2, 136.4 Hz), 48.40 (t, J = 3.7 Hz), 41.96 (s), 16.66 (d, J = 5.8 Hz), 16.35 (t, J = 6.1 Hz) ppm.

GC-MS (70 eV) m/z: 463 [M] $^+$, 433 [M -OEt] $^+$, 341 [M -PO(OEt)$_2$] $^+$, 203 [M - 2[PO(OEt)$_2$]] $^+$.
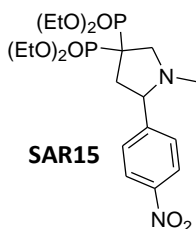
Tetraethyl 1-methyl-5-(4-nitrophenyl)pyrrolidine-3,3-diyldiphosphonate

^{1}H NMR (300 MHz, CDCl$_3$) δ 8.21 (d, J = 8.8 Hz, 2H), 7.59 (d, J = 8.7 Hz, 2H), 4.38–4.17 (m, 8H), 3.82–3.66 (m, 1H), 3.54 (dd, J = 10.0, 6.4 Hz, 1H), 2.99 (ddd, J = 22.5, 19.2, 10.7 Hz, 1H), 2.71 (ddd, J = 20.1, 13.8, 7.0 Hz, 1H), 2.41–2.18 (m, 1H), 2.16 (s, 3H), 1.45–1.34 (m, 12H) ppm.

^{31}P {^{1}H}-NMR (122 MHz, CDCl$_3$) δ 26.37 (d, J = 12.2 Hz, 1P), 25.63 (d, J = 12.2 Hz, 1P) ppm.

GC-MS, (70 eV) m/z: 478 [M] $^+$, 433 [M -OEt] $^+$, 341 [M -PO(OEt)$_2$] $^+$.

SAR11

(EtO)$_2$OP
(EtO)$_2$OP

Br

SAR12

(EtO)$_2$OP
(EtO)$_2$OP

O$_2$N

SAR15

(EtO)$_2$OP
(EtO)$_2$OP

NO$_2$

SAR18
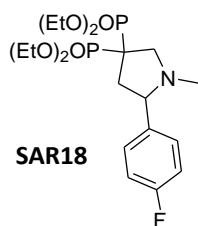
Tetraethyl 5-(4-fluorophenyl)-1-methylpyrrolidine-3,3-diyldiphosphonate

Not isolated as pure product.

^{31}P {^{1}H}-NMR (122 MHz, CDCl$_3$) δ 24.85 (d, J = 13.2 Hz, 1P), 24.06 (d, J = 13.1 Hz, 1P) ppm.

GC-MS, (70 eV) m/z: 451 [M]$^+$, 406 [M -OEt]$^+$, 314 [M -PO(OEt)$_2$]$^+$, 177 [M - (PO(OEt)$_2$)$_2$]$^+$.

SAR19
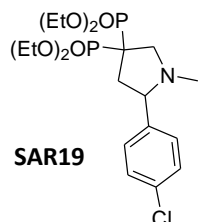
Tetraethyl 5-(4-chlorophenyl)-1-methylpyrrolidine-3,3-diyldiphosphonate

Not isolated as pure product

^{31}P {^{1}H}-NMR (122 MHz, CDCl$_3$) δ 26.33 (d, J = 12.1 Hz, 1P), 25.61 (d, J = 12.1 Hz, 1P) ppm.

GC-MS, (70 eV) m/z: 467 [M, Cluster Cl]$^+$, 422 [M -OEt, Cluster Cl]$^+$, 330 [M - PO(OEt)$_2$ Cluster Cl]$^+$.

SAR21
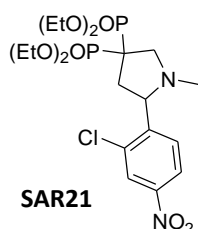
Tetraethyl 5-(2-chloro-4-nitrophenyl)-1-methylpyrrolidine-3,3-diyldiphosphonate

^{1}H NMR (300 MHz, CDCl$_3$) δ 8.54 (d, J = 2.8 Hz, 1H), 8.04 (dd, J = 8.7, 2.8 Hz, 1H), 7.49 (d, J = 8.7 Hz, 1H), 4.34–4.16 (m, 8H), 3.98 (dd, J = 9.6, 6.8 Hz, 1H), 3.76 (ddd, J = 17.1, 10.7, 6.3 Hz, 1H), 3.13–2.80 (m, 2H), 2.20 (s, 3H), 2.16–1.94 (m, 1H), 1.45–1.29 (m, 12H) ppm.

^{31}P {^{1}H}-NMR(122 MHz, CDCl$_3$) δ 24.51 (d, J = 16.3 Hz, 1P), 23.63 (d, J = 16.3 Hz, 1P) ppm

GC-MS, (70 eV) m/z: 512 [M, Cluster Cl]$^+$, 467 [M -OEt, Cluster Cl]$^+$, 375 [M - PO(OEt)$_2$]$^+$.

SAR22
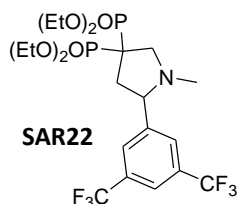
Tetraethyl 5-(3,5-bis(trifluoromethyl)phenyl)-1-methylpyrrolidine-3,3-diyldiphosphonate

Not isolated as pure product

^{31}P {^{1}H}-NMR (122 MHz, CDCl$_3$) δ 24.75 (d, J = 13.5 Hz, 1P), 23.83 (d, J = 13.5 Hz, 1P) ppm.

SAR26
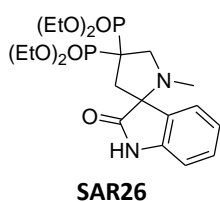
1'-methyl-2-oxospiro[indolyn-3,2'-pyrrolidin]-4',4'diildiphosphonate

^{1}H NMR (300 MHz CDCl$_3$) δ 7.71 (d, J = 6.7 Hz, 1H), 7.19 (t, J = 7.7 Hz, 1H), 7.04 (t, J = 7.5 Hz, 1H), 6.78 (d, J = 7.7 Hz, 1H), 4.40 – 4.09 (m, 8H), 3.85 (m, 1H), 3.61 – 3.45 (m, 1H), 2.94 (m, 1H), 2.85 – 2.67 (m, 1H), 2.11 (s, 3H), 1.35 (dt, J = 9.2, 3.6 Hz, 12H) ppm.

^{31}P {^{1}H}-NMR (122 MHz, CDCl$_3$) δ 25.40 (d, J = 11.5 Hz, 1P), 22.72 (d, J = 11.5 Hz, 1P) ppm.

5.3.6 *General procedure for base catalyzed addition of isonitriles to VBP*

In a vial equipped with magnetic stirring bar 0.2 mmol of VBP, 2 mL of chloroform was added followed by 0.2 mmol of isonitrile and 0.2 mmol of triethyl amine. The vial was thermostatted at 60°C for 12 h under vigorous stirring. Solvent was removed under reduced pressure and the product of the reaction was isolated by means of preparative TLC and characterized with ^{1}H, ^{31}P ^{13}C and GC-MS analyses.

NCEt
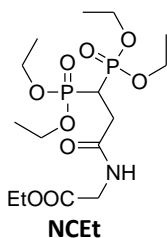
Ethyl 2-(3,3-bis(diethoxyphosphoryl)propanamido)acetate

^{1}H NMR (400 MHz, CDCl$_3$) δ 6.53 (t, *J* = 4.6 Hz, 1H), 4.23–4.10 (m, 10H), 4.02 (d, *J* = 5.1 Hz, 2H), 3.17 (tt, *J* = 23.6, 6.0 Hz, 1H), 2.78 (td, *J* = 16.3, 6.0 Hz, 2H), 1.37–1.29 (m, 12H), 1.27 (t, *J* = 7.1 Hz, 3H) ppm.

^{31}P {^{1}H}-NMR (162 MHz, CDCl$_3$) δ 22.65 (s, 2P) ppm.

^{13}C {^{1}H}-NMR (101 MHz, CDCl$_3$) δ 169.88 – 169.69 (m), 63.04 (d, *J* = 6.5 Hz), 62.73 (d, *J* = 6.7 Hz), 61.50 (s), 41.67 (s), 32.29 (t, *J* = 135.3 Hz), 31.92 (t, *J* = 4.5 Hz), 16.35 (d, *J* = 1.5 Hz), 16.28 (d, *J* = 1.5 Hz), 14.13 (s) ppm.

GC-MS, (70 eV) m/z: 431 [M] $^+$, 385 [M -OEt-H] $^+$, 358 [M -COOEt] $^+$, 329 [M - NHCH$_2$COOEt] $^+$, 301 [M -CONHCH$_2$COOEt] $^+$, 294 [M -PO(OEt)$_2$] $^+$.

NCMe
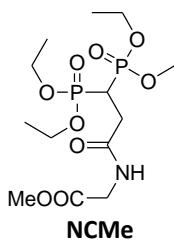
Methyl 2-(3,3-bis(diethoxyphosphoryl)propanamido)acetate

^{1}H NMR (400 MHz, CDCl$_3$) δ 6.52 (t, *J* = 4.2 Hz, 1H), 4.24–4.10 (m, 8H), 4.05 (d, *J* = 5.1 Hz, 2H), 3.75 (s, 3H), 3.16 (tt, *J* = 23.6, 6.0 Hz, 1H), 2.78 (td, *J* = 16.3, 6.0 Hz, 2H), 1.32 (t, *J* = 7.1 Hz, 12H) ppm.

^{31}P {^{1}H}-NMR (162 MHz, CDCl$_3$) δ 22.63 (s, 2P) ppm.

^{13}C {^{1}H}-NMR (101 MHz, CDCl$_3$) δ 170.18 (s), 63.07 (d, *J* = 6.5 Hz), 62.76 (d, *J* = 6.6 Hz), 41.52 (s), 32.34 (t, *J* = 135.3 Hz), 31.95 (t, J = 4.5 Hz), 16.50 – 16.22 (m) ppm.

GC-MS, (70 eV) m/z: 417 [M] $^+$, 385 [M -Me-H] $^+$, 329 [M -NHCH$_2$COOMe] $^+$, 301 [M - CONHCH$_2$COOMe] $^+$, 280 [M -PO(OEt)$_2$] $^+$.

5.3.7 *General procedure for AgOAc catalyzed addition of isonitriles to substituted BP precursors*

In a vial equipped with magnetic stirring bar 0.2 mmol of VBP precursor, 2 mL of acetonitrile was added followed by 0.2 mmol of isonitrile and 10 mol% of AgOAc with respect to BP. The vial was left at room temperature for 12 h under vigorous stirring. Solvent was removed under reduced pressure and the product of the reaction was isolated by means of preparative TLC and characterized with ^{1}H, ^{31}P ^{13}C and GC-MS analyses.
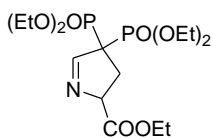
Ethyl 4,4-bis(diethoxyphosphoryl)-3,4-dihydro-2H-pyrrole-2-carboxylate

^{1}H NMR (400 MHz, CDCl$_3$) δ 7.53 (d, *J* = 3.0 Hz, 1H), 4.88 (dqd, *J* = 12.1, 6.1, 3.0 Hz, 1H), 4.27–4.04 (m, 10H), 2.81–2.50 (m, 2H), 1.34–1.26 (m, 15H) ppm.

^{31}P {^{1}H}-NMR (162 MHz, CDCl$_3$) δ 18.77 (d, *J* = 8.0 Hz, 1P), 17.36 (d, *J* = 8.0 Hz, 1P) ppm.

^{13}C {^{1}H}-NMR (101 MHz, CDCl$_3$) δ 170.98 (d, *J* = 4.3 Hz), 161.37 (dd, *J* = 7.8, 5.1 Hz), 75.42 (d, *J* = 5.3 Hz), 64.02 (d, *J* = 6.8 Hz), 63.73 (d, *J* = 6.9 Hz), 63.55 (d, *J* = 7.0 Hz), 63.34 (d, *J* = 7.1 Hz), 61.61 (dd, *J* = 137.3, 132.2 Hz), 61.50 (s), 30.50 (t, *J* = 3.4 Hz), 16.50–16.21 (m), 14.16 (s) ppm.

GC-MS, (70 eV) m/z: 413 [M] [+], 368 [M -OEt] [+], 340 [M -COOEt] [+], 276 [M -PO(OEt)$_2$] [+].
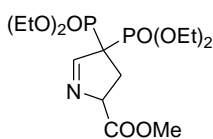
AG1Et

Methyl 4,4-bis(diethoxyphosphoryl)-3,4-dihydro-2H-pyrrole-2-carboxylate

^{1}H NMR (300 MHz, CDCl$_3$) δ 7.53 (d, *J* = 2.9 Hz, 1H), 4.90 (dqd, *J* = 12.1, 6.1, 3.0 Hz, 1H), 4.29–4.08 (m, 8H), 3.77 (s, 3H), 2.86–2.47 (m, 2H), 1.34–1.25 (m, 12H) ppm.

^{31}P {^{1}H}-NMR (122 MHz, CDCl$_3$) δ 17.40 (d, *J* = 8.0 Hz, 1P), 15.99 (d, *J* = 8.0 Hz, 1P) ppm.

GC-MS, (70 eV) m/z: 399 [M] [+], 368 [M -OMe] [+], 340 [M -COOMe] [+], 262 [M -PO(OEt)$_2$] [+].

AG1Me
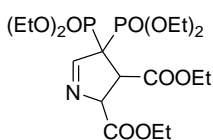
Diethyl 4,4-bis(diethoxyphosphoryl)-3,4-dihydro-2H-pyrrole-2,3-dicarboxylate

^{1}H NMR (400 MHz, CDCl$_3$) δ 7.45 (d, *J* = 3.1 Hz, 1H), 5.20 (dtd, *J* = 9.3, 6.1, 3.1 Hz, 1H), 4.40–3.96 (m, 13H), 1.37-1.24 (m, 18H) ppm.

^{31}P {^{1}H}-NMR (162 MHz, CDCl$_3$) δ 15.93 (t, *J* = 9.5 Hz, 2P) ppm.

^{13}C {^{1}H}-NMR (101 MHz, CDCl$_3$) δ 170.07 (d, *J* = 3.0 Hz), 168.80 (dd, *J* = 5.9, 3.2 Hz), 161.25 (dd, *J* = 8.0, 5.8 Hz), 77.66 (d, *J* = 5.0 Hz), 64.56 (d, *J* = 4.6 Hz), 64.19 (dd, *J* = 135.3, 131.0 Hz), 63.35 (d, *J* = 5.7 Hz), 63.05 (d, *J* = 5.9 Hz), 61.89 (s), 61.73 (s), 49.06 (t, *J* = 3.1 Hz), 16.40 (d, *J* = 4.6 Hz), 16.26 – 16.05 (m), 14.10 (s), 13.95 (s) ppm.

GC-MS, (70 eV) m/z: 485 [M] [+], 440 [M -OEt] [+], 412 [M -COOEt] [+], 348 [M -PO(OEt)$_2$] [+].

AG2Et
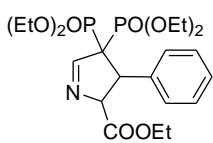
Ethyl 4,4-bis(diethoxyphosphoryl)-3-phenyl-3,4-dihydro-2H-pyrrole-2-carboxylate

^{1}H NMR (400 MHz, CDCl$_3$) δ 7.67–7.56 (m, 3H), 7.32–7.17 (m, 3H), 5.33 (tdd, *J* = 10.3, 5.1, 2.6 Hz, 1H), 4.46 (dddd, *J* = 29.6, 19.0, 10.7, 1.5 Hz, 1H), 4.37–4.29 (m, 2H), 4.28–4.11 (m, 4H), 3.97–3.87 (m, 2H), 3.84–3.75 (m, 1H), 3.69–3.58 (m, 1H), 1.36–1.32 (m, 6H), 1.30–1.25 (m, 3H), 1.13 (td, *J* = 7.1, 1.7 Hz, 3H), 1.07 (td, *J* = 7.1, 1.9 Hz, 3H) ppm.

^{31}P {^{1}H}-NMR (162 MHz, CDCl$_3$) δ 17.23 (d, *J* = 6.5 Hz, 1P), 15.97 (d, *J* = 6.5 Hz, 1P) ppm.

^{13}C {^{1}H}-NMR (101 MHz, CDCl$_3$) δ 170.74 (d, *J* = 3.3 Hz), 162.16 (dd, *J* = 8.9, 4.9 Hz), 134.00 (d, *J* = 5.1 Hz), 130.59 (s), 127.73 (s), 78.03 (dd, *J* = 8.8, 1.7 Hz), 66.76 (dd, *J* = 136.0, 128.6 Hz), 63.83 (d, *J* = 3.9 Hz), 63.76 (d, *J* = 3.8 Hz), 63.31 (d, *J* = 7.0 Hz), 62.89 (d, *J* = 7.2 Hz), 62.59 (s), 50.56 (s, *J* = 2.1 Hz), 16.44 (t, *J* = 6.2 Hz), 16.24 (dd, *J* = 6.1, 4.7 Hz), 14.42 (s).

GC-MS, (70 eV) m/z: 489 [M] [+], 444 [M -OEt] [+], 416 [M -COOEt] [+], 352 [M -PO(OEt)$_2$] [+].
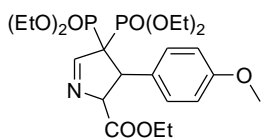
AG3Et

Ethyl 4,4-bis(diethoxyphosphoryl)-3-(4-methoxyphenyl)-3,4-dihydro-2H-pyrrole-2-carboxylate

Not isolated as pure product.

^{31}P {^{1}H}-NMR (162 MHz, CDCl$_3$) δ 17.35 (d, J = 6.0 Hz, 1P), 16.18 (d, J = 6.0 Hz, 1P) ppm.

GC-MS, (70 eV) m/z: 519 [M]$^+$, 474 [M -OEt]$^+$, 446 [M -COOEt]$^+$, 382 [M - PO(OEt)$_2$]$^+$.
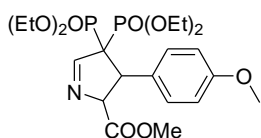
AG5Et

Methyl 4,4-bis(diethoxyphosphoryl)-3-(4-methoxyphenyl)-3,4-dihydro-2H-pyrrole-2-carboxylate

Not isolated as pure product.

^{31}P {^{1}H}-NMR (122 MHz, CDCl$_3$) δ 15.95 (d, J = 5.7 Hz, 1P), 14.74 (d, J = 5.7 Hz, 1P) ppm.

GC-MS, (70 eV) m/z: 505 [M]$^+$, 446 [M -COOMe]$^+$, 368 [M -PO(OEt)$_2$]$^+$.
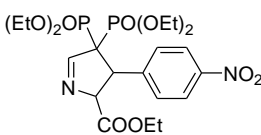
AG5Me

Ethyl 4,4-bis(diethoxyphosphoryl)-3-(4-nitrophenyl)-3,4-dihydro-2H-pyrrole-2-carboxylate

^{1}H NMR (400 MHz, CDCl$_3$) δ 8.14 (d, J = 8.9 Hz, 2H), 7.81 (d, J = 8.7 Hz, 1H), 7.62 (d, J = 3.0 Hz, 1H), 5.33 (dddd, J = 10.5, 7.8, 5.0, 3.1 Hz, 1H), 4.50 (ddd, J = 29.3, 19.0, 10.6 Hz, 1H), 4.29–4.13 (m, 6H), 4.00–3.92 (m, 2H), 3.91–3.84 (m, 1H), 3.83–3.75 (m, 1H), 1.36 (dd, J = 13.4, 6.7 Hz, 6H), 1.21 (t, J = 7.1 Hz, 3H), 1.13 (dt, J = 11.8, 7.1 Hz, 6H) ppm.

^{31}P {^{1}H}-NMR(162 MHz, CDCl$_3$) δ 16.67 (d, J = 6.1 Hz, 1P), 15.52 (d, J = 6.1 Hz, 1P) ppm.

^{13}C {^{1}H}-NMR (101 MHz, CDCl$_3$) δ 170.23 (d, J = 3.3 Hz), 161.84 (dd, J = 8.8, 4.9 Hz), 147.42 (s), 142.22 (d, J = 5.1 Hz), 131.57 (s), 122.74 (s), 77.97 (dd, J = 8.5, 1.8 Hz), 66.75 (dd, J = 136.4, 128.3 Hz), 64.18 (d, J = 3.0 Hz), 64.11 (d, J = 3.0 Hz), 63.68 (d, J = 7.1 Hz), 63.36 (d, J = 7.2 Hz), 62.00 (s), 50.08 (t, J = 2.4 Hz), 16.47 (dd, J = 5.9, 4.0 Hz), 16.28 (dd, J = 6.0, 4.0 Hz), 14.13 (s) ppm.

GC-MS, (70 eV) m/z: 534 [M]$^+$, 461 [M -COOEt]$^+$, 397 [M -PO(OEt)$_2$]$^+$.
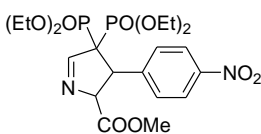
AG6Et

Methyl 4,4-bis(diethoxyphosphoryl)-3-(4-nitrophenyl)-3,4-dihydro-2H-pyrrole-2-carboxylate

^{1}H NMR (400 MHz, CDCl$_3$) δ 8.10 (d, J = 8.9 Hz, 2H), 7.76 (d, J = 8.7 Hz, 2H), 7.58 (d, J = 3.0 Hz, 1H), 5.31 (dddd, J = 10.5, 7.8, 5.1, 3.1 Hz, 1H), 4.47 (ddd, J = 29.1, 18.6, 10.5 Hz, 1H), 4.27–4.13 (m, 4H), 3.96–3.87 (m, 2H), 3.86–3.79 (m, 1H), 3.78–3.72 (m, 1H), 3.69 (s, 3H), 1.34–1.28 (m, 6H), 1.09 (dt, J = 13.8, 7.1 Hz, 6H) ppm.

^{31}P {^{1}H}-NMR (162 MHz, CDCl$_3$) δ 16.62 (d, J = 6.0 Hz, 1P), 15.45 (d, J = 6.0 Hz, 1P) ppm.

^{13}C {^{1}H}-NMR (101 MHz, CDCl$_3$) δ 170.60 (d, J = 3.4 Hz), 161.82 (dd, J = 8.7, 4.9 Hz), 147.34 (s), 142.01 (d, J = 4.7 Hz), 131.46 (s), 122.67 (s), 77.76 (dd, J = 8.5, 1.7 Hz), 66.69 (dd, J = 136.3, 128.4 Hz), 64.10 (d, J = 2.9 Hz), 64.03 (d, J = 2.9 Hz), 63.59 (d, J = 7.1 Hz), 63.26 (d, J = 7.2 Hz), 52.82 (s), 49.90 (t, J = 2.3 Hz), 16.36 (dd, J = 5.9, 4.0 Hz), 16.17 (dd, J = 6.1, 3.5 Hz) ppm.

GC-MS, (70 eV) m/z: 520 [M]$^+$, 461 [M -COOMe]$^+$, 383 [M -PO(OEt)$_2$]$^+$.

AG6Me

(EtO)$_2$OP PO(OEt)$_2$
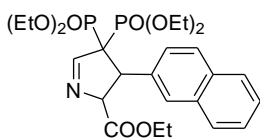
AG7Et

Ethyl 4,4-bis(diethoxyphosphoryl)-3-(naphthalen-2-yl)-3,4-dihydro-2H-pyrrole-2-carboxylate

Not isolated as pure product.

^{31}P {^{1}H}-NMR (122 MHz, CDCl$_3$) δ 15.92 (d, *J* = 6.0 Hz, 1P), 14.66 (d, *J* = 6.0 Hz, 1P) ppm.

GC-MS, (70 eV) m/z: 539 [M]$^+$, 466 [M -COOEt]$^+$, 402 [M -PO(OEt)$_2$]$^+$.

(EtO)$_2$OP PO(OEt)$_2$
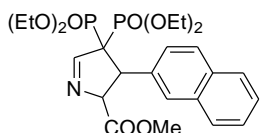
AG7Me

Methyl 4,4-bis(diethoxyphosphoryl)-3-(naphthalen-2-yl)-3,4-dihydro-2H-pyrrole-2-carboxylate

Not isolated as pure product.

^{31}P {^{1}H}-NMR (162 MHz, CDCl$_3$) δ 17.18 (d, *J* = 5.8 Hz, 1P), 15.88 (d, *J* = 5.8 Hz, 1P) ppm.

GC-MS, (70 eV) m/z: 525 [M]$^+$, 466 [M -COOMe]$^+$, 388 [M -PO(OEt)$_2$]$^+$.

5.3.8 *Tetraethyl 2-(2,3-dioxoindolin-1-yl)ethane-1,1-diyldiphosphonate (IST1)*

In a round bottom flask equipped with condenser and magnetic stirring bar, 0.33 mmol of VBP (100 mg) and 5 mL of toluene were added followed by 0.33 mmol of isatin (1 eq.) and 0.5 mmol of K$_2$CO$_3$ (1.5 eq.). The mixture was heated overnight at 60°C under vigorous stirring. Solvent was removed under reduced pressure. Crude product was diluted with 10 mL of ethyl acetate and washed twice with 5 mL of water. Organic phase was dried with Na$_2$SO$_4$, filtered and solvent was removed under reduced pressure. IST1 was obtained in 86% isolated yield and characterized with ^{1}H, ^{31}P ^{13}C and GC-MS analyses.

In a round bottom flask equipped with magnetic stirring bar, 0.2 mmol of IST1 was introduced followed by 5 mL of CH$_2$Cl$_2$ under anhydrous condition. To this, 2.4 mmol of bromotrimethylsilane (12 eq.) were added. The mixture was stirred under inert atmosphere at rt for 18 h. The crude mixture was concentrated under reduced pressure, diluted with a 9:1 solution of methanol and water, stirred for 4 h at room temperature and dried. The free bisphosphonic acid IST1-OH was obtained in quantitative yield and was characterized by ^{1}H and ^{31}P NMR.
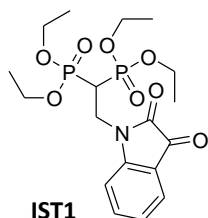
IST1

Tetraethyl 2-(2,3-dioxoindolin-1-yl)ethane-1,1-diyldiphosphonate
^{1}H NMR (300 MHz, CDCl$_3$) δ 7.61 (m, 2H), 7.17 – 6.90 (m, 2H), 4.36 – 4.00 (m, 10H), 3.11 (tt, *J* = 23.1, 7.0 Hz, 1H), 1.29 (td, *J* = 7.1, 2.9 Hz, 12H) ppm.
^{31}P {1H}-NMR (122 MHz, CDCl$_3$) δ 18.46 (s, 2P) ppm.
^{13}C {1H}-NMR (75 MHz, CDCl$_3$) δ 182.98 (s), 158.23 (s), 150.46 (s), 138.42 (d, *J* = 7.0 Hz), 125.27 (s), 123.71 (s), 117.57 (s), 110.97 (s), 63.39 (d, *J* = 6.8 Hz), 63.01 (d, *J* = 6.8 Hz), 37.12 (t, *J* = 3.3 Hz), 34.24 (s), 16.18 (dd, *J* = 6.6, 3.0 Hz) ppm.
GC-MS, (70 eV) m/z: 447 [M]$^+$, 402 [M -OEt]$^+$, 310 [M -PO(OEt)$_2$]$^+$.

IST1-OH
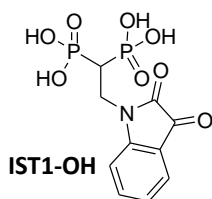
<u>2-(2,3-dioxoindolin-1-yl)ethane-1,1-diyldiphosphonic acid</u>
^{1}H NMR (300 MHz, D$_2$O) δ 7.62 (t, *J* = 7.8 Hz, 1H), 7.55 (d, *J* = 7.6 Hz, 1H), 7.12 (dd, *J* = 7.8, 5.2 Hz, 2H), 4.23 – 4.08 (m, 2H), 2.80 (tt, *J* = 21.7, 7.3 Hz, 1H) ppm.
^{31}P {^{1}H}-NMR (122 MHz, D$_2$O) δ 15.86 (s, 2P) ppm.

5.3.9 *General procedure for organocatalyzed aldol condensation between IST1 and ketones*

In a vial equipped with magnetic stirring bar 0.12 mmol of isatin BP, 3 mL of acetone (or 1 mL of ketone or 2M solution in 1 mL of MeCN of the same) and 25 mol% of catalyst were added. The vial was left at room temperature for 42 h under vigorous stirring. Solvent was removed under reduced pressure and the product of the reaction was isolated by means of preparative TLC with 7:3 ethyl acetate/acetone mixture as eluent and characterized with ^{1}H, [31]P [13]C. enantiomeric excess were determined by chiral HPLC analyses.

ALD1
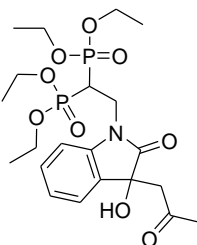
<u>Tetraethyl 2-(3-hydroxy-2-oxo-3-(2-oxopropyl)indolin-1-yl)ethane-1,1-diyldiphosphonate</u>
^{1}H NMR (300 MHz, CDCl$_3$) δ 7.35 – 7.25 (m, 2H), 7.04 (t, *J* = 7.4 Hz, 1H), 6.89 (d, *J* = 7.9 Hz, 1H), 4.56 – 4.37 (m, 2H), 4.24 – 4.05 (m, 8H), 3.35 – 3.07 (m, 3H), 2.14 (s, 3H), 1.41 – 1.22 (m, 12H) ppm.
^{31}P {^{1}H}-NMR (122 MHz, CDCl$_3$) δ 18.27 (d, *J* = 7.0 Hz, 1P), 17.84 (d, *J* = 7.0 Hz, 1P) ppm.
^{13}C {^{1}H}-NMR (75 MHz, CDCl$_3$) δ 206.46 (s), 176.63 (s), 142.08 (s), 130.94 (s), 129.47 (s), 123.65 (s), 122.95 (s), 109.04 (s), 77.22 (s), 73.07 (s), 63.25 (d, *J* = 3.5 Hz), 63.17 (d, *J* = 3.3 Hz), 62.96 (d, *J* = 6.4 Hz), 62.74 (d, *J* = 6.6 Hz), 48.50 (s), 36.47 (dd, *J* = 9.1, 2.9 Hz), 33.19 (d, *J* = 2.1 Hz), 31.44 (s), 30.93 (s), 16.29 (dd, *J* = 6.2, 1.9 Hz) ppm.

ALD2
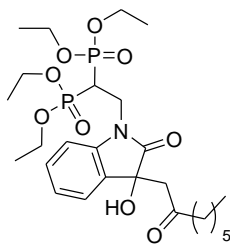
<u>Tetraethyl 2-(3-hydroxy-2-oxo-3-(2-oxooctyl)indolin-1-yl)ethane-1,1-diyldiphosphonate</u>
^{1}H NMR (300 MHz, CDCl$_3$) δ 7.30 (d, *J* = 7.2 Hz, 2H), 7.03 (t, *J* = 7.6 Hz, 1H), 6.89 (d, *J* = 7.8 Hz, 1H), 4.56 – 4.38 (m, 2H), 4.25 – 4.04 (m, 8H), 3.33 – 3.08 (m, 3H), 2.44 – 2.30 (m, 2H), 1.91 – 1.40 (m, 2H), 1.40 – 1.09 (m, 18H), 0.92 – 0.79 (m, 3H) ppm.
^{31}P {^{1}H}-NMR (122 MHz, CDCl$_3$) δ 18.33 (d, *J* = 7.0 Hz, 1P), 17.88 (d, *J* = 6.9 Hz, 1P) ppm.

ALD4
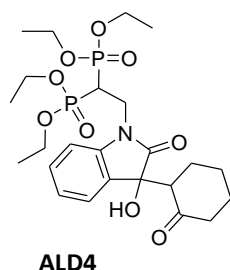
<u>Tetraethyl 2-(3-hydroxy-2-oxo-3-(2-oxocyclohexyl)indolin-1-yl)ethane-1,1-diyldiphosphonate</u>
^{1}H NMR (300 MHz, CDCl$_3$) δ 7.47 – 7.28 (m, 2H), 7.05 – 6.97 (m, 1H), 6.92 (d, *J* = 7.8 Hz, 1H), 4.51 (tt, *J* = 14.3, 8.6 Hz, 2H), 4.30 – 3.99 (m, 8H), 3.33 – 3.08 (m, 1H), 2.60 (t, *J* = 3.3 Hz, 1H), 2.41 – 2.21 (m, 2H), 2.09 – 1.55 (m, 6H), 1.39 – 1.21 (m, 12H) ppm.
^{31}P {^{1}H}-NMR (122MHz, CDCl$_3$) δ 18.55 (d, *J* = 7.4 Hz, 1P), 17.98 (d, *J* = 7.5 Hz, 1P) ppm.

ALD9
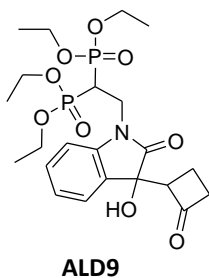
Tetraethyl 2-(3-hydroxy-2-oxo-3-(2-oxocyclobutyl)indolin-1-yl)ethane-1,1-diyldiphosphonate

^{1}H NMR (300 MHz, CDCl$_3$) δ 7.71 (d, J = 7.3 Hz, 1H), 7.32 (td, J = 7.8, 1.1 Hz, 1H), 7.10 (t, J = 7.1 Hz, 1H), 6.91 (d, J = 7.9 Hz, 1H), 4.39 (ddd, J = 23.1, 14.6, 8.5 Hz, 2H), 4.27 − 3.95 (m, 8H), 3.75 − 3.62 (m, 1H), 3.30 − 3.00 (m, 3H), 2.44 (dt, J = 9.9, 7.8 Hz, 1H), 2.10 (dt, J = 21.2, 9.3 Hz, 1H), 1.38 − 1.16 (m, 12H) ppm.

^{31}P {^{1}H}-NMR (122 MHz, CDCl$_3$) δ 18.30 (d, J= 5.9 Hz, 1P), 18.02 (d, J= 6.3 Hz, 1P) ppm.

^{13}C {^{1}H}-NMR (75 MHz, CDCl$_3$) δ 207.80 (s), 176.18 (s), 141.72 (s), 129.88 (s), 129.60 (s), 125.79 (s), 123.30 (s), 109.10 (s), 74.50 (s), 64.00 (s), 63.22 (dd, J = 9.2, 6.6 Hz), 62.88 (t, J = 6.7 Hz), 46.14 (s), 36.72 (t, J = 2.8 Hz), 30.92 (s), 16.27 (dd, J = 5.9, 2.2 Hz), 12.30 (s) ppm.
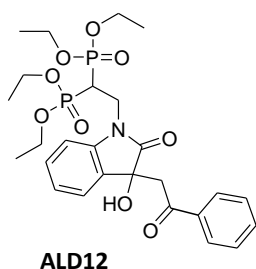
ALD12

Tetraethyl 2-(3-hydroxy-2-oxo-3-(2-oxo-2-phenylethyl)indolin-1-yl)ethane-1,1-diyldiphosphonate

^{1}H NMR (300 MHz, CDCl$_3$) δ 7.61 − 7.48 (m, 2H), 7.48 − 7.38 (m, 3H), 7.37 − 7.27 (m, 2H), 7.01 (t, J = 7.5 Hz, 1H), 6.92 (d, J= 7.9 Hz, 1H), 4.62 − 4.45 (m, 1H), 4.25 − 3.57 (m, 11H), 3.43 − 3.11 (m, 1H), 1.48 − 1.16 (m, 12H) ppm.

^{31}P {^{1}H}-NMR (122 MHz, CDCl$_3$) δ 18.29 (d, J = 7.5 Hz, 1P), 17.79 (d, J =7.4 Hz, 1P) ppm.

ALD13
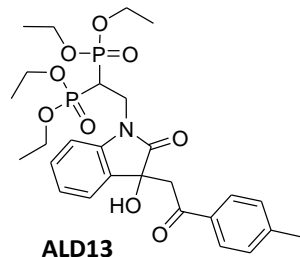
Tetraethyl 2-(3-hydroxy-2-oxo-3-(2-oxo-2-p-tolylethyl)indolin-1-yl)ethane-1,1-diyldiphosphonate

^{1}H NMR (300 MHz, CDCl$_3$) δ 7.78 (d, J = 8.2 Hz, 2H), 7.35 − 7.28 (m, 2H), 7.22 (d, J = 8.4 Hz, 2H), 7.00 (t, J = 7.5 Hz, 1H), 6.93 (d, J = 7.9 Hz, 1H), 4.57 − 4.46 (m, 1H), 4.29 − 4.00 (m, 8H), 3.83 (dd, J = 63.5, 17.7 Hz, 2H), 3.37 − 3.14 (m, 2H), 2.38 (s, 3H), 1.37 − 1.24 (m, 12H) ppm.

^{31}P {^{1}H}-NMR (122 MHz, CDCl$_3$) δ 18.38 (d, J = 6.3 Hz, 1P), 17.92 (d, J = 6.3 Hz, 1P) ppm.

^{13}C {^{1}H}-NMR (75 MHz, CDCl$_3$) δ 197.19 (s), 176.86 (s), 142.27 (s), 136.27 (s), 133.54 (s), 133.11 (s), 131.35 (s), 129.37 (s), 128.62 (s), 128.57 (s), 128.31 (s), 128.13 (s), 123.51 (s), 122.87 (s), 109.01 (s), 73.31 (s), 63.27 (dd, J = 6.3, 1.2 Hz), 62.97 (d, J = 6.6 Hz), 62.65 (d, J = 6.8 Hz), 44.28 (s), 36.48 (s), 33.17 (s), 29.70 (s), 16.30 (dd, J = 6.1, 3.7 Hz) ppm.

ALD14
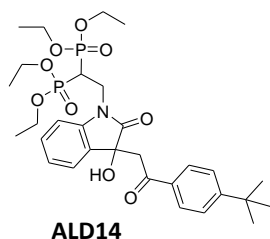
Tetraethyl 2-(3-(2-(4-tert-butylphenyl)-2-oxoethyl)-3-hydroxy-2-oxoindolin-1-yl) ethane-1,1-diyldiphosphonate

^{1}H NMR (300 MHz, CDCl$_3$) δ 7.83 (d, J = 8.6 Hz, 2H), 7.44 (d, J = 8.6 Hz, 2H), 7.34 − 7.28 (m, 2H), 6.99 (t, J = 7.5 Hz, 1H), 6.92 (d, J = 7.7 Hz, 1H), 4.64 − 4.47 (m, 2H), 4.29 − 4.00 (m, 8H), 3.85 (dd, J = 65.5, 17.7 Hz, 2H), 3.26 (tdd, J = 23.4, 9.0, 6.7 Hz, 1H), 1.42 − 1.23 (m, 21H) ppm.

^{31}P {^{1}H}-NMR (122 MHz, CDCl$_3$) δ 18.34 (d, J = 7.1 Hz, 1P), 17.87 (d, J = 7.1 Hz, 1P) ppm.
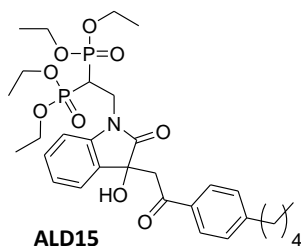
Tetraethyl 2-(3-hydroxy-2-oxo-3-(2-oxo-2-(4-pentylphenyl)ethyl)indolin-1yl) ethane-1,1-diyldiphosphonate

^{1}H NMR (300 MHz, CDCl$_3$) δ 7.81 (d, *J* = 8.3 Hz, 2H), 7.31 (td, *J* = 7.5, 1.0 Hz, 2H), 7.22 (d, *J* = 8.3 Hz, 2H), 7.00 (t, *J* = 7.2 Hz, 1H), 6.92 (d, *J* = 7.8 Hz, 1H), 4.55 (tt, *J* = 14.5, 8.3 Hz, 2H), 4.29 – 3.99 (m, 8H), 3.84 (dd, *J* = 63.8, 17.8 Hz, 2H), 3.26 (tdd, *J* = 23.4, 8.8, 6.7 Hz, 1H), 2.62 (dd, *J* = 14.4, 6.4 Hz, 2H), 1.60 (dt, *J* = 15.1, 7.4 Hz, 3H), 1.39 – 1.26 (m, 14H), 0.88 (t, *J* = 6.8 Hz, 3H) ppm.

^{31}P {^{1}H}-NMR (122 MHz, CDCl$_3$) δ 18.35 (d, *J* = 7.1 Hz, 1P), 17.88 (d, *J* = 7.1 Hz, 1P) ppm.

^{13}C {^{1}H}-NMR (75 MHz, CDCl$_3$) δ 196.96 (s), 176.86 (s), 149.42 (s), 142.27 (s), 134.04 (s), 131.40 (s), 129.32 (s), 128.65 (s), 128.28 (s), 123.54 (s), 122.84 (s), 109.00 (s), 73.40 (s), 63.30 (d, *J* = 2.6 Hz), 63.21 (d, *J* = 2.4 Hz), 62.96 (d, *J* = 6.6 Hz), 62.67 (d, *J* = 6.7 Hz), 44.12 (s), 35.96 (s), 31.38 (s), 30.70 (s), 22.46 (s), 16.29 (d, *J* = 4.8 Hz), 13.96 (s) ppm.
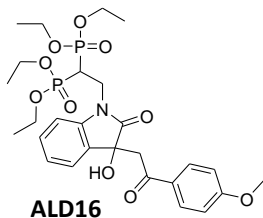
Tetraethyl 2-(3-hydroxy-3-(2-(4-methoxyphenyl)-2-oxoethyl)-2-oxoindolin-1-yl) ethane-1,1-diyldiphosphonate

^{1}H NMR (300 MHz, CDCl$_3$) δ 7.87 (d, *J* = 9.0 Hz, 2H), 7.36 – 7.28 (m, 2H), 7.12 (dd, *J* = 8.3, 6.1 Hz, 1H), 7.00 (t, *J* = 7.5 Hz, 1H), 6.95 – 6.84 (m, 2H), 4.62 – 4.45 (m, 2H), 4.34 – 3.98 (m, 8H), 3.95 – 3.64 (m, 5H), 3.40 – 2.99 (m, 1H), 1.41 – 1.21 (m, 12H) ppm.

^{31}P {^{1}H}-NMR (122 MHz, CDCl$_3$) δ 18.35 (d, *J* = 7.0 Hz, 1P), 17.92 (d, *J* = 7.0 Hz, 1P) ppm.
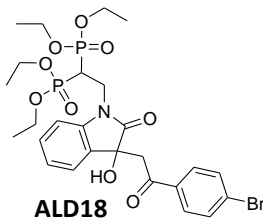
Tetraethyl 2-(3-(2-(4-bromophenyl)-2-oxoethyl)-3-hydroxy-2-oxoindolin-1-yl) ethane-1,1-diyldiphosphonate

^{1}H NMR (300 MHz, CDCl$_3$) δ 7.84 – 7.67 (m, 2H), 7.61 – 7.50 (m, 2H), 7.31 (t, *J* = 7.6 Hz, 2H), 7.02 (t, *J* = 7.6 Hz, 1H), 6.92 (d, *J* = 7.7 Hz, 1H), 4.56 (tt, *J* = 14.7, 8.1 Hz, 2H), 4.29 – 3.98 (m, 8H), 3.83 (dd, *J* = 58.0, 17.8 Hz, 2H), 3.41 – 3.13 (m, 1H), 1.41 – 1.24 (m, 12H) ppm.

^{31}P {^{1}H}-NMR (122 MHz, CDCl$_3$) δ 18.20 (d, *J* = 7.9 Hz, 1P), 17.68 (d, *J* = 8.0 Hz, 1P) ppm.

^{13}C {^{1}H}-NMR (75 MHz, CDCl$_3$) δ 196.14 (s), 176.79 (s), 142.22 (s), 135.02 (s), 131.94 (s), 131.21 (s), 129.65 (s), 129.45 (s), 128.82 (s), 123.49 (s), 122.93 (s), 109.01 (s), 77.21 (s), 73.18 (s), 63.28 (d, *J* = 6.5 Hz), 62.99 (d, *J* = 6.5 Hz), 62.64 (d, *J* = 6.8 Hz), 44.22 (s), 16.42 – 16.13 (m) ppm.
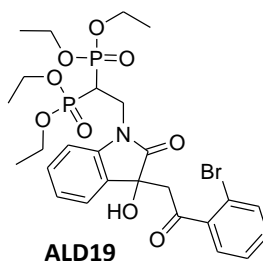
Tetraethyl 2-(3-(2-(2-bromophenyl)-2-oxoethyl)-3-hydroxy-2-oxoindolin-1-yl)ethane-1,1-diyldiphosphonate

^{1}H NMR (300 MHz, CDCl$_3$) δ 7.64 – 7.51 (m, 1H), 7.47 – 7.26 (m, 5H), 7.04 (t, *J* = 7.5 Hz, 1H), 6.91 (d, *J* = 7.8 Hz, 1H), 4.54 (ddd, *J* = 23.0, 14.3, 8.5 Hz, 2H), 4.29 – 4.00 (m, 8H), 3.80 (dd, *J* = 62.1, 17.6 Hz, 2H), 3.41 – 3.02 (m, 1H), 1.41 – 1.21 (m, 12H) ppm.

^{31}P {^{1}H}-NMR (122 MHz, CDCl$_3$) δ 18.32 (d, *J* = 7.0 Hz, 1P), 17.80 (d, *J* = 6.9 Hz, 1P) ppm.

ALD20
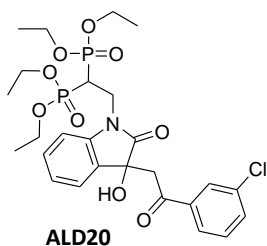
Tetraethyl 2-(3-(2-(3-chlorophenyl)-2-oxoethyl)-3-hydroxy-2-oxoindolin-1-yl)ethane-1,1-diyldiphosphonate

^{1}H NMR (300 MHz, CDCl$_3$) δ 7.87 (dd, J = 4.0, 2.1 Hz, 1H), 7.78 (d, J = 7.8 Hz, 1H), 7.55 – 7.50 (m, 1H), 7.41 – 7.24 (m, 4H), 7.02 (t, J = 7.5 Hz, 1H), 6.92 (d, J = 8.2 Hz, 1H), 4.55 (tdd, J = 14.3, 11.9, 5.6 Hz, 2H), 4.30 – 4.00 (m, 7H), 3.84 (m, 2H), 3.36 – 3.13 (m, 1H), 1.45 – 1.19 (m, 12H) ppm.

^{31}P {^{1}H}-NMR (122 MHz, CDCl$_3$) δ 18.20 (d, J = 8.0 Hz, 1P), 17.69 (d, J = 7.9 Hz, 1P) ppm.

^{13}C {^{1}H}-NMR (75 MHz, CDCl$_3$) δ 195.94 (s), 176.75 (s), 142.24 (s), 137.77 (s), 134.99 (s), 133.43 (s), 133.04 (s), 131.14 (s), 129.94 (s), 129.47 (s), 128.31 (s), 126.25 (s), 123.49 (s), 122.94 (s), 109.02 (s), 73.18 (s), 63.27 (d, J = 6.6 Hz), 62.99 (d, J = 6.5 Hz), 62.64 (d, J = 6.7 Hz), 44.36 (s), 36.44 (s), 26.65 (s), 16.45 – 16.13 (m) ppm.

5.3.10   *Tetraethyl-3-nitro-propane-1,1-bisphosphonate (γ-NO$_2$BP)*

1,8 mg (0.033 mmol, 1 eq) of sodium methylate was dissolved in nitromethane (0,62 mL, 350 eq, anhydrified with CaCl$_2$ and distilled) and 1 mL of dry THF was added. After stirring for 1 hour, 100 mg of VBP (10 eq) was added to the mixture very quickly. After stirring for two additional hours at r.t., 1 mL of saturated NH$_4$Cl solution was poured in and then nitromethane and THF was removed under reduced pressure. Precipitate was dissolved by adding water. The aqueous solution was extracted with chloroform (4 x 1 mL) and the organic phase was dried over Na$_2$SO$_4$ and solvent evaporated. The crude product, a clear oil, is used without any purifications. This procedure was repeated in multigram scale using 2 g of VBP.
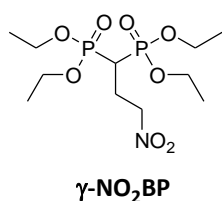
Tetraethyl-3-nitro-propane-1,1-bisphosphonate
^{1}H NMR (500 MHz, CDCl$_3$) δ 4.70 (t, J = 6.9 Hz, 2H), 4.20 (s, 8H), 2.64–2.44 (m, 3H), 1.35 (t, J = 6.9 Hz, 12H) ppm.
^{31}P {1H}-NMR (202 MHz, CDCl$_3$) δ 21.49 (s, 2P) ppm.
MS ESI, m/z: 361.9 [M+H]$^+$, 333.8 [M -CH$_2$CH$_3$+H]$^+$.

γ-NO$_2$BP

5.3.11   *Tetraethyl-3-amino-propane-1,1-bisphosphonate (γ-NH$_2$BP)*

The nitro compound γ-NO$_2$BP (50 mg, 6.5 eq) was dissolved in 5 mL of methanol containing a few drop of water and 45 mg of the catalyst (10% Pd on charcoal, 51% H$_2$O) was added. The system was degassed and then put under hydrogen atmosphere. The reaction proceeds at r.t. in 1 hour with vigorous stirring. The catalyst was filtered off and the resulting solution was evaporated to give the crude product, a clear oil, that was used without any purifications.
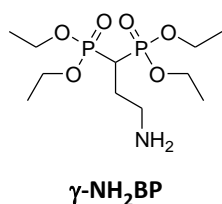
Tetraethyl-3-amino-propane-1,1-bisphosphonate
^{1}H NMR (500 MHz, CDCl$_3$) δ 4.20 (s, 8H), 3.08 (t, J = 6.6 Hz, 2H), 2.64 (tt, J = 24.2, 6.1 Hz, 1H), 2.27–2.13 (m, 2H), 1.36 (td, J = 7.1, 2.1 Hz, 12H) ppm.
^{31}P {1H}-NMR (202 MHz, CDCl$_3$) δ 23.38 (s, 2P) ppm.
MS ESI, m/z: 332.3 [M+H]$^+$, 354.3 [M +Na]$^+$.

γ-NH$_2$BP

5.3.12   *Tetraethyl-3-azido-propane-1,1-bisphosphonate (γ-N$_3$BP)*

The amino compound γ-NH$_2$BP (0.458 g, 1 eq) was dissolved in 50 mL of a solution of water in methanol (H$_2$O/MeOH 2/8 v/v) and 36,7 mg of the CuSO$_4$ catalyst (15% mol) was added under stirring. To the system was added in order 0.580 g (2 eq.) of ISA-HCl and 0.572 g (3 eq.) of K$_2$CO$_3$ (pH 8/10). After stirring overnight, the blue solution was diluted with water (50 ml) and extracted with EtOAc (3 × 50 ml). The organic phases were washed

with saturated aqueous brine (1 × 50 ml), dried (Na$_2$SO$_4$), filtered and concentrated in vacuo to give γ-N$_3$BP (0.3935 g, 80%) as a yellow oil. γ-N$_3$BP was purified by automated column chromatography under below conditions:

Experimental conditions for automated column chromatography	
column:	Silica 12g
Flow Rate:	30 mL/min
carrier	Ethyl acetate-Methanol
0-2 min	0% methanol
2-8 min	20% methanol
8-14 min	20% methanol

For the synthesis of ISA-HCl was followed the procedure reported by Goddard-Borger et al. [334]
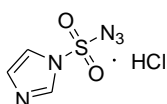
Imidazol sulphony azide hydrochloridric salt
^{1}H-NMR (500 MHz, D$_2$O): δ 8.62-8.38 (m, 1H), 7.66 (s, 1 H), 7.22 (s, 1H) ppm.
MS ESI, m/z: 174.1 [M+H]$^+$.

ISA-HCl
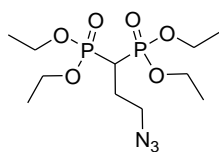
Tetraethyl-3-azido-propane-1,1-bisphosphonate
^{1}H NMR (500 MHz, CDCl$_3$) δ 4.26 – 4.12 (m, 8H), 3.58 (t, J = 6.8 Hz, 2H), 2.50 (tt, J = 23.9, 6.3 Hz, 1H), 2.18 (qd, J = 13.4, 6.6 Hz, 2H), 1.36 (t, J = 7.0 Hz, 12H) ppm.
^{31}P {1H}-NMR (202 MHz, CDCl$_3$) δ 22.78 (s, 2P) ppm.
MS ESI, m/z: 358.2 [M+H]$^+$.

γ-N$_3$BP

5.3.13 *Tetraethyl 3-(4-(2-hydroxyethyl)-1H-1,2,3-triazol-1-yl)propane-1,1-diyldiphosphonate (TRIA1)*

In a round bottom flask equipped with magnetic stir bar and condenser, 12,3 mg (0.034 mmol, 1 eq) of γ-N$_3$BP was dissolved in 2 mL of water/isopropanol 1:1 mixture. 4,8 µL of 3-butyn-1-ol (2 eq.), 5,5 mg of CuSO$_4$ (1 eq.) and 13,6 mg of ascorbic acid (2 eq.) were added to the mixture under vigorous stirring. Mixture was heated at 50°C for 2 hours and the crude was concentrated under reduced pressure. Resulting oil was dissolved by adding dichloromethane (5 mL) and washed with 5 mL of EDTA aqueous solution. The organic phase was dried over Na$_2$SO$_4$ and solvent evaporated.
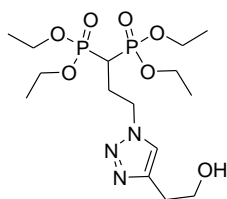
Tetraethyl 3-(4-(2-hydroxyethyl)-1H-1,2,3-triazol-1-yl)propane-1,1-diyldiphosphonate
^{1}H NMR (500 MHz, CDCl$_3$) δ 7.63 (s, 1H), 4.68 (t, J = 6.8 Hz, 2H), 4.22 – 4.13 (m, 8H), 3.95 (t, J = 5.6 Hz, 2H), 3.02 (t, J = 5.7 Hz, 2H), 2.60 – 2.46 (m, 2H), 2.30 (tt, J = 24.2, 5.9 Hz, 1H), 1.35 (td, J = 7.0, 2.8 Hz, 12H) ppm.
^{31}P {1H}-NMR (202 MHz, CDCl$_3$) δ 21.96 (s) ppm.
MS ESI, m/z: 428.6 [M+H]$^+$, 450.5 [M+Na]$^+$.

TRIA1

5.3.14 Tert-butyl 5-((1-(3,3-bis(diethoxyphosphoryl)propyl)-1H-1,2,3-triazol-4-yl)methyl)-1,4-dioxo-3,6-diphenyl-4,5-dihydropyrrolo[3,4-c]pyrrole-2(1H)-carboxylate (TRIA2)

In a round bottom flask equipped with magnetic stir bar and condenser, 37.8 mg (0.1 mmol, 1 eq) of γ-N₃BP was dissolved in 6 mL of water/isopropanol 1:1 mixture. 50 mg (1.1 eq.) of DPPBoc, 18,5 mg of $CuSO_4$ (1.1 eq.) and 46 mg of ascorbic acid (2.2 eq.) were added to the mixture under vigorous stirring. Mixture was heated at 50°C for 2 hours and the crude was concentrated under reduced pressure. Resulting red oil was dissolved by adding dichloromethane (5 mL), dried over Na_2SO_4 and concentrated again.

TRIA2 was purified by automated column chromatography under below conditions resulting in partial loss of Boc group:

Experimental conditions for automated column chromatography	
column:	Silica 24g
Flow Rate:	35 mL/min
carrier	Ethyl acetate-Methanol
0-5 min	0% methanol
5-10 min	10% methanol
10-17 min	10% methanol
17-20 min	20% methanol
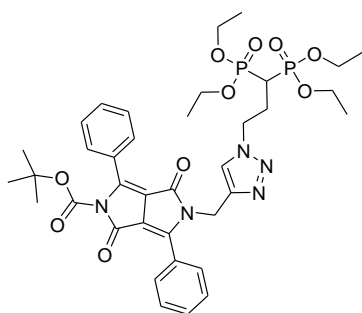
TRIA2

Tert-butyl 5-((1-(3,3-bis(diethoxyphosphoryl)propyl)-1H-1,2,3-triazol-4-yl)methyl)-1,4-dioxo-3,6-diphenyl-4,5-dihydropyrrolo[3,4-c]pyrrole-2(1H)-carboxylate

¹H NMR (500 MHz, CDCl₃) δ 8.10 – 8.06 (m, 2H), 7.80 – 7.76 (m, 2H), 7.75 (s, 1H), 7.58 – 7.55 (m, 2H), 7.52 – 7.48 (m, 4H), 4.99 (s, 2H), 4.61 (t, J = 7.2 Hz, 2H), 4.21 – 4.12 (m, 8H), 2.49 (ddt, J = 16.4, 14.1, 6.9 Hz, 2H), 2.40 – 2.26 (tt, 23.8, 6.3 Hz, 1H), 1.41 (s, 9H), 1.32 (td, J = 7.1, 3.5 Hz, 12H) ppm.

³¹P {1H}-NMR (202 MHz, CDCl₃) δ 22.04 (s) ppm.

MS ESI, m/z: 784.3 [M+H] ⁺, 806.2 [M+Na] ⁺, 684.4 [M-Boc+H] ⁺.

5.3.15 3-(4-((1,4-dioxo-3,6-diphenyl-4,5-dihydropyrrolo[3,4-c] pyrrol-2(1H)-yl)methyl)-1H-1,2,3-triazol-1-yl)propane-1,1-diyldiphosphonic acid (FLUOProbe)

In a pear flask equipped with magnetic stir bar and condenser, 191.6 mg (0.24 mmol, 1 eq) of TRIA2 was dissolved in 9 mL of anhydrous acetonitrile. 516 μL (d: 1.16 g/mL, 16 eq.) of TMSiBr were added. Mixture was strirred at 60°C under microwaves irradiation for 20 minutes. Solvent was evaporated under reduced pressure and to the sylil intermediate, 10 mL of water/methanol 1:1 solution was added. Mixture was stirred for 4 hours at room temperature and concentrated under reduced pressure.
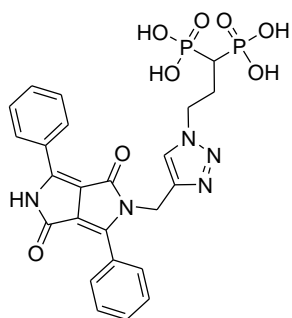
FLUOProbe

3-(4-((1,4-dioxo-3,6-diphenyl-4,5-dihydropyrrolo[3,4-c] pyrrol-2(1H)-yl) methyl)-1H-1,2,3-triazol-1-yl)propane-1,1-diyldiphosphonic acid

^{1}H NMR (500 MHz, DMSO-d6) δ 11.31 (s, 1H), 8.50 – 8.41 (m, 2H), 7.98 – 7.95 (m, 2H), 7.93 (s, 1H), 7.60 – 7.55 (m, 6H), 4.96 (s, 2H), 4.57 – 4.51 (m, 2H), 2.21 (qd, J = 15.5, 7.3 Hz, 2H), 2.07 – 1.94 (tt, 22.3, 6.6 Hz 1H) ppm.

^{31}P NMR (202 MHz, DMSO-d6) δ 19.49 (s, 2P) ppm.

MS ESI, m/z: 570.5 [M-H]$^-$.

Elemental Analysis $C_{24}H_{23}N_5O_8P_2$: Calculated C, 50.45; H, 4.06; N, 12.26; O, 22.40; P, 10.84; Found: C, 42.28; H, 4.17; N, 10.34

Chemical Formula Calculated: $C_{24}H_{23}N_5O_8P_2(HBr)(H_2O)_2$

6. <u>ACKNOWLEDGEMENTS</u>

7. <u>REFERENCES</u>

1 G. Brum, L. McKane, G. Karp, "*Biologia*", Zanichelli, Bologna, **2002**, pp. 319-324.

2 J. R. Porter, *Biothechnol. Prog.,* **2009***, 25*, 1539 - 1560.

3 D. A. Williams, T. L. Lemke, "*Foye's principi di chimica farmaceutica*", Piccin, Padova, **2005**, pp. 739-749.

4 T.A. Einhorn, R. Marcus, D. Feldman, J. Kelsey, "*Osteoporosis",* Elsevier Academic Press, San Diego, **2008**, pp. 3-22.

5 J.K. Gong, J.S. Arnold, S.H. Cohn, *Anat. Rec.*, **1964**, 149, 325-332.

6 H. Ou-Yang, E.P. Paschalis, W.E. Mayo, A.L. Boskey, *J. Bone Miner. Res.*, **2001**, 16, 893-900.

7 A.L. Boskey, S. Gadaleta, C. Gundberg, S.B. Doty, *Bone*, **1998**, 23, 187-196.

8 H. Fleish, "*Bisphosphonates in bone disease*", Academic Press, San Diego, **2000**, pp. 1-21.

9 E.J. Mackie, *Int. J. Biochem. Cell Biol.*, **2003**, 35, 1301-1305.

10 M. Tate, T. A. Adamson Jr. and T. W. Bauer, *Int. J. Biochem. Cell Biol*., **2004**, 36, 1–8.

11 J. M. Quinn, M. T. Gillespie, *Biochem. Biophys. Res. Commun*., **2005**, 328, 739–745.

12 G.D. Roodman, *Endocr. Rev.*, **1996**, 17, 308-332.

13 T.A. Einhorn, R. Marcus, D. Feldman, J. Kelsey, "*Osteoporosis",* Elsevier Academic Press, San Diego, **2008**, pp. 151-167.

14 A.M. Parfitt, *Med. J.*, **1988**, 36, 143–144.

15 A.M. Parfitt, G.R. Mundy, G.D. Roodman, D.E. Hughes, B.F. Boyce, J. Bone Min. Res., **1996**, 11, 150-160.

16 T.A. Einhorn, R.J. Majeska, *Clin. Orthop.Relat. Res*., **1991**, 262, 286–297.

17 H.K. Walker, W.D. Hall, J.W. Hurst, "*Clinical Methods: The History, Physical, and Laboratory Examinations 3rd edition*" Butterworths, Boston, **1990**.

18 G.R. Mundy, T.J. Martin, "*Physiology and Pharmacology of Bone*", Springer, Berlin, **1993**.

19 T. Wada, T. Nakashima, N. Hiroshi, J.M. Penninger, *Trends Mol. Med*., **2006**, 12, 17–25.

20 T. J. Martin, N. A. Sims, *Trends Mol. Med*., **2005**, 11,76–81.

21 G. J. Atkins, P. Kostakis, B. Pan, A. Farrugia, S. Gronthos, A. Evdokiou, K. Harrison, D.M. Findlay, A.C. Zannettino, *J. Bone Miner. Res*., **2003**, 18, 1088–1098.

22 FAO/WHO: Human Vitamin and Mineral Requirements, **2002**.

23 J. Rubin, C. Rubin, C. R. Jacobs, *Gene*, **2006**, 367, 1–16.

24 J. A. Kanis, L. J. Melton, C. Christiansen, C. C. Johnston, N. Khaltaev., *J. Bone Miner. Res.*, **1994**, 1137–1141.

25 NIH consensus statement, *J.Am.Med.Ass.*, **2001**, 285, 785–795 .

26 F. Albright, E.C. Reifenstein, *"The Parathyroid Glands and Metabolic Bone Disease: Selected Studies."*, Williams and Wilkins, Baltimore, **1948**.

27 B.L. Riggs, H.W. Wahner, E. Seeman, K.P. Offord, W.L. Dunn,L.J. Melton, *J. Clin. Invest.*, **1982**, 70, 716–723.

28 H. Fleish, "Bisphosphonates in bone disease", Academic Press, San Diego, **2000**, pp. 123-159.

29 M.L. Bouxsein, *Osteoporos Int.*, **2003**, 14(Suppl 5), 118–127.

30 J.C. Rice, S.C. Cowin,J.A. Bowman, *J. Biomech.*, **1988**, 21, 155–168.

31 T.M. Keaveny, E.F. Morgan, G.L. Niebur,O.C. Yeh, *Ann. Rev. Biomed. Eng.*, **2001**, 3, 307–333.

32 L. Gibson, *J. Biomech.*, **1985**, 18, 317–328.

33 A. Parfitt, *Calcif. Tissue Int.*, **1984**, 36, 123–128.

34 J.C. Van der Linden, J. Homminga, J.A. Verhaar, H. Weinans, *J. Bone Miner. Res.*, **2001**, 16, 457–465.

35 A.C. Looker, E.S. Orwell, C.C. Johnston, R.L. Lindsay, S.P. Heyse, *J. Bone Miner. Res.*, **1997**, 12, 1761–1768.

36 A.C. Looker, H.W. Wahner, W.L. Dunn, R. Lindsay, *Osteoporosis Int.*, **1998**, 8, 468–489.

37 J.S. Finkelstein, M. Sower, G.A. Greendale, M.L. Lee, B. Ettinger, *J. Clin. Endocrinol.Metab.*, **2002**, 87, 3051–3056.

38 E.S. Orwoll, *"Osteoporosis in Men"*, **1999**, Academy Press, San Diego.

39 M. Lunt, D. Felsenberg, J. Reeve, L. Benevolenskaya, T.W. O'Neill, A.J. Silman, *J. Bone Miner. Res.*, **1997**, 12, 1883–1894.

40 K.E. Ensrud, R.C. Lipschutz, J.A. Cauley, D. Seeley, S.R. Cummings, *Am. J. Med.*, **1997**, 103, 274–280.

41 K.L. Margolis, K.E. Ensrud, P.J. Schreiner, H.K. Tabor, *Ann. Intern. Med.*, **2000**, 133, 123–127.

42 S.R. Cummings, M.C. Nevitt, W.S. Browner, K. Stone, T.M. Vogt, *N. Engl. J. Med.*, **1995**, 332, 767–773.

43 E. Jequier, *Int. J. Obes. Relat.Metab.Disord.*, **2002**, 26(Suppl. 2), S12–S17.

44 WHO, World Health Organization*,"Obesity and overweight Fact sheet N°311"*, **2015**.

45 B. Dawson-Hughes, C. Shipp, L. Sadowski, G. Dallal, *Calcif. Tissue Int.*, **1987**, 40, 310–314.

46 A.P. Hermann, C. Brot, J. Gram, N. Kolthoff, L. Mosekilde, *J. Bone Miner. Res.*, **2000**, 15, 780–787.

47 E.X. Jensen, C. Fusch, P. Jaeger, E. Peheim, F.F. Horber, *J. Clin. Endocrinol.Metab.*, **1995**, 80, 2181–2185.

48 K. Landin-Wilhelmsen, L. Wilhelmsen, G. Lappas, T. Rosen, G. Lindstedt, *Calcif. Tissue Int.*, **1995**, 56, 104–108.

49 E.A. Krall, B. Dawson-Hughes, *J. Bone Miner. Res.*, **1999**, 14, 215–220.

50 R.T. Turner, L.S. Kidder, A. Kennedy, G.L. Evans, J.D. Sibonga, *J. Bone Miner. Res.*, **2001**, 16, 589–594.

51 R.T. Turner, *Alcohol Clin. Exp. Res.*, **2000**, 24, 1693–1701.

52 R.F. Klein, *Alcohol Clin. Exp. Res.*, **1997**, 21, 392–399.

53 R. B. Kimble, *Alcohol Clin. Exp. Res.*, **1997**, 21, 385–391.

54 J.L. Gonzalez-Calvin, A. Garcia-Sanchez, V. Bellot, D. Salvatierra-Rios, *Alcohol Alcoh.*, **1993**,28, 571–579.

55 J.Z. Ilich, R.A. Brownbill, L. Tamborini, Z. Crncevic-Orlic, *J. Am. Coll. Nutr.*, **2002**,21, 536–544.

56 O. Ganry, C. Baudoin, P. Fardellone, *Am. J. Epidemiol.*, **2000**, 151, 773–780.

57 http://www.iofbonehealth.org/

58 N.C. Wright, A.C. Looker, K.G. Saag, E.S. Delzell*, J. Bone Miner. Res.*, **2014**, 29, 2520–2526.

59 A. Svedbom,E. Hernlund, M. Ivergård, J.A. Kanis, M.L. Brandi, F. Silveri, *Arch. Osteoporos.*, **2013**, 8, 137.

60 E. Hernlund, A. Svedbom, M. Ivergård, J.A. Kanis., *Arch. Osteoporos.*, **2013**, 8, 136.

61 A. Randell, P.N. Sambrook, T.V. Nguyen, J.A. Eisman, *Osteoporos. Int.*, **1995**, 5, 427–432.

62 L.J. Melton, *Bone*, **1993**, 14(Suppl 1), S1–8.

63 D. Vanness A. Tosteson, *Topics Geriatric Rehab.*, **2005**, 21, 4–16.

64 Atti Parlamentari Doc. XVII, n. 12 del Senato della Repubblica, **23 maggio 2003**.

65 T.A. Einhorn, R. Marcus, D. Feldman, J. Kelsey, "Osteoporosis", Elsevier Academic Press, San Diego, **2008**, pp. 840-849.

66 B. Shea, D. Bonaiuti, R. Iovine, S. Negrini, V. Robinson, H.C.Kemper, A. Cranney, *Eur. Medicophys.*, **2004**, 40, 199–209.

67 T.A. Einhorn, R. Marcus, D. Feldman, J. Kelsey, "Osteoporosis", Elsevier Academic Press, San Diego, **2008**, pp. 799-836.

68 V. Matkovic, K. Kostial, I. Simonovic, R. Buzina, A. Brodarec,B.E.C. Nordin, *Am. J. Clin. Nutr.*, **1979**, 32, 540–549.

69 M.C. Chapuy, M.E. Arlot, F. Duboeuf, *N. Engl. J. Med.*, **1992**, 327, 1637.

70 K.L. Tucker, M.T. Hannan, H. Chen, *Am. J. Clin. Nutr.*, **1999**, 69, 727-736.

71 M.S. Morris, P.F. Jacques, J. Selhub, *Bone*, **2005**, 37, 234-242

72 J. Iwamoto, T. Takeda, Y. Sato, *Curr. Pharm. Des.*, **2004**, 10, 2557-2576.

73 J.R. Zanchetta, C.E. Bogado, J.L. Ferretti, O. Wang, S.L. Myers, *J. Bone Miner. Res.*, **2003**, 18, 539-543.

74 M.R. Vickers, A.H. MacLennan, B. Lawton, T.W. Meade, *BMJ*, **2007**, 335, 239-250.

75 K.E. Ensrud, J.L. Stock, E. Barrett-Connor, J.A. Cauley, *J. Bone Miner. Res.*, **2008**, 23, 112-120.

76 P.D. Miller, A.A. Chines, C. Christiansen, H.C. Hoeck, P.D. Delmas, *J. Bone Miner. Res.*, **2008**, 23,525-535.

77 P.J. Meunier, D.O. Slosman, P.D. Delmas, J.L. Sebert, J.Y. Reginster, *J. Clin. Endocrinol.Metab.*, **2006**, 87, 2060-2066.

78 S.R. Cummings, J. San Martin, M.R. McClung, C. Christiansen, *N. Engl. J. Med.*, **2009**, 361, 756-765.

79 H. Fleisch, R. G. Russell, M. D. Francis, *Science*, **1969**, 165, 1262–1264.

80 H. Fleisch, W.F. Neuman, *Am. J. Physiol.*, **1961**, 200, 1296–1300.

81 T.A. Einhorn, R. Marcus, D. Feldman, J. Kelsey, "Osteoporosis", Elsevier Academic Press, San Diego, **2008**, pp. 1725-1742.

82 R.G.G. Russell, M. Rogers, *Bone*, **1999**, 25, 97-106.

83 a) M. Rogers, *Curr. Pharm. Des.*, **2003**, 9, 2643–2658.

    b) G.H. Nancollas, R. Tang, R.G.G. Russell, F.H. Ebetino, *Bone*, **2006**, 38, 617–627.

84 European Medices agency, http://www.ema.europa.eu/ema/

85 F.H. Ebetino, M.D. Francis, M.J. Rogers, *Rev. Contemp. Pharmacother.*, **1999**, 9, 233–243.

86 S.P. Luckman, F.P. Coxon, F.H. Ebetino, *J. Bone Miner. Res.*, **1998**, 13, 1668–1678.

87 E. Van Beek, C. Löwik, I. Que, *J. Bone Miner. Res.*, **1996**, 11, 1492–1497.

88 Y. Zhang, R. Cao, F. Yin, F. Lin, H. Wang, K. Krysiak, J. No, D. Mukkamala, K. Houlihan, J. Li, C.T. Morita, E. Oldfield, *Angew. Chem. Int. Ed.*, **2010**, 49, 1136-1138.

89 B.J. Gertz, S.D. Holland, W.F. Kline, H. Quan, *Clin. Pharmacol.Ther.*, **1995**, 58, 288-298.

90 T. Chen, J. Berenson, R. Vescio, *J. Clin. Pharmacol.*, **2002**, 42, 1228.

91 K. Thompson, M.J. Rogers, F.P. Coxon, *Mol. Pharmacol.,* **2006**, 69, 1624–1632.

92 J.C. Frith, J. Monkkonen, G.M. Blackburn, *J. Bone Miner. Res.*, **1997**, 12, 1358–1367.

93 S.P. Luckman, D.E. Hughes, F.P. Coxon, *J. Bone Miner. Res.*, **1998**, 13, 581–589.

94 E. Van Beek, E. Pieterman, L. Cohen, *Biochem. Biophys. Res. Commun.*, **1999**, 264, 108-111.

95 J.E. Dunford, M.J. Rogers, F.H. Ebetino, R.J. Phipps, *J. Bone Miner. Res.*, **2006**, 21, 684–694.

96 H. Monkkonen, S. Auriola, P. Lehenkari, J. Monkkonen, *Brit. J. Pharmacol.*, **2006**, 147, 437–445.

97 R.G.G. Russell, N.B. Watts, F. H. Ebetino, M.J. Rogers, *Osteoporos. Int.*, **2008**, 19, 733–759.

98 J.M. Rondeau, F. Bitsch, E. Bourgier, M. Geiser, W. Jahnke, *ChemMedChem*, **2006**, 1, 267–273.

99 D.M. Black, A.V. Schwartz, K.E. Ensrud, S.R. Cummings, *JAMA*, **2007**, 296, 2927-2938.

100 H. Fleish, "Bisphosphonates in bone disease", Academic Press, San Diego, **2000**, pp. 56-62.

101 S. Maraka, K.A. Kennel, *BMJ,* **2015**, 351, 3783.

102 B. Cryer, D.C. Bauer, *Mayo Clin. Proc.,* **2002**, 77, 1031-1043.

103 I.R. Reid, G.D. Gamble, P. Mesenbrink, *J. Clin. Endocrinol.Metab.,* **2010**, 95, 4380-4387.

104 FDA drug safety communication, 2011, www.fda.gov/Drugs/DrugSafety/ucm270199

105 S. Khosla, D. Burr, J. Cauley, *J. Bone Miner. Res.,* **2007**, 22, 1479-1491.

106 C.J. Crandall, S.J. Newberry, A. Diamant, *Ann. Intern.Med.,* **2014**, 161, 711-723.

107 E. Cohen-Sela, M. Chorny, N. Koroukhov, G. Golomb, *J. Control Release*, **2009**, 133, 90-95.

108 M. Jian, H. Liandong, *J. Pharm. Pharmacology*, **2011**, 63, 400-408.

109 V. Dissette, P. Bozzi, C.A. Bignozzi, A. Dalpiaz, L. Ferraro, L. Pasti, *Eur. J. Pharm. Sci.*, **2010**, 41, 328-336.

110 S. Zhang, G. Gangal, H. Uludag, *Chem. Soc. Rev.*, **2007**, 36, 507-531.

111 M. Capuzzi, D. Perdicchia, K.A. Jørgensen, *Chem. Eur. J.*, **2008**, 14, 128-135.

112 S. Sulzer-Mossè, M. Tissot, A. Alexakis, *Org. Lett.*, **2007**, 9, 3749-3752.

113 M.T. Barros, A.M. Faisca Philllips, *Eur. J. Org. Chem.*, **2008**, 15, 2525-2529.

114 F.H. Ebetino, J.E. Dunford, M.W. Lundy, M. Pozzi, Z. Xia, R. Dobson, *Bone*, **2008**, 42 , 36.

115 B. Heuzé, M. Lemarié, M. Vazeux, M. Gulea, S. Masson, Phosphorus, Sulfur, Silicon and Rel. El., **2009**, 184, 820-829

116 J. J. Brophy, M. J. Gallagher, *Australian Journal of Chemistry*, **1967**, 20, 503-513.

117 O.E.O. Hormi, E.0. Pajiinen, A.C. Avall, P. Pennanen, *Synth. Comm.*, **1990**, 20, 1865-1867.

118 D. Meziane, J. Hardouin, A. Elias, E. Gu´enin, M. Lecouvey, *Heteroatom Chemistry*, **2009**, 20, 369-377.

119 J.B. Rodriguez, *Synthesis*, **2014**, 46, 1129–1142.

120 C.R. Degenhardt, D.C. Burdsall, *J. Org. Chem.,* **1986**,51, 3488-3490.

121 W. Lehnert, *Tetrahedro*n, **1973**, 30, 301-305.

122 D. Lecerclè, M. Sawicki, F. Taran,*Organic Letters*, **2006**, 8, 4283-4285.

123 A. Minto, "*Sintesi catalitiche selettive di bisfosfonati quali potenziali farmaci per il contrasto dell'osteoporosi*", tesi di laurea magistrale, **2012**.

124 J. Huang, M. Zhao, W. Duan, *Tetrahedron Letters*, **2014**, 55, 629–631.

125 H. Xiang,X. Qi,Y. Xie,G. Xub, C. Yang,*Org. Biomol. Chem.*, **2012**, 10, 7730-7738.

126 H. Ding, G. Xu, J. Wang, Y. Zhang, X. Wu, Y. Xie, *Heteroatom Chemistry*, **2004**, 15, 549-555.

127 Z. Xue, Q. Li, H. Tao, C. Wang, *J. Am. Chem. Soc.*, **2011**, 133, 11757–11765.

128 D. Villemin, F. Thibault-Starzyk, E. Esprimont, *Phosphorus, Sulfur and Silicon*, **1992**, 70, 117-120.

129 A. Köckritz, M. Schnell,*Phosphorus, Sulfur and Silicon*, **1992**, 73, 185-194.

130 W.M. Abdou, N.A. Ganoub, A.F. Fahmy, A.A. Shaddy, *Monatshefte für Chemie*, **2006**, 137, 105–116.

131 H. Xiang, J. Qi, Q. He, M. Jiang, C. Yang, L. Denga, *Org. Biomol. Chem.*, **2014**, 12, 4633-4636.

132 W.M. Abdou, A.A. Kamel, M.D. Khidre*, J. Heterocyclic Chem.*, **2015**, 52, 1654-1662.

133 A. Chiminazzo, "*Sintesi catalitiche selettive di bisfosfonati quali potenziali farmaci per il contrasto dell'osteoporosi*", tesi di laurea magistrale, **2012**.

134 S. Pei, C. Xue, L. Hai, Y. Wu,*RSC Adv.*, **2014**, 4, 38055-38058.

135 Y. Jie, L. Nan, C. Dian-Feng, L. Shi-Wei, *Tetrahedron Letters*, **2014**, 55, 2859–2864.

136 S.M. Nicolle, C.J. Moody, *Chem. Eur. J.*, **2014**, 20, 4420–4425.

137 X. Creary, *J. Org. Chem.*, **1987**, 52, 5026-5030.

138 C.E. McKenna, L.A. Khawli, W.Y. Ahmad, P. Pham, *Phosphorus, Sulfur, Silicon Rel. El.*, **1988**, 37, 1-12.

139 O. Bortolini, I. Mulani, A. De Nino, L. Maiuolo, M. Nardi, S. Avnet, *Tetrahedron*, **2011**, 67, 5635-5641.

140 C.E. McKenna, T. Higa, N. Cheung, M. McKenna, *Tetrahedron Lett.*, **1977**, 2, 155-158.

141 D.A. Nicholson, W.A. Cilley, O.T. Quimby, *J. Org. Chem.,* **1970**, 56, 3149-3150.

142 G. Sponchia, E. Ambrosi, A. Del Tedesco, P. Riello, A. Benedetti, *J. Mater. Chem. B*, **2015**,3, 7300-7306.

143 D. Simoni, N. Gebia, F. P. Invidiata, N. Cacamo, F. Dieli, *J. Med. Chem.*, **2008**, 51, 6800–6807.

144 P.C.B. Page, M.J. McKenzie, J.A. Galagher, *J. Org. Chem.*, **2001**, 66, 3704–3708.

145 H.J. Edwards, J.D. Hargrave, S.D. Penrose, C.G. Frost, *Chem. Soc. Rev.*, **2010**, 39, 2093–2105.

146 K. Kikushima, J.C. Holder, M. Gatti, B.M. Stoltz, *J. Am. Chem. Soc.*, **2011**, 133, 6902–6905.

147 G. Berthon, T. Hayashi "Catalytic Asymmetric Conjugate Reactions", Wiley-VCH, Weinheim, **2010,** 1-70.

148 N.R. Vautravers, B. Breit, *Synlett*, **2011**, 17, 2517–2520.

149 H. Zilaout, A. Van den Hogenband, J. de Vries, J.H.M. Lange, J.W. Terpstra, *Tetrahedron Lett.*, **2011**, 52, 5934–5939.

150 a) G.C. Tsui, M. Lautens, *Angew. Chem. Int. Ed.*, **2010**, 49, 8938–8941.

b) G. C. Tsui, F. Menard, M. Lautens, *Org. Lett.*, **2010**, 12, 2456–2459.

c) G. Pattison, G. Piraux, H.W. Lam, *J. Am. Chem. Soc.*, **2010**, 132, 14373-14375.

151 K.J. Wadsworth, F.K. Wood, C.J. Chapman, C.G. Frost, *Synlett*, **2004**, 11, 2022–2024.

152 T. Hayashi, T. Senda, Y. Takaya, M. Ogasawara, *J. Am. Chem. Soc.*, **1999**, 121, 11591-11592.

153 G. Bianchini, A. Scarso, A. Chiminazzo, L. Sperni, G. Strukul, *Green Chem.*, **2013**, 15, 656-662.

154 K. Takatsu, R. Shintani, T. Hayashi, *Angew. Chem. Int. Ed.*, **2011**, 50, 5548-5552.

155 L. Kamm, W. McIlwraith, C. Kawcak, *J. Equine Vet. Sci.*, **2008**, 28, 209-214.

156 D.W. Hutchinson, D.M. Thornton,*J. Organometallic Chemistry*, **1988**, 346,341-348.

157 R. Lenin,R.M. Raju, D.V.N. Srinivasa Rao,U.K. Ray, *Med. Chem. Res.*, **2013**, 22, 1624-1629.

158 C. Leung, A.M. Langille, J. Mancuso, Y.S. Tsantrizos, *Bioorganic & Medicinal Chemistry*, **2013**, 21, 2229–2240.

159 D. Granchi, A. Scarso, G. Bianchini, A. Chiminazzo, G. Di Pompo, S. Avnet, G. Strukul, *Eur. J. Med. Chem.,* **2013**, 65, 448-455.

160 C. Ornelas*, New J. Chem*., **2011**, 35, 1973–1985.

161 M.F.R. Fouda, M.M. Abd-Elzaher, R.A. Abdelsamaia, A.A. Labib, *Appl. Organometal. Chem.* **2007**; 21, 613–625.

162 H.E. Mukaya, X.Y. Mbianda, *J. Inorg. Organomet.Polym*., **2015**, 25, 411–418.

163 M. Recher, A.P. Barboza, M. Ferrer-Casal, J.B. Rodriguez, *Eur. J. Med. Chem*., **2013**, 60, 431-440.

164 E. Boanini, P. Torricelli, M. Gazzano, A. Bigi,*Biomaterials*, **2014**, 35, 5619-5626.

165 C. Capuccini, P. Torricelli, E. Boanini, M. Gazzano, A. Bigi,*J. Biomed. Mater. Res. A*, **2009**, 89, 594-600.

166 E. Boanini, P. Torricelli, M. Gazzano, R. Giardino, A. Bigi, *Biomaterials*, **2006**, 27, 4428–4433.

167 J. Kuljanin, I. Jankovi, J. Nedeljkovic, D. Prstojevic, V. Marinkovic, *J. Pharm. Biomed. Anal.*, **2002**, 28, 1215-1220.

168 R.S. Hong, K.H. Hwang, S. Kim, H.E. Cho, D.C. Moon, *J. Kor. Magn. Reson.*, **2013**, 17, 98-104.

169 V. Molinier, B. Fenet, J. Fitremann, A. Bouchu, Y. Queneau, *Carbohydr. Res*., **2006**, 341, 1890-1895.

170 S. Henzer-Schweizer, N. De Zanche, M. Pavan, A. Henning, *NMR Biomed*., **2010**, 23, 406-413.

171 M.C. Martinez-Bisbal, D. Monleon, M. Piotto, J. Piquer, J.L. Llacer, *NMR Biomed.*, **2009**, 22, 199-206.

172 S.G. Lee, *Bull. Korean Chem. Soc.*, **2007**, 28, 1635-1636.

173 S. Akoka, L. Barantin, M. Trierweiler, *Anal. Chem.*, **1999**, 71, 2554-2557.

174 J. Tsuji, "Palladium Reagents and Catalysts—New Perspectives for the 21st Century", John Wiley & Sons, Chichester, **2004**.

175 G. Knobloch, N. Jabari, S. Stadlbauer, A. Gohla, *Bioorg. Med. Chem*., **2015**, 23, 2819-2827.

176 H. Ding, G. Xu, J. Wang, Y. Zhang, X. Wu, Y. Xie, *Heteroat. Chem.*, **2004**, 15, 549–555.

177 C. Chen, J.M. Fang, *Org. Biomol. Chem.*, **2013**, 11, 7687–7699.

178 H. Xiang, X. Qi, Y. Xie, G. Xu, C. Yang, *Org. Biomol. Chem.*, **2012**, 10, 7730–7738.

179 P. Etayo, A. Vidal-Ferran, *Chem. Soc. Rev.*, **2013**, 42, 728-754.

180 P. Kleman, A. Pizzano, *Tetrahed. Lett*., **2015**, 56, 6944-6963.

181 B.T. Cho,*Aldrichim. Acta*, **2002**, 35, 3-16.

182 H. Xie, A. Song, X. Zhang, X. Chen, H. Li, C. Sheng, W. Wang,*Chem.Commun.*, **2013**, 49, 928-930.

183 S.G. Ouellet, A.M. Walji, D.W.C. MacMillan, *Acc. Chem. Res.*, **2007**, 40, 1327-1339.

184 M. Zhang, L. Chen, Y. You, Z. Wang, D. Yue, X. Zhang, X. Xu, W. Yuan, *Tetrahedron*, **2016**, 72, 2677-2682.

185 L.C. Morrill, L.A. Ledingham, J.P. Couturier, J. Bickel, A.D. Harper, C. Fallan, A.D. Smith, *Org. Biomol. Chem.*, **2014**, 12, 624-636.

186 D. Simoni, N. Gebbia, F.P. Invidiata, M. Eleopra, S. Provera, M. Tolomeo, E. Novellino, J. Dunford, F. Dieli, *J. Med. Chem*., **2008**, 51, 6800-6807.

187 N.H. Khan, R.I. Kureshy, S.H.R. Abdi, S. Agrawal, *Coord. Chem. Rev.*, **2008**, 252, 593-623.

188 A.K. Yadav, L.D.S. Yadav, *Synlett*, **2015**, 26, 1026-1030.

189 M. Morita, L. Drouin, R. Motoki, Y. Kimura, M. Shibasaki, *J. Am. Chem. Soc.*, **2009**, 131, 3858-3859.

190 L.D.S. Yadav, C. Awasthi, A. Ret, *Tetrahed. Lett.*, **2008**, 49, 6360-6363.

191 J. Wang, W. Li, Y. Liu, Y. Chu, L. Lin, X. Feng, *Org. Lett.*, **2010**, 12, 1280-1283.

192 G. Sturtz, J. Guervenou, *Synthesis*, **1991**, 8, 661-662.

193 Y. Liu, S. Shirakawa, K. Maruoka, *Org. Lett.*, **2013**, 15, 1230-1233.

194 Y. Xi, X. Shi, *Chem. Commun.*, **2013**, 49, 8583-8585.

195 A.K. Ghosh, K. Xi, K. Ratia, B.D. Santarsiero, S.C. Baker, A.D. Mesecar, *J. Med. Chem.*, **2005**, 48, 6767-6771.

196 T.J. Senter, M.C. O'Reilly, K.M. Chong, C.W. Lindsley, *Tetrahed. Lett.*, **2015**, 56, 1276-1279.

197 Y. Sohtome, B. Shin, N. Horitsugi, K. Noguchi, K. Nagasawa, *Angew. Chem. Int. Ed.*, **2010**, 49, 7299-7303.

198 G.A. Molander, S.K. Pack, *Tetrahedron*, **2003**, 59, 10581-10591.

199 S. Laval, W. Dayoub, A. Favre-Reguillon, M. Berthod, P. Demonchaux, M. Lemaire, *Tetrahed. Lett*., **2009**, 50, 7005-7007.

200 A. Lauria, R. Delisi, F. Mingoia, A. Terenzi, G. Barone, A.M. Almerico, *Eur. J. Org. Chem*., **2014**, 16, 3289-3306.

201 R. Alvarez, S. Velazquez, E. De Clercq, A. Karlsson, M.J. Camaras, *J. Med. Chem.*, **1994**, 37, 4185-4194.

202 M.J. Genin, D.A. Allwine,C.J. Hamel, D. Stapert, B.H. Yagi, *J. Med. Chem*., **2000**, 43, 953-970.

203 V.V. Rostovtsev, L.G. Green, V.V. Fokin, K.B. Sharpless, *Angew. Chem. Int. Ed*., **2002**, 41, 2596-2599.

204 C.W. Tornoe, C. Christensen, M. Meldal, *J. Org. Chem*., **2002**, 67, 3057-3064.

205 C. Xu, C. Yuan, *Eur. J. Org. Chem*., **2004**, 4410-4415.

206 J. Mortier, *Org. Lett*., **1999**, 7, 981-984.

207 B. Chamberlain, T. Upton, B. Kashemirov, C. McKenna,*J. Org. Chem*., **2011**, 76, 5132-5135.

208 J.P. Gourves, H. Couthon, G. Sturtz, *Phosph.Sul.Sil. Rel. Elem*., **1998**, 132, 219-229.

209 X. Chen, X. Li, J. Yuan, L. Qu, S. Wang, H. Shi, Y. Tang, L. Duan, *Tetrahedron*, **2013**, 69, 4047-4052.

210 M. Ferrer-Casal, A.P. Barboza, S.H. Szajnman, J.B. Rodriguez, *Synthesis*, **2013**, 45, 2397-2404.

211 D. Faulkner, *Nat. Prod. Rep*., **1999**, 16, 155-198.

212 a) J.H. Wynne, W.M. Stalick, *J. Org. Chem.*, **2002**, 67, 5850-5853.

b) A. Kumar, S. Sharma, R.A. Maurya, *Tetrahedron Lett*., **2009**, 50, 5937-5940.

c) Z. Wang, A.J. Kochanowska-Karamyan, M.T. Hamann, *Chem. Rev.*, **2010**, 110, 4489-4497.

213 a) J. Zhou, M. Ye, Z. Huang, Y. Tang, *J. Org. Chem.*, **2004**, 69, 1309-1320;

b) H. Kim, S. Kim, K. Oh, *Angew. Chem. Int. Ed.*, **2010**, 49, 4476-4478.

214 a) Y. Zhou, X. Sun, B. Zhu, J. Zheng, J. Zhou, Y. Tang, *Synlett*, **2011**, 935-938.

b) L. Liu, J. Li, M. Wang, F. Du, Z. Qin, B. Fu, *Tetrahedron: Asymm*., **2011**, 22, 550-557.

215 K.A. Jorgensen, *Synthesis*, **2003**, 1117-1125.

216 L. Wen, Q. Shen, X. Wan, L. Lu, *J. Org. Chem.*, **2011**, 76, 2282-2285.

217 H. Couthon-Gourv, G. Simon, J. Haelters, B. Corbel, *Synthesis*, **2006**, 81-88.

218 K. Manabe, N. Aoyama, S. Kobayashi, *Adv. Synth.Catal*., **2001**, 343, 174-176.

219 H. Johansson, T. Bogelov Jorgensen, D.E. Gloriam, D. Sejer Pedersen, *RSC Adv.*, **2013**, 3, 945-960.

220 J.Q. Weng, R.J. Fan, Q.M. Deng, R.R. Liu, Y.X. Jia, *J. Org. Chem.*, **2016**, 81, 3023-3030.

221 C.A. Palmerini, F. Tartacca, L. Granieri, A. Scrascia, S. Lepri, *Eur. J. Med. Chem.*, **2015**, 102, 403-412.

222 R. Huisgen, *Angew. Chem.*, **1963**, 2, 633-645.

223 O. Diels, K. Alder, *Liebigs Ann. Chem.*, **1928**, 460, 98-122.

224 M. Shankar Singh, S. Chowdhury, S. Koley, *Tetrahed.*, **2016**, 1603–1644.

225 R. Ruzziconi, G. Rici, A. Gioiello, H. Couthon-Gourvès, J.P. Gourvès, *J. Org. Chem.*, **2003**, 68, 736-742.

226 R.Y. Zhu, C.S. Wang, F. Jiang, F. Shi, S.J. Tu, *Tetrahed. Asymm.*, **2014**, 25, 617-624.

227 J. Adrio, J.C. Carretero, *Chem. Commun.*, **2014**, 50, 12434-12446.

228 R. Grigg, J. Kemp, G. Sheldrick, J. Trotter, *J. Chem. Soc., Chem. Commun.*, **1978**, 109-111.

229 G. Li, M. Wu, D. Kong, R. Liu, X. Zhou, F. Liu, *New J. Chem.,* **2014**, *38*, 3350-3353.

230 A.R. Katritzky, C.A. Ramsden, J.A. Joule, V.V. Zhdankin, "*Handbook of Heterocyclic Chemistry*", Elsevier, Oxford, **2010**.

231 S. Sadjadi, M.M. Heravi, N. Nazari, *RSC Adv.*, **2016**, 6, 53203-53272.

232 A. Dömling, Chem. Rev., **2006**, 106, 17-89.

233 I. Ugi, R. Meyr, U. Fetzer, C. Steinbrückner, *Angew. Chem.*, **1959**, 71, 386.

234 I. Ugi, C. Steinbrückner, Angew. Chem., **1960**, 72, 267-268.

235 V.P. Boyarskiy, N.A. Bokach,K.V. Luzyanin, V.Y. Kukushkin, Chem. Rev., **2015**, 115, 2698-2779.

236 B.P. Dalvi, L. Shu-Fen, P. Vijaykumar. S. Chung-Ming, *ACS Comb. Sci.*, **2015**, 17, 421-425.

237 M. Rouhania, A. Ramazania, S. Woo, *Ultrason. Sonochem.*, **2015**, 22, 391-396.

238 L.A. Polindara-García, E. Juaristi, *Eur. J. Org. Chem.*, **2016**, 6, 1095-1102.

239 R. Ramozzi, N. Che´ron,P.C. Hibertyd, P. Fleurat-Lessard, *New J. Chem.*, **2012**, 36, 1137-1140.

240 V. Ruth Pinney, Patent US6352032 B1, **March 2002**.

241 A.M. van Leusen, H. Siderlus, B.E. Hoogenboom, D. van Leusen, *Tetrahed. Lett*, **1972**, 52, 5337-5340.

242 M.J. Fan, B. Qian,L.B. Zhao, Y.M. Liang, *Tetrahedron*, **2007**, 63, 8987–8992.

243 a) U. Schollkopf,P.H. Porsch, *Chem. Ber.*, **1973**, 106, 3382-3390.

   b) U. Schollkopf, K. Hantke, *Liebigs Ann. Chem.*, **1973**, 1571-1582.

244 X. Zhao, X. Liu, H. Mei, J. Guo, L. Lin, X. Feng, *Angew. Chem. Int. Ed.*, **2015**, 54, 4032–4035.

245 J. Li, Y. Liu, C. Li, X. Jia, *Adv. Synth.Catal.*, **2011**, 353, 913–917.

246 Y. Wang, R.K. Kumar, X. Bi, *Tetrahedron Lett.*, **2016**, 57, 5730–5741.

247 R. Grigg, M.I. Lansdell, M. Thornton-Pett, *Tetrahedron*, **1999**, 55, 2025-2044.

248 C. Arróniz, A. Gil-González, V. Semak, C. Escolano, M. Amat, *Eur. J. Org. Chem.*, **2011**, 3755-3760.

249 C. Del Fiandra,M. Moccia,V. Cerullia, M.F.A. Adamo, *Chem. Commun.*, **2016**, 52, 1697-1700.

250 A. Dehnel, J. Kanabus-Kaminska, G. Lavielle, *Can. J. Chem.*, **1988**, 66, 310-318.

251 N. Ischia, A. Palumbo, G. Prota, *Tetrahedron*, **1988**, 44, 6441-6446.

252 J. F. M. Da Silva, S. J. Garden, A. C. Pinto, *J. Braz. Chem. Soc.*, **2001**, 12, 273-324.

253 a) M.S. Majik, C. Rodrigues, S. Mascarenhas, L. D'Souza, *Bioorg.Chem.*, **2014**, 54, 89-95.

   b) H.M. Zhang, H. Dai, P.J. Hanson, M.G. Hemida, Y. Tong , D. Yang, *ACS Chem. Bio.*, **2014**, 9, 1015-1024.

c) M. Kidwai, A. Jain, V. Nemaysh, R. Kumar, P.M. Luthra, *Med. Chem. Res*., **2013**, 22, 2717-2723.

254 S.N. Pandeya, P. Yogeeswari, E. De-Clercq, M. Wivrouw, *Chemother*., **1999**, 45, 192-196.

255 S. N. Pandeya, D. Sriram, G. Nath, E. De-Clercq, *Indian J. Pharm. Sci*., **1999**, 61, 358-361.

256 R. S. Varma, W. L. Nobles, *J. Med. Chem*., **1967**, 10, 972-974.

257 M. Flores, J. Pena, P. García-García, N.M. Garrido, D. Diez, *Curr. Org. Chem*., **2013**, 17, 1957-1985.

258 M.M.M. Santos, *Tetrahedron*, **2014**, 70, 9735-9757.

259 a) J. Frederick, D. Carlo, H.G. Lindwall, *J. Am. Chem. Soc*. **1945**, 67, 199-201.

b) G. Imanzadeh, T. Aghaalizadeh, M. Zamanloo, Y. Mansoori*, J. Chil. Chem. Soc*., **2011**, 56, 616-620.

c) C.Gang, T. Ying, Z. Jie, W. Ya, H. Xiao-Jiang, M. Shu-Zhen, *Lett. Org. Chem*., **2011**, 8, 614-617.

260 a) M.M. Heravi, S. Asadi, *Tetrahedron Asymm*., **2012**, 23, 1431-1465.

b) Y. Liu, P. Gao, J. Wang, Q. Sun, Z. Ge, R. Li, *Synlett*, **2012**, 23, 1031–1034.

261 T. Itoh, H. Ishikawa, Y. Hayashi, *Org. Lett.*, **2009**, 11, 3854-3857.

262 L. Li, S. Gou, F. Liu, *Tetrahedron Asymm*., **2014**, 25, 193-197.

263 Q. Guo, J. C.G. Zhao, *Tetrahedron Lett*., **2012**, 53, 1768-1771.

264 S. Abbarajua, J. C.G. Zhao, *Adv. Synth.Catal*., **2014**, 356, 237-241.

265 Y. Lu, Y. Ma, S. Yang, M. Ma, H. Chu, C. Song, *Tetrahedron Asymm*., **2013**, 24, 1082-1088.

266 G. Qunsheng, B. Mayur, Z. Cong-Gui, *Angew. Chem. Int. Ed.*, **2010**, 49, 9460-9464.

267 N. Marion , R.S. Ramón, S.P. Nolan, *J. Am. Chem. Soc*., **2009**, 131, 448-449.

268 G. Luppi, P. Cozzi, B. Kaptein, Q.B. Broxterman, C. Tomasini, *J. Org. Chem*., **2005**, 70, 7418-7421.

269 a) T. Marcelli, J.H. van Maarseveen, H. Hiemstra, *Angew. Chem. Int. Ed*., **2006**, 45, 7496-7504.

b) C. Ó Dálaigh, *Synlett*, **2005**, 5, 875-876.

270 D. Shu-Wen, L. Yi-Yin, D. Wei, L. Tian-Ren, X. Wen-Jing, *Synthesis*, **2013**, 45, 1647-1653.

271 K. Libson, E. Deutsch, B.L. Barnett, *J. Am. Chem. Soc*., **1980**, 102, 2476-2478.

272 L. Qiu, W. Cheng, J. Lin, S. Luo, L. Xue, J. Pan, *Molecules,* **2011**, 16, 6165-6178.

273 M. Meckel, M. Fellner, N. Thieme, V. Kubicek, F. Rösch, *Nuc. Med. Biol*., **2013**, 40, 823-830.

274 V. Lungu, D. Niculae, P. Bouziotis, *Radiolab. J. Radioanal. Nuc. Chem*., **2007**, 273, 663–667.

275 R. Bergmann, M. Meckel, J. Pietzsch, P. Hermann, F. Rösch, *EJNMMI Res.*, **2016**, 6:5, 1-12.

276 M.G. Lam, J.M. de Klerk, P.P. van Rijk, *Eur. J. Nuc. Med. Mol. Imag*., **2004**, Suppl 1, S162-S170.

277 K. Ogawa, H. Kawashima, K. Shiba, K. Washiyama, M. Uedab, H. Saji, *Nuc. Med. Biol*., **2009**, 36, 129-135.

278 S.J. Koopmans, L. van der Wee-Pals, S.E. Papapoulos, *J. Bone Miner. Res*., **1994**, 9, 241-246.

279 B.A. Kashemirov, J.L.F. Bala, X. Chen, F.H. Ebetino, F.P. Coxon, C.E. McKenna, *Bioconjugate Chem.*, **2008**, 19, 2308-2310.

280 S. Sun, K.M. Błażewska, B.A. Kashemirov, F.P. Coxon, M.J. Rogers, F.H. Ebetino, C.E. McKenna, *Phosph. Sulf. Sil.*, **2011**, 186, 970-971.

281 S. Sun, K.M. Błażewska, A.P. Kadina, B.A. Kashemirov, J.E. Dunford, F.H. Ebetino, C.E. McKenna, *Bioconjugate Chem*., **2016**, 27, 329-340.

282 T. Kowada, J. Kikuta, A. Kubo, S. Mizukami, K. Kikuchi, *J. Am. Chem. Soc*., **2011**, 133, 17772-17776.

283 G. Jinbo, L. Jinggong, Q. Yongge, C. Xiusheng, L. Ding, *Bioch. Bioph. Acta*, **2013**, 1830, 3635-3642.

284 M. Pramanik, N. Chatterjee, S. Das, K. Das Saha, A. Bhaumik, *Chem. Commun*., **2013**, 49, 9461-9463.

285 A. Zaheer, R.E. Lenkinski, A. Mahmood, L.C. Cantley, J.V. Frangioni, *Nat. Biotechnol*., **2001**, 19, 1148-1154.

286 K.M. Kozloff, L.I. Volakis, J.C. Marini, M.S. Caird, *J. Bone Min. Res*., **2010**, 25, 1748-1758.

287 H. Hyun, H. Wada, K. Bao, J. Gravier, Y. Yadav, H.S. Choi, *Angew. Chem. Int. Ed*., **2014**, 53, 10668-10672.

288 D.G. Parnum, G. Mehta, G.G.I. Moore, F.P. Siegal, *Tetrahed. Lett*., **1974**, 29, 2549-2552.

289 A. Iqbal, L. Cassar, Patent US4415685 A, **1983**.

290 M. Kaura, D.H. Choi, *Chem. Soc. Rev*., **2015**, 44, 58-77.

291 S. Luňák Jr., J. Vyňuchal, R. Hrdina, *J. Mol. Struc*., **2009**, 919, 239–245.

292 R. Beninatto, G. Borsato, O. De Lucchi, F. Fabris, V. Lucchini, E. Zendri, *Dyes Pigm*., **2013**, 96, 679-685.

293 a) Y. Li, P. Sonar, L. Murphy, W. Hong, *Energy Environ. Sci*., **2013**, 6, 1684-1710.

    b) C.B. Nielsen, M. Turbiez,I. McCulloch, *Adv. Mater*., **2013**, 25, 1859-1880.

    c) D. Chandran, K.S. Lee, *Macromol. Res*., **2013**, 21, 272-283.

294 a) Y. Qu, J. Hua, H. Tian, *Org. Lett*., **2010**, 12, 3320-3323.

    b) Y.H. Jeong, C.H. Lee, W.D. Jang, *Chem. Asian J*., **2012**, 7, 1562-1566.

295 a) G. Zhang, H. Li, S. Bi, L. Song, Y. Lu, L. Zhang, J. Yu, L. Wang, *Analyst*, **2013**, 138, 6163-6170.

    b) M. Kaur, D. H. Choi, *Sens. Actuators B*, **2014**, 190, 542-548.

296 M. Kaur, D.S. Yang, K. Choi, M.J. Cho, D.H. Choi, *Dyes Pigm*., **2014**, 100, 118-126.

297 L. Deng, W. Wu, H. Guo, J. Zhao, S. Ji, X. Zhang, X. Yuan, C. Zhang, *J. Org. Chem*., **2011**, 76, 9294-9304.

298 T. Yamagata, J. Kuwabara, T. Kanbara, *Tetrahedron Lett*., **2010**, 51, 1596-1599.

299 S. Schutting, S.M. Borisov, I. Klimant, *Anal. Chem*., **2013**, 85, 3271-3279.

300 J. Mizuguchi, T. Imoda, H. Takahashi, H. Yamakami, *Dyes Pigm*., **2006**, 68, 47-52.

301 H. Ftouni, F. Bolze, J.F. Nicoud, *Dyes Pigm*., **2013**, 97, 77-83.

302 H. Ftouni, F. Bolze, H. de Rocquigny, J.F. Nicoud, *Bioconjugate Chem*., **2013**, 24, 942-950.

303 G.M. Fischer, A.P. Ehlers, A. Zumbusch, E. Daltrozzo, *Angew. Chem., Int. Ed*., **2007**, 46, 3750-3753.

304 S. Wiktorowski, C. Rosazza, M.J. Winterhalder, E. Daltrozzo, A. Zumbusch, *Chem. Commun*., **2014**, 50, 4755-4758.

305 M. Shankar Singh, S. Chowdhury, S. Koley, *Tetrahedron*, **2016**, 72, 5257-5283.

306 L. Zhang, X. Chen, P. Xue, H.H.Y. Sun, I.D. Williams, K.B. Sharpless, V.V. Fokin, G. Jia, J. *Am. Chem. Soc.*, **2005**, 127, 15998-15999.

307 A.E. Speers, G.C. Adam, B.F. Cravatt, *J. Am. Chem. Soc.*, **2003**, 125, 4686-4687.

308 P.L. Golas, N.V. Tsarevsky, B.S. Sumerlin, K. Matyjaszewski, *Macromol*., **2006**, 39, 6451-6457.

309 H. Hagiwara, H. Sasaki, T. Hoshi, T. Suzuki, *Synlett*, **2009**, 4, 643-647.

310 K. Barral, A.D. Moorhouse, J.E. Moses, *Org. Lett*., **2007**, 9, 1809-1811.

311 M. Meldal, C.W. Tornøe, *Chem. Rev*., **2008**, 108, 2952-3015.

312 F. Himo, T Lovell, R. Hilgraf, V.V. Rostovtsev, L. Noodleman, K.B. Sharpless, V.V. Fokin, *J. Am. Chem. Soc.*, **2005**, 127, 210-216.

313 V.D. Bock, H. Hiemstra, J.H. van Maarseveen, *Eur. J. Org. Chem*., **2006**, 1, 51-68.

314 L. Delaine-Bioton, D. Villemin, J.F. Lohier, J. Sopkova, P.A. Jaffres, *Tetrahedron*, **2007**, 63, 9677-9684.

315 O.I. Artyushin, S.N. Osipov, G.V. Röeschenthaler, I.L. Odinets, *Synthesis*, **2009**, 21, 3579-3588.

316 P.A. Turhanen, *J. Org. Chem.*, **2014**, 79, 6330-6335.

317 L. Shuyun, B. Wenzhu, L. Xu, C. Xiaolan, Q. Lingbo, Z. Yufen, *Phosp. Sulf. Silic. Rel. Elem*., **2015**, 190, 1735-1742.

318 M.V. Makarov, E.Y. Rybalkina, Z.S. Klemenkova, G.V. Röschenthaler, *Russian Chem. Bull. Int. Ed*., **2014**, 63, 2388-2394.

319 V.S. Wills, C. Allen, S.A. Holstein, D.F. Wiemer, *Med. Chem. Lett*., **2015**, 6, 1195-1198.

320 X. Zhou, S.V. Hartman, E.J. Born, J.P. Smits, S.A. Holstein, D.F. Wiemer, *Bioorg. Med. Chem. Lett*., **2013**, 23, 764-766.

321 S. Díez-González, E.D. Stevens, S.P. Nolan, *Chem. Commun*., **2008**, 4747-4749.

322 H. Díaz Velázquez, Y. Ruiz García, M. Vandichel, A. Madder, F. Verpoort, *Org. Biomol. Chem*., **201**4, 12, 9350-9356.

323 S. Díez-González, E.D. Stevens, S.P. Nolan, *Angew. Chem. Int. Ed*., **2008**, 47, 8881–8884.

324 F. Lazreg, A.M.Z. Slawin, C.S.J. Cazin, *Organometallics*, **2012**, 31, 7969-7975.

325 H. Johansson, D. Pedersen, *Eur. J. Org. Chem*., **2012**, 4267-4281.

326 W. Winckler, T. Pieper, B. Keppler, *Phosp. Sulfur and Sil*., **1996**, 112, 137-141.

327 R. Lartia, P. Murat, P. Dumy, E. Defrancq, *Org. Lett*., **2011**, 13, 5672-5675.

328 A. Mishra, V.K. Tiwari, *J. Org. Chem.*, **2015**, 80, 4869-4881.

329 T.J. Sminia, D.S. Pedersen, *Synlett*, **2012**, 23, 2643-2646.

330 A.K. Pandiakumar, S.P. Sarma, A.G. Samuelson, *Tetrahed. Lett*., **2014**, 55, 2917–2920.

331 J. Zaloom, D. Roberts, *J. Org. Chem*., **1981**, 46, 5173-5176.

332 P. Alper, S. Hung, C. Wong, *Tetrahed. Lett*., **1996**, 37, 6029-6032.

333 A. Link, M. Vink, D. Tirrell, *Nat. Protoc*., **2007**, 2, 1879-1883.

334 E. Goddard-Borger, R. Stick, *Org. Lett*., **2007**, 9, 3797-3800.

335 N. Fischer, E. Goddard-Borger, R. Greiner, T. Klapotke, B. Skelton, J. Stierstorfer, *J. Org. Chem*., **2012**, 77, 1760-1764.

336 A. Khare, C.E. Mckenna, *Synthesis*, **1991**, 5, 405-406.

337 C.A. Lipinski, F. Lombardo, B.W. Dominy, P.J. Feeney, *Adv. Drug Deliv. Rev.*, **1997**, 23, 3-25.

338 A. Avdeef, B.Testa, *Cell. Mol. Life Sci*., **2002**, 59, 1681-1689.

339 C.A. Lipinski, F. Lombardo, B.W. Dominy, P.J. Feeney, *Adv. Drug Deliv. Rev.*, **2001**, 46, 3–26.

Università Ca'Foscari Venezia

DEPOSITO ELETTRONICO DELLA TESI DI DOTTORATO

DICHIARAZIONE SOSTITUTIVA DELL'ATTO DI NOTORIETA'
(Art. 47 D.P.R. 445 del 28/12/2000 e relative modifiche)

Io sottoscritto ..ANDREA CHIMINAZZO…………………………………………………….

nat o. a …TREVISO…………………………… (prov. .TV.) il ..08/06/1985………….

residente a .CASALE SUL SILE…… in ..via M. Buonarroti…………………………. n. ..15….

Matricola (se posseduta) ..800358…………. Autore della tesi di dottorato dal titolo:

.New synthetic routes to bisphosphonates as potential drugs for bone disease treatment…

……

……

Dottorato di ricerca in …SCIENZE CHIMICHE…………………………………………………….

(in cotutela con …………………………………………………………………………………)

Ciclo .XXIX……………

Anno di conseguimento del titolo ..2017……………

DICHIARO

di essere a conoscenza:

1) del fatto che in caso di dichiarazioni mendaci, oltre alle sanzioni previste dal codice penale e dalle Leggi speciali per l'ipotesi di falsità in atti ed uso di atti falsi, decado fin dall'inizio e senza necessità di nessuna formalità dai benefici conseguenti al provvedimento emanato sulla base di tali dichiarazioni;

2) dell'obbligo per l'Università di provvedere, per via telematica, al deposito di legge delle tesi di dottorato presso le Biblioteche Nazionali Centrali di Roma e di Firenze al fine di assicurarne la conservazione e la consultabilità da parte di terzi;

3) che l'Università si riserva i diritti di riproduzione per scopi didattici, con citazione della fonte;

4) del fatto che il testo integrale della tesi di dottorato di cui alla presente dichiarazione viene archiviato e reso consultabile via Internet attraverso l'Archivio Istituzionale ad Accesso Aperto dell'Università Ca' Foscari, oltre che attraverso i cataloghi delle Biblioteche Nazionali Centrali di Roma e Firenze;

5) del fatto che, ai sensi e per gli effetti di cui al D.Lgs. n. 196/2003, i dati personali raccolti saranno trattati, anche con strumenti informatici, esclusivamente nell'ambito del procedimento per il quale la presentazione viene resa;

6) del fatto che la copia della tesi in formato elettronico depositato nell'Archivio Istituzionale ad Accesso Aperto è del tutto corrispondente alla tesi in formato cartaceo, controfirmata dal tutor, consegnata presso la segreteria didattica del dipartimento di riferimento del corso di dottorato ai fini del deposito presso l'Archivio di Ateneo, e che di conseguenza va esclusa qualsiasi responsabilità dell'Ateneo stesso per quanto riguarda eventuali errori, imprecisioni o omissioni nei contenuti della tesi;

7) del fatto che la copia consegnata in formato cartaceo, controfirmata dal tutor, depositata nell'Archivio di Ateneo, è l'unica alla quale farà riferimento l'Università per rilasciare, a richiesta, la dichiarazione di conformità di eventuali copie;

Data ___07/12/2016___   **Firma** _____

NON AUTORIZZO

l'Università a riprodurre ai fini dell'immissione in rete e a comunicare al pubblico tramite servizio on line entro l'Archivio Istituzionale ad Accesso Aperto la tesi depositata per un periodo di 12 (dodici) mesi a partire dalla data di conseguimento del titolo di dottore di ricerca.

DICHIARO

1) che la tesi, in quanto caratterizzata da vincoli di segretezza, non dovrà essere consultabile on line da terzi per un periodo di 12 (dodici) mesi a partire dalla data di conseguimento del titolo di dottore di ricerca;

2) di essere a conoscenza del fatto che la versione elettronica della tesi dovrà altresì essere depositata a cura dell'Ateneo presso le Biblioteche Nazionali Centrali di Roma e Firenze dove sarà comunque consultabile su PC privi di periferiche; la tesi sarà inoltre consultabile in formato cartaceo presso l'Archivio Tesi di Ateneo;

3) di essere a conoscenza che allo scadere del dodicesimo mese a partire dalla data di conseguimento del titolo di dottore di ricerca la tesi sarà immessa in rete e comunicata al pubblico tramite servizio on line entro l'Archivio Istituzionale ad Accesso Aperto.

Specificare la motivazione:

☒ motivi di segretezza e/o di proprietà dei risultati e/o informazioni sensibili dell'Università Ca' Foscari di Venezia.

☐ motivi di segretezza e/o di proprietà dei risultati e informazioni di enti esterni o aziende private che hanno partecipato alla realizzazione del lavoro di ricerca relativo alla tesi di dottorato.

☐ dichiaro che la tesi di dottorato presenta elementi di innovazione per i quali è già stata attivata / si intende attivare la seguente procedura di tutela:

………………………………………………………………………………………………………;

☐ Altro (specificare):

………

………

………

A tal fine:

- dichiaro di aver consegnato la copia integrale della tesi in formato elettronico tramite auto-archiviazione (upload) nel sito dell'Università; la tesi in formato elettronico sarà caricata automaticamente nell'Archivio Istituzionale ad Accesso Aperto dell'Università Ca' Foscari, dove rimarrà non accessibile fino allo scadere dell'embargo, e verrà consegnata mediante procedura telematica per il deposito legale presso la Biblioteca Nazionale Centrale di Firenze;

- consegno la copia integrale della tesi in formato cartaceo presso la segreteria didattica del dipartimento di riferimento del corso di dottorato ai fini del deposito presso l'Archivio di Ateneo.

Data …07/12/2016……… **Firma** …………………………………………………………………

La presente dichiarazione è sottoscritta dall'interessato in presenza del dipendente addetto, ovvero sottoscritta e inviata, unitamente a copia fotostatica non autenticata di un documento di identità del dichiarante, all'ufficio competente via fax, ovvero tramite un incaricato, oppure a mezzo posta.

Firma del dipendente addetto ………………………………………………………………………